Deconstructing the ALT-associated Promyelocytic Leukemia Bodies

By

Martina Stagno d'Alcontres

MRC Toxicology Unit

University of Leicester

Thesis submitted for the degree of

Doctor of Philosophy (PhD)

2007

ProQuest LLC
789 East Eisenhower Parkway
P.O. Box 1346
Ann Arbor, MI 48106-1346

Abstract

Cells in which Alternative lengthening of telomeres (ALT) is activated have been reported to contain a novel PML nuclear body (PML-NB) known as ALT-associated PML body (APB). These large, donut-shaped nuclear structures are unique to telomerase-negative cells and contain, among others, PML, telomeric DNA, the telomere binding proteins TRF1 and TRF2, MRE11 and NBS1. APBs can be correlated with ALT in that they appear when the telomere length pattern becomes characteristic of ALT positive cells and are not found in telomerase positive cell lines. The exact role of these bodies in telomere maintenance and/or protection is as yet unclear as there have been few studies carried out to determine the functional involvement of the specific components. Our study aims at the identification of the essential components of this structure and, ultimately, at studying the effect of APB alterations on telomere length and genomic stability. We began by determining the percentage of APB-positive cells within our chosen cell lines, and found that there were a higher proportion of APB positive cells than reported in the literature. In order to determine the role of PML in formation of APB, we employed RNA interference oligonucleotides directed against nuclear PML. Interestingly, decreased speckled distribution of MRE11 and TRF1 was observed in PML-depleted cells. In contrast, TRF2 was not affected, and its down-regulation has no clear effect on MRE11 or TRF1 localization. TRF2 silencing results in telomere erosion, thus suggesting that in ALT cells TRF2 regulates telomere length. In addition, TRF2 depletion causes inhibition of colony formation, increased cell size, p21 upregulation and induction of genomic instability. Although in ALT cells active ATM is found at APBs, it is only following TRF2 silencing that the ATM target p53 becomes phosphorylated and activated. This study sheds new light on the role of the APB components PML and TRF2 in ALT cells.

Acknowledgements

The completion of this thesis is due to the opportunity given to me by my supervisor, Paolo Salomoni, and funding by the MRC. I would like to thank Paolo for all his support, patience and belief in me.

I owe a debt to everyone in the MRC Toxicology Unit for all their help and friendship. In particular I have to say a huge thank you to the people who put up with me everday. I would like to thank Cristian, Amel, Tarik, Valentina, Lorenza, Elena, and Eliana for their scientific help and, along with Lorraine Holland and John, ensuring that I always had a smile on my face. I owe the formatting and layout of this thesis to Colin and his never ending patience. I would also like to thank Dr Nicola Royle, Aaron, Jenny J and Jenny F for teaching me how to work with radiation and how to run Southern blots.

This would not have happened without the support of my family and friends who have stood by me. Their love and support has helped me accomplish my goal and ensured that I never gave up. I dedicate this thesis to them.

Table of Contents

LIST OF TABLES

LIST OF FIGURES

Abbreviations

µg Microgram

µl Microlitre

-/- Knockout

+/- Heterozygote

+/+ Wildtype

ALT Alternative lengthening of telomeres

AML Acute myelogenous leukemia

APB ALT-associated PML- nuclear body

APL Acute promyelocytic leukemia

ATM Ataxia telangiectasia mutated kinase

ATP Adenosine triphosphate

ATR Ataxia telangiectasia and RAD3-related kinase

ATRA All-trans retinoic acid

bp Base pair

BLM Bloom protein

BS Bloom syndrome

BRCA1 Breast cancer 1

CBP CREB binding protein

cDNA Complementary DNA

CNS central nervous system

cPML cytoplasmic PML

CREB Camp response element-binding protein

dH2O Distilled water

DISC Death inducing signalling complex

DMBA 9,10-Dimethylbenz-A-Anthracene

DNA Deoxyribonucleic acid

dNTPs Deoxynucleotide triphosphates

DSB Double strand break

dsRNA Double stranded RNA

ECTR Extrachromosomal telomeric repeats

ERCC1/XPF Excision repair cross complementation group1/xeroderma pigmentosum group F endonuclease

FACS Fluorescence activated cell sorter

FBS Feotal bovine serum

FCS Foetal calf serum

FISH Fluorescence *in situ* hybridization

γ-H2AX Phosphorylated histone H2AX

HAUSP Herpese associated ubiquitin specific protease

HIPK1/2 Homeodomain interacting kinase1/2

HR Homologour recombination

ICF Centromeric instability adn facial dysmorphy syndrome

IF Immunofluorescence

IFN Interferon

JNK c-Jun amino-terminal kinase

kb Kilo base

kD Kilo Dalton

MEF Embryonic fibroblasts

mg Milligram

ml Millilitre

MRE11 Meiotic recombination 11

MRN MRE11/RAD50/NBS1 complex

mRNA Messenger RNA

ng Nanogram

NB Nuclear body

NBS1 Nijmengen Breakage syndrome

NHEJ Non homologoue end joining

PBS Phosphate buffered saline

PI Propidium iodide

PML Promyelocytic leukemia protein

PNA Protein nucleic acid probe

POT1 Protection of telomeres 1

PTOP POT1-interacting protein

Rap1 Repressor/activator protein 1

RARα Retinoic acid receptor α

RBCC RING B box coiled-coil domain

RISC RNA-induced silencing complex

RNA Ribonucleic acid

RNAi RNA interference

SARA Smad anchor for receptor activation

SCE Sister chromatid exchange

shRNA Short Hairpin RNA

siRNA Small interfering RNA

SSB Single strand break

SV40 Simiam virus 40

Terc RNA C-rich sequence (telomerase)

TERT Reverse transcriptase catalytic subunit (telomerase)

TGFβ Transforming growth factor β

TIN2 TRF1 interacting nuclear protein 2

TNF Tumour necrosis factor

TPA 12-*O*-tetradecanoylphorbol-13-acetate

TPP1 Tripeptidyl peptidase 1

TRAP Terminal repeat fragment analysis

TRIM TRIpartite motif

TRF Terminal repeat fragment

TRF1 Telomere repeat binding protein 1

TRF2 Telomere repeat binding protein 2

TRF2$^{\Delta B \Delta M}$ Dominant negative TRF2

V(D)J Variable (Diversity) joining

UV Ultraviolet

WRN Werner protein

YFP Yellow fluorescent protein

Chapter 1) Introduction

1.1 PML and Acute Promyelocytic Leukemia

Acute promyelocytic leukaemia (APL) is a distinct subtype of acute myelogenous leukaemia (AML) and accounts for 10% of all AMLs. It is characterised by the accumulation of leukemic cells with promyelocytic features in the bone marrow, chromosomal translocations involving the retinoic acid receptor α (RARα) locus on chromosome 17, and lastly, the extreme sensitivity of the APL blasts to the differentiating action of retinoic acid (Rego et al., 2001). In the vast majority of cases the promyelocytic leukaemia protein (PML) gene locus, on chromosome 15, is fused to the RARα gene generating the PML-RARα and RARα-PML fusion proteins (Wang et al., 1998a). Numerous lines of evidence point to the PML-RARα fusion gene being the major contributor to APL pathogenesis. Whereas PML-RARα is consistently expressed in APL patients, the reciprocal RARα-PML is only present in 70-80% of cases (Alcalay et al., 1992; Grimwade et al., 1996). Although the mechanisms underlying formation of these translocations are currently unknown, it has been reported that PML and RARα are located adjacent to each other in the chromatin of haematopoietic precursors at various stages of the cell cycle (Neves et al., 1999). It is this fusion protein that appears to be one of the main players in the development and progression of the disease, as it interferes with the functions of the two proteins involved (Wang et al., 1998a).

APL cells blocked at the promyelocyte stage of differentiation display a different PML nuclear pattern from that seen in normal cells. PML is dispersed into hundreds of tiny dots in the nucleus and the cytoplasm in APL cells (Dyck et al., 1994; Koken et al., 1994; Weis et al., 1994). A remarkable feature of APL cells is that, upon treatment with all-trans retinoid acid (ATRA), the normal pattern of PML nuclear bodies is restored (Daniel et al., 1993) and the block on differentiation is released (Huang et al., 1988) (Figure 1.1). However, even though treatment of APL patients with ATRA often leads to complete remission, it is mostly short-lived (see review by (Degos and Wang, 2001)). It has been demonstrated that treatment with low doses of arsenic trioxide can induce apoptosis in leukaemic cells thus representing an alternative treatment for APL (Chen et al., 1996; Zhu et al., 1997). It is believed that the disruption of PML nuclear bodies plays an important role in the development of

APL.

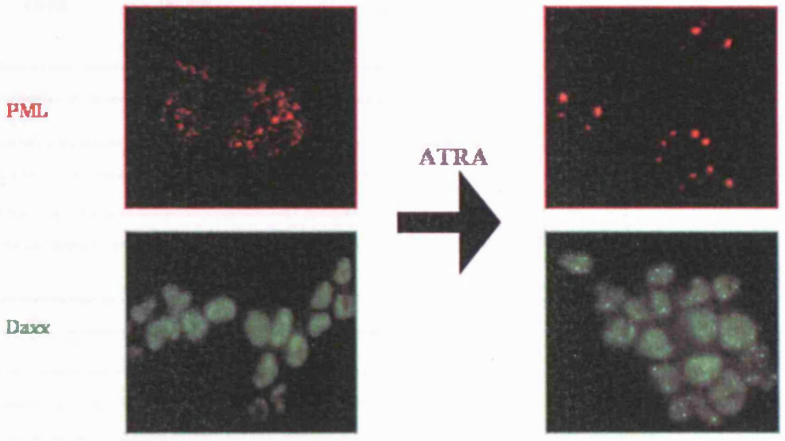

Figure 1.1 Localization of PML and Nuclear body components, such as Daxx, in APL cells before and after treatment with all-trans retinoic acid (ATRA). This confocal image was generated by Dr Paolo Salomoni, MRC Toxicology Unit.

1.2 PML Structure

The PML protein can be divided into three cysteine-rich zinc-binding domains, a RING-finger, two B-boxes (B1 and B2) and a predicted α-helical Coiled-Coil domain, which together form the RBCC motif (Borden et al., 1998; Saurin et al., 1996) or TRIpartite Motif or TRIM (Reymond et al., 2001). The order of these sub-domains is conserved, with the RING finger, B-box and the coiled-coil domains arranged from the N to the C terminus (Jensen et al., 2001) (Figure 1.2). The RBCC/ TRIM motif is found in all PML isoforms and in the PML/RARα fusion protein. Interestingly, it is not only PML that becomes oncogenic upon chromosomal translocation, but also two other members of the RBCC/TRIM family, TIF1 (transcriptional intermediary factor 1) and Rfp (RET finger protein) (Klugbauer and Rabes, 1999); (Le Douarin et al., 1995).

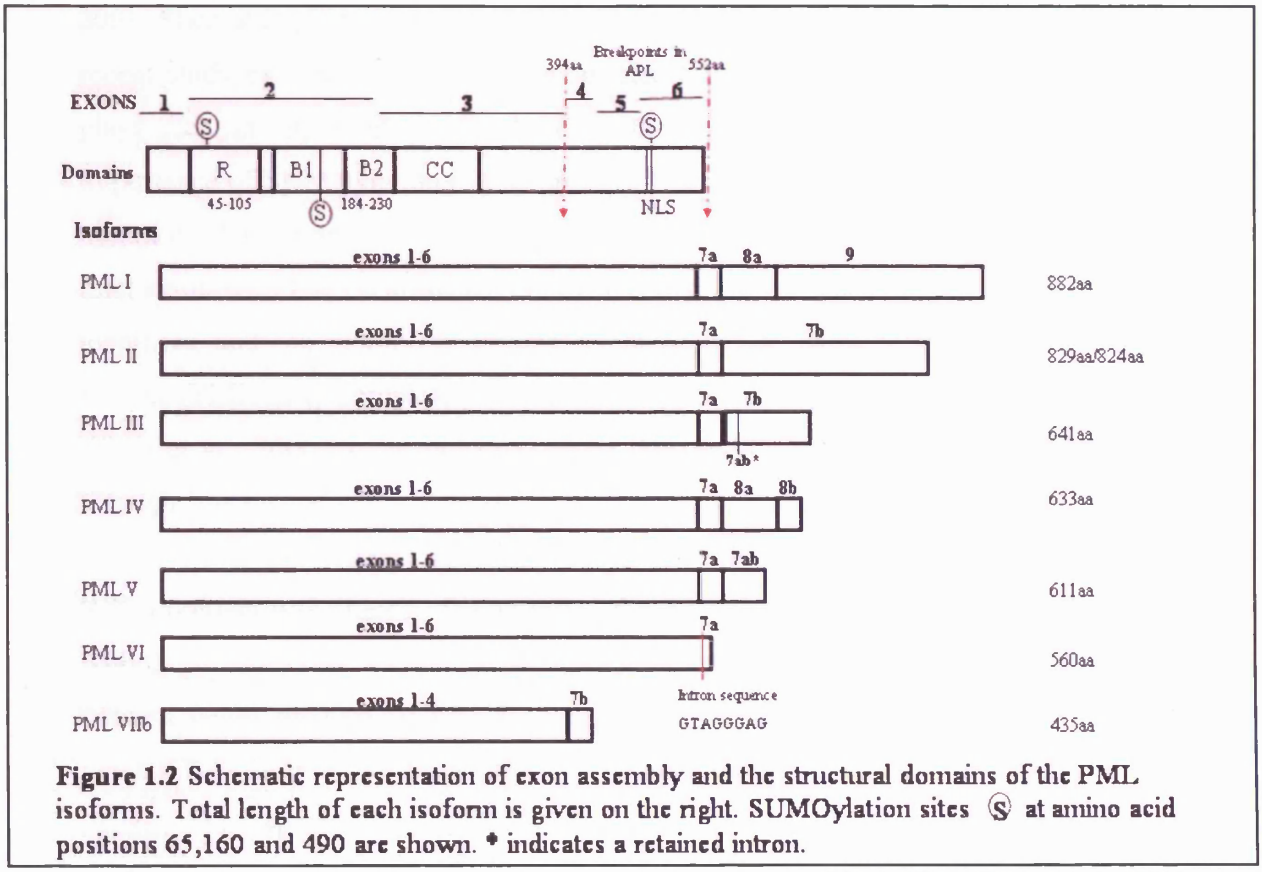

Figure 1.2 Schematic representation of exon assembly and the structural domains of the PML isoforms. Total length of each isoform is given on the right. SUMOylation sites Ⓢ at amino acid positions 65,160 and 490 are shown. * indicates a retained intron.

Adapted from (Jensen et al., 2001)

The RING finger domain is a cysteine-rich zinc binding domain found in a large number of proteins, in species ranging from plant to human. This domain is approximately 60 amino acids long and binds two zinc atoms (Borden, 2000; Kentsis and Borden, 2000). Many functions have been attributed to this motif; however the more commonly observed role is in regulating protein-protein interactions. Mutations of the conserved zinc binding domains cause disruption of PML nuclear bodies (NBs) *in vivo* (Borden et al., 1995; Kastner et al., 1992),. Furthermore, these mutations are correlated with loss of PML growth suppression (Fagioli et al., 1998; Mu et al., 1994), apoptotic and anti-viral activities (Borden et al., 1997; Regad et al., 2001). Interestingly, upon mutation of specific surface regions of the RING domain, PML bodies become enlarged in vivo in the absence of aberrant protein turnover (Boddy et al., 1997). The importance of the RING domain for NB formation may be solely dependent on its protein-protein interaction ability. Studies have shown that various proteins, including SUMO-1 E2 enzyme UBC9, the proline rich homeodomain PRH and the viral proteins Z, IE1 and Tas (Ahn et al., 1998; Borden et al., 1998; Duprez et al., 1999; Regad et al.,

2001; Shen et al., 2006; Topcu et al., 1999) bind to PML through the RING domain. A recent study by Shen and colleagues outlined a possible model to explain why PML plays such an important structural role in the formation of the nuclear body and the importance of SUMOylation in this process (Shen et al., 2006). The authors found that mutation of the known SUMOylated lysines to arginines of PML did not affect the interaction with PML and SUMO. A SUMO-binding consensus sequence was recently identified and the disruption of this sequence in the SUMOylation impaired PML mutant (PML 3M) completely abrogated any interaction between PML and SUMO (Shen et al., 2006; Song and Lee, 2004). Disruption of the RING domain structure through mutagenesis of key cysteine residues was found to decrease SUMO binding activity (Shen et al., 2006). Further investigations using PML 3M mutants, in which the RING domain was altered, demonstrated that there was a reduced interaction of PML with high molecular weight SUMOylated proteins. This suggested that the RING domain could mediate SUMO binding (Shen et al., 2006). Proteins with a RING domain have been suggested to behave in a manner reminiscent to that of E3 ubiquitin ligases. More specifically, the RING finger domain has been found to play a role in mediating the transfer of ubiquitin to heterologous substrates and other RING finger proteins (reviewed in (Joazeiro and Weissman, 2000)). *Mdm2* is a RING-type E3 ubiquitin ligase that has been shown to regulate its own levels and those of p53 through proteasome-mediated degradation (Fang et al., 2001; Honda and Yasuda, 2000) TRIM/RBCC proteins have also been proposed to act as ubiquitin ligases. Biochemical studies have shown that RING E3 ligases interact with E2 enzymes. It is believed that the tripartite domain acts to bring the E2 ligase in close proximity to the substrate resulting in ubiquitination of the target. E3 enzymes can be regulated by ubiquitination by other E3 ligases. TRIM/RBCC compartments contain many proteins including other TRIM/RBCC proteins, and can therefore be regulated through association with other proteins within these domains. However, more work needs to be done in order to fully understand the extent of specificity between the TRIM/RBCC proteins and the E2 enzymes (reviewed in (Meroni and Diez-Roux, 2005). RING finger proteins have also been shown to act as SUMO ligases. The RING finger protein PIAS-1 has been shown to SUMOylate p73 and p53 and regulate cell cycle reentry through binding and SUMOylation of p73 (Munarriz et al., 2004). Taken together, the data to date suggest that the RING finger is important for the formation of PML NBs *in vivo*, possibly

through its ability to mediate SUMO binding. Furthermore, the RING domain may act as an E3 ubiquitin ligase and is able to regulate other cellular processes such as the cell cycle via its SUMOylation activity.

Alongside the RING finger are the B-box domains, B1 and B2. These motifs are small (42 and 46 residues, respectively) and also bind zinc. However, they differ in the number and spacing of the conserved cystine and histidine ligands (Borden et al., 1996). The substitution of the conserved zinc ligands in either B1 or B2 obstructs nuclear body formation in vivo. However, this does not interfere with PML-PML oligomerization (Borden et al., 1996). B-boxes are believed to function with the RING finger to implement the growth suppressor function of PML (Fagioli et al., 1998). Molecular modelling has suggested that the orientation and position of the B-boxes could be important for the correct alignment of the α-helices that form the coiled-coil (Jensen et al., 2001). It is interesting to note that the B-box is only found in RBCC/TRIM family members, inferring the importance of this motif and its function (Reymond et al., 2001).

The coiled-coil domain is made up of interwoven α-helices that create rod-like structures (Lupas, 1996). Peng *et al.* demonstrated that coiled-coils mediate both homo and heterotrimeric interactions as well as higher order multimer interaction (Peng et al., 2000). Several studies have demonstrated that these regions are important for PML multimerization. Minucci and colleagues demonstrated that the coiled-coil domain was involved in the formation of PML-RARα oligomers (Minucci et al., 2000). The authors demonstrated that oligomerization, through the coiled-coil domain of PML-RARα, was sufficient to achieve transforming potential (Minucci et al., 2000). It has also been reported that this domain is important for nuclear body formation and the full growth suppressive activities of PML *in vivo* (Fagioli et al., 1998).

In summary the RBCC motif appears to regulate PML functions and nuclear body formation by inducing high-order homo or hetero protein-protein interactions. Mutations of these domains cause alterations in the function of PML and thus highlight the importance of these structures.

1.2.1 PML and Alternative Splicing

The PML gene consists of nine exons that are alternatively spliced, giving rise to multiple PML transcripts (de The et al., 1991; Fagioli et al., 1992; Goddard et al., 1991; Kakizuka et al., 1991; Kastner et al., 1992). Interestingly, all of the PML isoforms contain the N-terminal region comprising the RBCC/ TRIM motif, but differ either in the central region or in the C-terminal region (Figure 1.2 and Table 1a). All PML isoforms contain the three characterized SUMO-1 modification sites at position 65 in the RING finger, 160 in the B1- Box and 490 in the NLS, as well as a bipartite nuclear localization signal. This suggests that the functions carried out by these motifs are relevant to most PML isoforms. Fagioli and colleagues found that all PML isoforms were expressed more or less equally in all cell lines tested to date (Fagioli et al., 1992). In a more recent study, using isoform specific and total PML antibodies, Condemine *et al.* demonstrated that the longer isoforms, PML-II/PML-I, are the most abundantly expressed, followed by PML-III/V, whereas PML-IV is far less abundant than PML-I (Condemine et al., 2006).

Table 1.1a

Summary and exon assembly of PML isoforms

Isoforms	Exons	References
PML1	1-2-3-4-5-6-7a-8a-9	PML4 (Fagioli et al., 1992) PML-1 (Goddard et al., 1991) TRIM 19 alpha (Reymond et al., 2001)
PML II	1-2-3-4-5-6-7a-7b	PML-2 (Fagioli et al., 1992) PML-3 (Goddard et al., 1991) TRIM 19 gamma (Reymond et al., 2001) TRIM 19 delta (Reymond et al., 2001) TRIM 19 kappa (Reymond et al., 2001)
PML III	1-2-3-4-5-6-7a-7ab retained intron -7b	PML-L (de The et al., 1991)
PML IV	1-2-3-4-5-6-7a-8a-8b	PML-3 (Fagioli et al., 1992) Myl (Kastner et al., 1992)
PMLV	1-2-3-4-5-6-7a-7ab retained intron	PML1 (Fagioli et al., 1992) PML-2 (Goddard et al., 1991) TRIM 19 beta (Reymond et al., 2001)
PMLVI	1-2-3-4-5-6-intron sequence-7a	PML-1 (Kakizuka et al., 1991) PML-3b (Goddard et al., 1991) TRIM 19 epsilon (Reymond et al., 2001)
PML VIIb	1-2-3-4-7b	TRIM 19 theta (Reymond et al., 2001)

Adapted from (Jensen et al., 2001)

PML has many isoforms that can be divided into seven groups (PMLI – VIIb) (Jensen et al., 2001). These isoforms all share the same N-terminal domain but vary, due to splicing of the 3' exons, in the C-terminal domain (Figure 1.2 and Table 1a). These can then be further divided into sub-groups a/b/c, which reflect the alternative splicing of exons 4, 5 and 6 (Table 1b). It has been shown that PML III and PML IV can exist without exon 5 (de The et al., 1991; Fagioli et al., 1992) and that PML V can exist

without exons 5 and 6 or 4, 5 and 6 (Fagioli et al., 1992). Reymond *et al.* carried out a comprehensive study of all human proteins belonging to the RBCC/TRIM-family, in which one new PML isoform (PML VIIb/TRIM19 theta) and one new alternative spliced variant (PML VIb/TRIM19 iota/eta) were identified (Reymond et al., 2001). Since the b and c variants are missing the NLS, they are likely to be cytoplasmic. The functions of the PML splice variants are being studied. Reports have suggested that PMLIII is involved in centrosome regulation and PMLIV has been shown to function as a co-activator of p53 (Condemine et al., 2006).

Table 1.1b

PML alternative splice variants

Isoform	Length	References
PML I	882aa	PML4 (Fagioli et al., 1992)
	882aa	PML-1 (Goddard et al., 1991)
	882aa	TRIM 19 alpha (Reymond et al., 2001)
PML II	829aa	PML2 (Fagioli et al., 1992)
	824aa	PML-3 (Goddard et al., 1991)
	824aa	TRIM 19 gamma (Reymond et al., 2001)
	854aa	TRIM 19 delta[1] (Reymond et al., 2001)
	829aa	TRIM 19 kappa (Reymond et al., 2001)
PML III	641aa	PML-L (de The et al., 1991)
PML IIIa	593aa	PML-S (de The et al., 1991)
PML IV	633aa	PML3 (Fagioli et al., 1992)
	633aa	Myl (Kastner et al., 1992)
	633aa	TRIM 19 zeta (Reymond et al., 2001)
PML IVa	585aa	TRIM 19 lambda (Reymond et al., 2001)
PML V	611aa	PML-1 (Fagioli et al., 1992)
	611aa	PML-2 (Goddard et al., 1991)
	611aa	TRIM 19 beta (Reymond et al., 2001)
PML VI	560aa	PML-1 (Kakizuka et al., 1991)
	560aa	PML-3b (Goddard et al., 1991)
	560aa	TRIM 19 epsilon (Reymond et al., 2001)
PML VIb	423aa	TRIM 19 iota[2] (Reymond et al., 2001)
PMLVIb	423aa	TRIM 19 eta[2] (Reymond et al., 2001)
PML VIIb	435aa	TRIM 19 theta (Reymond et al., 2001)

[1]Similar to PML-3 with an extra 30aa repeat Adapted from (Jensen et al., 2001)

[2]Missing intron sequence GTAGGGAG before exon 7a

1.3 PML and the Nuclear body

Attention was focused on PML due to its occurrence within discrete nuclear bodies that redistribute into microspeckles in blast cells from APL patients, believed to be an important event for the progression of the disease (Zhu et al., 1997). PML nuclear bodies are present in most mammalian cell nuclei and typically a nucleus contains between 5 and 30 discrete foci whose diameter varies in size from 0.2-1μm (Melnick and Licht, 1999). Disruption of NBs is observed upon viral infection, heat shock, heavy metal exposure and rare pathological situations (Eskiw et al., 2003; Ishov et al., 1999; Kamei, 1997; Maul et al., 1995; Nefkens et al., 2003). The correlation seen between nuclear body disruption and interruption of normal cell function has led to the suggestion that the integrity of PML nuclear bodies is of major importance. An important feature of PML nuclear bodies is that in the absence of PML, all PML-NB components tested to date are delocalized, indicating that PML is required for the formation of these nuclear structures. In *Pml*-/- cells each nuclear body component analyzed to date acquires an aberrant nuclear localization pattern and Pml add-back is able to rescue normal localization (Lallemand-Breitenbach et al., 2001; Zhong et al., 2000a). Modification of PML by SUMO1, a ubiquitin-like protein, has been also shown to be essential for the correct formation of the nuclear body (Zhong et al., 2000a). SUMO1 has been demonstrated to covalently attach to PML and several other NB components such as Daxx, Sp100, p53 and CBP (CREB binding protein) (Girdwood et al., 2003; Gostissa et al., 1999; Jang et al., 2002; Rodriguez et al., 1999; Sternsdorf et al., 1997). $Pml^{-/-}$ cells reconstituted with a mutant PML that is not able to be SUMOylated do not reform PML-NBs. Shen *et al.* established that there were multiple SUMO1 binding sites as well as SUMOylation sites on PML and that these were important for the formation of PML nuclear bodies. They proposed a model whereby the construction of the PML-NB occurs through the covalent bonding of SUMO1 conjugated proteins to other SUMO1 attached proteins (Shen et al., 2006) (Figure 1.3). This implies that, although PML is the main component of nuclear bodies, it needs to be modified by SUMO1 in order to induce the correct assembly of these nuclear structures.

1.3.1 Shape and Movement of the PML Nuclear body.

There have been multiple investigations on the shape of this nuclear structure. Sternsdorf *et al.* have suggested that it is a doughnut shaped structure, whereas Weis *et al.* have implied that it is spherical (Sternsdorf et al., 1997; Weis et al., 1994) However, more recently a correlative microscopy and electron microscopy analysis in serial thin sections revealed the doughnut shaped PML-NB structure (Boisvert et al., 2000) (Figure 1.3), although the PML-NB dynamically changes its morphology during the cell cycle and in response to cellular stresses (Bernardi et al., 2004; Dellaire et al., 2006; Everett et al., 1999). It has also been reported that these nuclear structures are mobile. Using a well known component of the nuclear body, Sp100, fused to yellow fluorescent protein, the behaviour of these bodies was monitored in live BHK cells. This study revealed that, based on mobility, there were three populations of nuclear body: 25% were stationary, 63% displayed minor motion and 12% showed rapid movement (Muratani et al., 2002). It was also noted that different nuclear bodies moved at different times within the same nucleus and motion was not restricted to translational movements, but also bodies coalescing and smaller bodies budding off from larger ones. The velocity at which the rapidly moving bodies navigate the nucleoplasm was recorded at 4.0 to 7.2 μm/s, making PML bodies the fastest moving nuclear structure recorded. These movements seem to be ATP and myosin dependent and it seems that other cell type-specific factors may be involved, as HeLa cells did not display any moving NBs, whereas BHK and primary mouse embryo fibroblasts did (Muratani et al., 2002). These data imply that there is more than one type of PML-NB within the nucleus of some cells and that the behaviour and localization of these structures may determine a specific function.

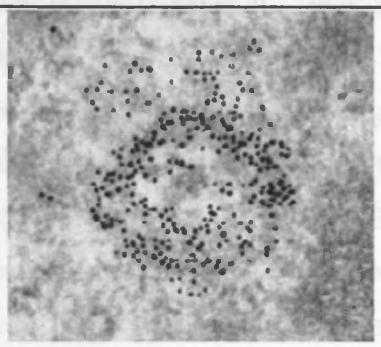

Figure 1.3 Electron micrograph of the PML nuclear body. PML is localized on the outer edge of a doughnut shaped nuclear structure (black dots). This EM image has been generated by Dr David Dinsdale, MRC Toxicology Unit.

1.4 Role of the PML Nuclear body in the Nucleus

A specific function has not been attributed to PML nuclear bodies. However PML protein has been implicated in growth control, transformation suppression, induction of apoptosis and Ras-induced senescence depending on the cellular context (Borden, 2002; Scaglioni et al., 2006). These functions are most likely due to the association of 50 or more known proteins within the PML nuclear body. The large number of proteins accumulating in these bodies has led many to believe that these nuclear structures may act as storage facilities within a cell (Maul et al., 2000). This hypothesis is supported by the observation that upon overexpression of foreign proteins such as the *lac* repressor and a variety of viral proteins, they were found to associate with the body (Maul et al., 2000; Tsukamoto et al., 2000). A number of overexpressed cytoplasmic proteins, such as Int6, have been shown to localize to nuclear bodies (Desbois et al., 1996). A similar localization pattern was noted for BRCA1 and GSN5 when ectopically expressed (Maul, 1998; Maul et al., 1998), as well as many viral proteins such as the mutated form of the influenza NP1 protein (Anton et al., 1999). These rationalizations infer a role for PML-NBs as sensors of foreign or incorrectly expressed proteins that eventually would be eliminated and allow normal function to continue. This hypothesis is further supported by the observation that several proteins involved in polyglutamine repeat disorders such as huntingtin, ataxin 1 and 3 are found to associate with NBs in their

expanded form. However, in these cases the PML-NBs appear larger and more like inclusions than normal nuclear bodies (Chai et al., 1999; Skinner et al., 1997; Yasuda et al., 1999). As mentioned above, the RING domain of PML may have E3 ubiquitin ligase activities that could be involved in proteasomal targeting of missfolded or foreign proteins. Data suggesting that NBs are found adjacent to proteosomal compartments further supports this role for the PML-NB (Lallemand-Breitenbach et al., 2001). In a recent study, Janer and colleagues demonstrated the importance of PML nuclear bodies in proteasomal degradation of poly-Q proteins. The authors showed that it is PMLIV bodies that specifically colocalize with mutant endogenous and exogenous ataxin 7 (ATXN7; mutated in spinocerebellar ataxia type 7) as overexpression of PML III led to the formation of elongated bodies that did not colocalize with ATXN7. It was noted that the coexpression of PMLIV with ATXN7 caused a decrease in the amounts of soluble and aggregated protein, implicating PMLIV bodies in the degradation of this protein. The addition of the proteosomal inhibitor MG132 caused an increase in the level of soluble and insoluble ATXN7, further implicating PMLIV bodies in the active degradation of poly-Q aggregates. The data presented in this article indicated that PMLIV induced the assembly of a nuclear structure dedicated to protein degradation, similar to clastosomes, a subset of PML nuclear bodies that are enriched in ubiquitin-proteasome S components suggested to be sites of nuclear protein degradation (Lafarga et al., 2002). These structures contained subunits of the 19S complex, involved in unfolding substrates, as well as subunits of the 20S catalytic core. Also found in these bodies were chaperones such as Hsp40 that recognises misfolded poly-Q proteins. These structures, enriched in proteasome components, have been implicated in the correct degradation of aggregated poly-Q proteins. More specifically it appears that PMLIV bodies resembling clastosomes are responsible for this function. A recent study by Fu *et al.* has demonstrated that it is not only poly-Q protein aggregates that associate with or near to PML nuclear bodies. The nonpoly-Q proteins golgin-160 (GFP170) and G3 were also shown to form nuclear aggregates in the vicinity of PML nuclear bodies. It was found that the formation of these aggregates was dynamic and that the initial step of the process was the deposition of small aggregates close to PML-NBs. These small structures were then seen to coalesce with larger structures to form larger inclusions. In this study it was also demonstrated that PML-NBs were involved in degradation and the authors hypothesized that PML-NBs represented dedicated domains specialized in

handling foreign particles within the nucleus. It was also implied that the association of nonpoly-Q aggregates with PML-NBs was due to the organization of the nucleus, and these sites were designated degradative regions. These results suggest that the PML nuclear body plays an important role in the expulsion of harmful nuclear aggregates and that these bodies could be spatially defined degradative regions.

It has also been hypothesized that PML Nuclear bodies are storage compartments for functional cellular proteins that modulate biochemical cellular processes (Maul et al., 2000). Daxx is a known DNA binding protein found to accumulate in PML-NBs. Daxx has been shown to be a repressor of PAX3 (Hollenbach et al., 1999) and therefore it is reasonable to assume that controlled release or sequestration of Daxx will effect the level of PAX3 transcription. It has been reported that the localization of Daxx to nuclear bodies is dependent on the modification of PML by SUMO1. Upon localization to NBs, Daxx is SUMOylated and it is believed that the level of SUMOylation can determine the intensity with which Daxx is associated to these structures, thus keeping Daxx away from alternative binding sites and functions. In *Pml*$^{-/-}$ cells it was noted that Daxx is no longer found in discrete nuclear speckles, but was found to localize to nuclear patches that, when counterstained for DNA, were identified as condensed chromatin (Ishov et al., 1999). Daxx was removed from these areas of condensed chromatin upon re-expression of PML, either through overexpression or by cell fusion experiments (Maul et al., 2000). It is plausible that the balance between the Daxx found in NBs and that found in areas of condensed chromatin may constitute a potential cellular homeostatic control mechanism. Alternatively these bodies have been suggested to be catalytic surfaces that allow specific modifications of associated proteins to take place (Kentsis and Borden, 2000). One such protein appears to be p53. It is believed that upon association with NBs p53 is acetylated and phosphorylated to allow its activation upon receipt of the correct cellular stimulus (discussed below). There has been no data to suggest that either of these hypotheses is wrong and all would provide a molecular basis for the biochemical functions described to date.

1.5 PML and Tumour suppression

Multiple in vitro experiments have shown that PML can act as a tumour suppressor. Wang *et al.* demonstrated that $Pml^{-/-}$ mice were resistant to the lethal effects of γ-irradiation, thus suggesting it could regulate cell survival (Wang et al., 1998b). It was also demonstrated that upon treatment with dimethylbenzanthracene (DMBA) and the tumour promoter 12-0-tetradecanoylphorbol-13-acetate (TPA) $Pml^{-/-}$ mice developed more papillomas than control mice as well as fibrosarcomas and sarcomas when treatment was applied to the salivary glands. Unexpectedly 50% of the tumours found in $Pml^{-/-}$ mice were T and B cell lymphomas and 21% were fibrohistiocytoma-like lesions (Wang et al., 1998a). The lymphomas that developed in these mice were more metastatic and aggressive than those seen in control mice. The authors concluded that PML could antagonize the initiation, promotion, and progression of tumours of different histological origins. These data demonstrate that PML can act as a tumour suppressor upon exposure to cancer inducing agents. In order to determine whether PML acted as a tumour suppressor in a relevant disease context, the same laboratory looked at the role of PML in PMLRARα-induced leukemogenesis and neu-induced breast tumorigenesis (Rego et al., 2001). The inactivation of PML was found to dramatically contribute to APL leukemogenesis and the inactivation of one PML allele was found to have a striking effect on the incidence and latency of the disease (Rego et al., 2001). However, PML inactivation did not modify the frequency, the latency, the size of breast tumours, or the frequency of metastasis (Rego et al., 2001). Another study showed that *Pml* loss noticeably accelerates tumour onset, incidence, and progression in *Pten*-heterozygous mutants. Pten heterozygosity predisposes the prostate epithelium to the development of preneoplastic lesions, but not full blown carcinomas (Trotman et al., 2003). Trotman *et al.* found that the male cohort of mice examined displayed a Pml dose-dependence for development of prostate cancer (Trotman et al., 2006). The intestines of $Pten^{+/-}Pml^{-/-}$ mice were also found to have invasive adenocarcinomas of the colon (Trotman et al., 2006). Gurrieri and colleagues examined the status and expression of the PML gene in solid tumours of various histological origins and found that PML protein expression was lost or reduced in prostate adenocarcinomas, colon adenocarcinomas, breast and lung carcinomas, lymphomas, central nervous system (CNS) tumours, and germ cell tumours (Gurrieri et al., 2004). The loss of protein

expression was associated with progression in prostate cancer, breast cancer and CNS tumours (Gurrieri et al., 2004). The above data implicate PML as a tumour suppressor, with loss of protein expression occurring in cancers of various histological origins. The mechanisms through which PML exerts its tumour suppressive functions are discussed in detail below. It has become apparent that PML is able to carry out these functions in both a PML-NB dependent and independent manner.

1.6 Role of PML in Apoptosis

PML is important for numerous stress and DNA damage-activated apoptotic pathways. Myeloid haemopoietic progenitor cells from PML-RARα mice are resistant to apoptotic stimuli such as CD95 and γirradiation (Wang et al., 1998b). Furthermore, apoptotic resistance is increased upon reduction of PML to hemizygosity in *Pml-RARα/Pml*$^{+/-}$ transgenic mice, emphasizing the importance of PML proapoptotic activity *in vivo* and in the progression of APL (Rego et al., 2001). These findings are mirrored in studies conducted in *Pml*$^{-/-}$ mice and cells, confirming the importance of PML in the control of apoptosis. Wang *et al.* demonstrated that *Pml*$^{-/-}$ mice were resistant to the lethal effects of γ-irradiation and CD95. Primary *Pml*$^{-/-}$ splenocytes, thymocytes, mouse embryonic fibroblasts (MEFs) and hematopoietic cells showed impaired caspase activation upon treatment with ceramide, TNFα and interferon INF type I and type II as well as CD95 and γ irradiation (Wang et al., 1998b).

In vitro overexpression studies have also shown that PML induces cell death. Upon PML overexpression cells undergo cell death, but do not show any of the hallmarks of apoptosis such as DNA condensation. This is enhanced upon addition of the caspase inhibitor z-VAD-fmk. Quignon *et al.* found that caspase-3 was not activated in this system, thus implying that overexpression of PML can cause caspase-independent apoptosis (Quignon et al., 1998). However, further investigation into the involvement of other caspases is necessary to completely rule out their involvement in PML-induced cell death. Many other conditions under which caspase-independent apoptosis occurs have been reported, including serum deprivation, staurosporine, overexpression of oncogenes such as c-MYC and E1A, DNA damage and IL-3 withdrawal (Rathmell and Thompson, 1999). However this does not eliminate the contradiction seen between *in*

vivo $Pml^{-/-}$ mice and cells and the *in vitro* overexpression studies. One explanation could be that lower levels of PML are necessary for the correct function of proapoptotic transcription factors that eventually lead to caspase activation. It is possible that elevated levels of PML trigger apoptosis independently of transcription or caspase activation via sequestration of multiple proteins to the nuclear body. The physiological relevance of these findings is as yet to be determined, as it is likely that the levels of PML reached in overexpression studies are not physiologically relevant and there are still no mechanistic insights that corroborate these observations.

Although most reports indicate that PML mainly acts from its PML-NB location, several lines of evidence suggest that PML also exerts PML-NB independent functions. For instance, PML can promote apoptosis in both a PML-NB-dependent and PML-NB-independent manner. This is going to be the subject of the following paragraphs.

1.6.1 PML-NB dependent Apoptosis

1.6.1.1 PML and p53

There are several lines of evidence that suggest a role for PML-NBs and their components in the activation of p53 in response to various stimuli. Multiple factors that regulate p53 activity are found in, or associated with, PML-NBs, including CBP, Hdm21, HIPK2, Chk2, hSir2, herpesvirus-associated ubiquitin-specific protease (HAUSP) and of course PML itself (D'Orazi et al., 2002; Ferbeyre et al., 2000; Fogal et al., 2000; Guo et al., 2000a; Hofmann et al., 2002; Langley et al., 2002; Le et al., 1996; Louria-Hayon et al., 2003; Pearson et al., 2000; Yang et al., 2002). This large accumulation of p53 regulating factors to NBs suggests that the nuclear body could be creating a microenvironment suitable for efficient post-translational modification of a portion of p53. p53 is not constitutively found in PML nuclear bodies, much like multiple other components. However, all PML isoforms are able to mediate its localization to the NB but only one, PML IV, is able to regulate p53 activity (Fogal et al., 2000; Guo et al., 2000a; Wang et al., 1998b)

Guo and co-workers demonstrated that *Pml*$^{-/-}$ mice were resistant to lethal doses of γ-irradiation, implicating PML in the apoptotic response to DNA damage. They also demonstrated that p53 is an essential component of this pathway through the finding that *p53*$^{-/-}$ thymocytes were completely resistant to γ-irradiation-induced apoptosis. *Pml*$^{-/-}$ thymocytes were also resistant to γ-irradiation, but to a lesser extent, suggesting that PML may be necessary for mediating correct p53 proapoptotic functions *in vivo* (Guo et al., 2000a). Upon γ-irradiation, p53 is activated through acetylation, among other mechanisms. Acetylation of p53 enhances its ability to bind DNA and activate transcription. *Pml*$^{-/-}$ thymocytes show impaired acetylation of p53, suggesting that PML may regulate p53 transcriptional function by favouring its acetylation. These data are supported by the finding that *Pml*$^{-/-}$ thymocytes lack induction of downstream target genes of p53, the proapoptotic gene bax, and the inhibitor of cell cycle p21 (Guo et al., 2000a). Acetylation of p53 has also been shown to be controlled by PML upon the onset of premature cellular senescence triggered by oncogenic Ras overexpression (Pearson et al., 2000)(discussed below). Although PML does not possess intrinsic acetyltransferase activity, it interacts with CBP and colocalizes with CBP and p53 in PML-NBs (Guo et al., 2000a; Pearson et al., 2000). Upon exposure to high doses of UV-radiation HIPK2 localizes to PML-NBs along with CBP and p53. The homeodomain-interacting protein kinase-2 (HIPK2) directly interacts with and phosphorylates p53 at serine 46 resulting in the activation of p53 proapoptotic transcription (D'Orazi et al., 2002; Hofmann et al., 2002). There is data to suggest that the nucleoplasmic fraction of PMLIV mediates the effect on p53 Ser46 phophorylation during premature senescence, indicating that PML and p53 can interact independently of the nuclear body (Bischof et al., 2002). Another component of the PML nuclear body able to stabilize p53 is Chk2. Chk2 is a serine kinase that phosphorylates human p53 on serine 20 in response to genotoxic stress (Louria-Hayon et al., 2003). Overxpression of PML increased Ser20 phosphorylation of p53 and protected it against mdm2-mediated ubiquitination and degradation, leading to increased p53 stability and activity (Louria-Hayon et al., 2003).

Negative regulators of p53 activity have also been found to localize to PML-NBs such as the NAD-dependent histone deacetylase hSir2. This protein inhibits p53 activity through deacetylation of lysine 382, thus antagonising genotoxic stress-induced

apoptosis (Luo et al., 2001; Vaziri et al., 2001). A potential mechanism for the regulation of p53 function in PML-NBs is probable due to the presence of two antagonistic proteins, CBP and hSir2. This is likely to be regulated by the molecular context and stimulus received (Hofmann and Will, 2003).

1.6.1.2 PML and Daxx

PML has been shown to be an important component for Fas and TNF-induced apoptosis. This indicates that PML is able to mediate p53-independent proapoptotic pathways (Bernardi and Pandolfi, 2003). However, p53-independent apoptosis is triggered by signals initiating from the death-inducing signalling complex (DISC) at the plasma membrane. Therefore the signal would have to be transduced from the plasma membrane to the PML-NB. One of the more attractive candidates to carry the signal is Daxx. Originally cloned as Fas-interacting partner that specifically binds to the Fas death domain (Yang et al., 1997), Daxx was found to act as a positive mediator of Fas and TGFβ-induced apoptosis (Perlman et al., 2001). Daxx directly interacts with PML in the PML-NB as well as PML-RARα (Torii et al., 1999; Zhong et al., 2000b). Torii and colleagues have shown that Daxx and PML cooperate to potentiate Fas-induced apoptosis (Torii et al., 1999). In the absence of PML Daxx is delocalized from the nuclear body and is found to accumulate in heterochromatin dense nuclear regions (Ishov et al., 2004). The overexpression of PML in $Pml^{-/-}$ cells is able to recruit Daxx almost completely to nuclear structures considered PML-NBs, due to the presence of other PML-NB–associated proteins (Maul et al., 2000). This was also found to be the case in fusion experiments where $Pml^{-/-}$ mouse cells were fused to $Pml^{+/+}$ human cells and the physiological levels of PML were still able to recruit Daxx to the PML-NBs (Maul et al., 2000). Additionally, the ability of Daxx to trigger apoptosis and potentiate the Fas apoptotic signal is significantly impaired in $Pml^{-/-}$ cells (Zhong et al., 2000b). Daxx is a transcriptional repressor and its sequestration to the PML-NB has been shown to interfere with this activity. Delocalization from the nuclear body through the expression of PML-RARα enhances Daxx-mediated transcriptional repression (Li et al., 2000b). It has been demonstrated that the localization of Daxx to the NBs is dependent on the SUMO modification of PML. Experiments carried out interfering with the number of available PML SUMOylation sites determined that the level of

posttranslational modification of PML might dictate the amount of Daxx recruited, and the avidity with which it is retained in the nuclear body (Kamitani et al., 1998) (Maul et al., 2000). The localization of Daxx to PML nuclear bodies was also reported upon mitogenic stimulation of mature splenic lymphocytes. In this case Daxx was upregulated and localized to the NB were it was involved in a pathway for lymphocyte apoptosis (Zhong et al., 2000b).

There are various lines of evidence that suggest that Daxx is able to shuttle between the nucleus and the cytoplasm upon specific stimuli. Fas stimulation (Charette and Landry, 2000), oxidative stress and glucose deprivation (Song and Lee, 2003a; Song and Lee, 2003b; Song and Lee, 2004) cause the relocalization of Daxx from the nucleus to the cytoplasm. Work carried out by Ecsedy and co-workers demonstrated that the movement of Daxx from the nuclear body could be regulated by homeodomain-interacting kinase 1 (HIPK1) through physical interaction (Ecsedy et al., 2003). Other groups have reported that upon overexpression of Daxx it is phosphorylated by HIPK1 causing it to relocalize to the nucleus where it interacts with and activates ASK1, the upstream JNK kinase (Song and Lee, 2003b). The majority of these studies have been carried out in cancer cell lines. However, a report by Khelifi and colleagues demonstrated a pro-apoptotic role for Daxx in physiological settings. Upon exposure to either UV or hydrogen peroxide Daxx was induced and primary fibroblasts in which Daxx had been downregulated by RNAi became resistant to UV- and hydrogen peroxide-induced cell death (Khelifi et al., 2005). The above data all support the view that Daxx is a pro-apoptotic protein.

Despite the many reports implicating Daxx as a pro-apoptotic factor, there are many contradicting reports suggesting that it functions as an anti-apoptotic protein. Daxx has been shown to be important in development as *Daxx*$^{-/-}$ mice have increased apoptosis at embryonic day 7.5 and die at embryonic day 9.5 (Michaelson et al., 1999). There have been reports in which Daxx RNAi in tumour cell lines led to their sensitization to UV, Fas and tumour necrosis factor α (TNFα) induced cell death (Chen and Chen, 2003; Michaelson and Leder, 2003). However, in these studies Daxx was not found to completely localize to the NBs, but was also found in different speckles within the nucleus. Daxx has also been reported to be required for the stability of Mdm2 (Tang et al., 2006). Daxx is found to associate with Mdm2 and the p53 deubiquitinase HAUSP

and mediate the stabilizing activity of HAUSP on Mdm2. DNA damage was found to cause Daxx to dissociate from Mdm2 which correlated with the degradation of Mdm2 (Tang et al., 2006). The authors suggested that this interaction is important for p53 activation in response to DNA damage.

It is plausible that the localization of Daxx dictates its role in apoptosis and that physiological settings and the developmental stage dictate this, thus giving Daxx both anti- and pro-apoptotic functions.

1.6.2 PML-NB independent Apoptosis

1.6.2.1 PML, p53 and other nuclear structures

Although PML was originally identified as part of the PML nuclear body and studies have focused on the structure and function of these nuclear compartments, it is important to note that PML does also have PML-NB-independent functions. It is well established that PML is required for the appropriate post-transcriptional modifications of p53 that potentiate its activity (Ferbeyre et al., 2000; Guo et al., 2000b; Pearson et al., 2000). Furthermore, overexpression of PML recruits p53 to the nuclear body where the transcription of p53 target genes is enhanced and p53-dependent cell cycle arrest is promoted (Bischof et al., 2002; Ferbeyre et al., 2000; Fogal et al., 2000; Guo et al., 2000b; Pearson et al., 2000). p53 is a short-lived protein maintained at low levels in normal cells by Mdm2-mediated ubiquitination and consequent degradation via the proteasome. It is therefore important to stabilize the protein in order for it to be able to carry out its tumour suppressive activities. PML has been shown to recruit Mdm2, the negative regulator of p53, to the nuclear body and protect p53 from Mdm2 mediated degradation (Kurki et al., 2003; Louria-Hayon et al., 2003; Wei et al., 2003). All these functions have been seen to occur within the nuclear body. However, recent evidence suggests that PML influences p53 and Mdm2 function also from outside the nuclear body. A recent study by Kurki and colleagues revealed relocalization and novel interactions of Mdm2 and PML in response to cellular stress and DNA damage (Kurki et al., 2003). They demonstrated a direct interaction between PML and Mdm2 through

the C-terminus and the RING finger domain of the two proteins respectively, and that the overexpression of PML led to the recruitment of Mdm2 to the nuclear bodies. Interestingly, upon cellular stress and DNA damage caused by ultraviolet (UV)-radiation, proteasome down-regulation by MG132 or arsenic trioxide, PML was found to relocalize to perinuclear areas resembling a nuclear necklace structure. This observed pattern was similar to that seen with Mdm2 post UV-C treatment (Kurki et al., 2003). It was noted that Mdm2 and PML colocalized in these regions and that the damage-specific relocalization and interaction were independent of p53. *In vitro* analyses showed that PML, Mdm2 and p53 were able to form trimeric complexes. UV-irradiation caused reorganization of the nuclear body structure, which led to the formation of two distinct complexes, PML/p53 and PML/Mdm2. These complexes were found to form in coincidence with the stabilization of p53, but before the formation of the p53/Mdm2 complex, implying that these are temporally distinct complexes. The above data suggest that PML can participate in the activation and stabilization of p53 in response to cellular stress through a direct interaction with Mdm2 (Kurki et al., 2003).

Another study has shown that PML redistributes to the nucleolus after DNA damage (Bernardi et al., 2004). This work demonstrated that PML was able to enhance p53 stability through the sequestration of Mdm2 to the nucleolus. Accordingly, PML-null cells had increased p53 ubiquitination and displayed a consequent decrease in its stability. It is also important to note that SUMO1 was seen to localize to the nucleolus upon doxorubicin treatment, implying that SUMOylation of PML or associated factors could contribute to its nucleolar localization (Bernardi et al., 2004). The same study demonstrated that the accumulation of PML and Mdm2 in the nucleolus is Arf-independent but dependent on the phosphorylation of PML by ataxia telangiectasia- and RAD3-related kinase (ATR)(Bernardi et al., 2004). ATR is one of two known kinases that are major regulators of cellular responses to DNA damage resulting in either cell cycle arrest and DNA repair or apoptosis (Abraham, 2001). The authors treated cells with caffeine, a known inhibitor of both ATM and ATR, and found that nucleolar localization of PML was markedly impaired after doxorubicin treatment. Using $ATM^{-/-}$ cells it became apparent that there was no effect on the nucleolar relocalization of PML thus implicating ATR. ATR phosphorylation of PML was determined using an antibody

against phophorylated targets of ATM/ATR. Immunoprecipitation of PML after doxorubicin treatment was recognized by the phospho-specific antibody. This was not seen in untreated cells and the effect was abrogated in cells expressing a dominant negative construct of ATR and cells treated with caffeine. All these data imply that PML is phosphorylated by ATR in response to DNA damage as part of an ATR-dependent checkpoint. p53 was not found to colocalize with Mdm2 or PML in response to DNA damage. The localization of the Mdm2 to the nucleolus was found to be dependent on PML, as cells lacking PML demonstrated an impaired nucleolar sequestration of Mdm2 as well as an increased stabilization of p53 and the induction of apoptosis. Interestingly PML was seen to physically associate with the nucleolar protein L11 and PML nucleolar localization was dependent on this association. Taken together the above studies have demonstrated new and unexpected roles for PML in a PML-NB-independent, nucleolar network for tumour suppression.

1.6.2.2 DNA damage by UV-C irradiation.

Another indication of a PML role outside the PML-NB came from the analysis of the cellular response to UV irradiation. The response to short wave length UV light is p53-independent in primary fibroblasts, as cells null for p53 and p21 are more sensitive to UV-induced apoptosis (Bissonnette and Hunting, 1998; Brugarolas et al., 1995; Lackinger and Kaina, 2000; Smith and Fornace, 1997; Waldman et al., 1996). It is interesting to note that primary embryonic fibroblasts lacking c-Jun-N-terminal kinases (JNKs), which are upstream activators of c-Jun, are resistant to UV-induced apoptosis (Tournier et al., 2000). However the role of c-Jun in UV-induced apoptosis is still a matter of debate. A recent report by Salomoni and colleagues suggests a role for c-Jun in UV-induced apoptosis. As previously stated, PML redistributes into microspeckles upon UV exposure. These PML microspeckles have been shown to colocalize with c-Jun and have been shown to be specific to DNA damage, as there is no c-Jun-PML colocalization seen in untreated control cells (Salomoni et al., 2005). *Pml* null cells exposed to UV show a decrease in apoptosis and mitochondrial membrane potential; however p53 was still functional in these cells. This implies that PML can regulate UV-dependent apoptosis in a p53-independent manner. This hypothesis was corroborated by similar results obtained when cells were treated with varying doses of cisplatin, which,

like UV irradiation, induces DNA adducts (Salomoni et al., 2005). Experiments using a dominant-negative c-Jun construct showed that it can inhibit UV-induced apoptosis in fibroblasts; however the effect is reduced in *Pml*$^{-/-}$ cells suggesting c-Jun is impaired in Pml-deficient cells. The transcriptional activity of c-Jun is enhanced upon UV treatment and this is strongly potentiated in cells overexpressing PML in a dose dependent manner. This co-activation is only seen in cells exposed to UV, demonstrating that this regulation of transcriptional activity by PML is UV-dependent. This transcriptional activation is impaired in cells null for PML and reintroduction of PML into these cells almost completely rescued this phenotype (Salomoni et al., 2005). The authors also suggest that the PML-RARα oncoprotein acts as a constitutive and UV-independent co-activator of c-Jun, thus constitutively triggering the oncogenic potential of c-Jun.

1.6.2.3 Role of PML cytoplasmic isoforms

Until recently the tumour suppressive functions of PML have been attributed to its ability to regulate the transcriptional activity of tumour suppressors such as p53 and Rb within the nucleus. However, several cytoplasmic PML (cPML) isoforms, whose function has not been characterized, have been described (Jensen et al., 2001). Only recently a number of studies have started to elucidate the possible functions of these isoforms. A study by Lin and colleagues suggests that cPML plays an important role in TGF-β signalling (Lin et al., 2004). The authors were able to demonstrate that PML affects TGF-β-induced gene expression, as in *Pml*$^{-/-}$ MEFs this was markedly impaired. Treatment with TGF-β1 of both MEFs and B cells isolated from *Pml*$^{-/-}$ mice showed that growth inhibitory functions were impaired implying that PML does affect TGF-mediated biological functions. The induction of TGF-β-mediated senescence has been documented in cancer cells (Katakura et al., 1999) and in this study proven to have the same function in wild type MEFs but not in *Pml* deficient MEFs (Lin et al., 2004). This phenotype was rescued by add-backs of cPML and partially rescued by PMLIV. However mutant forms of PMLIV lacking either the nuclear localization signal or the RBCC, both therefore displaying cytoplasmic localization, were found to completely restore TGF-β-induced transcriptional activity. This was believed to be due to the interactions with Smad3, as mutants of cPML and cytoplasmic PMLIV that could no

longer bind this protein were not able to restore TGF-β-induced growth inhibition or senescence (Lin et al., 2004). TGF-β was shown to phosphorylate both Smad2 and 3 and this was impaired in *Pml*$^{-/-}$ MEFs. Overexpression of cPML was able to enhance phosphorylation of Smad2 and 3 in HepG2 cells upon TGF-β exposure. The authors came to the conclusion that cPML levels could have a critical function in the modulation of TGF-β-induced Smad phospharylation (Lin et al., 2004). It became apparent that there was a direct interaction at endogenous levels of both Smad2 and 3 with cPML. SARA (Smad anchor for receptor activation), a Smad interacting protein was also found to associate with this complex. In the absence of PML this complex is not formed, but upon reintroduction of PML the interaction between these proteins is fully restored. cPML has been shown to be essential for the formation of a stable and functional SARA/Smad2/3 complex (Lin et al., 2004) cPML has been shown to associate with both TGF-β receptors and was found to dissociated upon TGF-β treatment. This suggested that cPML was present in the TGF-β receptor I/II/SARA/Smad complex and its role was to facilitate the localization of the complex to the early endosome. APL blasts have impaired TGF-β signalling similar to that seen in *Pml*$^{-/-}$ cells, supporting the theory that PML-RARα antagonizes cPML function resulting in TGF-β-unresponsiveness (Lin et al., 2004). Again there is data to support the assertion that PML is a potent tumour suppressor.

A more recent study has demonstrated that there is a more complex association between cPML, SARA and the Smad proteins that involves c-Jun and the Terminal Growth Interacting Factor (TGIF). The authors suggest that the interaction between TGIF and cPML through c-Jun may negatively regulate TGF-β signalling by controlling the localization of cPML and consequently the assembly of the cPML/SARA complex (Seo et al., 2006). The homeodomain protein TGIF was reported to inhibit Smad2 phosphorylation, through a Smad2-association-independent mechanism. This inhibitory function of TGIF occurs in coincidence with c-Jun facilitating the interaction of TGIF with cPML, resulting in the nuclear sequestration of cPML and the disruption of the cPML-SARA complex. The elimination of TGIF by siRNA resulted in an increased association of cPML with SARA and the cytoplasmic accumulation of cPML. Furthermore, *c-Jun*$^{-/-}$ fibroblasts were found to have an enhanced association of cPML with SARA and lose their sensitivity to TGIF-mediated disruption of the cPML-SARA

complex and the nuclear sequestration of cPML. The authors suggest that the interaction of cPML with TGIF mediated by c-Jun could negatively regulate TGF-β signalling by controlling the localization of cPML and consequently the formation of the cPML/SARA complex (Seo et al., 2006).

The above studies have shown mechanisms through which cPML is able to control TGF-β signalling and highlight the fact that further work needs to be done to more clearly understand the role of cPML in cellular signalling. However all the above studies have clearly demonstrated that PML is a multifunctional protein that is able to exert its tumour suppressive activities not only outside the nuclear body, but also in the cytoplasm.

1.7 The role of PML in genomic stability

Cancer is a disease characterized by high genomic instability. Genomic instability is both a cause and a consequence of tumourigenesis. Several tumour suppressors act as guardians of the genomes and tightly control genomic stability. In this paragraph, we discuss the several lines of evidence suggesting a role of the tumour suppressor PML in the control of genomic stability.

1.7.1 PML-NB –dependent roles

1.7.1.1 PML and BLM

Recent reports have implicated PML and the NB in the process of DNA recombination and repair as well as checkpoint activation. Studies in this area were initiated due to the observation that several proteins involved in maintenance of genomic stability and/or DNA recombination localized to the NB at specific stages of the cell cycle or upon DNA damage. Zhong and colleagues were the first to demonstrate that PML and the NB are implicated in the control of genomic stability and the regulation of normal Bloom (BLM) function (Zhong et al., 1999). The BLM gene encodes a DNA helicase of the RecQ family (Ellis et al., 1995) that plays a direct role in the maintenance of

genomic stability, possibly through the control of non-homologous recombination (Hanada et al., 1997; Harmon and Kowalczykowski, 1998). BLM protein is mutated and defective in Bloom Syndrome (BS), which is characterized by, at the cellular level, genomic instability that includes excessive chromosome breakage and sister chromatid exchange (SCE) (Ellis et al., 1995). The hypermutability and hyper-recombinability of BS cells is likely to be the reason behind some of the clinical features of the syndrome, including the high predisposition to develop cancer. Interestingly, BLM was found to be concentrated in both primary and transformed cells with approximately 85% of cells displaying PML and BLM in nuclear speckles, with a coincidence greater than 90% (Zhong et al., 1999). In the study carried out by Zhong *et al.* it became apparent that PML was necessary for the localization of BLM into nuclear speckles, but not vice versa, as PML was unperturbed in cells derived from BS patients. BLM, on the other hand, failed to accumulate into nuclear structures in *Pml* null cells and was delocalized from nuclear bodies in APL cells. One of the hallmarks of BS cells is the high rate of SCE (Ellis et al., 1995). Intriguingly, primary fibroblasts from $Pml^{-/-}$ mice also display a higher rate of spontaneous SCE compared to wild type cells, suggesting a possible role for PML in the maintenance of genomic stability, either directly or in cooperation with DNA repair proteins such as BLM (Zhong et al., 1999).

Reports have shown that BLM expression and localization is cell cycle regulated and reaches its peak at S/G2. It was noted that BLM was found to predominantly localize to PML-NBs, except during S phase when its distribution became nucleolar (Yankiwski et al., 2000). The colocalization between BLM and PML was predominantly seen in late S/G2 of the cell cycle, when other proteins involved in recombination and repair, replication factor A (RP-A) and the *E. coli* and *S. cerevisiae* RecA homolog, (RAD51), were also found to localize in a portion of PML-NBs. This colocalization in normal primary human fibroblasts became more apparent after γ-irradiation (Bischof et al., 2001). The authors believed that the appearance of these foci post irradiation was cell cycle-dependent and due to the block in G2 imposed by the DNA damage. It was also noted that both PML and BLM associated with sites of DNA repair after irradiation. These observations led the authors to conclude that BLM was part of a nuclear matrix-based complex that resided in PML-NBs and formed during G2 phase of the cell cycle

in undamaged cells and in response to recombinogenic DNA damage (Bischof et al., 2001).

1.7.1.2 PML and the MRN complex

The repair of DNA double strand breaks (DSBs) is critical for the maintenance of genomic stability. Defects in the cellular response to DSBs have been linked to inherited human cancer-prone syndromes (Carney et al., 1998; Shiloh, 1997; Stewart et al., 1999) and the accumulation of frequently occurring genomic rearrangements in cancer cells (Ferguson et al., 2000). DSBs can be repaired by two different processes; homologous recombination (HR) where correction of the break requires an intact homologous duplex to direct the process or non-homologous end-joining (NHEJ). In *Saccharomyces cerevisiae* recombinational repair of DSBs is in great part carried out by the RAD52 epistasis group. These proteins can be divided into two subgroups; those involved in homologous recombination, namely ScRAD51, ScRAD52, ScRAD55, and ScRAD57 and those involved in non homologous end joining, namely ScRAD50, ScMRE11 and ScXRS2 (Maser et al., 1997) and references therein). Mutations in these genes cause recombination defects and increase sensitivity to DSB causing agents. Human homologues of meiotic recombination 11 (MRE11), RAD50 and XRS2 (NBS1) have been identified as well as those for RAD51, RAD52 and RAD54 (Maser et al., 1997; Petrini et al., 1995). The sequence homology between yeast and mammals of these proteins, as well as the conserved function of the MRE11-RAD50 complex in mammalian cells implies conservation of mechanistic functions also (Dolganov et al., 1996). In yeast this complex has been shown to be involved in checkpoint activation and telomere length homeostasis (Ritchie and Petes, 2000). In meiosis the MRN complex is required for the formation and resection of meiotic DSBs to generate 3` single stranded overhangs (Cao et al., 1990; Nairz and Klein, 1997). It is also important for the formation of 3` single stranded DNA at mitotic DSBs (Ivanov et al., 1994; Tsubouchi and Ogawa, 2000). A report by Ghoshal and Muniyappa suggested that in *Saccharomyces cerevisiae*, MRE11 was likely to play a major role in the generation of the appropriate substrates for DNA synthesis by telomerase and telomere-binding proteins (Ghosal and Muniyappa, 2005). Recently it has been reported that Drosophila MRE11 mutants display an unusually high incidence of telomeric fusions (Bi et al.,

2004; Ciapponi et al., 2004) confirming a possible role of MRE11 in telomere maintenance. These observations strongly suggest that human MRE11 and RAD50 are involved in NHEJ much like their yeast counterparts. The nibrin/NBS1 protein has been shown to associate with MRE11 and RAD50 *in vivo* by directly interacting with MRE11 via sequences in its C-terminus and it is believed that this interaction is necessary for the nuclear localization of the complex (Cerosaletti and Concannon, 2003). MRE11 and NBS1, along with RAD50, form the MRN complex. This complex has been implicated in DNA repair and the initiation of the response to DNA damage via ATM. NBS1 is a target of ATM, and its phosphorylation on Ser343 is required for the phosphorylation of other substrates like CHK2 and histone H2AX (Buscemi et al., 2001; Lee and Paull, 2004). It is believed that the MRN complex is recruited, via NBS1, to sites of DNA damage, where it is then modified by ATM along with Chk2, which goes on to act as a downstream effector, eventually leading to cell cycle arrest (Petrini and Stracker, 2003). It was recently shown that ATM binds the C-terminal domain of NBS1 (Falck et al., 2005; Henson et al., 2005). A study by Uziel at al demonstrated that full activation of ATM, particularly after treatment of cells with low doses of DSB-inducing agents, requires the nuclease activity of MRE11 (Uziel et al., 2003). There have been further studies documenting the necessity of this interaction in yeast, mouse, Xenopus and human cells (Costanzo et al., 2004; Falck et al., 2005; Kang et al., 2005; Lee and Paull, 2005; Myers and Cortez, 2006; Stiff et al., 2005; Uziel et al., 2003). Lee and Paull have shown that MRN is essential for the activation of ATM *in vitro* and that MRN binds tightly to both DNA and ATM, further implicating MRN in the recruitment of ATM to sites of DNA damage (Lee and Paull, 2004; Lee and Paull, 2005).Work by Dupré and colleagues have demonstrated that ATM is activated in two steps, both requiring MRN. The first step involves the recruitment of inactive dimeric ATM to DSBs and the formation of unphosphorylated monomers. The second step is the activation of these monomers through autophosphorylation. This model implies that the activation of ATM requires physical interaction of ATM/MRN complex with DSB ends (Dupre et al., 2006). Taken together these data demonstrate the importance of the MRN complex in the DNA damage signalling cascade.

RAD50 is a member of the structural maintenance of chromosomes (SMC) protein family and has DNA binding activity (Hopfner et al., 2000). The RAD50 protein

contains a Walker A and B domain at the C and N termini that are separated by a large coiled-coil domain. The two Walker domains are brought together to generate a functional nucleotide binding domain through intramolecular assembly. The dimerization potential is mediated by a zinc-binding motif at the base of the coiled coil region. Electron microscopy studies have revealed that a RAD50 dimer binds to two MRE11 molecules to form a stable tetrameric complex with nuclease activity (Chen et al., 2001; Gorski et al., 2004). MRE11 is a DNA binding protein that has both 3' and 5' exonuclease and endonuclease activity that enables it to cleave hairpin DNA structures. These activities have been shown to increase when MRE11 is in a complex with RAD50 (Paull and Gellert, 1999). MRE11 is an essential mammalian gene as knockout mice and cells are not viable (Xiao and Weaver, 1997). The partner of MRE11 and RAD50 is the product of the *NBS1* gene found on chromosome 8q21. The end terminus of this protein contains a forkhead associated domain (FHA) and a breast cancer C-terminal domain (BRCT) that have been shown to be important for focus formation and phosphorylation of this protein (Cerosaletti and Concannon, 2003). Hypomorphic mutations in MRE11 and NBS1 are the cause of diseases characterized by predisposition to cancer and chromosomal instability: Ataxia teleangectasia-like syndrome (ATLD) and Nijmengen Breakage syndrome (NBS) respectively. All of the mutations of the *NBS1* gene found in patients with this disorder cause a premature truncation of the protein, leaving the amino-terminal portion which contains the BRCT domain and the FHA domain. Cell lines from NBS patients do not form MRE11 and RAD50 foci after exposure to ionizing radiation (Carney et al., 1998), and do not postpone DNA synthesis in response to DNA damage (Shiloh, 1997). In addition, these cells show an elevated frequency of chromosomal translocations, especially at *V(D)J*-related loci, and patients have a higher incidence of malignancies. The phenotypes of these disorders are very similar and cells derived from patients do not correctly respond to DSBs and have chromosomal abnormalities, display hypersensitivity to ionizing radiation, radio-resistant DNA synthesis and S-phase checkpoint defects (Shiloh and Kastan, 2001).

Interestingly there is evidence to suggest that NBS1 and hMRE11 are found in PML-NBs (Mirzoeva and Petrini, 2001b). Both proteins have been found to colocalize with PML in primary human fibroblasts with normal telomeres in the absence of DNA

damage (Lombard and Guarente, 2000; Mirzoeva and Petrini, 2001a). Mammalian cells respond to γ-irradiation induced DSB by initiating the NHEJ process, especially during G1 and early S-phase of the cell cycle ((Bernardi and Pandolfi, 2003) and references therein). The MRE11/RAD50/NBS1 (MRN) complex, immediately after exposure to γ-irradiation, appears to localize in nuclear speckles known as irradiation induced foci (IRIF). However, these foci are not present in cells exposed to UV irradiation (Maser et al., 1997). These sites are now known to be sites of DNA damage and repair (Haber, 1998). However, association of MRE11 and NBS1 with PML is lost at early time points after exposure to ionizing radiation and was found to return at later time points (Mirzoeva and Petrini, 2001a). The authors suggested that MRE11 returns to the nuclear bodies at later time points upon completion of DNA repair. A later study, carried out by Carbone and colleagues, confirmed PML and MRE11 colocalization in undamaged cells as well as the loss of colocalization at the early stages post irradiation. What was interesting in this study was that upon resumption of PML/MRE11 colocalization, p53 was also found in the same foci (Carbone et al., 2002). As stated above, PML has also been shown to colocalize with BLM/RAD52/RP-A foci (Bischof et al., 2001) at later time points post irradiation. These are likely to be different foci to those containing MRE11/RAD50 and PML, as it has been reported that MRE11 and RAD51 do not colocalize (Maser et al., 1997). From the studies carried out to date it is as yet unclear what the exact role of PML is upon irradiation-induced DNA damage. It remains to be determined whether PML is able to relocate to different complexes at various stages of repair, or if it is a fixed platform that allows DNA repair proteins to associate more readily with sites of DNA damage. However, taken together, the above observations suggest that PML may play a role in the DSB repair pathways.

1.7.2 PML-NB –independent role of PML in genomic stability

1.7.2.1 PML and the Centrosome.

Most of the work on PML has focused on one of its isoforms, (see above) PML IV. However, several lines of evidence suggest that other isoforms are important. In particular, a recent report demonstrated a role for PMLIII in centrosome duplication and

genome stability (Xu et al., 2005). *Pml*$^{-/-}$ MEFs were shown to have amplified centrosomes in more than 35% of cells examined. In normal cells centrosome duplication occurs in G1/S phase of the cell cycle. In primary and immortalized MEFs lacking PML, the mechanism that regulates centrosome reduplication is impaired allowing continued duplication in the absence of DNA replication. They later demonstrated that PMLIII was the isoform responsible for the control of this cellular process with the use of isoform specific siRNAs. Furthermore, a physical interaction with Aurora A, a serine/threonine protein kinase associated with the centrosome and implicated in the regulations of mitotic microtubles and centrosome maturation (Xu et al., 2005), was discovered. Interestingly they were able to demonstrate, using a PMLIII specific antibody, that colocalization of PMLIII and γ-tubulin was not impaired in APL cells. This indicated that, although other PML isoforms form heterodimers with PML-RARα and become delocalized in the nucleus of APL blasts, PMLIII apparently retains normal function through its interaction with the centrosome in the cytoplasm (Xu et al., 2005). Another fact worthy of note is that Aurora A is able to phosphorylate and destabilize p53 (Katayama et al., 2004). Upon activation, p53 induces the transcription of p21 that in turn binds and inhibits Cdk2/cyclin E functions, essential for regulating centrosome duplication. In the absence of PML there is a decrease in p21 binding and inhibition of Cdk2/cyclin E complex causing it to increase. This whole cycle was shown to be controlled by the inhibition of Aurora A by PMLIII. Taken together these data suggest that PML has an important role for the correct duplication of centrosomes by preventing reduplication through repression of Aurora A activation and highlight a possible role for specific PML isoforms in genomic stability. However, a more recent study contradicts the above findings. Condemine and colleagues were not able to reproduce the centrosomal localization of PMLIII (Condemine et al., 2006). PMLIII was stably expressed in Chinese hamster ovary cells and *Pml*$^{-/-}$ MEFs and there was no detectable colocalization with the centrosome. The same was found to be true of HeLa cell, MRC5 primary human fibroblasts, APL-derived cell line NB4 or APL primary cells, using antibodies directed specifically against PMLIII or total PML (Condemine et al., 2006). These data suggest that there is not a significant amount of PMLIII at the centrosome. However, further studies need to be carried out to determine other isoform specific roles and if there is cross talk between specific isoforms and the pathways in which they are involved.

1.8 PML, Cellular proliferation and Senescence

DNA damage is inevitable as over time cells suffer insults that result in either single strand breaks (SSBs) or DSBs. Mechanisms have evolved to ensure the correct repair is carried out and minimal damage is passed on to daughter cells. If the damage sustained is too great to repair, cells will enter senescence and eventually a cell death mechanism will be activated. Senescence was originally defined by the observation that primary cells have a genetically determined limit to their proliferative capacity, after which they permanently arrest with characteristic features (Campisi, 1997; Hayflick, 1965). Telomeres shorten during each cell division; this is known as the "end-replication problem." It has become apparent that some aspect of telomere malfunction induces the senescent cell-cycle arrest (Artandi and DePinho, 2000). Interestingly there have been many studies that have implicated PML in the onset of growth arrest and cellular senescence upon oncogenic transformation. More specifically, expression of oncogenic RAS (RAS^{val12}) in primary cells induces cellular senescence through the expression of tumour suppressors such as p53, p15INK4b, p16INK4a and p19ARF, which consequently leads to the hypophosphorylation of Rb in several normal human and rodent cell types (Ferbeyre et al., 2000). Ferbeyre and colleagues also found that there was a 7.5 fold increase in PML in Ras-arrested cells. Several PML isoforms appeared to be upregulated. Oncogenic Ras was also found to induce the accumulation of PML-NBs containing both PML and Sp100 and this accumulation was coincident with the onset of premature senescence and appeared unique to the senescent state (Ferbeyre et al., 2000). This study went on to show that overexpression of PML causes a reduction in BrdU incorporation, inferring a growth arrest function to PML. Cells expressing either PML or oncogenic ras displayed similar cell cycle profiles with a prominent arrest in G1/G2 and loss of S Phase DNA content. The authors suggest that PML is sufficient to promote cell-cycle arrest and premature senescence (Ferbeyre et al., 2000). There is further evidence to suggest that PML is essential for cellular senescence upon oncogenic transformation. Pearson *et al.* demonstrated that in $Pml^{-/-}$ cells RAS^{val12}-induced senescence was dramatically impaired, as was p53 acetylation (Pearson et al., 2000). As mentioned above, PML has been found to be important for p53 transcriptional activity, but not its stability or expression as Ras-dependent induction of p53 was not significantly impaired in $Pml^{-/-}$ MEFs (Pearson et al., 2000). It was also

demonstrated that Ras-dependent induction of the p53 target gene, p21 was impaired in *Pml*$^{-/-}$ cells (Pearson et al., 2000). The above data suggest that RAS^{val12} induces PML expression which leads to the acetylation and transcriptional activation of p53. This, in turn, causes the upregulation of p21 leading to growth arrest.

PML has been shown to physically interact with the retinoblastoma protein (pRb), which has been found in the PML-NB and implicated in the control of cell cycle entry and cellular senescence (Alcalay et al., 1998). pRb, like PML, has been shown to associate with a large number of proteins, the relevance of which has been proven for very few. It has been reported that corepressors, such as histone deacetylase 1 (HDAC1), Ski/Sno and mSin3, are associated with PML in the PML-NB (Khan et al., 2001a; Khan et al., 2001b). This complex was found to be important for the transcriptional repression function carried out by the tumour suppressors MAD and pRb. In *Pml*$^{-/-}$ MEFs the ability of both Mad and pRb are impaired further underlining a role for PML in transcriptional repression (Khan et al., 2001a; Khan et al., 2001b). It was also made apparent that PML was able to potentiate pRb transcriptional repression whereas PML-RARα was found to antagonise it (Khan et al., 2001a). This, once again, highlights the importance of the nuclear body and its correct assembly.

1.9 Other PML nuclear structures

Interest in the PML nuclear body grew when it was discovered to be disrupted in APL (Seeler and Dejean, 1999) and other tumours (Gurrieri et al., 2004). Over time other PML nuclear structures have been found that appear in specific settings such as the onset of centromeric instability and facial dysmorphy (ICF) syndrome (Figure 1.4) (Luciani et al., 2006). Interestingly, ICF cells were found to contain enlarged nuclear structures to which multiple heterochromatin protein 1 (HP1) isoforms localized as well as PML and other PML-NB proteins such as ATRX and Daxx (Luciani et al., 2006). These bodies were also found to contain undercondensed juxtacentromeric satellite DNA which was later shown to also be present in PML-NBs at G2 (Luciani et al., 2006). Taking advantage of the large size of these nuclear bodies the authors were able to analyse their spatial organization and found that both PML and SP100 signals were organized in concentric spheres with PML appearing larger that SP100. The HP1β

signal was found in the area enclosed by PML and SP100 and Daxx and ATRX appeared to be organized in concentric circles around HP1β. It was also noted that at G2 phase, the protein organization is similar in both the giant body and the normal PML-NB (Luciani et al., 2006). Another type of nuclear body was described in cells that maintain telomeres by alternative lengthening of telomeres (ALT) (Figure 1.4) (Yeager et al., 1999). These nuclear structures were reported to contain PML and a number of DNA repair proteins as well as telomeric DNA. These are more thoroughly discussed below. The discovery of different PML nuclear structures in various pathological backgrounds suggests that the formation of these nuclear structures plays an important role in pathogenesis. A clearer understanding of the function and structure of these bodies may be useful for developing treatments.

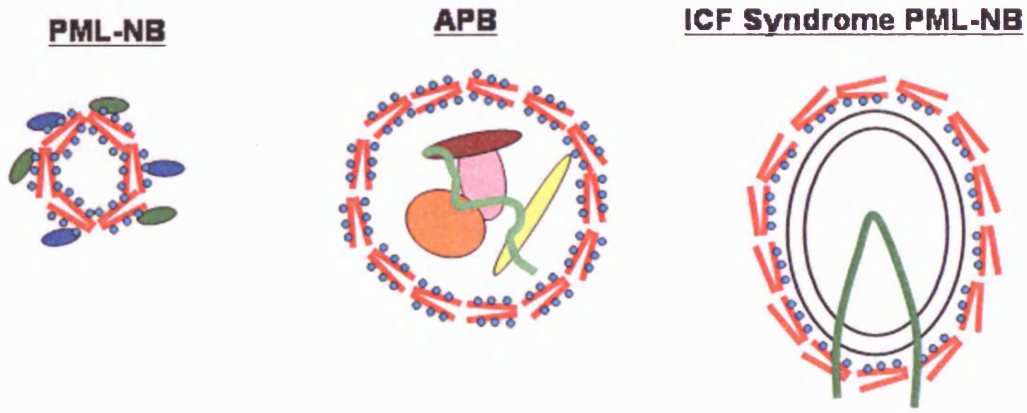

Figure 1.4 Cartoon representation of the various PML nuclear bodies illustrating the predicted organization and size differences. Red rods, PML dimers; light blue circles, SUMO; blue circle joined to light blue circle, SUMOylated proteins; bright green line, telomeric DNA; dark green line, juxtacentromeric satellite DNA; coloured circles, other nuclear body components; concentric black ovals, Daxx and ATRX. This was adapted from (Shen et al., 2006) and (Luciani et al., 2006).

1.10 A Brief History of Telomeres

If the single linear double stranded DNA molecule of a eukaryotic chromosome were completely sequenced from end to end, the first and last sequences would be the telomeric DNA sequences. These terminal sequences stand out from internal DNA sequences because of both their primary sequence and their functional properties (Blackburn, 1991). Telomeres are highly conserved DNA-protein complexes located at the ends of all linear eukaryotic chromosomes. They consist mainly of tandem repeats of short G-rich sequences, TTAGGG in humans and other vertebrates, slime moulds and trypanosomes (Blackburn, 1994) Table 2 shows representative examples of telomeric repeated sequences. Human chromosomes carry 2-30kb of double-stranded TTAGGG repeats and telomere termini carry long (approximately 150 nucleotides) protrusions of single stranded repeats (Makarov et al., 1997; McElligott and Wellinger, 1997; Wright et al., 1997). Telomere length stabilization is required for cellular immortality.

DNA genomes tend to be circular as seen with bacterial genomes, plasmids, bacteriophages and mitochondrial DNAs. Many eukaryotic DNA viruses, such as SV40, polyoma, and hepatitis B virus, also have circular genomes (Griffith et al., 1999). In contrast, eukaryotic chromosomes are predominantly linear (Naito et al., 1998). DNA replication occurs through the use of short RNAs to prime DNA synthesis. The removal of these primers results in 8-12 nucleotide gaps that do not impede the duplication of circular genomes as each gap is resolved through the extension of the preceding Okazaki fragment. However, on a linear template, as in mammalian cells, the last RNA that primed lagging strand synthesis will leave a gap that can not be filled. In the absence of a telomere maintenance mechanism a modest rate of terminal sequence loss will occur (3-5 base pairs(bp)/end/cell division) (Johnson et al., 2001; Levis, 1989; Lundblad and Szostak, 1989; Smogorzewska and de Lange, 2004). However, this loss is much greater in human and mouse cells (50-150bp/end cell division) (Blasco et al., 1997; Harley et al., 1990; Niida et al., 1998) implying that telomeres are actively degraded in these organisms.

Table 1.2 Telomeric DNA sequences

Square brackets have been used when either nucleotide may be in the motif. Round brackets indicate that the nucleotide may or may not be present

Telomeric Repeat	**Group**	**Organisms**
TTAGGG	Mammals	Homo sapiens
	Slime moulds	Physarum Didymium
	Filamentous Fungi	Neurospora
	Kinetoplastid Protozoa	Trypanosoma Crithidia
GGGGTT	Ciliated protozoa	Tetrahymena Glaucoma
GGG[GT]TT		Paramecium
GGGGTTTT		Oxytricha Stylonychia Euplotes
AGGGTT[TC]	Coccidial Protozoa	Plasmodium
AGGGTTT	Higher plants	Arabidopsis
TTTTAGGG	Algae	Chlamydomonas
$(A)G_{2-5}TTAC$	Fission yeast	Schizo sacchromyces pombe
$G_{1-3}T$	Budding yeast	Sacchromyces cerevisiae
$G_{1-8}A$	Cellular slime moulds	Dictyostelium

Adapted from (Blackburn, 1991)

The telomere hypothesis of cellular senescence was independently proposed by Olovnikov and Watson. They proposed that the ends of linear chromosomes were not able to be fully replicated during each round of cell division. Consequently, in somatic

cells this results in the progressive shortening of telomeres with each cell division, which could be the cause of cell cycle arrest in senescent cells (Olovnikov, 1971; Watson, 1972). Later, Harley and colleagues demonstrated that telomeres shorten as a function of age in human cells both *in vitro* and in vivo (Harley, 1991). The telomere hypothesis suggested that critically short telomeres may act as a mitotic clock to signal cell cycle arrest at senescence. Benchimol and Vaziri proposed that the consequence of telomere loss was the generation of single or double strand breaks that in turn activated p53-dependent and independent DNA-damage pathways, culminating in the G1 block of senescence (Vaziri and Benchimol, 1996). Correspondingly, inactivation of p53 and pRb by antisense neutralization (Hara et al., 1991) or by viral oncoproteins (Shay et al., 1991) can extend the replicative potential of cells which may lead to further telomere erosion and prompt the onset of a period of massive cell death and chromosomal instability termed crisis (Counter et al., 1992).

The synthesis and maintenance of telomeres are mediated by telomerase, a specialized ribonucleoprotein complex made up of an RNA C-rich sequence (Terc) that acts as a template for the synthesis of the G-rich telomeric DNA strand both *in vitro* and *in vivo* (Blackburn, 1991) and a reverse transcriptase catalytic subunit (Tert). Telomerase is the key enzyme for the stabilization of telomeres via the addition of TTAGG repeats. Its activity is not detectable in most human somatic cells, but is found in germ cells and immortalized cells. Recent studies have implied that hTert can maintain cell survival and proliferation independently of telomerase activity through pro-survival and anti-apoptotic activity (Cao et al., 2002). The first evidence to suggest that TERT may be involved in cellular functions other than telomere maintenance came from studies that implicated TERT in neuroprotection. In the presence of β-amyloid peptide (a neurotoxic protein fragment believed to promote neuronal degeneration in Alzheimer's disease) neurons in which TERT levels were reduced showed increased oxidative stress and mitochondrial dysfunction, whereas overexpression of TERT resulted in decreased vulnerability to β-amyloid-induced cell death (Zhu et al., 2000). Transgenic mouse models have shown that telomerase is upregulated in a number of developing tumour types implying that telomerase activation can confer enhanced proliferative and survival potential in tumorigenesis, independent of its role in telomere maintenance (Blasco et al., 1996; Broccoli et al., 1996; Greenberg et al., 1999). Mouse models, where targeted

expression of telomerase in basal epidermal keratinocytes resulted in increased telomerase activity and normal telomere length, displayed an increase in wound-healing rates and an increased incidence of carcinogen-induced tumours compared to littermate controls (Gonzalez-Suarez et al., 2001). Taken together these studies support the existence of telomere-independent functions for TERT in mediating cellular proliferation, survival and tumorigenesis.

1.11 ATM and telomere maintenance

Several factors involved in double-strand break repair are found at telomeres and have been shown to have important roles in chromosome stability. Studies have focused on the PIKK (phosphatidyl inositol 3-kinase-like kinase) family proteins, ATM and ATR (ATM and Rad3-related). Inactivation of these proteins leads to major defects in telomere length control and telomeric stability in all organisms studied to date. Recent observations have revealed an important role for PIKK proteins in telomere maintenance. Inactivating ATM in human cells, Tel1p in *S. cerevisiae* and Rad3p in *S. pombe* causes telomere shortening (Dahlen et al., 1998; Greenwell et al., 1995; Metcalfe et al., 1996; Naito et al., 1998). Bi *et al.* and others have shown that mutating the *Drosophila* ATM homologue (*tefu*) causes telomere fusions and genomic instability (Bi et al., 2004; Oikemus et al., 2004; Silva et al., 2004; Song et al., 2004). Further studies carried out by this group demonstrated that ATM and ATR controlled partially redundant telomere-protecting pathways, as seen in yeast. This redundancy appeared to be specific for telomeres regardless of how they are elongated (Bi et al., 2005). In mammalian cells, the role of ATM in telomere maintenance was initially noticed in ataxia-telengiectasia (A-T) patient cells where accelerated telomere loss and genomic instability were characteristic features (Lavin and Shiloh, 1997). ATM was later shown to be activated and mediate p53-dependent apoptosis in the absence of TRF2, possibly because the uncapped telomeres resembled damaged DNA (Karlseder et al., 1999). Other studies have confirmed the role of ATM in telomere-induced senescence activated above a certain threshold by critically short telomeres (d'Adda di Fagagna et al., 2003; de Lange, 2002; Karlseder et al., 1999; Smogorzewska and de Lange, 2002). More recently it was demonstrated that TRF2 is able to inhibit ATM activation by directly interacting with the region of ATM containing S1981 (serine phosphorylated

upon activation of ATM) (Karlseder et al., 2004a). The authors suggested that ATM was also involved in a mechanism directed specifically to telomeres that was inhibited by TRF2. TRF2 is abundant only at telomere ends within the nucleus of cells and therefore its inhibition of ATM would not affect the response to internal DNA damage. The same group also demonstrated that the activation of the ATM pathway at chromosome ends was independent of obvious DNA processing and did not require telomere overhang degradation. Therefore, alterations in telomere structure are not necessary but rather telomere length is important for ATM activation.

Despite the importance of telomere maintenance, it has become apparent that telomeres do not just function as a buffer zone that prevents the loss of essential sequences, but act as a cap that allows cells to distinguish natural chromosome ends from broken DNA. Work carried out in unicellular organisms proposed two possible ways in which this function may occur: either a specific DNA structure at the most terminal single-stranded end of the telomere (Williamson et al., 1989) or proteins bound to the 3` end of the telomere (Gottschling and Zakian, 1986; Horvath et al., 1998) were responsible. However, a single terminus-specific protein has as yet not been reported in mammalian cells. Nevertheless, duplex telomeric DNA-binding proteins have emerged as key players in the capping of mammalian chromosomes.

1.12 Telomere binding proteins

An important aspect of telomere structure and function is the interaction between the repeat sequences and specific binding proteins and associated factors essential for both telomere homeostasis and the capping function. Over the past ten years components of the protein complex formed by telomere-specific proteins have been identified.

1.12.1 Telomere repeat binding factor 1 (TRF1)

The first mammalian telomeric protein to be identified was a 60kDa protein known as TRF1. It was isolated based on its *in vitro* specificity for double-stranded TTAGGG repeats typical of vertebrate telomeres (Chong et al., 1995; Zhong et al., 1992). TRF1 was shown to bind specifically to double-stranded DNA as single-stranded repeats were

not recognised. The optimal site for TRF1 was shown to contain more than six contiguous TTAGGG repeats and be more specific to mammalian chromosome ends as other tandem arrays such as TAGGG, TTTAGGG, TTGGGG, and TTAGGC were not recognised (Zhong et al., 1992). TRF1 mRNA and protein have been detected in all cells and tissue analysed implying that this factor is required in every nucleated cell (Smith and de Lange, 1997). TRF1 displayed a punctate staining pattern by indirect immunofluorescence and was found to colocalize with telomeric DNA upon FISH (Chong et al., 1995; Luderus et al., 1996). In human metaphase cells, TRF1 was seen at chromosome ends (Chong et al., 1995) in concordance with the observation that TRF1 was found to localize with telomeric DNA. Co-fractionation experiments found TRF1 with telomeric DNA in the nuclear matrix and this localization was confirmed by double labelling experiments of nuclear matrix preparations (Luderus et al., 1996). These reports confirm that TRF1 is a telomeric protein that caps all telomeres *in vivo* in interphase as well as mitosis. TRF1 is detected in nuclear extracts from human, monkey, rodent and chicken cells suggesting that all vertebrates have a similar telomeric protein. The isolation and DNA sequence analysis of the full length cDNA of both human and mouse TRF1 led to the prediction of the primary structure and an interspecies comparison (Broccoli et al., 1997a; Chong et al., 1995). It is interesting to note that human and mouse TRF1 are not strongly conserved implying rapid evolution (Smith and de Lange, 1997); however this has allowed the identification of the conserved domains of the mammalian protein. TRF1 was found to contain an acidic amino terminal domain. This is followed by a conserved TRF1-specific domain of 200 amino acids. Alongside this is the least conserved region of the protein that contains the putative nuclear localization signals. The last 50 amino acids are the most conserved region of the protein, and show sequence homology to the DNA-binding domain of the MYB family of proto-oncogenes (Smith and de Lange, 1997) (Figure 1.5). This DNA binging domain, however, differs from the MYB oncoproteins in that it only contains one MYB repeat and it is located at the extreme carboxy terminus of the protein rather than the amino terminus. TRF1 was found to bind DNA as a dimer in a yeast two-hybrid screen (Bianchi et al., 1997). Dimerization occurs through a conserved domain at the N terminus of the protein. Dimerization was found to be important for the DNA binding activity of TRF1 as both MYB domains are required, indicating a resemblance between TRF1 and other MYB-related proteins. Similarities between TRF1 and the

yeast DNA-binding protein Rap1 have been reported (Bianchi et al., 1997; Shore, 1994). For instance, both proteins require two MYB motifs for DNA binding and both bind along their cognate telomeric sequences. Although they are not homologous proteins both display a similar pattern of behaviour in that both TRF1 and Rap1 are able to bend DNA in the order of 120° (Bianchi et al., 1997).

Interestingly, TRF1 has been found to have transcriptional activation potential when targeted to a promoter via a heterologous DNA-binding domain (Smith and de Lange, 1997). However the significance of this function is not clear.

The role of TRF1 in telomere length control was understood through the use of a Tetracycline (Tet)-inducible system. The overexpression of TRF1 caused telomeres to gradually shorten and the partial inhibition of TRF1 through the use of a dominant-negative allele caused the progressive elongation of telomeres to a new equilibrium length (Smogorzewska and de Lange, 2004). The amount of TRF1 did not affect the rate of telomere shortening in telomerase negative cells implying that TRF1 alters telomere length through an effect on telomere elongation (Karlseder et al., 2002). It was proposed that TRF1 controls the action of telomerase at each individual telomere and this was proven by Gilson and colleagues who demonstrated that TRF1 can limit telomere elongation in cis (Gilson et al., 1993; van Steensel and de Lange, 1997). It has been demonstrated that the number of TRF1 molecules bound to the telomere depends on telomere length. Chromatin immunoprecipitation (ChIP) experiments on different cell lines showed that TRF1 immunoprecipitates 20-30% of the telomeric DNA regardless of telomere length, indicating that longer telomeres contain more TRF1 (Loayza and De Lange, 2003). Furthermore, immunofluorescence studies demonstrated that TRF1 signal increases with telomere length (Smogorzewska et al., 2000). These data suggest that TRF1 behaves in a similar fashion to Rap1 given that the amount of TRF1 present at telomeres reflects their length. According to this model longer telomeres recruit more TRF1 and this blocks telomerase from adding more telomeric repeats. Therefore, shorter telomeres, that contain less TRF1, have a greater chance of being elongated. As a consequence, all telomeres in a given cell line will eventually converge to a similar median telomere length. At this length equilibrium there is sufficient TRF1 bound to avoid inappropriate elongation by telomerase but enough to avoid shortening to a critical length and thus prevent senescence.

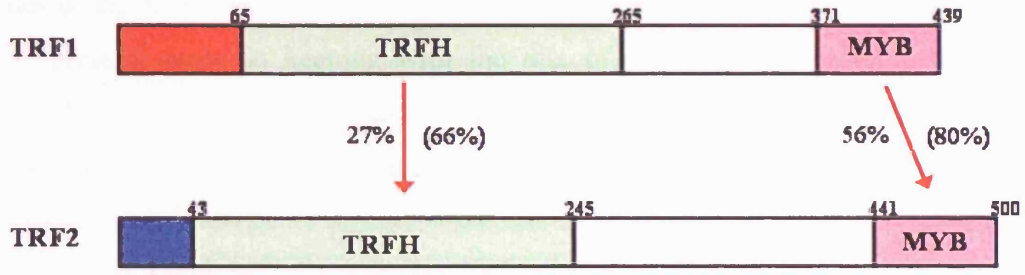

Figure 1.5 Schematic representation of TRF1 and TRF2 proteins highlighting the two domains of homology; the TRFH dimerization domain (green) and the Myb DNA-binding motif (pink). The basic (blue) and acidic (red) regions are marked. The percentage of sequence identity and homology are indicated. Adapted from (Court et al., 2005).

1.12.2 Telomere repeat binding factor 2 (TRF2)

1.12.2.1 Cloning and structure

TRF2 was initially identified as a TRF1 paralogue (Bilaud et al., 1997; Broccoli et al., 1997b). The sequence information was used to isolate the full length human and mouse cDNAs representing TRF2. Human TRF2 cDNA was found to hybridize to a 3.1kb mRNA with a ubiquitous expression pattern similar to that of TRF1 (Broccoli et al., 1997b). *In vitro* translated human and mouse TRF2 appeared to have a larger molecular weight than TRF1. The alignment of the predicted sequences for TRF1 and TRF2 showed that the strongest conservation between these two proteins was in the C-terminal MYB domain. There was also a moderate level of conservation in the regions

from position 45 to 245 in TRF2 that coincided with the dimerization domain of TRF1 (Figure 1.5) (Broccoli et al., 1997b). The dimerization domains of TRF1 and TRF2 did not interact, implying that these proteins are not able to heterodimerize and exist predominantly as homodimers. Unlike TRF1, TRF2 contained predominantly basic residues in the N-terminus and displayed a much higher level of conservation with the murine protein, more in keeping with the rate of divergence of other mammalian proteins. It was also found to localize to human telomeres in metaphase chromosomes. The above data strongly suggest that mammalian telomeres bind two related proteins.

1.12.2.2 TRF2 inhibition, apoptosis and senescence

TRF2 coats the length of all human telomeres at all stages of the cell cycle and is estimated to be present at more than 100 copies per chromosome end (Bilaud et al., 1997; Broccoli et al., 1997b). It has been demonstrated that TRF2 is a crucial factor in the protection of telomeres. Expression of a mutant telomerase which adds sequences to chromosome ends lacking TRF2 binding sites results in a phenotype similar to that seen upon inhibition of TRF2 (Guiducci et al., 2001; Kim et al., 2001), where chromosome ends are perceived as sites of DNA damage (Karlseder et al., 1999; van Steensel et al., 1998). Karlseder *et al.* demonstrated that the inhibition of TRF2 in many cell types, including primary lymphocytes resulted in the immediate induction of p53-dependent apoptosis (Karlseder et al., 1999). It was also noticed that ATM was required for the induction of this cell death program, as two B-cell lines from ataxia telangiectasia patients lacking this kinase and cells from mice lacking functional ATM failed to undergo apoptosis upon TRF2 inhibition (Karlseder et al., 1999). It is the involvement of ATM that leads to the belief that telomeres lacking TRF2 are perceived as sites of DNA damage. Activation of ATM has been shown to be a central player in the cellular response to γ-irradiation-induced Double strand breaks (DSBs), where it is involved in the activation of cell cycle checkpoints that lead to DNA-damage-induced arrest at G1/S, S and G2/M (Bakkenist and Kastan, 2003; Banin et al., 1998; Canman et al., 1998; Canman et al., 1994; Gatei et al., 2003; Kurz and Lees-Miller, 2004; Suzuki et al., 1999). Apoptosis was also seen to occur in mouse cells lacking telomerase once telomeres became critically short (Chin et al., 1999). However, this can be by-passed through the inhibition of p53, as is the case in cells lacking TRF2. A study by Karlseder

et al. found that the inhibition of TRF2, through the use of a dominant negative form of TRF2 lacking both the basic domain and the Myb domain ($TRF2^{\Delta B \Delta M}$), caused apoptosis in a selection of mammalian cells by reducing the amount of TRF2 bound to telomeres (Karlseder et al., 1999). They found that the induction of apoptosis by telomere malfunction was dependent on the activation of p53 by ATM. However, the induction of apoptosis caused by TRF2 inhibition was independent of the DNA damage resulting from broken dicentric chromosomes. The authors concluded that TRF2 was important to "mask" telomeres from a response pathway that could lead to cell death. The inhibition of TRF2 led to the inappropriate exposure of telomeric DNA that resembled double-strand breaks resulting in ATM-mediated p53 activation (Karlseder et al., 1999). These data demonstrate that in some mammalian cell types, telomere malfunction can result in apoptosis. Mice that have critically short telomeres have also been shown to have an increased rate of apoptosis (Lee et al., 1998). Telomere erosion can lead to the disruption of the telomere capping complex and cause apoptosis in some human cells (human T cells) and senescence in others (fibroblasts). The onset of tumorigenesis has been shown to cause telomere shortening (de Lange et al., 1990). Therefore, cells that are deficient in p53 function have a survival advantage compared to those in which the pathway is intact, suggesting that the activation of the DNA damage pathway upon telomere erosion is a tumour suppressive mechanism. It became apparent that there is also a p53-independent response involved since both telomerase-deficient mouse cells and tumour cell lines expressing a dominant negative allele for telomerase reverse transcriptase eventually undergo apoptosis, even in the absence of p53 (Chin et al., 1999; Hahn et al., 1999; Zhang et al., 1999).

Primary human fibroblasts react to TRF2 inhibition by entering senescence rather than apoptosis (Karlseder et al., 1999; Smogorzewska and de Lange, 2002). The cells were shown to display all the morphological and molecular characteristics of senescence, including a large and flat cell shape, multiple nuclei, a diploid (2n) DNA content or polyploid (4n) DNA content, and staining with the senescence marker SA-β-gal (Smogorzewska and de Lange, 2002). This observed response to TRF2 inhibition is very similar to that seen upon shortening of telomeres, with the upregulation of p53 and its targets (p21), as well as effects on the Rb pathway (Smogorzewska and de Lange, 2002). However, the suppression of both the p53 and the p16/Rb pathways can abolish

replicative senescence in human cells. This is clearly demonstrated by the effects of SV40 large T antigen or the combined effects of the HPV16 E6 and E7 proteins that can fully suppress senescence and extend life span (Shay et al., 1991; Shay and Wright, 1989). In both cases cells are able to continue growing and their telomeres continue to shorten, as oncoproteins that suppress p53 or Rb are not able to persuade cells to ignore their shortening telomeres (Shay et al., 1991). Cells that no longer had a functional p53 pathway, due to the presence of E6 protein, transfected with a dominant negative allele for TRF2 ($TRF2^{\Delta B\Delta M}$) still underwent cell cycle arrest. The same was seen to be true with cells lacking functional Rb pathway due to the presence of E7 protein. It was the combined effect of both E7 and E6 or the SV40 large T that was able to induce cell cycle arrest in the presence of $TRF2^{\Delta B\Delta M}$ (Smogorzewska and de Lange, 2002). Both p53 and Rb pathways have been implicated in the prevention of S phase entry upon telomere damage. These data closely reflect the steps leading to senescence in cells undergoing replicative aging (Sherr and DePinho, 2000), implying that telomeres lacking TRF2 resemble critically short telomeres.

The above data suggest that the general response to loss of TRF2 or telomere shortening resembles that seen upon extensive DNA damage. In both situations p53 and p21 are induced and there is an increase in the levels of p16 responsible for the reduction of Rb phosphorylation. It is therefore not unreasonable to believe that telomere-directed senescence may mimic the effects of persistent damage.

1.12.2.3 TRF2 and DNA damage

TRF2 has been found to associate with proteins involved in DSB repair, including the MRN complex, Ku70, Werner protein (WRN) and Bloom protein (BLM) (discussed below) (Opresko et al., 2002; Song et al., 2000; Zhu et al., 2000). These associations have led many to believe that TRF2 is involved in the DNA damage response. Karlseder *et al.* demonstrated that upon overexpression, TRF2 was able to inhibit the response of the ATM kinase to damage and cell cycle arrest upon irradiation, along with several other damage responses, including NBS1 phosphorylation, p53 induction and upregulation of p53 target genes (Karlseder et al., 2004b). TRF2 was shown to directly interact with ATM *in vitro* through a region comprising the S1981 autophosphorylation site of ATM. This led to the discovery that TRF2 was able to

inhibit the activation of ATM at telomeres and act as a control mechanism that specifically blocked the DNA damage response at telomeres without affecting the surveillance of chromosome internal damage. Two recent studies have reported a role for TRF2 away from the telomere upon DNA damage. Bradshaw and colleagues demonstrated that TRF2 associated with photo-induced DSBs in human fibroblasts (Bradshaw et al., 2005). This association was found to occur rapidly and transiently after irradiation and depended on the presence of a functional basic domain. The localization of TRF2 to sites of DNA damage was independent of its interaction with other DNA damage proteins such as Ku70, WRN and BLM and the overexpression of TRF2 was also found to inhibit the DSB-induced phosphorylation of ATM signalling targets. Tanaka and colleagues demonstrated that TRF2 itself was phosphorylated in response to DNA damage, and that this phosphorylated form of the protein was not bound to telomeric DNA (Tanaka et al., 2005). However, phosphorylated TRF2 was present at telomeres in cells that were undergoing telomere-based crisis, most likely due to the telomere-induced damage signalling cascade. These data implicate TRF2 in the initial stages of DNA repair and are the first to propose a non-telomeric role for this protein.

Having determined that TRF2 was essential for the protection of telomeres from being detected as DSBs, it was important to determine what impact TRF2 down-regulation had on the structure of telomeres. Celli and de Lange were able to eliminate TRF2 from MEFs using the 'hit and run' method. These authors generated a conditional allele of *Trf2* (*Trf2*^{flox}), in which gene excision can be achieved by expressing a Cre recombinase. To avoid onset of senescence and apoptosis, *Trf2*^{flox} mice were crossed with *p53*$^{-/-}$ mice to generate *Trf2*$^{flox/flox}$; *p53*$^{-/-}$ animals. *Trf2*$^{flox/flox}$; *p53*$^{-/-}$ MEFs were infected with Cre recombinase to induce TRF2 deletion. This resulted in extensive telomere fusions, which progressively increased until nearly all the telomeres had undergone end joining (Celli and de Lange, 2005). This telomere fusion phenotype was rescued upon the reintroduction of TRF2, demonstrating that it was caused by TRF2 deficiency. The authors were also able to confirm that the fusions were dependent on the non homologous end joining mechanism (NHEJ) by deleting the DNA ligase IV gene. In fact, in cells lacking TRF2, p53 and LigIV (*Trf2*$^{-/-}$ *LigIV*$^{-/-}$ *p53*$^{-/-}$) there was

approximately a 120 fold decrease in fusions compared to control cells. Interestingly, the telomeres of *Trf2*$^{-/-}$ *LigIV*$^{-/-}$ *p53*$^{-/-}$ cells persisted in a free state without undergoing significant DNA degradation (Celli and de Lange, 2005). Remarkably, the 3` overhang was maintained, but the telomeres were recognised as sites of DNA damage, accumulating DNA damage response factors such as 53BP1 and γ-H2AX, and activating ATM. This study implies that the activation of the DNA damage pathway does not require the degradation of the overhang or any other obvious DNA processing.

All of the above mentioned studies have shown that upon TRF2 deletion cells activate either the ATM DNA damage signalling pathway or undergo senescence. A study carried out on mouse liver cells, known to be highly resistant to extensive telomere damage, resulted in telomeric accumulation of γ-H2AX and frequent telomere fusions upon conditional TRF2 knock out, indicating telomere deprotection. However, there was no induction of p53 or apoptosis and liver function did not appear to be impaired (Lazzerini Denchi et al., 2006). Liver regeneration was not compromised in the absence of TRF2. BrdU incorporation was identical in cells lacking TRF2 when compared to controls implying that TRF2 was not essential for DNA replication or entry into the cell cycle. Hepatocytes lacking TRF2 were found to not be able to complete mitosis with a large proportion of cells seemingly arrested in prophase. The authors reasoned that the large number of end-to-end fusions created structures morphologically identical to those seen in prophase. The combination of normal levels of DNA replication and the reduction of cell division was found to be due to cells undergoing endoreduplication (Lazzerini Denchi et al., 2006). This was believed to allow cells to overcome chromosome segregation problems associated with telomere fusions. This report demonstrates that non-dividing hepatocytes can maintain and regenerate liver function, even in the absence of telomere integrity.

Taken together, the above reports demonstrate that TRF2 is important for maintaining genomic stability and that the response to lack of TRF2 varies from senescence in primary human fibroblasts to endoreduplication in the mouse regenerating liver. The common phenotype observed in all these studies was genomic instability and chromosome fusions, implicating TRF2 as an important factor in the control of genomic stability.

1.12.2.4 TRF2 and cancer

In contrast to primary cells, most transformed cells, including cancer cells, maintain short but stable telomeres through the activation of telomerase. It has therefore been suggested that telomere maintenance, along with telomerase activation, act as a general mechanism of tumorigenesis. TRF2 interacts with a number of factors involved in DNA repair that have been shown to have roles in telomere homeostasis (Blasco, 2005). Many chromosomal instability syndromes, characterized by premature aging, increased cancer incidence and short telomeres, have been found to have mutations in TRF2-interacting proteins. Some of these proteins have been extensively characterized, such as Werner (WRN, mutated in Werner syndrome), Bloom (BLM, mutated in the Bloom syndrome) the excision repair cross complementation group 1/xeroderma pigmentosum group F (ERCC1/XPF) endonuclease (mutated in *Xeroderma pigmentosa*), and the MRE11/RAD50/NBS1(MRN) complex (NBS1 is mutated in Nijmegen breakage syndrome) ((de Lange, 2005; Munoz et al., 2006; Munoz et al., 2005; Opresko et al., 2005; Zhu et al., 2003). TRF2 has also been reported to interact with ATM (mutated in Ataxia telangiectasia syndrome) preventing its activation at telomeres (Bradshaw et al., 2005). As many of the TRF2-interacting proteins are involved in chromosomal instability syndromes, it is likely that TRF2 itself may play an important role in the onset of human disease. TRF2 overexpression has been seen in multiple human cancers including lung, liver, breast, and gastric tumours (Matsutani et al., 2001); (Munoz et al., 2005); (Oh et al., 2005). The overexpression of TRF2 has also been reported in human skin carcinomas, further implicating TRF2 in tumourigenesis (Munoz et al., 2005). Munoz and colleagues demonstrated that increased TRF2 levels caused premature aging and increased skin carcinogenesis in a transgenic mouse model (Munoz et al., 2005), strongly supporting the idea that TRF2 is important in cancer and aging. A more recent report from the same group demonstrated that TRF2 acts as a potent oncogene in the absence of telomerase *in vivo* (Blanco et al., 2007). It was noted that the overexpression of TRF2 in a telomerase deficient background dramatically accelerated carcinogenesis in parallel with increased genomic instability and DNA damage. The authors, based on this data, suggest that telomerase inhibition may not be sufficient to block tumour growth if TRF2 expression is upregulated and new therapeutic strategies may be required.

1.13 The telomere capping complex: Shelterin

Telomere deprotection has been implicated in a number of processes including apoptosis, senescence and tumorigenesis. It is therefore important to maintain these structures in order to allow cells to proliferate normally. A telomere cap structure, comprising six telomere-specific proteins, has been identified and termed shelterin. The components of this complex have been identified gradually over the last 10 years, with TRF1 being the first component (Zhong et al., 1992) and then TRF2 (Bilaud et al., 1997; Broccoli et al., 1997b). TRF1-interacting nuclear protein 2 (TIN2) and repressor/activator protein (Rap1) were identified through a yeast two-hybrid screen using TRF1 and TRF2 respectively (Kim et al., 1999); (Li et al., 2000a) and tripeptidyl peptidase 1 (TPP1) (Houghtaling et al., 2004), POT1-interacting protein (PTOP) (Liu et al., 2004) also referred to as PIP1 (Ye et al., 2004) were recently identified as TIN2-interacting proteins. The most conserved component of this complex is POT1 (protection of telomeres 1). POT1 was identified based on sequence homology to telomere-binding factors in hypotrichous ciliates (Baumann and Cech, 2001). These principal components of the shelterin complex have been found in a single complex in fractionated cellular extracts (Liu et al., 2004).; (Ye et al., 2004). TIN2 has been identified as a key player of this complex as it is able to tether TPP1/POT1 to TRF1 and TRF2 and has also been shown to connect TRF1 with TRF2, thereby aiding in the stabilization of TRF2 at the telomere (Liu et al., 2004); (Ye et al., 2004).

Shelterin has been found to be abundant only at chromosome ends and nowhere else in the cell. There is no change in its localization or abundance during the cell cycle and it is known to function only at telomeres (de Lange, 2005). It is important to note that not all proteins found to localize to telomeres are part of the shelterin complex, as many do not meet one or any of the above criteria. The specificity of shelterin for the telomere is mainly due to the multiple Myb-like DNA binding domains of TRF1 and TRF2 dimers and higher order oligomers that show a low tolerance for single base changes in the TTAGGG sequence (Bianchi et al., 1999; Hanaoka et al., 2005). POT1 has also been found to have a strong sequence specificity, binding single stranded 5`-(T)TAGGGTTAG-3` sites both at the 3` end and at internal positions (Bailey et al., 2004); (Loayza et al., 2004). As all of the above mentioned proteins are connected

through protein-protein interactions, the complex can bind telomeric DNA with at least five DNA binding domains and is able to clearly distinguish telomeres from all other DNA ends. Shelterin-like complexes have also been identified in other eukaryotes, such as yeast, implying that this is a conserved complex that is important for telomere maintenance.

1.13.1 Shelterin and the t-loop

Shelterin is believed to aid in the formation of the t-loop. The single stranded tail of the telomere has been proposed to invade the double stranded telomeric DNA, base-pairing with the C-strand and displacing the G-strand (Figure 1.6). This strand invasion can occur at a distance from the physical end of the telomere and it therefore results in the formation of a large duplex loop known as the t-loop (Figure 1.6). This structure allows the end of the telomere to be tucked in and protected.

T-loops were first identified using electron microscopy (Griffith et al., 1999). TRF2 was found to be important for the formation of this structure as it was able to remodel an artificial telomeric substrate into t-loop structures (Griffith et al., 1999); (Stansel et al., 2001). These structures were stabilized upon psoralen cross-linking, suggesting that a strand invasion event had occurred (Griffith et al., 1999). Interestingly, the formation of t-loops by TRF2 *in vitro* does not appear to require ATP, nor does TRF2 have a helicase domain. The reaction is not efficient and it is believed that TRF2 requires help from other factors to generate these structures, implying that other components of the shelterin complex are involved.

TRF1 has also been shown to have DNA remodelling activity *in vitro*, where it can bend, loop and pair telomeric repeat arrays. These activities may all contribute to the formation of the t-loop in vivo (Bianchi et al., 1997); (Bianchi et al., 1999); (Griffith et al., 1998). TIN2 is thought to be involved due to its ability to alter TRF1 conformation, favouring a tertiary telomeric structure able to hinder telomerase access (Kim et al., 2003). As more components of the shelterin complex are identified, the role of each component, with respect to t-loop formation, will soon be elucidated.

T-loops are conserved structures and it has been proposed that they protect telomeres and regulate telomerase activity. However, more work needs to be done to gain a clearer understanding of the precise role these structures play in telomere maintenance.

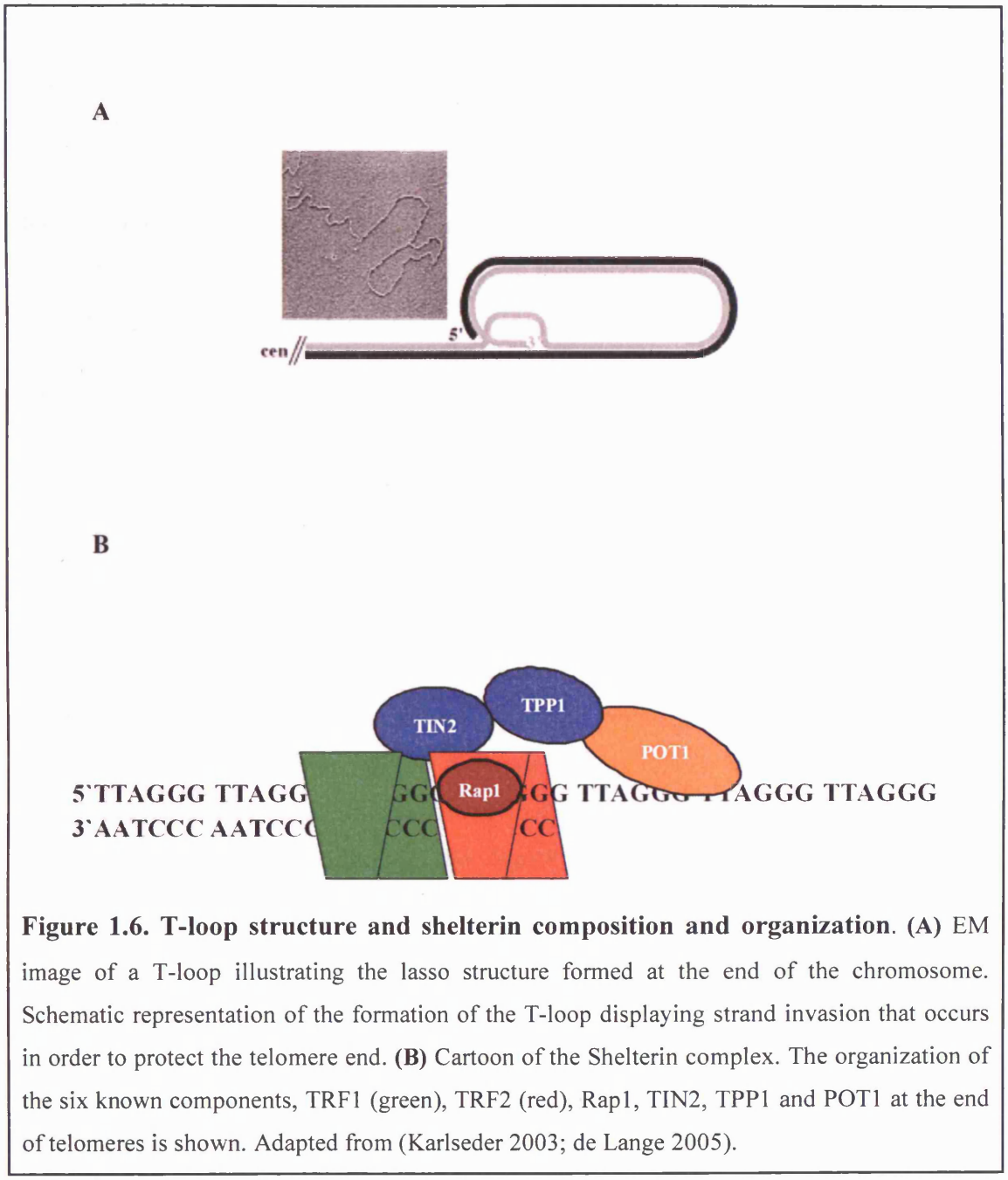

Figure 1.6. T-loop structure and shelterin composition and organization. **(A)** EM image of a T-loop illustrating the lasso structure formed at the end of the chromosome. Schematic representation of the formation of the T-loop displaying strand invasion that occurs in order to protect the telomere end. **(B)** Cartoon of the Shelterin complex. The organization of the six known components, TRF1 (green), TRF2 (red), Rap1, TIN2, TPP1 and POT1 at the end of telomeres is shown. Adapted from (Karlseder 2003; de Lange 2005).

1.13.2 Shelterin in telomere structure and length

In the absence of either TRF2 or POT1 the overall amount of single stranded telomeric DNA is reduced by 30-50% (van Steensel et al., 1998), (Hockemeyer et al., 2005). Upon TRF2 inhibition it is the ERCC1/XPF that cleaves the 3` overhang, just inside the neighbouring duplex DNA (Zhu et al., 2003). The involvement of ERCC1/XPF suggests that some of the telomeres will lose the entire single-stranded overhang in the absence of TRF2. The protection of the overhang by shelterin, through the formation of the t-loop, may be enough to protect against this cleavage. Additionally, the binding of POT1 to single-stranded DNA could impede nucleolytic degradation (Hockemeyer et al., 2005).

Shelterin has also been implicated in the processing of the 5` strand in the generation of the telomeric overhang. Sfeir *et al.* found that the sequence of the 3` end was more or less randomly generated whereas the 5` end was more specifically organized (Sfeir et al., 2005). Almost all human chromosomes have the AATCCAATC-5` sequence suggesting that nucleolytic processing is a controlled process. POT1 has been implicated in this control as its inhibition leads to the loss of homogeneity of the 5` end (Hockemeyer et al., 2005). In the natural structure of the telomere the first POT1 binding site is just two nucleotides from the end of the telomeric DNA duplex and this appears to be the preferred binding substrate. This suggests an interaction between POT1 and the duplex end of the telomere (Hockemeyer et al., 2005). It is plausible that the binding of POT1 so close to the duplex is what inhibits further nucleolytic processing. This activity could be increased further through the binding of POT1 with other shelterin components. It is interesting to note that recent data suggest that there are two POT1 paralogues in mouse; POT1a and POT1b. Strikingly, both are required to prevent the DNA damage signal, endoreduplication and senescence. However, they were dispensable for the repression of telomere fusion. Both proteins were found to have distinct functions, with POT1a involved in repression of the DNA damage signal and POT1b responsible for the regulation of single stranded DNA at the telomere terminus (Hockemeyer et al., 2006). This raises implications about the modelling of human telomere biology in mice.

In yeast and mammals telomeres are maintained within a set size range through a negative feedback loop that is able to block telomerase at individual chromosome ends (reviewd (Smogorzewska and de Lange, 2004). Long telomeres have been proposed to be able to block telomerase from elongating them further, whereas short telomeres will allow telomerase to elongate them. Shelterin has been found to represent the cis-acting inhibitor. The proposed model suggests that telomerase activity is influenced by the total amount of shelterin present at the telomere, which in turn is proportional to the length of the telomere. Longer telomeres are proposed to have more shelterin than shorter telomeres. This inhibition has been suggested to be due to the presence of POT1 (Loayza and De Lange, 2003). Loayza and colleagues found that a mutated POT1 not able to bind telomeres caused telomerase-dependent elongation even in the presence of increasing shelterin (Loayza and De Lange, 2003). POT1 DNA binding activity has been found to be necessary for telomerase inhibition as POT1 was not able to inhibit telomeric repeat addition to substrate primers defective for POT1 binding (Kelleher et al., 2005). From these data it was postulated that the amount of shelterin on a telomere determines the positioning of POT1 in such a way as to inhibit telomerase.

Taken together the above data suggest that shelterin is involved in every aspect of telomere maintenance. It is not necessarily the activity of the individual components, but the combination of all the involved proteins interacting and reinforcing one another's functions that make this such an effective complex.

1.14 Telomeres immortalization and cancer

1.14.1 The role of senescence and immortalization in cancer

Normal human and rodent cells in culture exhibit a finite life span at the end of which they exhibit morphological changes and cease proliferating, a process termed cellular senescence or cellular aging (Barrett et al., 1993). Cells become enlarged and express pH-dependent galactosidase activity (Dimri et al., 1995). Senescent cells can remain metabolically active for long periods of time even though they have permanently stopped proliferating (Campisi et al., 1996; Goldstein, 1990). Senescence has been proposed to form a barrier against tumorigenesis, as the ability to proliferate infinitely is

essential for the malignant transformation of normal cells (O'Brien et al., 1986; Sager, 1991). Senescence has been shown to occur upon progressive telomere shortening during serial cell division (Harley et al., 1990; Levy et al., 1992), through extensive DNA damage (Robles and Adami, 1998), or through ectopic expression of certain oncogenes, such as oncogenic Ras (H-RasV12) (Serrano et al., 1997; Zhu et al., 1998). Cells have been shown to be able to overcome or bypass senescence upon ectopic expression of the telomerase reverse transcriptase catalytic subunit (Cao et al., 2002; Harrington et al., 1997). Telomerase activity is not readily detectable in most human somatic cells, but is found in germ cells and immortalized cells. Malignant cells that express telomerase have been found to have shorter telomeres than normal cells (Elmore et al., 2002). However, some immortalized cells will undergo senescence in response to certain anticancer agents, suggesting that gain of immortality does not necessarily mean a loss in DNA damage response (Chang et al., 1999).

Senescence has been shown to depend on the presence of functional p53 and Rb pathways (Rheinwald et al., 2002; Serrano et al., 1997; Shay et al., 1991) reviewed in (Garkavtsev et al., 1998; Stein and Dulic, 1995). Inactivation of the p53 and pRb/p16^{INK4a} pathways is the most important oncogenic event in cancer. p53 is a known tumour suppressor and has a key role in monitoring genomic integrity in human cells. The p53 gene is the most commonly mutated gene in human cancer, having been found to be inactivated in approximately 50% of human tumours (Harris and Hollstein, 1993). p53 was discovered in 1979 as a 53kDa protein that binds the SV40 large T antigen (Lane and Crawford, 1979) and was later found to bind to the HPV E6 viral oncoprotein (Scheffner et al., 1990) that targets it for ubiquitin-mediated degradation (Bond et al., 1999). Fibroblasts in which the normal function of p53 has been altered by transduction with a mutant p53 (Bond et al., 1994) or which experience spontaneous loss of the single wild-type p53 gene, as in Li-Fraumeni cells (Rogan et al., 1995), have an extended lifespan, thus suggesting they can escape from senescence. However, these cells eventually enter terminal proliferation arrest, even in the absence of a functional p53 pathway. Accordingly, rodent cells deficient in either p53 or p16 are efficiently transformed by oncogenic Ras (Serrano et al., 1997; Zhu et al., 1998) suggesting that the onset of senescence is a defense mechanism to prevent oncogene-driven proliferation.

Another frequently altered pathway in human cancers is the pRb/p16^{INK4a} pathway. Both HPV and SV40 oncoproteins have been shown to interact with members of the retinoblastoma (Rb) protein family and cause their inactivation (Ahuja et al., 2005). The Rb protein is physiologically active in a hypophosphorylated form and it inhibits progression through the cell cycle by binding various transcription factors (Sherr, 1996; Stein et al., 1990). Cell cycle progression is allowed upon phosphorylation of Rb by the holoenzyme complex containing cyclin D and cyclin dependent kinases (cdk4 or cdk6), which causes the release of the transcription factors and DNA synthesis. Serrano and colleagues identified an inhibitor of the cyclin D complex, p16^{INK4a} (Serrano et al., 1993), that maintains Rb in its active state. Loss of function of p16^{INK4a} occurs in multiple tumour types and can be due to point mutations, gene deletions or even loss of expression through hypermethylation of the CpG island in the upstream control region of the gene (Huschtscha and Reddel, 1999). Significantly, p16^{INK4a} levels are increased in a number of human cell types at the onset of senescence, including fibroblasts and epithelial cells (Palmero et al., 1997; Reznikoff et al., 1996). Reintroduction of Rb into cells lacking both Rb and p53 has been found to induce senescence (Alexander and Hinds, 2001; Xu et al., 1997). Certain cancers have been found to retain functional p53 and Rb genes. However, these are usually sequestered by E6 and E7 HPV viral proteins (Shay et al., 1991). Upon introduction of E2 viral protein, which represses both E6 and E7 cells, the same cells rapidly undergo senescence (Goodwin and DiMaio, 2000; Wells et al., 2003). These data all demonstrate the importance of Rb in the inhibition of tumorigenesis through its role in activating senescence.

It is interesting to note that PML is involved in p53- and pRb-mediated senescence. Overexpression of PML has been shown to inhibit oncogenic transformation (Le et al., 1996);(Mu et al., 1994) and induce hyperphosphorylation of Rb and increase expression of p53 and p21 (Le et al., 1998). Transformation by RasVa^{12} caused p53 accumulation in the PML-NB and its acetylation and transcriptional activation (Pearson et al., 2000) which is impaired in PML$^{-/-}$ cells. PML was found to potentiate pRb transcriptional repression (Khan et al., 2001b) and in PML$^{-/-}$ MEFs this was markedly impaired (Khan et al., 2001a; Khan et al., 2001b). These data demonstrate the involvement of PML in regulating tumour suppressor functions.

1.14.2 Telomere maintenance is important in both immortalized and tumour cells

Recently, the discovery that most cancer cells contain telomerase activity, a known marker of immortalization, has implied that immortalization is an essential factor for cancer development (Kim et al., 1994). There are examples of normal tissues that express telomerase, but most normal human somatic cells have low or undetectable levels of telomerase activity (Table 3). This is consistent with the telomere hypothesis of senescence where cells from explanted tissue were seen to have a finite lifespan (Hayflick, 1965; Hayflick and Moorhead, 1961). It became apparent that cancers could be transplanted indefinitely, but normal tissues could only be transplanted a finite number of times (Daniel et al., 1975).

Table 1.3

Examples of normal human cells and tissues that express telomerase

Cell Type	**Reference**
Haemopoietic cells	(Broccoli et al., 1995; Counter et al., 1995; Hiyama et al., 1995)
Epidermal keratinocytes	(Harle-Bachor and Boukamp, 1996; Taylor et al., 1996; Yasumoto et al., 1996)
Hair follicle cells	(Ramirez et al., 1997)
Intestine	(Hiyama et al., 1996)
Uroepethelial cells	(Belair et al., 1997)
Endothelial cells	(Hsiao et al., 1997)
Liver	(Burger et al., 1997)
Endometrium	(Brien et al., 1997; Kyo et al., 1997; Saito et al., 1997)

Telomerase activation is closely followed by immortalization, with the majority of immortalized cells having detectable levels of telomerase activity (Bryan et al., 1995; Counter et al., 1992; Kim et al., 1994). It has been demonstrated that the expression of the catalytic subunit of human telomerase is sufficient to extend the lifespan of normal cell types in the absence of senescence or crisis (Vaziri and Benchimol, 1998). Also, the expression of hTERT in pre-crisis cells has been found to bypass crisis (Counter et al.,

1998; Zhu et al., 1999). These reports have demonstrated that telomerase activity, and therefore the maintenance of telomeres, are vital for cellular immortalization.

The majority of human tumours and tumour-derived cell lines, approximately 85%, have been shown to have detectable telomerase activity (Shay and Bacchetti, 1997). This led to the assumption that telomerase activation plays a key role in cancer development. Interestingly, not all immortalized cells have detectable telomerase activity. Furthermore, it has been demonstrated that a number of tumours are able to maintain long telomeres in the absence of telomerase (Bryan et al., 1995). This phenomenon has been named ALT (alternative lengthening of telomeres), which is active in a variety of *in vitro* immortalized (Bryan et al., 1995) and tumour cell types (Bryan et al., 1997). Understanding the molecular mechanisms underlying ALT is one of the aims of this study.

1.15 Alternative lengthening of telomeres (ALT)

There are multiple studies that demonstrate the ability of a variety of eukaryotic organisms to maintain telomere length in the absence of telomerase. The yeast *Saccharomyces cerevisiae* undergoes senescence and cell death in the absence of telomerase ((Lundblad and Blackburn, 1993). The authors demonstrated that *est1*$^{-}$ (yeast telomerase homologue) survivors arise as a result of the amplification and acquisition of subtelomeric elements by a large number of telomeres. Even when the primary pathway for telomere replication is defective, an alternative backup pathway can restore telomere function and keep the cell alive. This study uncovered a role of RAD52 in telomere maintenance in the absence of telomerase (Lundblad and Blackburn, 1993). This was also reported to be the case in another yeast strain *Klyveromyces lactis* (McEachern and Blackburn, 1996). The authors found that in the absence of the telomerase RNA gene there was gradual loss of telomeric repeats and the cell growth capability gradually declined. Survivors eventually emerged that displayed lengthened telomeres, often seen to be much longer than wild type telomeres, and this was dependent on the RAD52 gene (McEachern and Blackburn, 1996). The authors concluded that telomeres became uncapped and this allowed telomeres to recombine between themselves and become lengthened.

Through experiments carried out in the *S. cerevisiae* telomerase-negative survivors it was noted that there were two subtypes of cells able to elongate their telomeres, these were termed type I and type II survivors (Lundblad and Blackburn, 1993; Teng and Zakian, 1999). Type I survivors were found to represent the majority of survivors and to display amplified subtelomeric elements followed by telomeric tracts (Lundblad and Blackburn, 1993; Teng and Zakian, 1999). In contrast, type II survivors have longer telomeres made up of amplified yeast telomeric repeats (Teng and Zakian, 1999). Taken together, the above data implies that there is more than one alternative telomere lengthening pathway present in yeast in the absence of telomerase. Teng *et al.* went on to demonstrate that type I survivors needed RAD51 whereas type II survivors needed RAD50 in order to elongate telomeres (Teng et al., 2000). Elongation in type II survivors was RAD51-independent and was inhibited by the telomere binding proteins Rif1 and Rif2 (Teng et al., 2000). The authors also noted that type II telomeres continuously shortened but experienced sudden episodic and dramatic lengthening.

Yeast is not the only eukaryotic organism reported to be able to elongate telomeres in the absence of telomerase. *Drosophila melanogaster* and the mosquito *Anopheles gambiae* have been shown to maintain telomeres in a telomerase-independent manner. Roth *et al.* demonstrated that mosquito telomeres were maintained in a telomerase-independent manner using a transgenic vector inserted at the end of a chromosome. Over a period of 3 years the authors monitored chromosome length and found that chromosome ends had become heterogeneous in length with some being shorter than the initial length and some elongated through the regeneration of part of the integrated plasmid (Roth et al., 1997). *Drosophila* telomeres are also not maintained by telomerase, but by retrotransposition to chromosome ends of three specialized retrotransposons ((Mason and Biessmann, 1995). The above data suggest that telomerase is not the only way to maintain telomeres. There are organisms that arise either through elimination of telomerase or naturally that are able to maintain telomere length in the absence of telomerase. Interestingly a telomerase-independent mechanism has also been reported in mammalian cells (Bryan et al., 1995).

1.15.1 Telomerase-independent telomere maintenance in immortalized human cells

Immortalization of human cells is often associated with reactivation of telomerase. Kim and colleagues developed a highly sensitive assay for measuring telomerase activity; telomere repeat amplification protocol (TRAP) (Kim et al., 1994). They found that telomerase was repressed in normal somatic tissues, but reactivated in cancer. Other studies, using the TRAP assay, demonstrated that there were some *in vitro* immortalized cell lines that did not appear to have detectable telomerase activity (Bryan et al., 1995; Rogan et al., 1995). Bryan *et al.* tested cell lysates from telomerase-negative cell lines to determine if these contained inhibitors of telomerase. They found that telomerase negative cells were not repressing telomerase activity through a specific telomerase inhibitor and that the lack of telomerase detection was not due to lack of sensitivity of the TRAP assay (Bryan et al., 1995).

Terminal repeat fragment (TRF) analysis of these samples revealed a striking telomere length phenotype. Using the enzymes Hinf1 and Rsa1 that digest genomic DNA at points outside, but not within, the TTAGGG repeats, Bryan at al and other groups found that telomerase negative cells had very heterogeneous telomeric smears with the peak of the smears ranging from 10 to 50 kb and this pattern was very different to that observed with telomerase-positive cell lines (Bryan et al., 1995; Henderson et al., 1996). This result was not due to incomplete digestion as a single-locus fingerprinting probe detected the two discrete bands that are expected upon Hinf1 digestion. As all the telomerase-negative cell lines displayed a similar pattern this implies a common mechanism for telomere elongation in these cells (Bryan et al., 1995). This phenomenon was termed alternative lengthening of telomeres (ALT) (Bryan et al., 1997)

In cells that become immortalized and activate ALT during culturing *in vitro*, a temporal correlation between the immortalization event and the occurrence of the characteristic telomere length phenotype has been noticed (Yeager et al., 1999). Using fluorescence in situ hybridization (FISH) Henson *et al.* were able to demonstrate that that the telomere length heterogeneity characteristic of ALT cell populations reflects the heterogeneity seen within individual cells. Within the same cell it was found that some

chromosome ends had no detectable telomeric signal while others had very strong telomere signals (Perrem et al., 2001).

1.15.2 Which immortalized human cells use ALT?

The types of tumours and tumour cell lines in which ALT has been found include osteosarcoma, soft tissue sarcoma, glioblastoma multiforme, renal cell carcinoma, non-small cell carcinoma of the lung, and ovarian carcinoma (Bryan et al., 1997; Mehle et al., 1996; Reddel, 2003; Scheel et al., 2001). ALT has been predominantly found to be activated in tumours of neuroepithelial and mesenchymal origin. The reason for this is still unknown. However, it has been suggested to be because these cells are able to regulate telomerase activity more tightly than epithelial cells and therefore have a higher relative probability of activating ALT. The activation of ALT has been associated with cells that have complex karyotypes, which could be either a cause or a result of the activation of ALT. Not all soft tissue sarcomas with complex karyotypes have been found to activate ALT, suggesting that the observed chromosomal instability is not soley due to ALT but requires the contribution of other factors (Henson et al., 2005; Ulaner et al., 2004). Bryan *et al.* found that the fibroblast cell line derived from a Li-Fraumeni patient that either underwent spontaneous immortalization or was transfected with SV40 or HPV-16 was telomerase negative and maintained telomeres through ALT (Bryan et al., 1995). The above data suggested that immortalized fibroblasts are more likely to activate ALT, especially if they have been transformed by SV40. However, fibroblasts transduced with HPV genes or chemical carcinogens can also use ALT.

1.15.3 The significance of ALT in human tumours

All immortalized cell lines tested to date have been found to have either telomerase activity or display a telomere length pattern characteristic of ALT. For human tumours the situation is more complex. It has been reported that approximately 85% of all human tumours have detectable telomerase activity (Shay and Bacchetti, 1997). However, it is not possible to say that the remaining 15% of tumours is ALT positive as

an extensive survey to determine the prevalence of ALT is yet to be done. Table 4 illustrates some tumours in which telomerase and ALT activity has been assessed. Also important to remember is that it is not known whether activation of telomere maintenance mechanisms and immortalization are necessary for all tumours. Another fact that renders the specific distinction of ALT and telomerase positive tumours difficult is that both mechanisms have been reported to occur in the same tumour (Bryan et al., 1997). Also it is possible to induce the expression of telomerase in GM847 ALT-positive cells, causing the lengthening of the shortest telomeres (Perrem et al., 2001). However, some of the hallmarks of ALT were still present. Thus exogenous expression of hTERT did not inhibit ALT, suggesting that the two mechanisms can occur at the same time within a given cell. In contrast, when GM847 cells were fused with two different telomerase-positive tumour cell lines, the ALT phenotype was repressed. The authors came to the conclusion that telomerase-positive cells contain an ALT-repressing factor, but this was not telomerase (Perrem et al., 2001). However, it is as yet unclear whether the two mechanisms exist within the same cell within a given tumour or whether there are different subpopulations of cells that have activated the different mechanisms separately. A study by Hakin-Smith on glioblastoma multiforme patient samples found that a patient that had a telomerase-positive tumour then had an ALT-positive recurrent tumour, supporting the latter hypothesis (Hakin-Smith et al., 2003). It is also interesting to note that in this study it was clear that those patients with ALT-positive tumours had a longer median survival than those that had telomerase positive tumours. For this reason the authors concluded that ALT could be a prognostic indicator for patients with glioblastoma multiforme.

ALT may be more common in tumours derived from mesenchymal tissues due to the higher occurrence of ALT in immortalized cell lines of fibroblastic origin compared with tumour derived cell lines (Perrem et al., 2001). Mesenchymal tissues have been found to have slower cell turnover and less telomere attrition in comparison to many epithelia. It is therefore possible that cells derived from these tissues are able to repress telomerase activity more readily, thus increasing the probability of ALT activation (Henson et al., 2002). Li-Fraumani syndrome immortal cells and tumours appear to activate ALT frequently (Bryan et al., 1997). The reason behind this is still unclear but could be due to the loss of p53. Buchhop and colleagues demonstrated that p53 interacts

with RAD51 and a study by Bertrand *et al.* demonstrated that, in the absence of p53, homologous recombination is increased (Bertrand et al., 1997; Buchhop et al., 1997). These data imply that the inactivation of p53 could be an important factor in the activation of ALT in cells of a specific origin.

Table 1.4

Tumours tested for the presence of both telomerase and ALT activation

Tumour Type	**Number of Samples**	**Number of telomerase negative (%)**	**Number with abnormally long TRFs: Telomerase negative**	**Number with abnormally long TRFs: Telomerase positive**
Melanoma	9	1(11)	0	1
Osteosarcoma	6	5(83)	1	0
Breast carcinoma	14	4(29)	1	0
Ovarian carcinoma	15	2(13)	0	2
Lung carcinoma	7	1(14)	0	0
Adrenocortical carcinoma	6	5(83)	2	0
Total	**57**	**18(31)**	**4**	**3**

1.15.4 Morphological markers of ALT: the ALT–associated PML nuclear body

Structures seen in a normal interphase nucleus include nucleoli, coiled bodies, and PML nuclear bodies. As described previously (Section 1.3 and 1.4), the PML-NB is a doughnut-shaped nuclear structure to which multiple proteins localize. The precise function of these bodies has yet to be defined; however, there have been reports implying a role for these nuclear structures in tumour suppression and a direct role in apoptosis (Quignon et al., 1998; Salomoni and Pandolfi, 2002; Wang et al., 1998b). Yeager *et al.* described a novel PML body present in 1-5% of interphase nuclei of ALT-positive cells and not telomerase-positive or normal cells (Yeager et al., 1999). These structures were termed the ALT-associated PML body (APB). The composition of APBs is significantly different to that of PML-NBs. APBs are unique due to the presence of TTAGGG repeat sequences, telomere binding proteins TRF1 and TRF2, PML, replication factor A, homologous recombination gene products RAD51 and RAD52, components of the MRN complex, the 911 DNA clamp complex, RAD17 the

clamp loader, phosphorylated histone H2AX (γ-H2AX) and the telomere associated protein Rap1 (Nabetani et al., 2004; Wu et al., 2003; Wu et al., 2000; Yeager et al., 1999). In addition APBs have also been demonstrated to contain proteins found in PML-NBs, such as BLM and Sp100 (Jiang et al., 2005; Naka et al., 2002). APBs can be detected by immunostaining cells with antibodies against proteins that colocalize to these structures, such as TRF1 and TRF2, in conjunction with PML (Yeager et al., 1999) Additionally, FISH with a peptide nucleic acid (PNA) probe against telomeric repeats can be used to reveal telomeric DNA associated with APBs. It has become evident that these structures are specific to ALT-positive cells, since other cell types examined show no evidence of such aggregates and display diffuse nuclear staining (Yeager et al., 1999). APBs were also detected in ALT tumour tissue suggesting that they are not an artefact of in vitro culturing. A nude mouse tumour model based on injection of EJ-ras (containing the activated c-Ha-ras oncogene from the EJ bladder carcinoma cell line) transformed ALT fibroblasts clearly showed that APBs are indeed present in tumours in vivo. Similarly, APBs are found in tissue section from an ALT breast carcinoma patient sample (Yeager et al., 1999).

The role of APBs in ALT is not clear. However, it is being investigated by many groups including ours. What has been taken into account is the composition of these bodies. The fact that telomere binding proteins and DNA damage repair proteins localize to these structures may be of relevance to the ALT mechanism. Multiple reports have implied that the presence of APBs is required for the ALT mechanism. Overexpression of Sp100, a constituent of the PML-NB, has been found to suppress APB formation through the sequestration of the MRN complex. NBS1 has been found to be vital for the correct assembly of APBs by recruiting MRE11, Rad50 and BRCA1 and this is dependent on its interaction with Sp100 (Naka et al., 2002; Wu et al., 2003) This correlates with ALT repression as determined by the rate of progressive telomere shortening which is found to be comparable to telomerase negative normal cells (Jiang et al., 2005). A recent paper by Blanco and colleagues found that the overexpression of the APB component TRF2 in a telomerase-negative mouse resulted in increased features of ALT at late generations including the appearance of APBs (Blanco et al., 2007). Despite recent advances, the precise function of these nuclear structures in this pathway remains unclear.

A topic of debate is whether or not the detection of APBs coincides with a particular stage of the cell cycle, consistent with the observation that APBs are only present in a proportion of cells, or whether APB positive cells are those that have permanently ceased to divide or are programmed to die. Indeed, a few reports have suggested that APBs are associated with various stages of the cell cycle. Grobelny *et al.* demonstrated that the percentage of APB-positive cells increased when cultures were enriched for cells in G2/M phase of the cell cycle (Grobelny et al., 2000). Another study by Wu and colleagues suggest that specific components of APBs are translocated to these structures in a cell cycle-dependent manner. The authors conclude that the translocation of NBS1 to APBs occurs specifically during late S to G2 phases of the cell cycle and coincides with active DNA synthesis in these structures (Wu et al., 2000). Interestingly a study by the same group also revealed that NBS1 plays a vital role in the assembly of APBs (Wu et al., 2003). It is possible that, depending on the component of APBs that is used to identify these structures, different results are obtained due to the dynamics of the associated proteins. A more recent report has demonstrated that reversible cell cycle arrest in G0/G1 by methionine restriction resulted in the appearance of APBs in most cells within an ALT positive population (Jiang et al., 2007). However, it is not clear whether it is the block in a specific stage of the cell cycle or it is an effect of the restriction that causes this increase in APB formation. Although the above mentioned studies suggest that APBs are present at specific phases of cell cycle, more work needs to be done to determine the functional implication of this association.

The earliest methods of detection of ALT were through terminal repeat fragment (TRF) Southern analysis or TRAP. As APBs have been found only in a small percentage of cells it is not the best morphological marker for the detection of ALT and has only been used to detect ALT in archival tumour material in paraffin sections (Yeager et al., 1999). This has proven to be a good screening method for large samples of tumours and, in future, will allow clinical correlations to be made between tumour type and telomere maintenance mechanisms. Once made apparent which tumours activate ALT over telomerase, it will make determining the choice of anticancer therapy either directed against telomerase inhibition or disruption of ALT, more efficient.

1.15.5 Molecular details of ALT in human cells

Several studies have proposed that the ALT mechanism is likely to involve recombination-mediated DNA replication. *Saccharomyces cerevisiae* cells that survive in the absence of telomerase require the RAD52 gene, which encodes a protein required for DNA recombination, to be functional (Lundblad and Blackburn, 1993). The type II yeast survivors are those that most closely resemble the ALT phenotype in human cells, and they require functional RAD50, a member of the MRN complex implicated in DNA recombination (Teng and Zakian, 1999). Individual telomeres in ALT cells undergo cycles of shortening and sudden lengthening in a way that is indicative of recombination (Murnane et al., 1994). There have been multiple investigations into the genomic stability of ALT cells. Sister chromatid exchange (SCE) was reported to occur at high frequencies in ALT cells compared to non-ALT cells (Londono-Vallejo et al., 2004). However, the overall frequency of homologous recombination did not differ between ALT and telomerase-positive cells (Bechter et al., 2003) implying that there is not a global increase in recombination. Interestingly, a recent study has shown that a specific minisatellite (MS32) was highly unstable in some ALT cell lines, but not in telomerase positive cells lines (Jeyapalan et al., 2005). MS32 instability was also demonstrated in a subset of ALT-positive soft tissue sarcomas. In contrast, other examined minisatellites were not found to be unstable in ALT tumours despite being highly recombinogenic in the germline.(Jeyapalan et al., 2005).

Recent evidence supports the belief that post-replicative telomeric exchanges occur in ALT cells with a higher frequency than telomerase positive cells (Londono-Vallejo et al., 2004) (Bechter et al., 2003). It could be argued that ALT cells have a higher probability of recombination due to the extreme length of some of the telomeres. However this does not appear to be a reason, as telomerase-positive cells with very long telomeres did not display any increase in recombination compared to mortal cells (Londono-Vallejo et al., 2004). The evidence suggests that telomeric recombination is a specific feature of ALT. This could be due to the recruitment of proteins involved in recombination to telomere ends. It is important to note that the method used to detect telomeric SCEs (t-SCEs) is not able to detect whether the exchanges involved sister chromatids, other telomeres or extrachromosomal DNA. It is also likely that there is more than one source of telomeric exchange.

An explanation for the rapid elongation and attrition of telomeres in ALT cells has recently been proposed (Bailey et al., 2004). Prior to mitosis homologous recombination occurs between symmetrically paired chromosomes or sister chromatids resulting in the exchange of equal amounts of DNA. Because telomeres are repetitive sequences of DNA, sister chromatids can find sites of homology along the length of the telomere. If alignment were to occur asymmetrically, this would result in the net gain of telomeric sequences for one chromatid and the net loss for the other. The daughter cell that ends up with the short telomere would eventually senesce and die, leaving the other cell with the long telomeres and extended proliferation potential. If this were to occur with a specific frequency within a given population it would effectively become immortal (reviewed in (Muntoni and Reddel, 2005). This is an intriguing hypothesis that will have to be tested experimentally in the future.

1.16 ALT and extrachromosomal repeats

Genetic data from *K. lactis* suggests that the maintenance of telomeric DNA in survivors is mediated by a roll and spread mechanism in which small extrachromosomal telomeric repeat (ECTR) circles are used as a template for rolling circle replication (Natarajan and McEachern, 2002). This creates long tracts of telomeric DNA that can be incorporated into telomeres through homologous recombination and in doing so increase their length. A study by Cesare and Griffith demonstrated that ECTR circles were present in ALT cell lines, but not telomerase-positive cells such as HeLa, or telomerase-negative primary human fibroblasts (Cesare and Griffith, 2004). This suggested that the ETCR circles were a specific feature of ALT. The authors came to the conclusion that human ALT cells may maintain their telomeric DNA in a similar way to *K. lactis*, using the roll-and-spread mechanism.

The evidence presented in the above section indicates that ALT is a recombination-based mechanism. However the exact method used to elongate telomeres is still an area of great debate and more research needs to be done in order to gain a clearer picture of the exact molecular mechanism(s) of ALT. Furthermore, another unanswered question is whether the APB is required for recombination.

1.17 Controlling the ALT mechanism

Multiple studies have been carried out to identify ALT repressors. One such used the GM847 ALT cell line in somatic cell hybrids. These cells were fused with normal cells to suppress the immortal phenotype. The clones that resulted from these fusions showed rapid loss of telomere tracts associated with the repression of ALT and cells underwent senescence (Perrem et al., 2001). Another study that resulted in the suppression of ALT was recently published by Jiang and colleagues (Jiang et al., 2005). The authors transfected ALT cells with a YFP-Sp100 construct and found that the formation of APBs was suppressed in cells that expressed high levels of this fusion protein. The stable expression of this construct resulted in the progressive shortening of telomeres over a number of population doublings and that the characteristic telomere length fluctuation of ALT was inhibited. Analysis of clones stably expressing the Sp100 construct revealed that the suppression of ALT occurred through the sequestration of the MRN complex by the full length Sp100 protein. This study identified a potential player in the suppression of ALT (Jiang et al., 2005).

In contrast, a recent report by Blanco and colleagues demonstrated that ALT can be induced upon the overexpression of the telomere binding protein TRF2 in mice deficient for telomerase (Blanco et al., 2007). The authors found that the overexpression of TRF2 caused telomere shortening and end-to-end fusions that were all increased in the absence of telomerase. Extrachromosomal telomeres, interstitial telomeres and multitelomeric signals were also observed. Extrachromosomal telomeres have been associated with the onset of ALT (Muntoni and Reddel, 2005). It was also noted that keratinocytes from mice overexpressing TRF2 displayed a significant increase in the percentage of cells with APBs than control cells. The authors concluded that the overexpression of TRF2 resulted in increased features of ALT which could act to maintain telomere lengths in the absence of telomerase.

The above reports have demonstrated that ALT is a recessive phenotype that can be inhibited through the sequestration of DNA repair proteins found in APBs or activated through the overexpression of TRF2, the telomere capping protein.

Although, our understanding of the mechanisms behind ALT is increasing, further studies need to be carried out in order to gain a more complete picture of the essential players involved in ALT. This is one of the main aims of this study.

1.18Aims of the Project

The purpose of this study was to investigate the role of PML and TRF2 in APB formation and telomere maintenance. The effect of the absence of PML and TRF2 on APB formation was analysed through the use of siRNA. Localization of other APB components was analyzed by immunofluorescence. Due to the transient nature of this method, clones stably downregulating either PML or TRF2 were obtained through the use of shRNA. This enabled us to study the long term effects of TRF2 and PML depletion on APB formation, cell cycle and morphology, and telomere length. Telomere length was assessed by pulse fieled gel electrophoresis and mean telomere lengths were obtained through densitometric analysis with Telomertrics program.

The Production of clones stably downregulating TRF2 allowed study of ALT cell response to telomere uncapping. The effect of TRF2 downregulation on the DNA damage response was investigated.

Chapter 2) Materials and Methods

This chapter describes the general materials and methods used throughout these studies. More specific methods and experimental protocols can be found in individual chapters.

2.1 Cell Culture

Cell culture procedures were carried out aseptically in a class II laminar flow cabinet. Cells were maintained in a Heraeus CO_2 Auto-Zero incubator at 37°C with 5% CO_2. The human cell lines used in these studies were: SAOS-2 and U2OS osteosarcoma cell lines purchased from American Type Culture Collection (ATCC). These cell lines were maintained in Dulbecco's Modified Eagle's Medium (DMEM) (Gibco) supplemented with 10% (v/v) heat inactivated fetal bovine serum (FBS) and 100 U/ml penicillin and 100 μ/ml streptomycin (Sigma). IIICF/A2 spontaneously immortalised cells derived from a Li-Fraumeni patient were a kind gift from Dr Roger Reddel (Children's Medical Research Institute, University of Sydney). These cells were grown in RPMI 1640 (Gibco) supplemented with 20% (v/v) heat inactivated FBS, 2mM glutamax (L-glutathione) (Sigma) and 100 U/ml penicillin and 100 μ/ml streptomycin (Sigma). JFCF6-T.1J/11E and JFCF6-T.1J/11C SV40 immortalized subclones of JFCF jejunal fibrablosts were also donated by Dr Roger Reddel. These fibroblasts were maintained in low glucose DMEM (Gibco) supplemented with 15% (v/v) heat inactivated FBS and 100 U/ml penicillin and 100 μ/ml streptomycin (Sigma). SUSM-1 carcinogen transformed liver fibroblasts and GM847 SV40 transformed skin fibroblasts from Lesch-Nyhan syndrome, were obtained from ATCC. WI38 VA13/2RA SV40 transformed lung fibroblasts were a gift from Dr. Nicola Royle (Department of Genetics, Leicester University). The above mentioned cells were maintained in Modified Eagle's Medium (MEM) supplemented with 15% (v/v) heat inactivated FBS, 1% (v/v) Non- Essential Amino Acids (NEAA) (Gibco) and 100 U/ml penicillin and 100 μ/ml streptomycin (Sigma). HeLa human cervical carcinoma cell line and MCF7 human breast adenocarcinoma cell line were obtained from ATCC and grown in DMEM (Gibco) supplemented with 10% (v/v) heat inactivated FBS and 100 U/ml penicillin and 100 μ/ml streptomycin (Sigma). BJ primary human foreskin fibroblasts were obtained from ATCC and maintained in DMEM (Gibco) supplemented with 10% (v/v) heat inactivated FBS and 100 U/ml penicillin and 100 μ/ml streptomycin (Sigma).

Cells were passaged routinely before they reached confluence, to maintain a logarithmic growth. The cells were routinely frozen in liquid nitrogen during culture to ensure stocks of all passages. To detach and subculture cells they were washed with warm sterile phosphate buffer saline (PBS, Sigma) and detached with a solution of 10X trypsin/EDTA (Sigma). The trypsin activity was stopped by adding double the volume of medium. After centrifugation at 1200 rpm for 5 minutes, cells were resuspended in the appropriate medium, counted with a haemocytometer and seeded at the desired density.

2.1.1 Long term storage of cells

To generate and maintain batches of cells, exponentially growing cells were washed twice with PBS and centrifuged at 1200 rpm for 5 minutes at room temperature. The cell pellet was resuspended in freezing medium (50% (v/v) FBS, 10% (v/v) DMSO and 40% (v/v) DMEM) to a desired density of cells/ml. Aliquots of 1 ml were placed in cryogenic boxes at -80°C for a week and then immersed in liquid nitrogen. Cells were recovered from the cell bank by rapid thawing to 37°C in a water bath, and then instantly resuspended in the appropriate culture medium and transferred to a tissue culture flask.

2.2 Small interfering RNA transfection (siRNA)

RNA interference (RNAi) is the name given to the process in which double stranded RNA (dsRNA) directs sequence-specific degradation of messenger RNA in both animal and plant cells. In mammalian cells, RNAi can be triggered by 21-nucleotide duplexes of small interfering RNA (siRNA). There have been a number of theories regarding the mechanism of gene silencing as a result of RNA interference. The most accepted model involves two stages: 1) an initiation step and 2) an effector step. The initiation step consists of the introduction of long double-stranded RNA molecules into the cell (via injection, electroporation, lipofection, etc.). The double-stranded RNA (dsRNA) is then cleaved into short RNA duplexes (21-23 nucleotides) by the DICER enzyme (RNase III family of dsRNA-specific ribonucleases) (Fig 2.2) (Agrawal et al., 2003; Hannon, 2002). In some cases, the dsRNA may induce a non-specific interferon response

resulting in non-specific gene silencing. To prevent or minimize this non-specific response, small interfering RNAs (siRNAs) can be injected directly into the cell. During the effector step, siRNA molecules and cellular proteins combine to form the RNA Induced Silencing Complex (RISC). The RISC is believed to target and destroy mRNA transcripts by complementary base pairing with the siRNA molecule and subsequent denaturation (via ATP-dependant helicase) thus activating the RISC complex. Once the RISC is activated, the antisense strand of the siRNA directs the RISC to the target mRNA through complementary base-pairing. RISC cuts the complex approximately in the middle of the region paired with the antisense RNA. This cleavage destroys the transcript and thus leads to silencing of the target gene (Fig 2.2) (Agrawal et al., 2003; Fuchs et al., 2004; Hammond et al., 2000; Hannon, 2002).

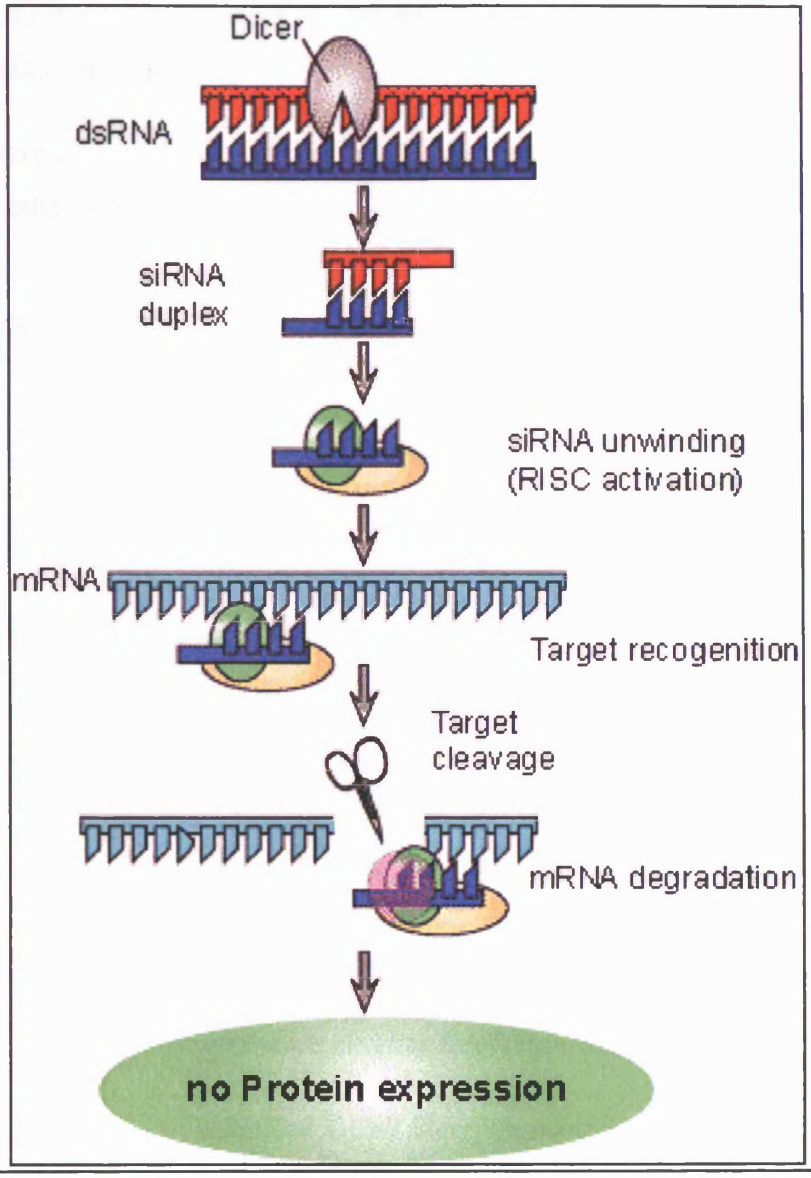

Figure 2.1 Simplified schematic representation of the proposed RNAi interference mechanism. dsRNA processing proteins (RNase III-like enzymes) bind to and cleave dsRNA into siRNA. The siRNA is then incorporated into a multicomponent nuclease complex, the RNA-induced silencing complex (RISC). The RISC complex then recognizes the target mRNA and is cleaved in the centre of the region complementary to the siRNA and quickly degraded.

2.2.1 Short interfering RNA Transfection

Introduction of double stranded RNA has proven to be a powerful tool for gene suppression. This, however, is known to provoke strong cytotoxic responses in mammalian cells. These can be avoided through the use of synthetic, 21 to 22

nucleotide, short interfering RNAs (siRNAs) that are capable of specific and strong gene expression suppression.

All oligos were ordered from Ambion in a 2'-deprotected, annealed and desalted duplex form unless otherwise stated.

2.2.2 Reagents and Buffers

P-ALL: CGCCAGCCCAGAAGAGGAAtt (sense)

UUCCUCUUCUGGGCUGGCGtt (antisense)

TRF2: GAGGAUGAACUGUUUCAAGtt (sense)

CUUGAAACAGUUCAUCCUCtt (antisense)

Scrambled oligo

OptiMEM serum-free medium (Invitrogen)

Phosphate Buffered Saline (PBS) (Sigma)

2mm electroporation cuvettes (Molecular Bioproducts)

BioRad X-Cell Electroporator

Trypan Blue (Sigma)

2.2.3 Protocol

Oligos were resuspended in RNase free water to a stock concentration of 40 μM and 50 μM for control scrambled oligos and stored in aliquots at -20°C. Cells were plated in T175 tissue culture flasks (NUNC) three days before. Cells were washed twice in PBS, trypsinised and haversted. After centrifugation at 1200 rpm for 5 minutes, cells were resuspended in the appropriate medium, counted with a haemocytometer and spun again for a further 5 minutes. Cells were washed twice in OptiMEM and then resuspended to a density of two million cells/ml. Eight million cells were removed and spun at 1200

rpm for 5 minutes. Supernatant was carefully aspirated to leave the cell pellet that was then resuspended in 100 µl OptiMEM. The oligos were then carefully added and the suspension was gently mixed, transferred into 2 mm electroporation cuvettes and left on ice for 5 minutes. Cells were electroporated at 160 V using an exponentially decaying pulse and then placed on ice for a further 5 minutes. Electroporated cells were then transferred to a Falcon tube containing the correct medium and cell viability was determined following electroporation using the trypan blue exclusion assay. Three hundred thousand cells were seeded in 6cm dishes for Western blot and one hundred and fifty thousand cells were seeded on glass coverslips in 6 well dishes for immunofluorescence. Pellets were collected and cells were fixed 48 and 72 hours post transfection.

2.3 Short Hairpin RNA interference

As previously described, the use of double stranded RNA to suppress gene expression has become a very powerful tool. To avoid cytotoxic effects siRNA synthetic oligos are used. However, the reduction in gene expression is only transient thus severely restricting its applications. This limitation has been overcome with the use of the pSUPER RNAi system, which provides a mammalian expression vector that directs intracellular synthesis of siRNA-like transcripts. The vector uses the polymerase-III H1-RNA promoter to produce a small RNA transcript lacking a poly adenosine tail and has a well defined start and stop signal. This system has been used for efficient and specific down-regulation of gene expression resulting in functional inactivation of target genes. This vector system allows stable and persistent suppression of gene expression thus allowing the analysis of loss of function phenotypes that develop over time.

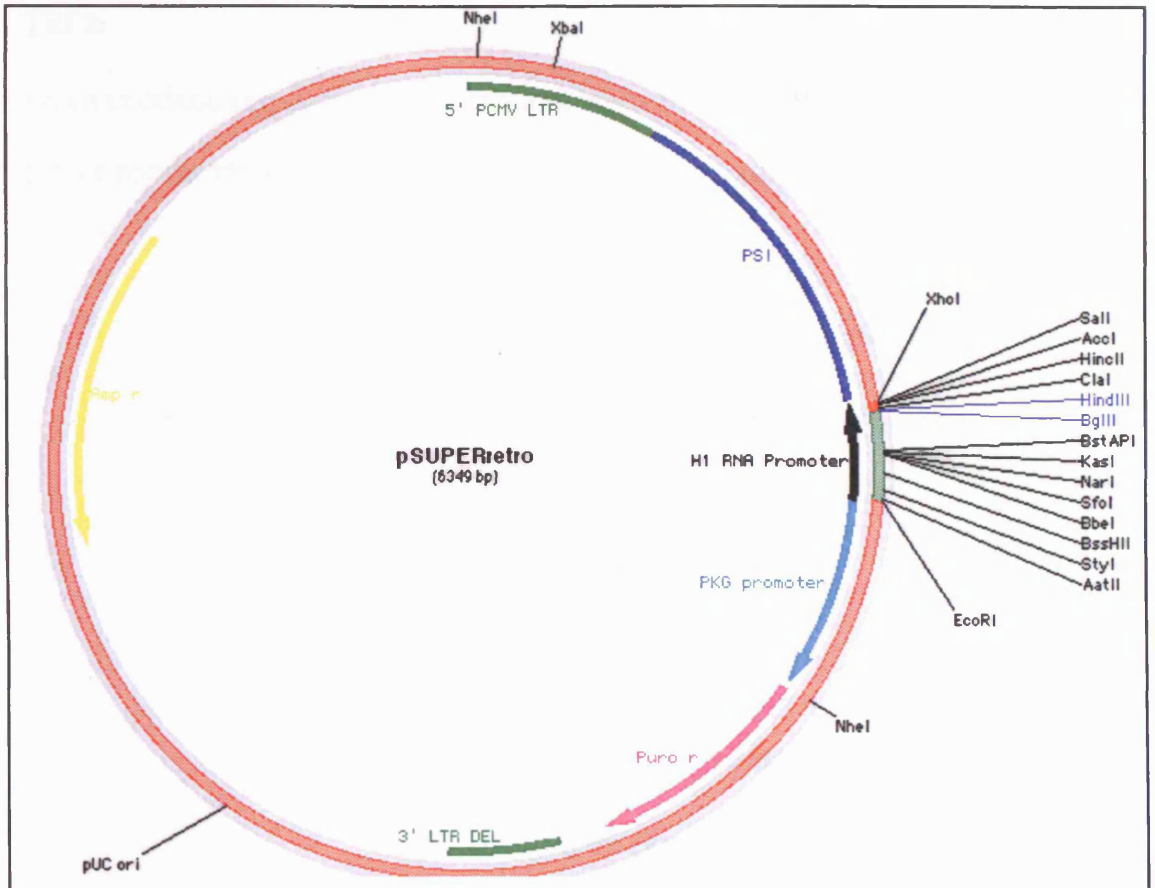

Figure 2.2 6349bp circular plasmid for cell transformation. List of enzymes present within the multi-cloning site are reported on the right side of the plasmid with the two used for shRNA cloning highlighted in blue.

2.3.1 Buffers and Reagents

pSUPER.retro vector (oligoengine)

PML EXOII:

5'GATCCCC**GGAGGATTCCAGTTTCTG**TTCAAGAGA**CAGAAACTGGAACTCCTCC**TTTTT3'

3'GGG**CCTCCTAAGGTCAAAGAC**AAGTTCTCT**GTCTTTGACCTTGAGGAGG**AAAAATTCGA5'

P-ALL:

5'GATCCCC**CGCCAGCCCAGAAGAGGAA**TTCAAGAGA**TTCCTCTTCTGGGCTGGCG**TTTTT3'

3'GGG**GCGGTCGGGTCTTCTCCTT**AAGTTCTCT**AAGGAGAAGACCCGACCGC**AAAAATTCGA5'

TRF2:

5'GATCCCC**GAGGATGAACTGTTTCAAG**TTCAAGAGA**CTTGAAACAGTTCATCCTC**TTTTT3'

3'GGG**CTCCTACTTGACAAAGTTC**AAGTTCTCT**GAACTTTGTCAAGTAGGAG**AAAAATTCGA5'

Polynucleotide Kinase (PNK) (New England Biolabs)

10X TNE buffer (100mM Tris; 2.0M NaCl; 10mM EDTA; pH7.4)

Hind III enzyme (Roche)

Bgl II enzyme (Roche)

Buffer B (Roche)

Alkaline Phosphatase (New England Bioloabs)

T4 DNA Ligase (Roche)

DH5α Bacterial competent cells

Luria Broth (LB)

Luria Broth Agar

Ampicillin

2.3.2 Production of the pSUPER.retro constructs

The shRNAs were designed based on the oligoengine design tool. The 19 nucleotide target sequences that were used and validated by siRNA were used as templates (2.211). The sense and antisense strands were ordered from Ambion. These were resuspended to a concentration of 1μg/μl and were phosphorylated using PNK at 37°C for 30 minutes. 10X TNE buffer was added and the final volume brought to 200μl and

boiled at 95°C for 5 minutes. The block was then removed from the heat and allowed to cool gradually and the oligos to anneal.

The pSUPER.retro vector was linearized using HindIII and BglII. After digestion, the plasmid was treated with shrimp alkaline phosphatase at 37°C for 30 minutes to remove the 5' phosphates and to reduce the probability of the plasmid to recircularise without insert. The linearized vector was run on an agarose gel and purified using the Quiagen gel purification kit. The purified linearized host plasmid was ligated with the annealed oligos in 10 microliters of a solution containing 1U of T4 DNA ligase (Promega) and 1X ligase buffer (30 mM Tris-HCl, pH 7.8, 10 mM $MgCl_2$, 10 mM DTT and 1 mM ATP, supplied with the ligase) over night at 16°C. A five microliter volume of this solution was then used to transform competent bacteria.

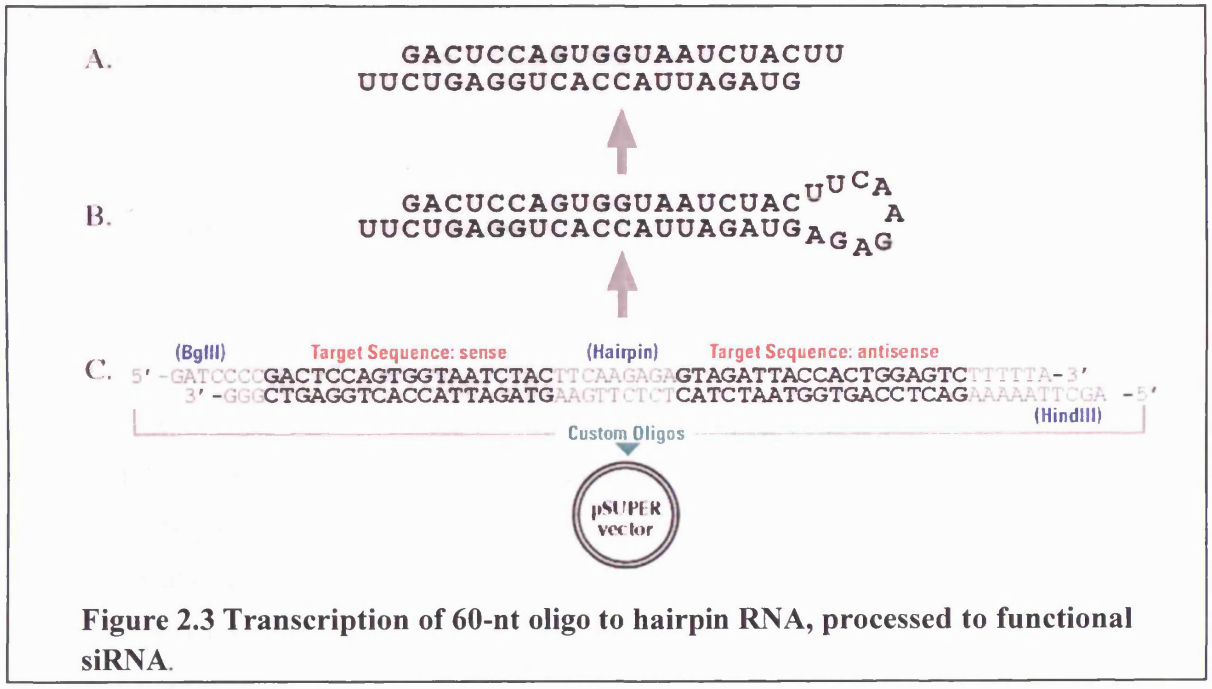

Figure 2.3 Transcription of 60-nt oligo to hairpin RNA, processed to functional siRNA.

DH5α competent bacterial cells were used to transform the pSUPER.retro constructs. Cells were defrosted on ice and then the ligation added. The cells were left on ice for 30 minutes and then heat shocked before being left a further 2 minutes on ice. 900 µl volume of LB medium (without antibiotic) was added, and the tube was placed into a heated shaking incubator (37°C, 220 rpm, 1.5 h) before being plated on ampicillin agar

plates and allowed to grow over night at 37°C. Each colony, representing ampicillin-resistant/transformed growing bacterial cells, was picked with a sterile disposable loop, resuspended in a 50 ml falcon tube containing 5 ml of liquid LB medium supplemented with ampicillin (50 μg/ml final concentration), and allowed to grow over night (37°C, 220 rpm shaking).

2.4 Purification of DNA from bacteria by miniprep

Plasmid DNA was purified from bacterial suspension using the miniprep system (Qiagen). The procedure, starting from 2 ml of bacterial suspension, was exactly as described by the manufacturer. The recovered DNA, in 50 μl of water, was subjected to restriction digestion with appropriate restriction enzymes to verify that the insert was indeed present in the colony isolated. After digestion and separation by electrophoresis on an agarose gel, the fragments of DNA were visualized by using an UV transilluminator. The positive colonies were in turn used to inoculate larger bacterial preparations.

2.4.1 Large scale preparation of plasmid by maxiprep

To obtain sufficient DNA to transfect cells, a maxi prep purification was set up. Using a sterile tip, 100 μl of bacterial suspension obtained from the mini prep were added to 250 ml of liquid LB containing 50 μg/ml ampicillin (contained in a 500 ml conical tube), and allowed to grow at 37°C in a shaking incubator at 220 rpm over night. Bacterial cells were then pelleted by a 30 min centrifugation at 9000 rpm at 4°C. After removal of LB medium, plasmid DNA was purified with the Qiagen Plasmid Maxi Kit (Qiagen) according to the manufacturer's instructions. The DNA recovered from the maxi preparation was quantified using a spectrophotometer, by reading the absorbance at 260 nm and 280 nm. The quality of the DNA prepared was determined by the ratio between 260 nm and 280 nm absorbances, which should be 1.8.

2.5 Tansfection of pSUPER.retro constructs.

2.5.1 Cell preparation for transfection

One day prior to transfection, cells were plated in 10 cm tissue culture dishes such that they were logarithmically growing on the day of transfection (i.e. 50-60% confluent at the time of transfection.

2.5.2 Calcium phosphate precipitate

Calcium phosphate precipitation is a widely used transfection method due to its efficiency of transfection in many cell types, especially highly transformed adherent cells. The necessary components are easy to make and the procedure is easy and relatively non toxic. This method is efficient for the generation of stable cell lines.

2.5.3 Buffers and reagents

$CaCl_2$ 1M

HBS 2X

Hepes pH7.1 50mM
NaCl 300mM
Na2HPO4 1.5mM

2.5.4 Procedure

18 µg DNA (pSUPER.retro constructs) was dissolved in 250 µl of 1 M $CaCl_2$ and 750 µl sterile water in a sterile 15 ml falcon tube to give a final concentration of 125mM $CaCl_2$. In a different sterile tube, 1 ml of HBS 2X was added. The HBS solution was gently vortexed and the DNA-$CaCl_2$ solution was added drop-wise. When all the DNA had been added, the tube was kept at room temperature for 30 minutes. The solution was then added drop wise to the cells seeded in a 10 cm dish and incubated 16 hours at 37°C. The cells with the DNA-$CaPO_4$ solution were then visualized under the

microscope to verify the presence of small precipitates of $CaPO_4$ on all the surface of the flask. Once this was verified, the medium was removed and the cells extensively washed with PBS. After washing, the cells were incubated in complete medium.

2.6 Isolation of cell clones stably expressing the gene of interest

When clones of cells stably expressing the gene of interest were to be recovered, 48 hours after the end of transfection the medium was removed and the cells detached with trypsin EDTA solution. Cells were replated into larger 15cm tissue culture dishes in complete medium containing 1μg/μl of puromycin (Sigma). At these antibiotic concentrations parental cells are killed and the only cells growing are likely to be those which have integrated the transfected plasmid in their DNA. The plates were then kept at 37 °C and the medium renewed regularly. When colonies were formed, they were visualized under the microscope and isolated from the plate by using 3mm diameter sterile paper cloning discs (Sigma) which were soaked in trypsin. Before isolation cells were washed thouroughly with sterile PBS. The soaked discs were then placed over the selected colonies left for a minute. The removed discs were placed in 96 well dish in medium containing 0.5μg/μl of puromycin. The plates were incubated at 37 °C for a few days before removing the discs from the wells and allowing cells to grow. The different clones picked from the original plates were grown and passaged until they were enough to plate 300,000 in a 6cm dish for Western blot analysis, to confirm the presence of the plasimid, and for some to be frozen in liquid nitrogen. The clones demonstrating down-regulation of the gene of interest are then expanded and stored in different aliquots in liquid nitrogen.

2.6.1 Colony Forming Assay

Cells were seeded in 10cm dishes and transfected as described above. Forty-eight hours after transfection medium was changed and 1μg/μl of puromycin was added to the fresh medium. Cells were monitored for one week and then colony formation was determined by crystal violet staining. Crystal violet is a cationic dye that binds DNA and is soluble in ethanol. This dye allows visualization of cells that remain attached to the plate and therefore enables colony counting and cell viability to be determined. Plates were

placed on ice and washed twice with ice-cold 1X PBS. Cells were then fixed with ice-cold methanol (stored at –20°C) for 10 minutes. Methanol was aspirated from the plates, and 0.5% crystal violet solution (made in 25% methanol and stored at room temperature) was added to cover bottom of plate and incubated at room temperature for 10 minutes. The crystal violet solution was poured off into a beaker and the plates were carefully rinsed ddH_20 until no color came off in the rinse. Plates were left to air dry at room temperature and colony formation was determined by eye.

2.7 Southern blot analysis

Briefly, DNA molecules are transferred from an agarose gel onto a nitrocellulose membrane. Southern blotting is designed to locate a particular sequence of DNA within a complex mixture. Telomeres in ALT cells range in size form 200bp to 30kb making visualising them difficult by continuous field electrophoresis. This is due to DNA fragments above 30kb migrating with the same mobility and appearing as a single large diffuse band. To overcome this problem we used clamped homogeneous electric field (CHEF) electrophoresis. This forces the DNA to change direction during electrophoresis allowing different sized fragments within this diffuse band to separate from each other. With each reorientation of the electric field relative to the gel, smaller sized DNA changes direction more quickly than the larger DNA, causing the larger fragments to lag behind and providing better separation of DNA.

The CHEF technique takes into account important variables such as the electric field and the reorientation angle. The electric field is homogenous and the direction is altered by electronically changing the polarity of the electrodes that are organized as shown in Figure 2.7. The reorientation angle is important as this is what controls the separation and the resolution. Increasing the separation range and the resolution of large DNA requires smaller reorientation angles, generally 96-140°, with 120° most common. The smaller angles increase the mobility of the DNA without seriously affecting resolution. The lower limit is approximately 96°. Below this, separation is seriously compromised.

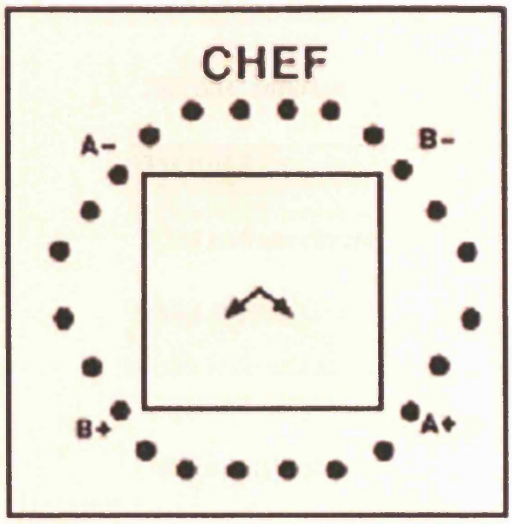

Figure 2.4 Schematic representation of a CHEF tank. This cartoon demonstrates the layout of the electrodes (A-, A+ and B-, B+) with respect to the gel (square in the middle). THE central arrows represent the constantly changing polarity of the electrodes.

2.7.1 DNA extraction

All DNA extractions were carried out in Phase Lock tubes from Eppendorf. These were used according to the manufacturers instructions.

2.7.2 Buffers and Reagents

2X Lysis buffer
100mM Tris HCl pH 7.5
100mM NaCl
10mM EDTA
1% Sarkosyl

20X SSC solution

3M NaCl

0.3M sodium citrate

1mM EDTA.

RNase (10mg/ml)

Proteinase K (20mg/ml)

Phenol/chloroform/isoamylalcohol (25:24:1)

Nuclease free water

100% Ethanol

2M Sodium Acetate pH 5.6

Hinf1(New England Biolabs)

Rsa1(New England Biolabs)

2.7.3 Protocol

Approximately 10^7 cells were harvested as described in section 2.1. Cells were washed twice in 1X SSC pelletted and resuspended in 500µl of 1X SSC. 500µl of 2X lysis buffer was added to the cell suspension plus 10µl of RNase to give a final concentration of 50µg/ml. This was then left to stand for 20 minutes at room temperature before adding 25µl of proteinase K and incubating over night in a rotating oven at 55°C. After overnight lysis 1ml of phenol chloroform was added to the tube and mixed gently but thoroughly to avoid any shearing. The tubes were then spun for 5 minutes at 2000rpm and the aqueous phase was poured into 10ml tubes containing 2.75ml of 100% ethanol and 100µl of sodium acetate and mixed gently to form a precipitate. The ethanol was then decanted and the DNA precipitate transferred to a clean eppendorf and washed with 80% ethanol. This was then decanted and the pellet left to air dry. Once dry the

pellet was resuspended in an appropriate amount of nuclease free water. The concentration of the DNA was checked as described in section 2.41. Samples were stored at + 4°C.

2.7.4 DNA Restriction Endonuclease Digestion

Before loading onto an agarose gel, genomic DNA must be digested with one or more restriction endonuclease enzymes. Six to ten micrograms of genomic DNA were digested in a total volume of 30 µl containing 3 µl of appropriate 1X dilution buffer and 1 µl of Rsa I and Hinf I restriction enzymes. The mixture was incubated at 37°C overnight. When the digestion was finished samples would be kept on ice whilst DNA concentration was checked to ensure equal loading.

2.7.5 DNA electrophoresis

Four micrograms of digested DNA were used to run on a 1% agarose gel. All samples were made up to 20µl with nuclease free water and 1/6 of the volume was loading buffer.

After loading, the gel electrophoresis was performed in TAE buffer (1X) for 21 hours at a 120° angle, 5 volts per centimetre with a 1-6 second ramped voltage and maintained at 14°C. Before the cooling pump was switched on, samples were allowed to run into the gel to minimize loss of DNA. At the end of the run the gel was briefly inspected under UV-light to visualize a smear which is indicative of a good digestion and separation. The DNA was then denaturated into single stranded form before blotting onto a membrane.

2.7.6 DNA denaturation

The agarose gel was placed in a box and submerged in denaturation solution. The gel was gently rocked on a shaker for 30 minutes and the denaturation solution was changed after 15 minutes.

Denaturation solution

NaCl 150M
NaOH 0.5M

After this incubation, the agarose gel was rapidly washed in deionised water and incubated for 30 minutes in neutralization solution.

Neutralization solution

Tris-HCl 0.5M pH 7.5
NaCl 150mM

The gel was washed again in deionised water to ensure that any excess salt was removed.

2.7.7 Blotting procedure

A capillary blot was set up using a solution of 20X SSC (recipe in section 2.7.2) as transfer buffer. The wick was made up of 1 piece of 3MM paper with each end dipping into the transfer solution. The gel was placed on the wick with wells facing down, and air bubbles were gently removed. A nylon membrane of exactly the same size of the gel was soaked in 6X SSC briefly and then carefully placed on top of the gel and any air bubbles removed. Two sheets of 3MM paper, cut to the same size as the membrane and gel, where then added over the membrane. The blot was then covered in Kim-Tech tissues and a balanced weight added to maximise transfer. The blot system was left for 16-24 hours after which the membrane was removed, gently towel dried, and baked at 80°C for at least 10 minutes and then UV cross-linked to ensure minimal DNA loss. The blot was stored between to sheets of 3MM paper until ready for hybridization.

2.7.8 Preparation of probes for Southern blot analysis

Probes suitable for determining the telomere length were prepared by using PCR amplified fragment from cell extracts.

2.7.8.1 Buffers and reagents

Primers Tel1: TTAGGGTTAGGGTTAGGG

Tel2: CTAACCCTAACCCTAACC

11.1X PCR buffer	Final Concentration
Tris HCl pH8.8	45mM
Ammonium sulphate	11mM
$MgCl_2$	4.5mM
β-mercaptoethanol	6.7mM
EDTA pH8.0	4.4μM
dATP	1mM
dCTP	1mM
dGTP	1mM
dTTP	1mM
BSA	113μg ml^{-1}
dH_2O	To final volume

Taq polymerase 5U/μl

*Telomere probe 1ng/*μl

OLB

Solution A	Volume
Tris HCl pH8.0 2M	625μl
$MgCl_2$ 5M	25μl
H_2O	350μl

β-mercaptoethanol	18µl
dATP 0.1M	5µl
dTTP 0.1M	5µl
dGTP 0.1M	5µl

(each triphosphate dissolved in 3mM Tris HCl, 0.2 mM EDTA pH 7.0 at a concentration of 0.1M).

***Solution B*:** 2M Hepes titrated to pH 6.6 with NaOH

***Solution C*:** Hexadeoxyribonucleotides (Pharmacia) suspended in 3mM Tris HCl, 0.2 mM EDTA pH7.0 at 90 OD units/ml.

Solutions mixed to ratio of 2:5:3 to make OLB. These were stored at -20°C for up to 3 months.

BSA 10mg/ml (Pharmacia)

dCTP Amersham PB10205, 3000 Ci/mmol, 10µCi/µl

Klenow 1U/µl

Stop solution

20 mM NaCl,
20 mM Tris HCl pH7.5,
2mM EDTA pH8.0,
0.25% SDS,
1μM dCTP

2.7.8.2 Procedure

One microlitre of telomere probe along with 4μl of each primer, 3.6μl of 11.1X PCR buffer and 0.8μl of Taq polymerase were mixed together and brought to a final volume of 40μl with dH_2O in a PCR eppendorf. The cycling conditions for amplification were: 96°C 40 sec, 65°C 40 sec, 70°C 5 mins for 25 to 30 cycles in an MJ Research PTC200 DNA engine, with heated lid. The products were checked on a 1% HGT agarose gel in 1X TAE or 0.5X TBE. The product was seen as a smear that extended from about 300bp to the wells (native DNA) or about 150b to 7kb (denatured DNA). Products from 300bp to about 12kb were gel purified from a 1% HGT agarose gel. These were then ethanol precipitated and dissolved in dH_2O and the concentration read on a spectrophotometer as described previously.

The labelling reaction was carried out at room temperature by adding: 6μl of OLB, 1.2μl of BSA, 10ng of DNA, 2.5μl dCTP, 1.5μl of Klenow and brought to 30μl with distilled water. The labelling reaction was allowed to run overnight, however the plateau is reached after approximately 3 hours. Smaller amounts of DNA take longer than 3 hours to label. Once the labelling reaction was finished the probe was recovered. Fifty microlitres of stop solution, 30μl of high molecular weight salmon sperm, 25μl of 2M NaAc and 425μl of 100% ethanol were added to the labelling reaction and flicked to precipitate the DNA. The excess solution was carefully aspirated and discarded and the DNA was washed with 500μl 80% ethanol and resuspended in 500μl of distilled

water. The probe was denatured by boiling at 95°C for 3-5 minutes just prior to adding to the blot.

2.7.9 Probing, Washing and Developing the Blot

2.7.9.1 Buffers and Reagents

Modified Church buffer	*Final Concentration*
EDTA	1mM
$NaHPO_4$ pH7.2	0.5M
SDS	7%

Made up to 800ml with distilled water.

Wash Solution	*Final Concentration*
SSC	1%
SDS	0.1%

2.7.9.2 Procedure

Once the transfer of the DNA was complete, the membrane was placed between two pieces of nylon mesh in a tray with distilled water. The membrane and mesh sheets were rolled into a cylinder and placed in a hybridization bottle. The Modified Church buffer was heated to 65°C and then added to the membrane which was then placed in a rotating hybridization oven at 65°C for 20 minutes or longer to prehybridize the blot and reduce any background non-specific binding of the probe. After the blot was prehybridized the church buffer was removed and replaced with 25ml of fresh buffer containing the labelled telomeric probe. This was left rotating in the hybridization oven at 65°C overnight.

Once hybridized the excess probe was drained and the blot was washed in wash solution three times for 10 to 15 minutes. The wash solution was heated to 65°C before adding to the blot which was then placed back in the hybridization oven. The blot was checked with the Geiger counter to determine when it was ready to be exposed. If the counts were between 5 and 10 the blot was removed from the bottle and dried gently between two sheets of 3MM paper. It was then fixed to a piece of 3MM paper of equal size, covered in Saran wrap and exposed to a phosphor screen overnight. The blot was then envisaged using a PhosphorImager and the image was examined using Image J and Adobe Photoshop.

2.8 Modified Southern protocol

A 1% HGT agarose gel was poured using 0.5X TBE without ethidum bromide. The CHEF tank was filled with 2 litres 0.5X TBE without ethidum bromide Run at 6v for 9 hrs with 0.5-1.5 switch time. If the gel was run overnight the conditions were altered to 5v for 13 hrs with the same switch time. Once the gel had run it was rinsed and placed ina tray with water and ethidium bromide on a shaker for 20min to allow the DNA to be visualized and a photograph of the gel to be taken. The gel was then exposed to UV light for 5minutes to depurinate the DNA and blotting was carried out as described before with two 10 minute washes in denaturing solution and two 10 minute washes in neutralizing solution. The gel was blotted using N+ nylon membrane for 24hrs using the same techinique described previously. The blotted membrane was hybridized as described previously.

2.9 In Gel Hybridization Southern Protocol

2.9.1 Buffers and Reagents

Denhardt solution 100X	*Final volume*
Ficoll 400	10g
Polyvinylpyrrolidone	10g
BSA	10g
dH_2O	500ml

Hybridization solution	*Final Concentration*
SSC	5X
Denhardt solution	5X
Na_2HPO_4	10mM
$Na_2H_2P_2O_7$	1mM

Radiolabeled Telomeric repeat probe

$(TTAGGG)_4$ probe (Ambion)

[γ-^{32}P]ATP (3000Ci/mmol) (Amersham)

T4 Polynucleotide kinase (PNK) 10U/µl

T4 ligase reaction buffer 10X

G25-column (Roche Biosciences)

2.9.2 Making the Radiolabeled Telomeric Repeat Probe

It has been shown that a G-rich probe gives higher signals than a C-rich probe; possibly due to G-quartet formation by the target G-strands which inhibits hybridization. One microlitre of oligonucleotide, 5µl of [γ-^{32}P]ATP, 2µl of 10X reaction buffer, 1µl of T4 PNK and made up to 20µl with dH_2O. The mixture was then incubated at 37°C for 30 minutes. The unicorporated label was removed using theG25-column nucleotide removal kit following the manufacturer's instructions. The cpm were determined using a counter. Fresh probe was made for each gel hybridization. [γ-^{32}P]ATP was not used if older than 3 weeks.

2.9.3 In-Gel Hybridization Protocol 1

This protocol was used as it is believed that there is less loss of smaller fragments of DNA and better visualization larger fragments due to the absence of transfer. DNA samples were prepared and digested as in section 2.7.3 and 2.7.4. Digested DNA samples were separated on a 0.7% (w/v) agarose gel stained with ethidium bromide (0.5µg/ml) for 16 hours at 70 volts in 1X TAE or 0.5X TBE buffer. Non radioactive λ HindIII DNA ladder was loaded at each end of the gel. The gel was denatured for 20 minutes in denaturing solution and rinsed for 10 minutes in distilled water. The gel was then dried upside down on two sheets of 3MM filter paper under vacuum for 1 hour at 50°C. Whilst the gel was drying the probe was labelled. After drying the gel was placed in neutralizing solution for 15 minutes and rinsed for 10 minutes in distilled water. The gel was then prehybridized for 10 minutes in 10ml of hybridization solution. The gel was then placed in a hybridization bag and fresh hybridization solution containing the radiolabelled probe was added and the bag sealed and left over night at 42°C. The gel was washed twice in 2X SSC and then one to three times for 10 minutes each in 0.1X SSC/0.1% SDS at room temperature. The gel was checked before it was gently dried and wrapped in saran wrap before being exposed to a phosphor screen and then scanned with a PhosphorImager and visualized using ImageQuant software.

2.9.4 In-Gel Hybridization Protocol 2

2.9.4.1 Buffers and Reagents

Church buffer	*Final Concentration*
SDS	35g (7% w/v)
BSA	5g (1% w/v)
1M Na_2HPO_4	250ml (0.5M)
0.5M EDTA pH8.0	1ml (1mM)

Wash Solution	*Final Concentration*
SSC	4X
SDS	0.1%

2.9.4.2 Procedure

A 0.7% agarose gel was poured in 0.5X TBE and run in 0.5XTBE, without ethidium bromide, overnight. The gel was then stained with ethidium to visualize the DNA smear and a photo taken. The gel was soaked in 2X SSC for 30 minutes on an orbital shaker before being dried on a gel drier for 30 to 90 minutes at room temperature until the gel was very thin. The gel was flipped half way through drying. The gel was then completely covered in denaturing solution and left at room temperature for 30 minutes. The denaturing solution was then removed and the gel rinsed once in distilled water before being submerged in neutralizing solution for 25 minutes on an orbital shaker. The gel was rinsed again in distilled water and then transferred to a sealable bag and enough pre-warmed church buffer to completely cover the gel. The bag was sealed removing all bubbles and placed on a shaking platform in a hybridization oven at 55°C for 1 hour for equilibration. The probe, made as above, was added to 20ml of pre-

warmed fresh church buffer which replaced that which was used to equilibrate the gel. The bag was sealed again taking care to remove any air bubbles and it was incubated overnight on the shaking platform in the hybridization oven at 37°C. The gel was then transferred to Tupperware containers and 55°C wash solution was added and left for 15 minutes on a shaker at room temperature. The gel was repeatedly checked with a Geiger counter and washed until radioactivity was confined only to areas where the probe should have bound. The gel was then blotted dry on Whatmann 3MM paper, wrapped in saran wrap exposed to a phosphor screen and then scanned with a PhosphorImager. The image was visualized using ImageQuant software.

2.9.5 In-Gel Hybridization Protocol 3

2.9.5.1 Buffers and Reagents

10X P-Wash

5mM PPi (inorganic phosphate)
100mM Na_2HPO_4

Hybridization solution	*Final Volume*
20X SSC	25ml
10X P-Wash	1ml
100X Denhardts solution	5ml
0.1mM ATP	40µl
Make to 100ml with distilled water	

2.9.5.2 Procedure

After having run a 0.5-0.75% agarose gel in 1X TBE buffer, staining the gel with ethidium bromide and photographing the smear the gel was immersed in 2X SSC for 30 minutes at room temperature. The gel was then placed with the open wells facing down on 2 layers of Whatman 3MM paper and covered in Saran wrap. The gel was then dried for 12-14 minutes at room temperature then the vacuum was stopped, the gel was flipped over and dried for another 12-14 minutes. Thirty minutes of drying was not exceeded. The thin, dry gel was then denatured for 25 minutes at room temperature. The denaturing solution was removed and replaced with 500ml of neutralizing solution and shaken gently at room temperature for 20 minutes. The gel was rinsed in distilled water and then placed in a sealable bag with 5ml of hybridization solution for 10 minutes. Hot probe is then added to 20ml of hybridization solution which was then directly poured into the sealable bag onto the gel. The bag was then sealed taking care to remove any air bubbles and hybridized overnight on a shaker at 30-37°C. The gel was then removed from the bag and placed in a plastic tray and washed in 2X SSC for 90 minutes at room temperature on a shaker. The gel was checked with a Geiger to determine any non-specific binding of the probe. Depending on the noise to signal ration the gel was washed again in decreasing concentrations of SSC solution until the background had gone down enough and the area where the probe was meant to bind was still hot. The gel was then blotted dry on Whatmann 3MM paper, wrapped in saran wrap exposed to a phosphor screen and then scanned with a PhosphorImager. The image was visualized using ImageQuant software.

2.10 Protein Electrophoresis and Western Blotting

2.10.1 Principle of Protein Electrophoresis

Electrophoresis is the name given to the movement of charged particles in solution by applying an electrical field across the mixture. The speed at which the molecules move is dependant on their size, shape and charge making this a useful tool for the separation of large molecules such as proteins. Most proteins are separated using polyacrylamide

gels. These cross-linked sponge-like structures act as size selective sieves such that molecules smaller than the gel pore size move more freely through the gel than those that are larger. Gel pore size is regulated by the concentration of polyacrylamide used where the higher the concentration the smaller the pore size. SDS polyacrylamide gel electrophoresis (SDS-PAGE) is the technique we chose to use as this allowed us to separate proteins on the basis of their molecular weight. Sodium dodecylsulfate (SDS) is an anionic detergent that is used to denature proteins. It does this by wrapping around the polypeptide backbone and conferring a net negative charge in proportion to the length.

2.10.2 Principle of Western Blotting

The transfer of proteins separated by SDS-PAGE from a gel to a membrane by electrophoretic elution is known as Western blotting. Nitrocellulose membranes are the more commonly used material. For a wet transfer the membrane is soaked in water and 2 pieces of 3MM paper are soaked in transfer buffer and the sandwich is then assembled. Following transfer the membrane is then incubated in blocking solution to block all non-specific binding sites and thus reduce any background. The blot is then probed with a protein-specific primary antibody followed by a secondary antibody specific for the general class of primary antibodies. Secondary antibodies are generally tagged with either a peroxidase or alkaline phosphatase thus allowing immunoreactive bands to be detected by either colour development of enhanced chemoluminescence (ECL) upon application of the appropriate enzyme substrates.

2.10.3 Principle of Enhanced Chemoluminescence (ECL) Detection.

Chemoluminescence is the emission of light without heat as a result of a chemical reaction. One of the most well characterised systems is the horseradish peroxidase (HRP)/hydrogen peroxide catalysed oxidation of luminol in alkaline conditions. The emission of light is due to the decay of excitation of the luminol. To enhance the light emission the oxidation reaction can be done in the presence of chemical enhancers such as phenols. This process is known as enhanced chemoluminescence (ECL).

2.10.4 Buffers and Reagents

10X Buffer stock solution

30g TriZma Base (Sigma)

140g Glycine (Sigma)

Made up to 1L with distilled water.

1X Running buffer

100ml of Buffer stock solution

5ml 20% SDS

Made up to 1L with distilled water

1X Transfer buffer

100ml of Buffer stock solution

200ml 100% methanol (Sigma)

Made up to 1L with distilled water

20% SDS

40g powdered SDS (Sigma)

200ml distilled water

Phosphate Buffered Saline

1 tablet/100ml distilled water (Gibco)

PBS-Tween (0.1%) (PBS-T)

1 L PBS
5ml of a 20% Tween-20 solution (Sigma)

Membrane Blocking solution

PBS
0.1% Tween-20
5% dry-powdered milk (Marvel)

Primary/Secondary antibody solution

PBS
0.1% Tween-20
3 % dry-powdered milk (Marvel)
Primary/ secondary antibody

Primary antibody for phosphorylated targets

PBS
0.1% Tween-20
5% BSA (Sigma)
Primary antibody

2.10.5 Protein Extraction

Total proteins were extracted from cells growing in culture by a lysis method. Cell cultures were washed with PBS and harvested as in section 2.1. Cell pellets were washed once in PBS and excess liquid was aspirated and pellets frozen in dry ice and stored at -80°C until needed. Thirty microlitres of lysis buffer were directly added to cell pellets. Frozen pellets were left to thaw on ice in lysis buffer for 10 minutes before mixing with a pipette. Non frozen samples were mixed as soon as buffer was added and then left on ice for 10 minutes before centrifuging at 13000 rpm for 5 minutes at +4°C. Cellular debris was pelleted and the total protein present in the supernatant was recovered and placed in a fresh Eppendorf tube (1.5 ml). An aliquot (1 µl) was used for determination of protein concentration.

Lysis Buffer	*Final Concentration*
Triton X-100	*0.5%*
Tris 1M, pH 7.6	*50 mM*
NaCl	*150 mM*
Protease inhibitor cocktail 100X (Sigma)	*1X*
Sodium Fluoride	*2.5 mM*
Sodium Orthovenadate	*10 mM*
Make to 200ml with distilled water.	

2.10.6 Protein Concentration Measurement

Protein concentration in the cellular extract was determined according to the Bradford protocol. Firstly a stock solution of bovine serum albumin (BSA) of 2mg/ml and dilutions ranging from 1 to 20 µg/µl were prepared by adding the appropriate amount of stock solution directly to 1ml aliquots of Bradford reagent (Sigma). The blank sample

was Bradford reagent alone. The absorbance at 595 nm was measured in the spectrophotometer and the calibration curve stored.

The concentration of proteins in the samples was determined by adding 1µl of protein extract to 1ml of Bradford reagent and the absorbance read on a spectrophotometer. Samples were processed as for the calibration curve and the amount of protein calculated.

2.10.7 SDS-PAGE

One fifth of the volume of sample buffer was added to the protein lysates and they were boiled at 95°C for 5 minutes.

5X Sample buffer	*Final concentration*
SDS	*10%*
Tris pH6.8	*312.5 mM*
Glycerol (Sigma)	*50%*
β-mercaptoethanol (Sigma)	*25%*
Bromophenol-blue (Sigma)	*0.025%*

After a brief spin 60µg of lysates were loaded in wells of a 5% stacking gel on an 8 or 12% polyacrylamide gel along with BenchMark™ Prestained marker (Invitrogen).

Stacking gel	*Final concentration*
Acrylamide mix (Protogel, Gene Flow National Diagnostic)	*5%*
Tris pH6.8	*0.13M*
SDS	*0.01%*
APS	*0.01%*
TEMED	*1000 X*
dH_2O	

8%Running Gel	*Final Concentration*
Acrylamide mix (Protogel, Gene Flow National Diagnostic)	*8%*
Tris pH8.8	*0.4M*
SDS	*0.01%*
APS	*0.01%*
TEMED	*1600 X*
Distilled Water	

12%Running Gel	*Final Concentration*
Acrylamide mix (Protogel, Gene Flow National Diagnostic)	*12%*
Tris pH8.8	*0.4M*
SDS	*0.01%*
APS	*0.01%*
TEMED	*2500 X*
Distilled Water	

Stacking and separating gels were prepared shortly before pouring. Ammonium persulphate (APS) catalyses polymerisation and TEMED accelerates the reaction and therefore these reagents are added last.

Proteins were resolved on a minigel apparatus (BioRad) and run at 40V until the dye front exited the stacking gel and then at 80V until the dye front reached the bottom of the gel.

2.10.8 Protein Transfer and Detection

The separated proteins were transferred onto nitrocellulose (at 65V for 2 h) using BioRad Mini transfer blot equipment in 1X transfer buffer. Blots were placed in a box with 5% non-fat dried milk dissolved in PBS-T 0.1% and shaken for 30 minutes at room temperature to block non-specific binding. Blots were exposed for either 1 h at room temperature or over night at 4°C to the desired antibodies diluted to the optimal working solution. After incubation, the blots were washed three times for 5 minutes in PBS-T 0.1% and incubated with the appropriate horseradish-peroxidase linked anti-mouse or anti-rabbit IgG secondary antibody (Amersham) for 1 h using appropriate dilutions. Blots were washed as previously described, and detection was performed with an enhanced chemiluminescent detection system (ECL, Amersham-Life Science). The blots were exposed to film for different time ranging from 15 to 20 minutes and developed.

2.10.9 Antibodies

2.10.9.1 Primary Antibodies

Antibody	Host	Source	Dilution
PML	Rabbit	Chemicon	**1:1000**
TRF2 (N-20)	Rabbit	Santa Cruz	**1:200**
P53 (DO-1)	Mouse	Santa Cruz	**1:500**
Phospho-p53 (Ser15)	Rabbit	Cell Signaling Technology	**1:1000**
P 21	Mouse	Santa Cruz	**1:200**
Actin	Mouse	Sigma	**1:5000**

2.10.9.2 Secondary Antibodies conjugated to HRP

Antibody	Host	Source	Dilution
Anti-mouse	Sheep	Amersham Bioscience	**1:10,000**
Anti-rabbit	Donkey	Amersham Bioscience	**1:10,000**

2.11 Immunocytochemistry

Immunocytochemistry can be described as the staining of cells grown in culture and fixed allowing the detection of specific antigens. This method permits the visualization of the localization of specific antigens using antibodies, which have been raised against the protein of interest.

2.11.1 Buffers and Reagents

PBS

10% Goat Serum

Goat Serum (Sigma) 1ml

Made to 10ml with 1X PBS

4% Paraformaldehyde (PFA)

1X PBS 100ml

Paraformaldehyde 4g (Sigma)

Cytoskeleton Buffer

10 mM piperazine-N,N9-bis (2-ethanesulfonic acid) (PIPES; pH 6.8) (Sigma)

100 mM NaCl, (Sigma)

300 mM sucrose (Sigma)

3 mM $MgCl_2$ (Sigma)

1 mM EGTA (Sigma)

0.5% Triton X-100 (Sigma)

PNA/FISH Hybridization solution

30% formamide
0.1% Triton-X 100
0.3X SSC

PNA/FISH Wash solution

4X SSC
0.05% Tween-20

2.11.2 Cell Preparation

Immunocytochemistry was performed on cells fixed with 4% PFA on glass coverslips. Breifly, cells were seeded on 22mm x 22mm glass coverslips that had been dipped in methanol and allowed to dry in the laminar flow cabinet, to ensure sterility. The dry coverslips were placed in 6 well dishes (NUNC) and covered with the appropriate medium. Cells were seeded at the appropriate density directly on the coverslips and allowed to attach for at least 24 hours.

This immunostaining procedure used to visualize MRE11 was adapted from the previous published work of Mirzoeva and Petrini. Coverslips were washed in phosphate-buffered saline (PBS), incubated in cytoskeleton buffer for 5 min on ice. After several washes with ice-cold PBS, the cells were fixed using 4% PFA, for 10 minutes, and washed with PBS. For all other staining cells were fixed in 4% formaldehyde for 10 minutes at room temperature and then permeabilized with ice-cold 0.1% Triton-X100 for 3 minutes. Once fixed and permeabilized, cells were blocked with 10% goat serum in PBS and incubated with primary antibody for 1 h and with secondary antibody for 1 h at room temperature. All antibodies were diluted in 10% goat serum–PBS. Cells were then washed, counterstained with 49, 69-diamidino-2-

phenylindole (DAPI), and mounted as using the ProLong Anti-fade kit (Molecular Probes). Primary antibody dilutions were as follows: Anti-human PML PG-M3 (Santa Cruz), human PML (Chemicon), Mre11 (Abcam), TRF1 (Genetex), TRF2 (Imgenex), TRF2 (N-20) (Santa Cruz), anti-phospho-ATM (ser1981) (Chemicon), anti-phospho-(Ser/Thr)ATM/ATR (Cell Signaling Technology), p95 NBS1 (phospho S343) (abcam), anti-p53 (DO-1) (Santa Cruz): 1:200, 1:1000, 1:500, 1:1000, 1:2000, 1:200, 1:200, 1:200, 1;200, 1:200 respectively. Alexa Fluor 488 and 568 conjugated secondary antibodies were used at 1:1000. Slides were analyzed by confocal microscopy.

2.11.3 Confocal microscopy

The confocal used was a Zeiss LSM 510 and detection was via photomultiplier tubes (PMT) intrinsic to the system. To acquire a green image using Alex Fluor 488, 5% laser power of a 30 mW argon 458/477/488/514 laser was used and a bandpass filter 505-550 nm, with a pinhole size of 0.78 Airy Units (129 um) giving an optical slice of 0.7um. To acquire a red image using Alexa Fluor 543, 80% laser power of a 1 mW HeNe 543 laser was used and a longpass filter 560 nm, with a pinhole size of 0.72 Airy Units (130 um) giving an optical slice of 0.8um. To acquire DAPI 405, 5% laser power of a 30 mW 405 diode laser was used and a bandpass filter 420-480 nm, with a pinhole size of 0.93 Airy Units (131 um) giving and optical slice of 0.7 um. PMTgain settings varied to give the appropriate level of signal for each image.

2.11.4 PNA/FISH with IF

Cells were grown on coverslips and fixed with ice-cold methanol-acetic acid. They were then prepared as for immunofluorescence but were not mounted. After secondary antibody exposure, coverslips were washed in PBS 3 times for 5 mins and post-fixed in 4% PFA for 2mins. After three quick rinses in PBS the coverslips were dehydrated in EtOH in series 70%, 85%, 96% for 2mins each. Coverslips were then completely air dried. The PNA (Panagene, South Korea) stock was diluted 1/1000 in hybridization solution and heated at 80°C for 5mins. Coverlips were then incubated in the dark at

room temp for 30 mins, rinsed in wash solution for 5 mins, counterstained with Dapi, mounted and stored at 4°C.

2.12 Apoptosis/cell cycle (PI staining)

To determine cell death PI staining and FACS analysis was carried out. Briefly, cells were fixed in 70% EtOH, spun, washed in PBS and spun again. The pellet was resuspended in 60µl of PBS with 300 µg/ml RNase and incubated for 30 min at room temperature. 10µg/ml of propidium iodide was then added and samples were incubated in the dark for 30 mins before being fed through a Becton Dickinson (BD) FACS machine. DNA profiles were analyzed using the CellQuest acquisition/analysis software.

Chapter 3) Characterization of PML bodies in telomerase negative and positive cell lines.

3.1 Introduction.

The vast majority of cancers are able to avoid the telomere-imposed proliferation block by activating telomere length maintenance mechanisms (TMM) (Ulaner et al., 2004). In most cancers, approximately 85% thereof, telomere length is maintained by telomerase, an enzyme composed of human telomerase RNA (hTR) and human telomerase reverse transcriptase (hTERT), which synthesizes telomere repeat sequences to replace those lost during DNA replication (Gana et al., 2002). Some cancers, however, are telomerase-negative and maintain telomeres by an alternative lengthening of telomeres (ALT) mechanism (Reddel, 2003). It has been hypothesized that cells using this mechanism maintain their telomeres through the annealing of one strand of a telomere with the complimentary strand of another, thus priming the synthesis of new telomeric DNA using the complimentary strand as a template (Reddel, 2003). Recent evidence suggests that this mechanism is common in a variety of cancers including osteosarcoma and glioblastoma multiforme, the most common type of primary brain tumor in adult humans (Londono-Vallejo et al., 2004). PML has been shown to have tumor suppressive functions. In APL, PML-containing nuclear bodies (PML-NBs) redistribute to microspeckles, suggesting that PML-NB disruption is important for disease progression (Carbone et al., 2002). In experimental animal models of APL where *PML* gene dosage has been reduced, an acceleration of the disease and a increased incidence are observed, emphasizing the role PML plays in the progression of the disease (Rego et al., 2001). Several proteins involved in apoptosis and growth inhibition co-localize to these structures in response to stress and transformation, such as p53 and Daxx (Guo et al., 2000b; Zhong et al., 2000b), suggesting that these nuclear organelles could play a role in tumor suppression. A variety of functions have been attributed to PML and PML nuclear bodies in telomerase positive cells. However, the recent discovery of a novel type of PML nuclear body suggests that there are still other undisclosed functions of PML. The appearance of the novel PML nuclear body coincided with the onset of the ALT mechanism and so these bodies became known as ALT-associated-PML-Nuclear bodies (APBs). APBs are remarkably different from PML-NBs as they are comprised of different components including telomeric DNA, DNA repair proteins such as MRE11,

NBS1 and Rad50, RPA, Rad52 and the telomere repeat binding factors TRF1 and TRF2 (Naka et al., 2002; Wu et al., 2003; Wu et al., 2000; Yeager et al., 1999; Zhu et al., 2000). TRF1 is the protein known to be involved in the negative regulation of telomere length, whereas TRF2 has been shown to play a key role in the protection of telomeres (See 1.13). TRF2 helps in the formation of the cap structure that protects the 3' overhang of the telomere from being recognized as a double strand break. It does so by helping the overhang to invade the double stranded region of the telomere and form what is known as the T-Loop (de Lange, 2002; de Lange, 2005; Griffith et al., 1999; van Steensel et al., 1998). Both of these telomeric binding proteins are essential for the maintenance of the telomere. MRE11, on the other hand, is a protein known to be part of the MRN (MRE11, NBS1, and RAD 50) DNA repair complex. Mre11 is a multifunctional protein that plays critical roles in homologous recombination used for processing DNA double-strand breaks, non-homologous DNA end-joining, meiotic recombination, DNA damage response, and telomere maintenance (Dong et al., 1999). The presence of all three of these proteins implicates APBs in telomere maintenance.

In this chapter, data will be presented on the characterization of seven different ALT cell lines and three telomerase positive cell lines. Our findings confirm already published data on the composition and frequency of APBs, and determine differences in APB number and occurrence in our system. Immunofluorescence analysis allowed a clear distinction between APBs and PML-NBs using the presence of MRE11, TRF1 and TRF2 with PML as markers of APBs.

3.2 Materials and Methods

Detailed methodology of cell culture and immunofluorescence techniques can be found in Chapter 2. To obtain percentages, 200 cells were assessed for PML colocalization with either MRE11, TRF1 or TRF2 per cell line. The number of positive cells was expressed as a percentage of the total number of cells counted. Counting was carried out manually.

3.3 Results

3.3.1 MRE11 Localization in ALT cells.

The localization of MRE11 was determined by immunofluorescence double labelling in conjunction with PML. To ensure more defined staining, cells were pre-permeabilized with CSK buffer prior to fixation, in order to remove any excess protein not connected to the cytoskeleton. U2OS, SAOS, IIICF, GM847, SUSM1, JFCF6 and VA13 cells were all treated equally allowing MRE11 and PML colocalization to be examined by confocal microscopy. Figure 3.1 and 3.2 show that all these ALT positive cell lines tested contain a percentage of cells displaying colocalization of MRE11 with PML (Table 3.1). MRE11 can be seen in defined speckles within the nuclei of cells. All the MRE11 speckles colocalize with PML. However, not all the PML speckles contain MRE11. Some of the cell lines have many nuclear PML speckles that vary in size. The larger bodies are those that colocalize with MRE11. SAOS and GM847 cells are those that have fewer large nuclear speckles most of which colocalize with MRE11. SUSM-1 and U2OS cells have more PML speckles; however there are a small proportion of these that are larger in size and colocalize with MRE11. In the nuclei of JFCF6 and IIICF cells the difference in nuclear body size is more apparent as there are a greater number of smaller bodies and only a few large bodies containing both PML and MRE11. VA13 cells are different from all the aforementioned cell lines as there does not appear to be a significant size difference between the bodies that colocalize with PML and those that do not, similar to what was reported by Yeager *et al.* (Yeager et al., 1999). This cell line also appears to have a greater number of bodies within the nuclei of cells ranging from

25 to 40 nuclear speckles compared to the 8-15 speckles per nucleus seen in other tested ALT cell lines.

Figure 3.1

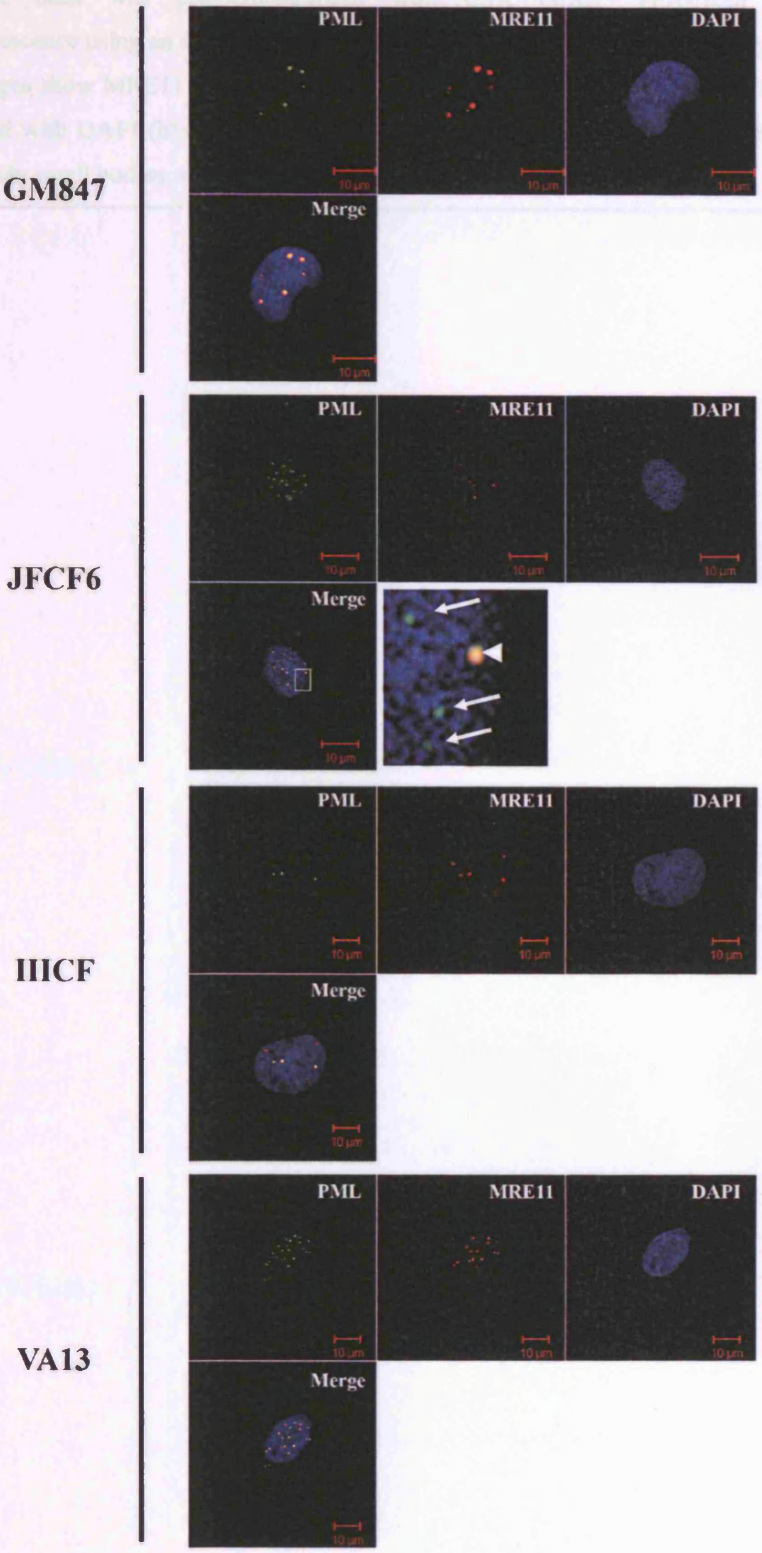
GM847
PML
MRE11
DAPI
Merge
JFCF6
PML
MRE11
DAPI
Merge
IIICF
PML
MRE11
DAPI
Merge
VA13
PML
MRE11
DAPI
Merge

Figure 3.1 MRE11 colocalizes with PML in ALT positive cell lines. A panel of ALT positive cell lines was pre-permeabilized with CSK buffer, PFA-fixed and stained by immunofluorescence using an anti-PML antibody (green) and an anti-MRE11 antibody (red). The merged confocal images show MRE11 localization in nuclear speckles that colocalize with PML. The nuclei are counterstained with DAPI (blue). The close up demonstrates the different sized bodies in JFCF6 cells. Arrows indicate small bodies, arrow head indicates large body (APB).

Figure 3.2

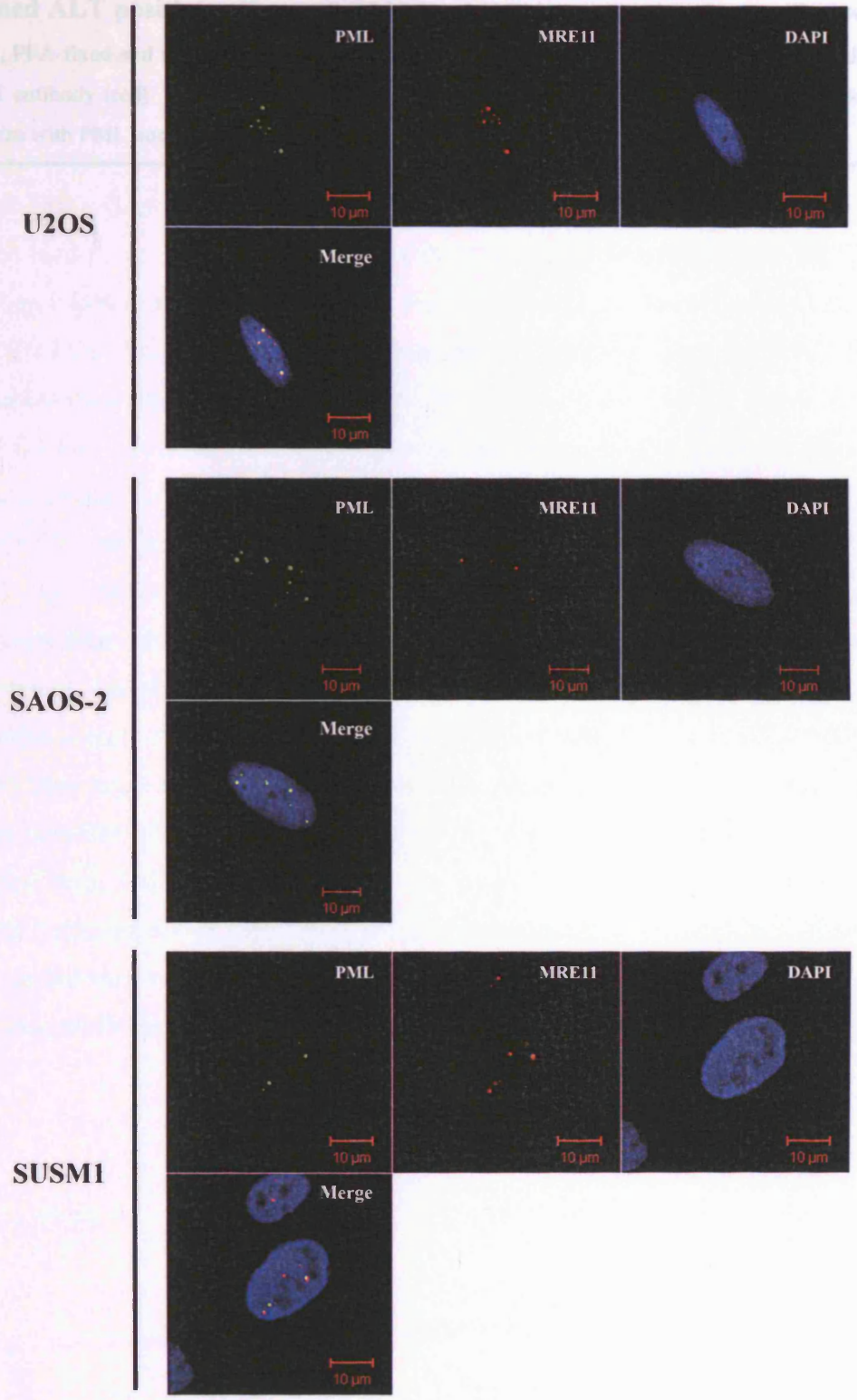
U2OS
PML
MRE11
DAPI
Merge
SAOS-2
PML
MRE11
DAPI
Merge
SUSM1
PML
MRE11
DAPI
Merge
10 µm

Figure 3.2 MRE11 colocalizes with PML in nuclear speckles in non-SV40 transformed ALT positive cells. U2OS, SAOS-2 and SUSM1 cells were pre-permeabilized with CSK buffer, PFA-fixed and stained by immunofluorescence using an anti-PML antibody (green) and an anti-MRE11 antibody (red). The merged confocal images show MRE11 localization in nuclear speckles that colocalize with PML nuclear. The nuclei counterstained with DAPI (blue).

3.3.2 PML Colocalization with TRF1

Using double labelling immunofluorescence, cells that were fixed in 4% PFA were probed with antibodies against TRF1 and PML to determine their localization. As TRF1 is a known component of APBs we used this as a marker to distinguish between PML bodies and APBs. Confocal imaging established the presence of TRF1 in the nuclei of all the ALT cell lines examined. However, a closer analysis determined that TRF1 is found in large speckles and microspeckles. Figures 3.3 and 3.4 show that VA13 and SUSM1 cells have many PML speckles throughout the nucleus. There are few TRF1 large speckles; however these can all be found to colocalize with the larger PML bodies. SAOS and U2OS cells, on the other hand, contain few bodies within the nucleus all of which contain both PML and TRF1 (Figure 3.4). GM847 cells also have few bodies within the nucleus; however there are smaller PML bodies that do not colocalize with TRF1 large speckles (Figure 3.3). Once again it is the larger PML speckles that are found to colocalize with TRF1 large speckles. IIICF cells display a larger number of nuclear speckles. The majority are PML-positive only, but it is clear that the few TRF1 large speckles seen in these nuclei completely colocalize with the larger PML bodies. JFCF6 also have large and small PML bodies with the larger bodies colocalizing with TRF1 large speckles (Figure 3.3). There are only one or two speckles that are not found to colocalize with PML. As mentioned above, in all the cell lines tested there are several TRF1 microspeckles within the nucleus. These speckles do not colocalize with PML and are not very bright. An explanation for this is that the microspeckles represent telomere ends, while large speckles constitute APBs.

Figure 3.3

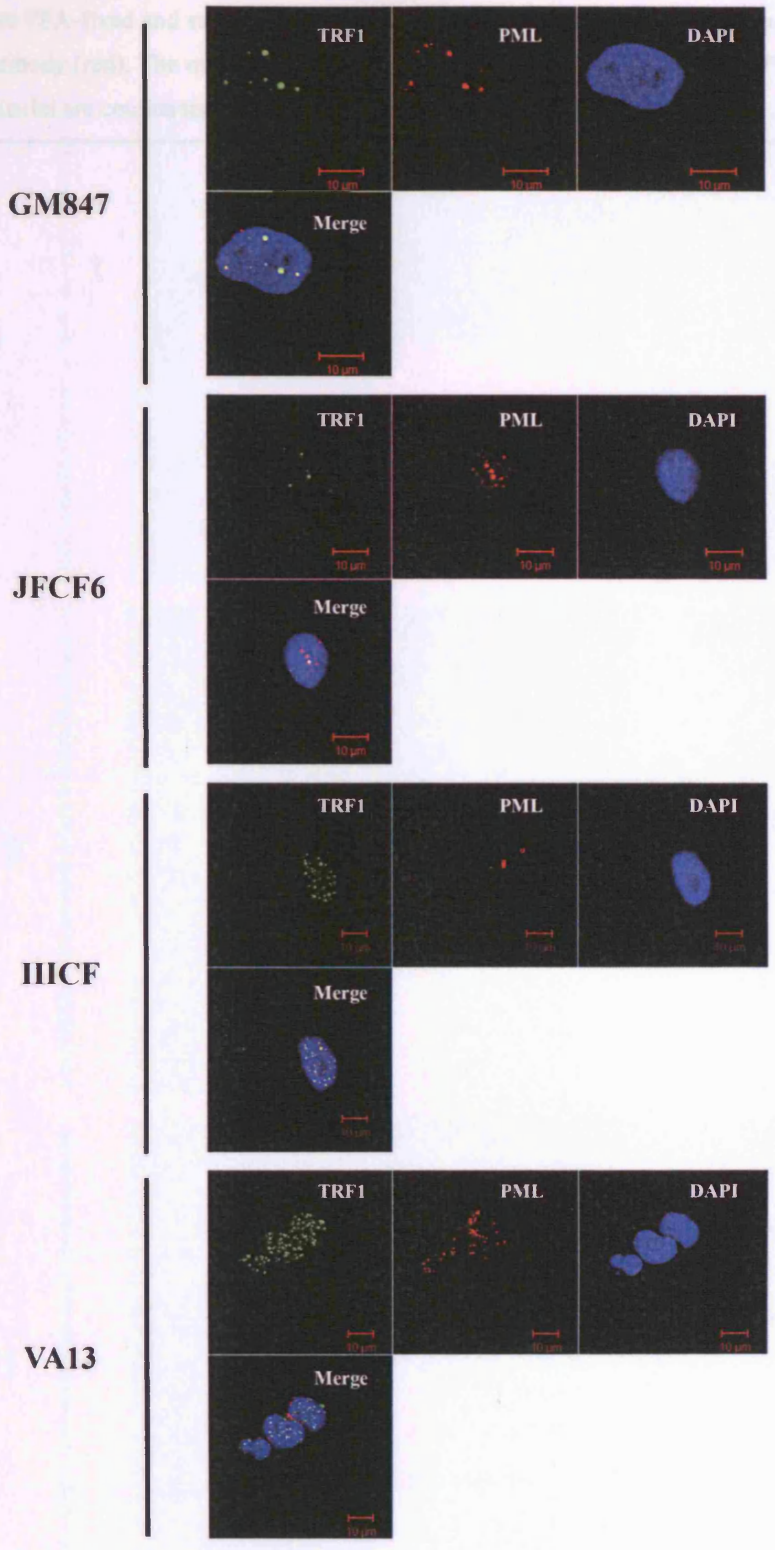
GM847
TRF1
PML
DAPI
Merge
JFCF6
TRF1
PML
DAPI
Merge
IIICF
TRF1
PML
DAPI
Merge
VA13
TRF1
PML
DAPI
Merge

Figure 3.3 TRF1 nuclear localization in ALT positive cell lines. A panel of ALT positive cell lines were PFA-fixed and stained by immunofluorescence with an anti-TRF1 antibody (green) and an anti-PML antibody (red). The merged confocal images show the colocalization of TRF1 nuclear speckles with PML. Nuclei are counterstained with DAPI (blue).

Figure 3.4

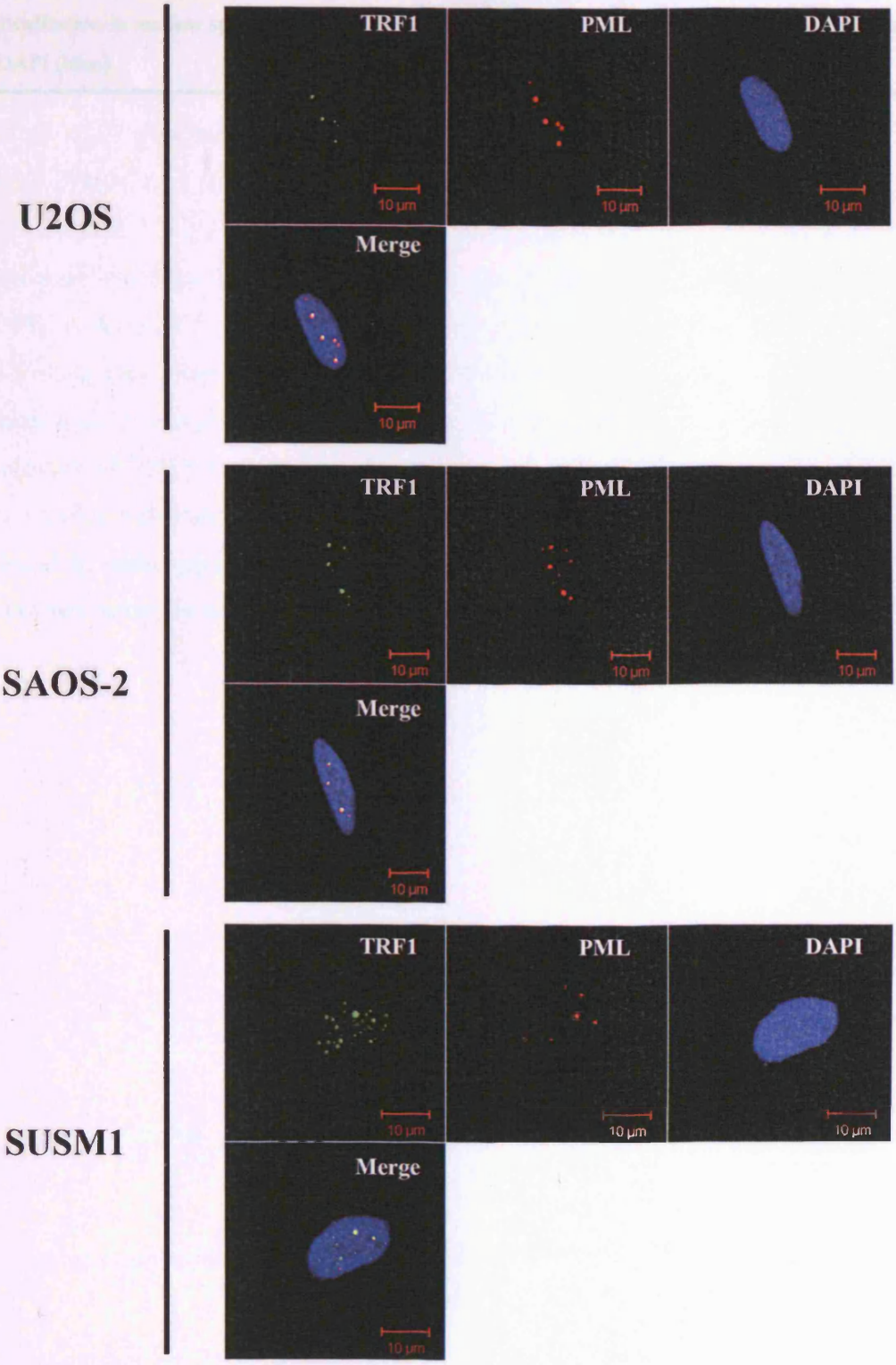
U2OS
TRF1
PML
DAPI
Merge
SAOS-2
TRF1
PML
DAPI
Merge
SUSM1
TRF1
PML
DAPI
Merge
10 µm

Figure 3.4 TRF1 nuclear localization in non-SV40 immortalized ALT positive cell lines. U2OS, SAOS-2 and SUSM1 cells were PFA-fixed and stained by immunofluorescence using an anti-PML antibody (red) and an anti-TRF1 antibody (green). The merged confocal images show TRF1 localization in nuclear speckles colocalizaing with PML nuclear speckles. The nuclei counterstained with DAPI (blue).

3.3.3 TRF2 Speckle Localization in the Nucleus of ALT Cells.

TRF2 is essential for the protection of telomeres from the activation of the DNA damage response. As it has been found to localize to APBs we are using this protein as a marker for APBs. Figures 3.5 and 3.6 show that TRF2 is seen in speckles in the nuclei of all ALT cell lines in percentages ranging from 10% in WI36VA13 to 40% in IIICF cells (Table 3.1). These speckles were found to colocalize with PML in all the cells lines tested. IIICF, JFCF6, SUSM-1, U2OS and SAOS cells all have defined TRF2 speckles in the nucleus of cells (Figure 3.5 and 3.6). These speckles all colocalize with PML. Like TRF1 and MRE11 there are more PML speckles than TRF2 speckles allowing easy identification of APBs. GM847 and VA13 cells have many more TRF2 bodies all of which are found to colocalize with PML (Figure 3.5). Irrespective of the number of TRF2 speckles seen in different cell lines they are mainly all found to colocalize with PML as do the other markers of APBs. Also in this case, TRF2 is also found in microspeckles that do not colocalize with PML and most probably represent 'normal' telomere ends.

Figure 3.5

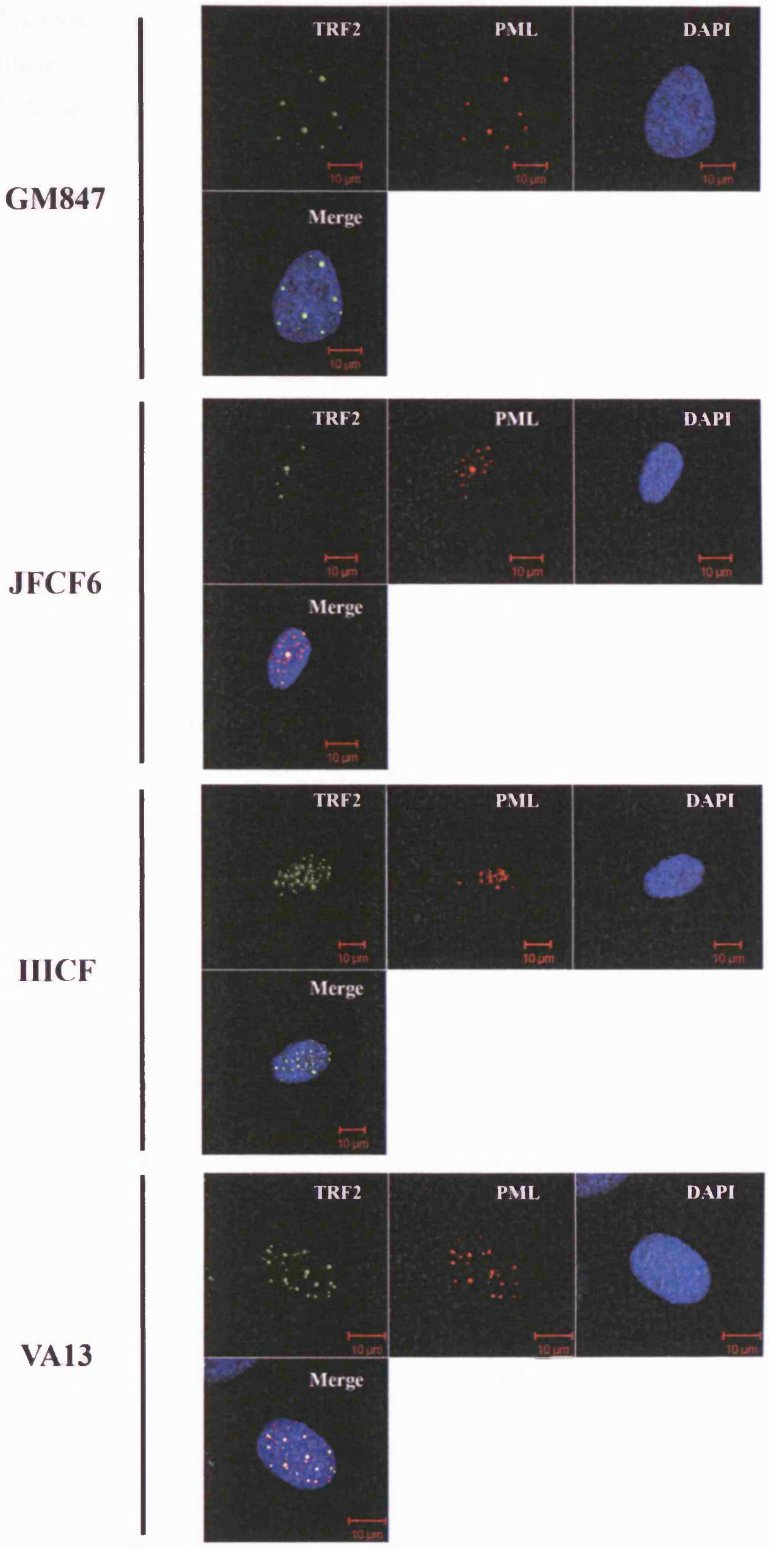
GM847
TRF2
PML
DAPI
Merge
JFCF6
TRF2
PML
DAPI
Merge
IIICF
TRF2
PML
DAPI
Merge
VA13
TRF2
PML
DAPI
Merge

Figure 3.5 TRF2 colocalization with PML in ALT cell lines. A panel of ALT positive cell lines were PFA-fixed and stained by immunofluorescence with an anti-TRF2 antibody (green) and an anti-PML antibody (red). The merged confocal images show the colocalization of TRF2 nuclear speckles with PML. Nuclei are counterstained with DAPI (blue).

Figure 3.6

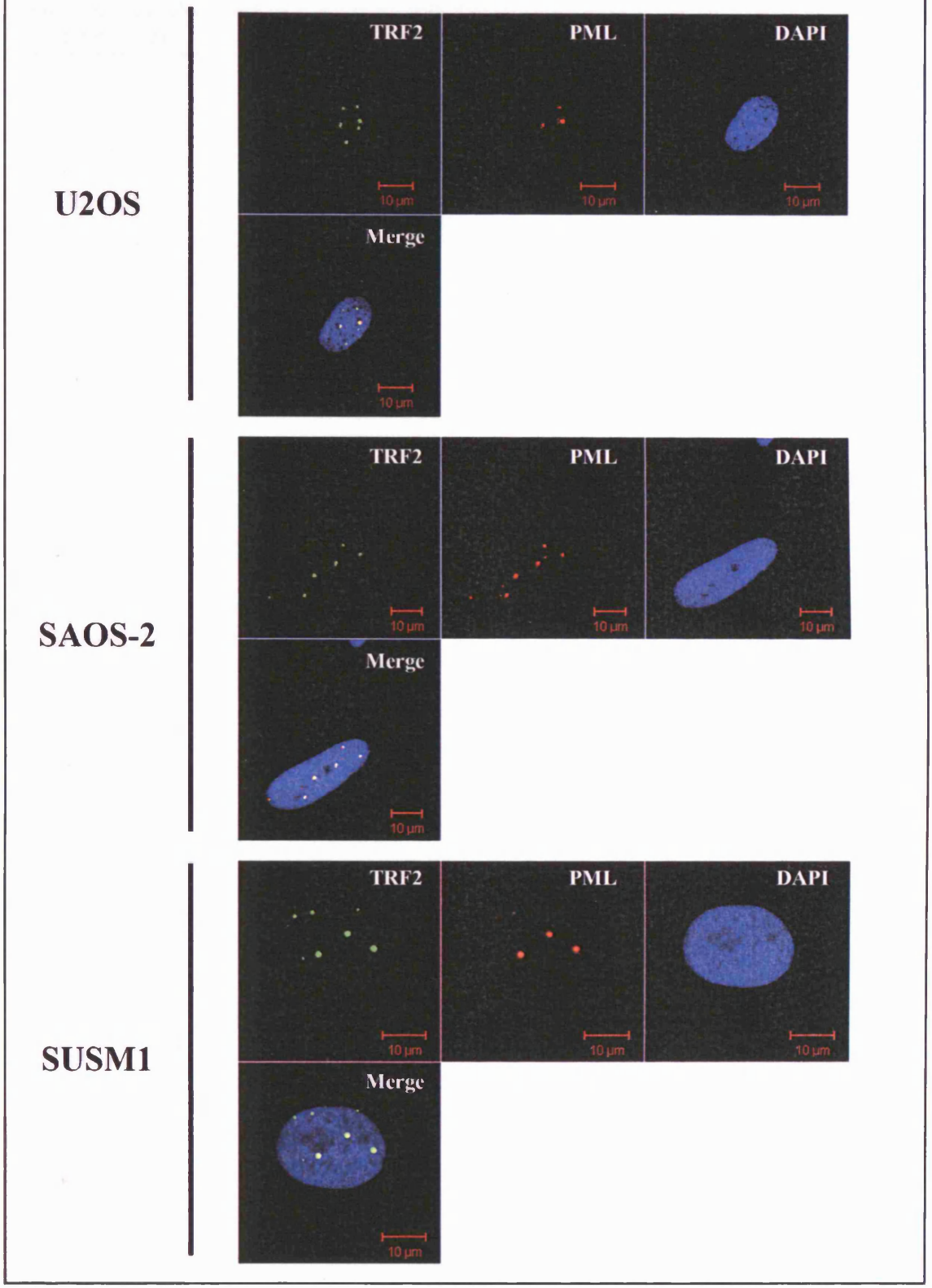
U2OS
TRF2
PML
DAPI
Merge
SAOS-2
TRF2
PML
DAPI
Merge
SUSM1
TRF2
PML
DAPI
Merge
10 µm

Figure 3.6 TRF2 colocalization with PML in non-SV40 transformed ALT positive cell lines. U2OS, SAOS-2 and SUSM1 cells were PFA-fixed and stained by immunofluorescence using an anti-PML antibody (red) and an anti-TRF2 antibody (green). The merged confocal images show TRF2 localization in nuclear speckles colocalizing with PML nuclear speckles. The nuclei are counterstained with DAPI (blue).

3.3.4 MRE11, TRF1, TRF2 and PML Colocalization in Telomerase Positive Cells.

To ensure that the speckles of MRE11, TRF1 and TRF2 we were seeing in the ALT cells we examined were specific markers for APBs, we looked at MCF7 and HeLa telomerase positive cells as well as JFCF6-T.1J/11C, the telomerase positive subclone of JFCF6-T cells. Using MRE11, TRF1 and TRF2 as markers for APBs in conjunction with PML the above cell lines were screened. Figure 3.7 shows that in HeLa cells MRE11 does not show a defined punctate staining, but rather a more diffuse nuclear staining that does not colocalize with PML. MCF7 cells also do not display any punctate MRE11 staining, but still maintain the speckled nuclear patter for PML as do JFCF6-T.1J/11C cells (Figure 3.7). TRF1 staining is undetectable in HeLa cells (Figure 3.8). However, there are microspeckles of TRF1 in JFCF6-T.1J/11C and MCF7 cells (Figure 3.8). These speckles do not colocalize with PML and resemble the microspeckles seen in ALT cell lines, suggesting that they are not APBs but rather 'normal' telomeres. PML is present in nuclear speckles in all three of the telomerase positive cell lines in the absence of TRF1 colocalization. The pattern seen for TRF2 staining is much the same, with no punctate nuclear staining (Figure 3.9). MCF7 cells show a diffuse nucleolar staining whereas JFCF6-T.1J/11C display weak microspeckled pattern and HeLa cells do not have any TRF2 visible by confocal microscopy. The protein that constantly displays a nuclear speckled pattern in the above mentioned cell lines is PML.

Table 3.1

Percentage of APB positive cells in ALT cell lines.

Cell Type	% APB Positive cells
WI38VA13 (ALT +ve)	10%
SAOS-2 (ALT +ve)	20-30%
U2OS (ALT +ve)	20%
IIICF (ALT +ve)	30-40%
JFCF6 (ALT +ve)	30-40%
GM847 (ALT +ve)	20%
SUSM1 (ALT +ve)	70%

Figure 3.7

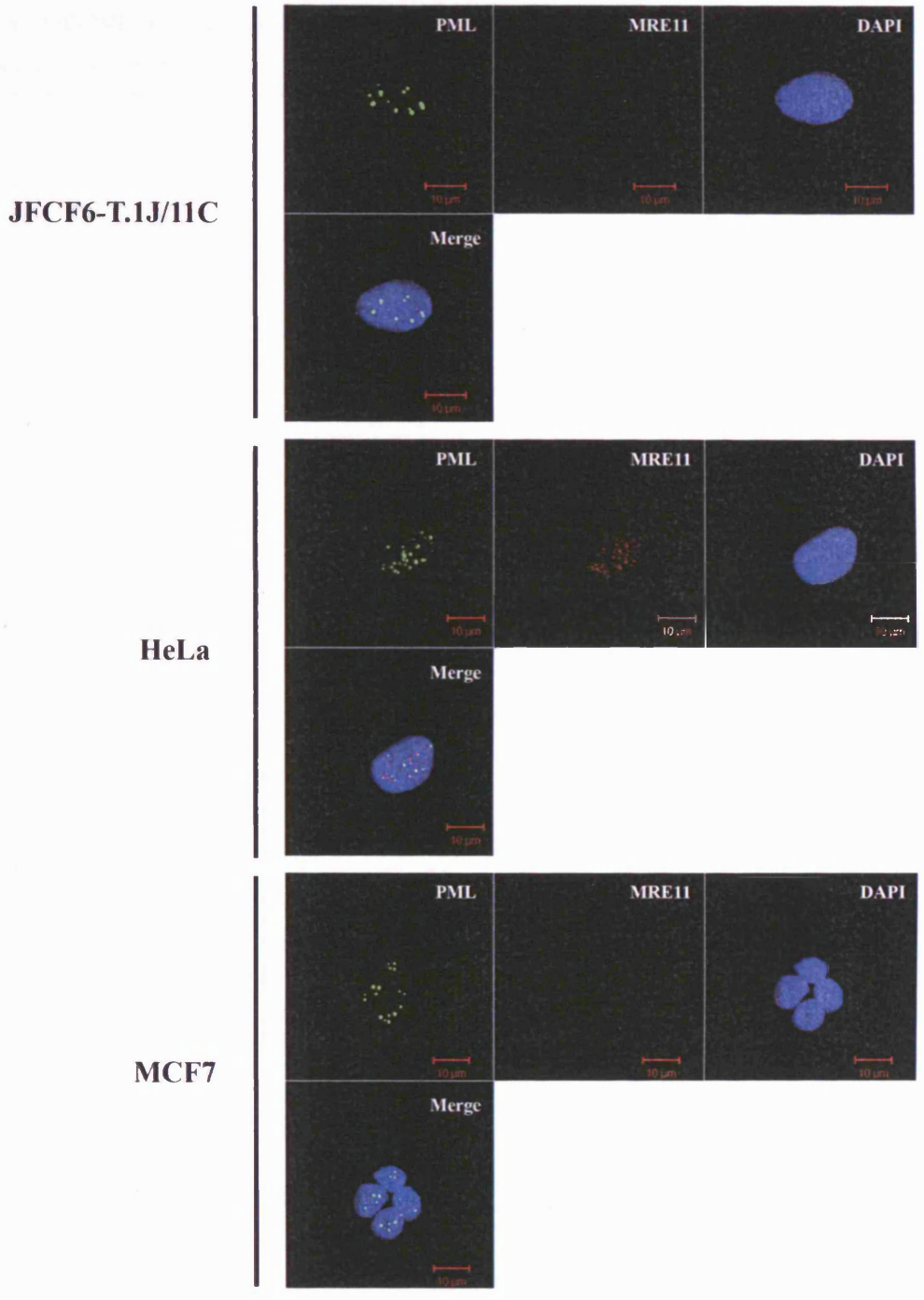
JFCF6-T.1J/11C
PML
MRE11
DAPI
Merge
HeLa
PML
MRE11
DAPI
Merge
MCF7
PML
MRE11
DAPI
Merge

Figure 3.7 Telomerase positive cell lines do not contain MRE11 in nuclear speckles that colocalize with PML. JFCF6-T.1J/11C, HeLa and MCF7 cells were pre-permeabilized with CSK buffer and then PFA-fixed and stained by immunofluorescence with an anti-MRE11 antibody (red) and an anti-PML antibody (green). The merged confocal images show no MRE11 nuclear speckles colocalizing with PML nuclear speckles. Nuclei are counterstained with DAPI (blue).

Figure 3.8

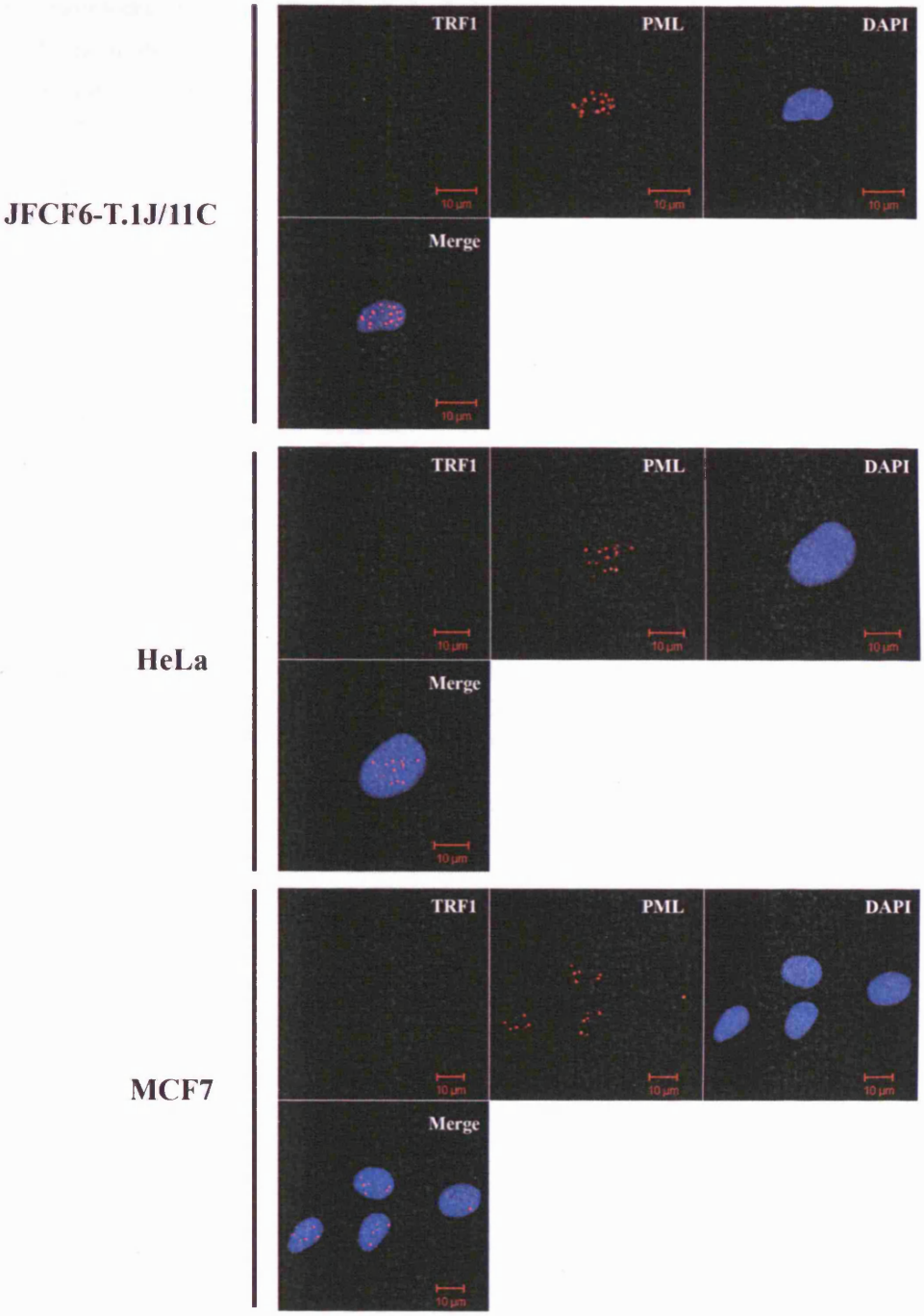
JFCF6-T.1J/11C
TRF1
PML
DAPI
Merge
HeLa
TRF1
PML
DAPI
Merge
MCF7
TRF1
PML
DAPI
Merge

Figure 3.8 Telomerase positive cell lines do not contain TRF1 in nuclear speckles that colocalize with PML. JFCF6-T.1J/11C, HeLa and MCF7 cells were PFA-fixed and stained by immunofluorescence with an anti-TRF1 antibody (green) and an anti-PML antibody (red). The merged confocal images show no TRF1 nuclear speckles colocalizing with PML nuclear speckles. Nuclei are counterstained with DAPI (blue).

Figure 3.9

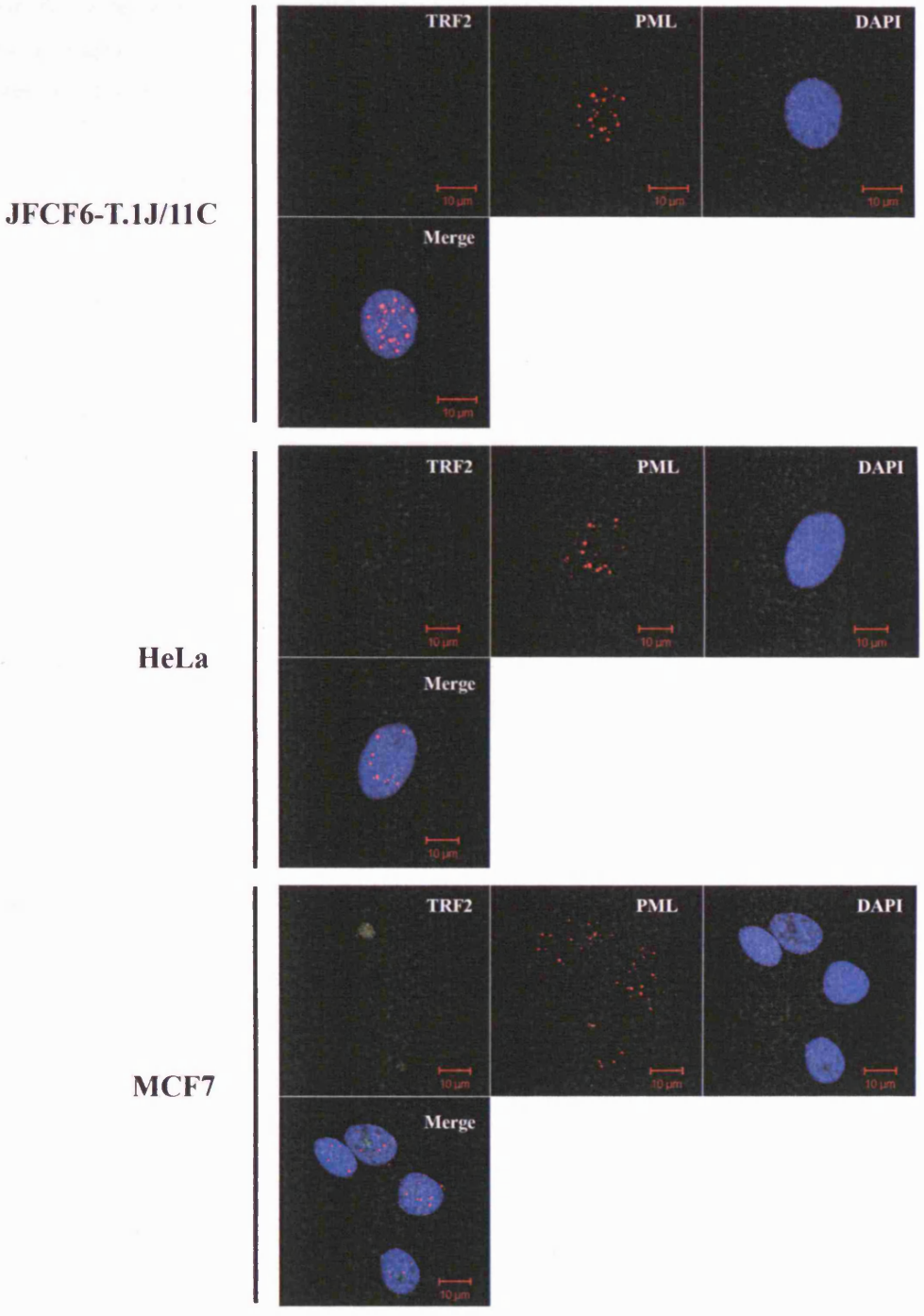
JFCF6-T.1J/11C
TRF2
PML
DAPI
Merge
HeLa
TRF2
PML
DAPI
Merge
MCF7
TRF2
PML
DAPI
Merge

Figure 3.9 Telomerase positive cell lines do not contain TRF2 in nuclear speckles with PML. JFCF6-T.1J/11C, HeLa and MCF7 cells were PFA-fixed and stained by immunofluorescence with an anti-TRF2 antibody (green) and an anti-PML antibody (red). The merged confocal images show no TRF2 nuclear speckles colocalizing with PML nuclear speckles. Nuclei are counterstained with DAPI (blue).

3.4 Discussion

It has been found that approximately 15% of human tumours are telomerase-negative and maintain their telomeres through ALT (Shay and Gazdar, 1997). ALT cells have some defining characteristics, including heterogeneous telomere length and a novel type of PML nuclear body known as the ALT-associated PML nuclear-body (APB). These too are doughnut shaped nuclear protein aggregates. However, these differ from PML-NBs due to their content which includes telomeric DNA, the telomere repeat binding proteins TRF1 and TRF2, and a range of proteins involved in DNA recombination and replication (RAD51, RAD52, RPA, MRE11, RAD50, NBS1, BLM and WRN). As these proteins are known components of APBs we chose to use TRF1, TRF2 and MRE11 as markers of APBs when determining the presence or absence of APBs in ALT and telomerase-positive cells.

The appearance of these nuclear structures has been reported to tightly coincide with the presence of ALT within a cell line. APBs have been found in 17/17 ALT positive and 0/20 telomerase-positive cell lines and in 0/5 mortal cell strains (Yeager et al., 1999). Our data reflects what is said in this report, with APBs being found only in the ALT cells we tested and not in the telomerase positive HeLa or MCF7 cells or in the telomerase positive subclone of the JFCF6-T cells. This therefore confirms the specificity of these bodies as hallmarks of ALT.

The exact function of these bodies is unknown. Speculations have been made implying these are by-products of the ALT pathway or that these bodies appear in cells that are senescent. This, however, is not the case as there is no senescence-associated β-galactosidase activity in these cells (Yeager et al., 1999). Another possibility is that APBs are reservoirs of telomeric DNA and associated proteins necessary in cells undergoing telomere repair and maintenance. APBs may simply be a platform for telomere maintenance where recombination between telomeres is facilitated. These hypotheses are mainly based on the observation that only a small percentage of ALT cells display APBs. It has been reported that less than 5% of interphase nuclei contained APBs (Yeager et al., 1999). In contrast, we have found that a larger number of ALT cells contain APBs. We found that the percentage of APB positive cells varied between

cell types and ranged from 10% to 30 or 40%. There was a great deal of variation in the number and size of these bodies between cell strains. We noticed that it was the predominantly larger bodies that showed colocalization of PML with all three of the chosen APB markers, implying that it is the larger bodies within the nuclei of these cells that are APBs. The size difference among these bodies was clear in the majority of the observed ALT cells. However there was one cell line, WI38-VA13/2RA, in which there was no apparent significant difference in nuclear speckle size. This has been previously reported by Yeager *et al.*, where it is reported that this cell line contained nuclear aggregates whose size was intermediate between the "nuclear sprinkles" found in telomerase-positive cells and the speckles found in other ALT cell lines (Yeager et al., 1999). Previous studies have shown that ALT is genetically recessive and that upon fusion of ALT cells with telomerase positive cells the ALT phenotype was repressed (Perrem et al., 2001). It has also been reported that WI38-VA13/2RA ectopically expressing hTERT and hTR, the enzymatic subunits of telomerase, maintained telomere length using both pathways for at least 90 population doublings (Cerone et al., 2001). Therefore ALT and telomerase can work together in the correct environment. It may be possible that some cells are more predisposed to this co-operation between mechanisms than others.

APBs, like PML nuclear bodies, are composed of a number of proteins. The main component of PML nuclear bodies is the tumour suppressor PML, without which all other associated proteins known to date no longer aggregate in these structures. A study by Wu *et al.*. suggested that the Nijmegen Breakage Syndrome 1 (NBS1) was necessary for the correct functional assembly of APBs (Wu et al., 2003). NBS1 is part of the DNA damage sensor complex along with MRE11 and RAD50. The report states that NBS1 directly interacts with TRF1 and is necessary for the recruitment of MRE11 and RAD50 but not TRF1 and RAD51 to APBs. It was also found that TRF1 was dispensable for the assembly of the bodies. However, it is not known what roles TRF2 and PML play in the establishment of these structures (Jiang et al., 2005; Naka et al., 2002).

3.5 Summary

This study confirmed the specificity of APBs as markers of cells that maintain their telomeres through ALT and not telomerase. It also became apparent that the percentage of cells displaying APBs in the nucleus was higher than that reported in the literature (<5% of interphase nuclei) (Yeager et al., 1999). All ALT positive cell lines examined displayed a similar pattern of colocalization of TRF1, TRF2 and MRE11 with PML, which were not seen in telomerase-positive cells. The components involved in the specific assembly of these structures have yet to be determined, and this will be discussed in the following chapters.

Chapter 4) Transient Down-regulation of Selected APB components.

4.1 Introduction.

PML has 9 exons which give rise to many isoforms due to alternative splicing (Figure 1.3). In all mammalian cells examined to date, PML is found in a heterogenous multi-protein complex known as the PML nuclear body. These structures are defined by the presence of PML. The importance of PML for the integrity of these structures was first defined in studies carried out in APL patient samples. In these cells PML is fused to RARα and this fusion product impedes the formation of nuclear bodies and causes the cells to arrest in the promyelocytic stage of development. These cells no longer display the punctuate nuclear patter of PML but a more diffuse micro speckled staining. Alteration of the structure of PML through the chromosomal translocation (t15:17) not only blocks the localization of PML to nuclear bodies but also causes all other proteins known to be found in nuclear bodies to disperse. Upon treatment with all-trans retinoic acid (ATRA) or arsenic trioxide the PML-RARα fusion protein is degraded. PML nuclear bodies reform and patients go into remission. This evidence strongly links the integrity of PML nuclear bodies with the maintenance of correct cellular function (Grimwade and Solomon, 1997)

Experiments carried out using PML knock out mice demonstrated that nuclear body components such as Daxx, SUMO-1 and CBP were no longer found in nuclear speckles in these cells. The exogenous expression of PML relocalized these factors to nuclear bodies demonstrating that PML, although not directly linked to all components, is able to establish a supramolecular scaffold required for the recruitment of the components of this nuclear domain (Ishov et al., 1999; Lallemand-Breitenbach et al., 2001; Zhong et al., 2000a).

TRF2 is a protein that is essential for the capping of the telomere. It coats the length of all human telomeres at all stages of the cell cycle and is said to be present at 100 copies per telomere. The protection of human telomeres crucially depends on this factor, as the inhibition of this protein using a dominant negative construct of TRF2 ($TRF2^{\Delta B\Delta M}$), in cancer cell lines studied to date, leads to immediate induction of apoptosis (Karlseder et al., 1999). In primary human fibroblasts induction of senescence, resembling that brought about by extremely short telomeres, is observed upon inhibition of TRF2 (Karlseder et al., 1999; Smogorzewska and de Lange, 2004). In the absence of

functional TRF2 a large fraction of telomeres become fused to one another resulting in dicentric chromosomes (van Steensel et al., 1998). These fused products go on to cause problems during anaphase for chromosome separation. Consequently, anaphase cells with dicentric chromosomes display characteristic chromosome bridges (Smogorzewska et al., 2002).

In this chapter, data will be presented on the effect of transient down-regulation of PML and TRF2, two potentially important APB components, on the structure of APBs. Using RNAi specific for these two proteins we were able to achieve significant down-regulation of both PML and TRF2 by western blot. Immunofluorescence analysis allowed us to determine effects on other APB components such as MRE11 and TRF1. PML was found to be important for the localization of MRE11 and TRF1 as seen by the significant decrease of nuclear speckles of these components in cells lacking PML. Transient TRF2 down-regulation on the other hand, does not appear to affect the localization of PML, MRE11 or TRF1.

4.2 Methods

Detailed methodology of RNAi, Western blotting and immunofluorescence techniques can be found in Chapter 2. To quantify downregulation approximately 200 cells were counted per experiment. Cells no longer displaying PML or TRF2 nuclear speckles were analysed for the presence of other nuclear body components and expressed as a ratio of control cells. Counting was carried out manually.

4.3 Results

4.3.1 PML transient down-regulation in SAOS and U2OS cells.

U2OS and SAOS cells were chosen as they are both osteosarcoma cell lines, the former with intact p53 and the latter without. Previous reports have stated that telomere alterations lead to cell death via p53. Therefore the use of these cells allows us to work within a good control system.

Cells were grown to the necessary confluency and 8 x 10^6 were used per electroporation. As a control, cells were electroporated with a scrambled oligo (S/O) generated by Ambion that does not have any targets within the cell. To downregulate all nuclear isoforms of PML an oligo against the nuclear localization signal on exon VI (P-ALL) was used. An oligo against exon II was also designed to allow down-regulation of all PML isoforms both nuclear and cytoplasmic. Cells were electroporated and collected for western blot analysis 48 and 72 hours post transfection. Western analysis showed that there was a significant decrease in the levels of PML after electroporation compared to the S/O control in both SAOS and U2OS (Figure 4.1a). U2OS cells show a marked decrease of the smaller isoforms (below 110 kDa) with the 110 kDa isoforms remaining noticeably less affected both at 48 and 72 hours post transfection. SAOS cells exhibited a different pattern of down-regulation. Again it is the smaller isoforms of PML that appear to be greatly affected however in this case the 90 kDa isoform is not completely downregulated as in U2OS cells as is the 110 kDa band. The degree of down-regulation is more noticeable 72 hours post transfection. Down-regulation of PML with the exon II oligo gave similar results with the smaller PML isoforms more efficiently downregulated and the larger, 110kDa band(s), only partially affected (Figure 4.1b).

Figure 4.1

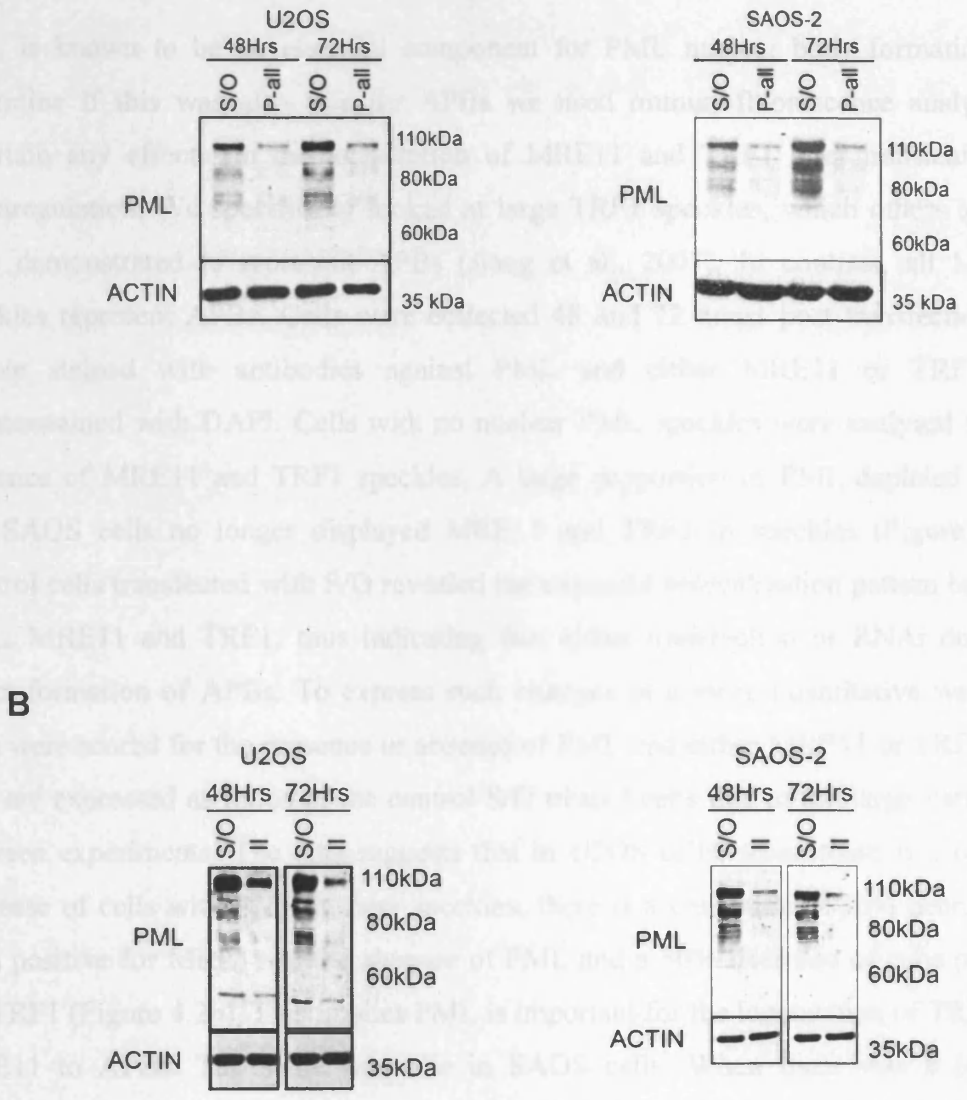

Figure 4.1 PML silencing by RNAi in SAOS and U2OS ALT cell lines. Cells were electroporated with scrambled oligo (S/O), PML oligo against the nuclear loaclization signal (P-ALL), or PML oligo against exon II (II) and cell lysates were prepared at 48, 72 hours. Western blot analysis of the cell lysates shows PML protein down-regulation at the indicated time points following introduction of the PML oligos. (**A**) PML proteins levels are significantly reduced upon P-ALL introduction at both time points in both U2OS and SOAS cells and exon II oligo (**B**).

4.3.2 Localization of MRE11 and TRF1 upon Transient PML Down-regulation.

PML is known to be an essential component for PML nuclear body formation. To determine if this was also true for APBs we used immunofluorescence analysis to ascertain any effects on the localization of MRE11 and TRF1 after transient PML downregulation. We specifically looked at large TRF1 speckles, which others and we have demonstrated to represent APBs (Jiang et al., 2007). In contrast, all MRE11 speckles represent APBs. Cells were collected 48 and 72 hours post transfection and double stained with antibodies against PML and either MRE11 or TRF1 and counterstained with DAPI. Cells with no nuclear PML speckles were analysed for the presence of MRE11 and TRF1 speckles. A large proportion of PML-depleted U2OS and SAOS cells no longer displayed MRE11 and TRF1 in speckles (Figure 4.2a). Control cells transfected with S/O revealed the expected colocalization pattern between PML, MRE11 and TRF1, thus indicating that either transfection or RNAi does not affect formation of APBs. To express such changes in a more quantitative way, 200 cells were scored for the presence or absence of PML and either MRE11 or TRF1. The data are expressed as ratios of the control S/O treated cells due to the large variability between experiments. The data suggests that in U2OS cells, when there is a 60-70% decrease of cells with PML nuclear speckles, there is a concomitant 30% decrease of cells positive for MRE11 in the absence of PML and a 50% decrease of cells positive for TRF1 (Figure 4.2b). This implies PML is important for the localization of TRF1 and MRE11 to APBs. The same was true in SAOS cells. When there was a 60-70% decrease of cells positive for PML speckles there was a 20% decrease of MRE11 positive cells in the absence of PML and a 30% decrease of TRF1 speckles, confirming the observation that PML is important for the localization of MRE11 and TRF1 to APBs. To determine if the decrease in MRE11 and TRF1 nuclear speckles in the absence of PML was delocalization and not due to degradation of the proteins, were checked MRE11 and TRF1 protein levels after electroporation (Figure 4.3b). Upon depletion of PML there is no difference in either MRE11 or TRF1 protein levels, suggesting that the decrease in nuclear speckles is due to delocalization and not degradation of these proteins. Again, using the RNAi oligo against exon II we see

similar effects on the localization of TRF1 and MRE11 in cells lacking PML nuclear speckles compared to control cells (not shown). The percentage of cells lacking PML was similar to that seen using P-ALL and the MRE11 and TRF1 were no longer seen in nuclear speckles in cells lacking PML. The use of two RNAi oligos directed against different exons of PML yielding similar results implies that what we see is not due to off target effects.

Multiple reports have demonstrated that PML is not required for viability *in vitro* and *in vivo* (Wang et al., 1998a; Xu et al., 2003). Accordingly, we found that there was no significant effect on cell death and proliferation upon transient PML downregulation (not shown).

4.3.3 TRF2 Localization upon Transient PML Down-regulation

It is known that TRF2 is an important protein for the protection of telomeres and that its loss results in either senescence or cell death. We wanted to determine the effect of PML down-regulation on TRF2 localization. U2OS and SAOS cells were examined by double immunofluorescence labelling, 48 and 72 hours post-transfection with the P-ALL and S/O oligos. It became apparent that TRF2 behaved in a different manner to TRF1 and MRE11 in the absence of PML. In fact there was no change in the localization of TRF2 to large speckles (APBs) in cells lacking PML in either U2OS or SAOS (Figure 4.3). The data suggest that PML is not necessary for the localization of TRF2 to APBs.

Figure 4.2

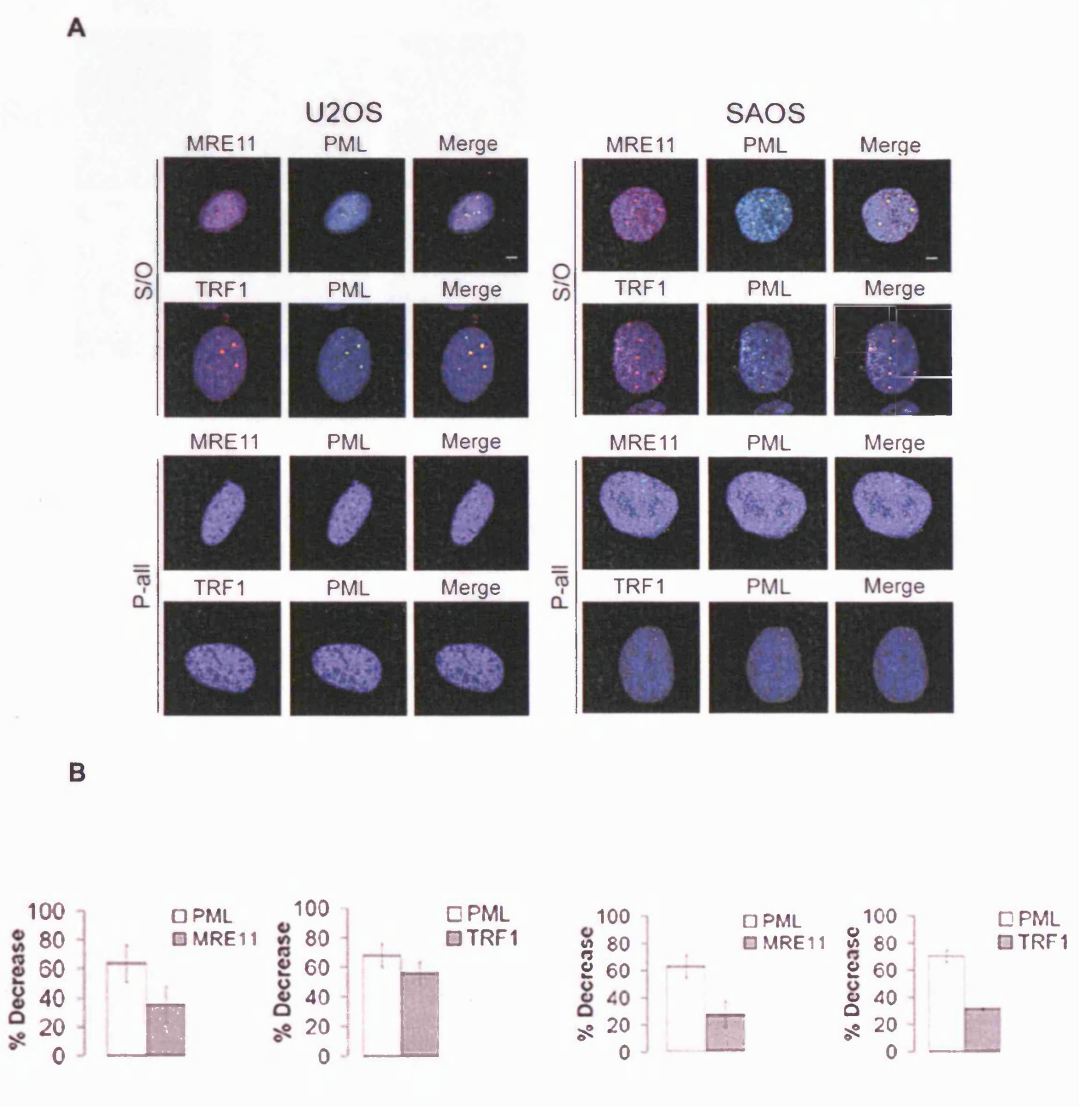

Figure 4.2 PML down-regulation affects MRE11 and TRF1 localization in ALT cells.(**A**) SAOS and U2OS cells were electroporated with control oligo (S/O)or PML oligo (P-ALL) and PFA-fixed at 48 hours. The merged confocal images show PML (green), MRE11 (red) and TRF1 (red) stained by immunofluorescence using an anti-PML antibody, anti-MRE11 antibody and anti-TRF1 antibody, respectively. Nuclei were counterstained with DAPI (blue). (**B**) Assessment of the percentage decrease of PML, MRE11 and TRF1 speckles in PML-depleted cells expressed as a ratio with control oligo transfected cells. Data are means of at least three experiments. Error bars are standard deviations.

Figure 4.3

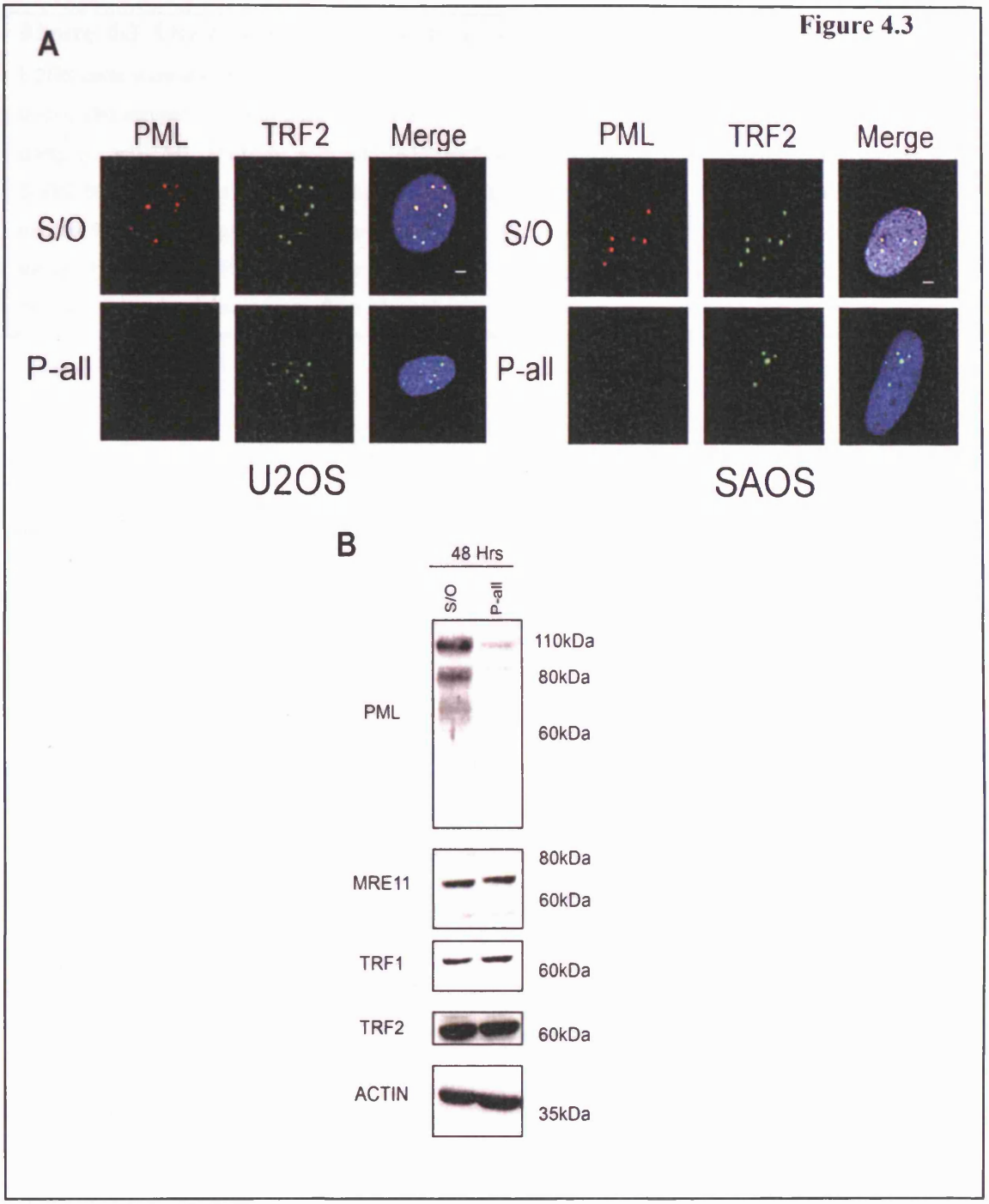
A
PML
TRF2
Merge
S/O
P-all
U2OS
SAOS
B
48 Hrs
S/O
P-all
110kDa
80kDa
60kDa
PML
80kDa
60kDa
MRE11
60kDa
TRF1
60kDa
TRF2
35kDa
ACTIN

Figure 4.3 TRF2 is not delocalized upon PML depletion by RNAi. **(A)** SAOS and U2OS cells were electroporated with control oligo (S/O) or PML oligo (P-ALL) and PFA-fixed at 48 hours. The merged confocal images show PML (red) and TRF2 (green) stained by immunofluorescence using an anti-PML antibody and anti-TRF2 antibody, respectively. Nuclei were counterstained with DAPI (blue). **(B)** Cells were electroporated with either scrambled oligo (SO) or PML oligo against the nuclear loaclization signal (P-ALL) and cell lysates were prepared at 48 hours. Western blot analysis of the cell lysates shows PML protein down-regulation and no effect on the protein levels of MRE11, TRF1 or TRF2 following introduction of the PML oligo.

4.3.4 The Effect of Transient TRF2 down-regulation on APB formation

Unlike other tested components, TRF2 localization was not affected by the transient down-regulation of PML. Would other APB components be affected upon the transient down-regulation of TRF2? A siRNA oligo designed against TRF2 was used to transfect both U2OS and SAOS cells along with the S/O control oligo. Cells were collected and TRF2 down-regulation was assessed by western blot, both 48 and 72 hours post-transfection. TRF2 protein was almost completely knocked down in both cell lines when examined by western blot in comparison to those transfected with the control oligo (Figure 4.4a). Having determined that the protein levels were significantly lowered upon transfection with the TRF2 oligo, determination of any effect on APB components was assessed through immunofluorescence double labelling. Upon down-regulation of PML, both TRF1 and MRE11 were partially delocalized from APBs. Using TRF1, MRE11 and PML to determine any compositional effects of TRF2 down-regulation on APBs, it became apparent that there was no difference in the localization of the above mentioned proteins (Figure 4.4c).Interestingly cells that were TRF2 depleted did not appear to undergo a significant increase in cell death compared to scrambled oligo transfected cells (Figure 4.4b). FACS analysis of TRF2 depleted cells showed that thre was 8.51% cells death compared to the 14.32% of control cells (Figure 4.4b). In cells that no longer displayed TRF2 in speckles in the nucleus PML, MRE11 and TRF1 maintained a speckled pattern. To ensure that the speckles remaining after TRF2 down-regulation were APBs, the colocalization of MRE11 with TRF1 was analysed. The remaining speckles were large and well defined and all displayed MRE11 and TRF1 colocalization (Figure 4.4c). These results implied that TRF2 was not necessary for the localization of PML, MRE11 and TRF1 to APBs.

Figure 4.4

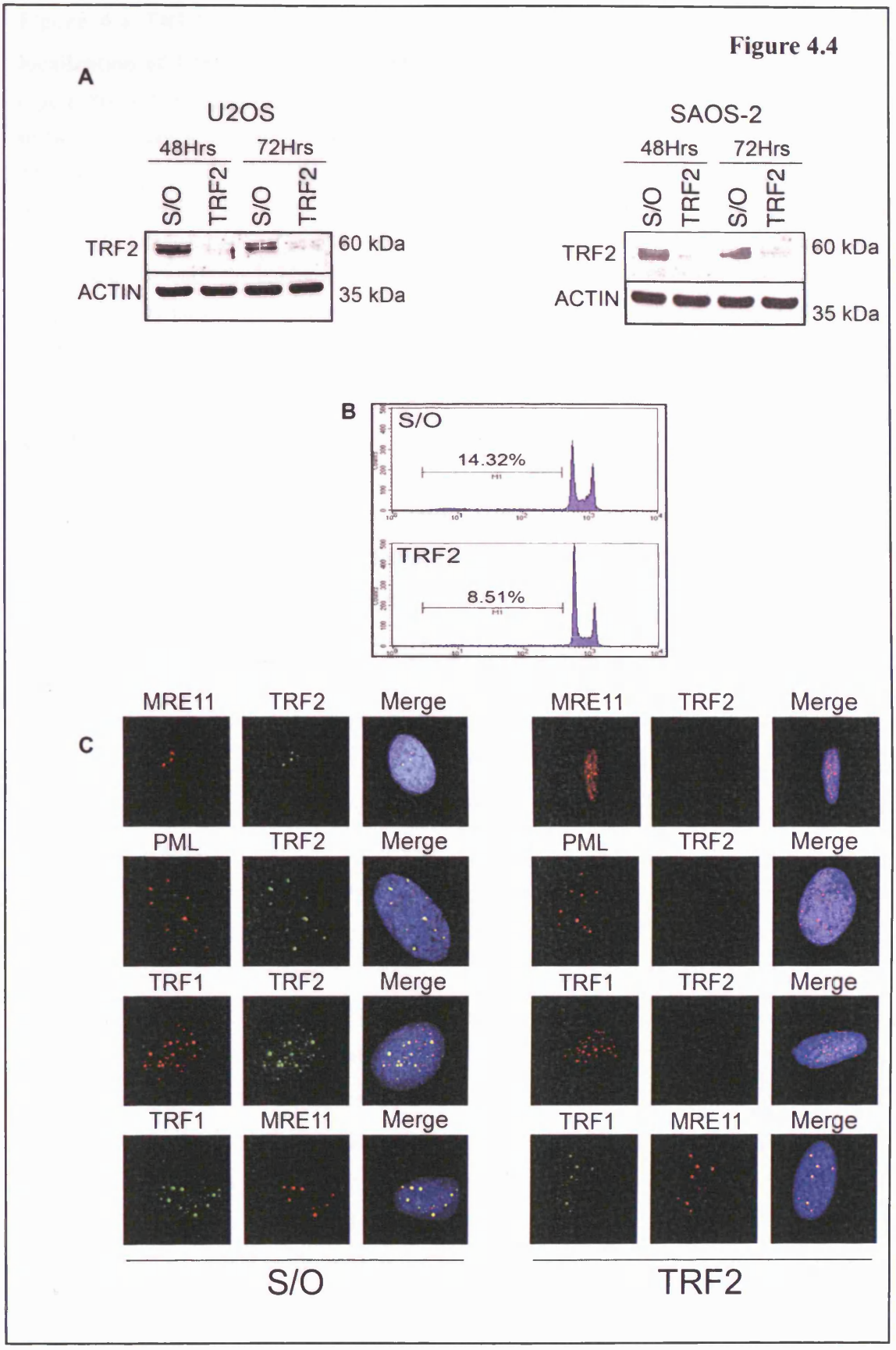
A
U2OS
48Hrs
72Hrs
S/O
TRF2
S/O
TRF2
TRF2
ACTIN
60 kDa
35 kDa
SAOS-2
48Hrs
72Hrs
S/O
TRF2
S/O
TRF2
TRF2
ACTIN
60 kDa
35 kDa
B
S/O
14.32%
TRF2
8.51%
C
MRE11
TRF2
Merge
PML
TRF2
Merge
TRF1
TRF2
Merge
TRF1
MRE11
Merge
S/O
TRF2

Figure 4.4 TRF2 down-regulation by RNAi does not affect cell death or the localization of PML, MRE11 or TRF1. **(A)** U2OS cells were electroporated with scrambled oligo (S/O) or TRF2 oligo (TRF2) and cell lysates were prepared at 48 and 72 hours. Western blot analysis of the cell lysates shows TRF2 protein down-regulation at the indicated time points following introduction of the TRF2 oligo. **(B)** Cells electroporated with the S/O and TRF2 oligos were fixed and stained with propidiuim iodide and run through FACS. The cell cycle profile shows no significant cell death in TRF2 depleted cells. **(C)** U2OS cells were electroporated with control oligo or TRF2 oligo and PFA-fixed at 48 hours. The images show TRF2 (green) and PML (red), MRE11 (red), and TRF1 (red, green) stained by immunofluorescence using an anti-TRF2 antibody, anti-PML antibody, anti-MRE11 antibody and an anti-TRF1 antibody respectively. Nuclei were counterstained with DAPI (blue).

4.4 Discussion

Previous reports have implied that the integrity of PML nuclear bodies is important for different cellular functions, from differentiation to induction of cellular senescence. The precise function of PML has not been found, however it has been implicated in many cellular processes such as transformation suppression, apoptosis and growth control. The involvement in such a variety of cellular processes has been attributed to its role in the formation of nuclear bodies and its association with the proteins within this complex. By contrast, the role of PML in APB formation and in general in ALT cells has not been defined. Although the essential components of these bodies have not been determined, it is reasonable to believe that PML is important for the formation of these nuclear structures. Transient down-regulation of PML using siRNA enabled a significant, although not complete, decrease of PML protein to be obtained. The incomplete dowregulation was possibly due to the large number of isoforms present, making it more difficult for a RNAi oligonucleotide to target all of them uniformly. There are many other factors that could influence the siRNA efficiency such as the secondary structures of the sense and anti-sense strands of the siRNA, secondary structures of target mRNAs, and sequence characteristics of siRNAs and specificity of siRNA to its target. A list of criteria have be developed to ensure maximum efficiency of the siRNA designed (Reynolds et al., 2004). However, many siRNAs have been published that do not comply with these rules. A number of groups suggest that the structure at the target site may influence siRNA activity (reviewed in (Kurreck, 2006). A parameter for target site accessibility was developed by Luo and Chang (Luo and

Chang, 2004), where the number of hydrogen bonds formed between nucleotides in the target region and the rest of the mRNA were taken into account. It was found that there was an inverse correlation with the value of the "hydrogen bond index" and gene silencing effect. More recently it was found that the thermodynamic properties of the siRNA were also important for efficiency. Schubert *et al.* recently proposed a model in which asymmetric strand incorporation into the RISC is controlled by the thermodynamic properties of the siRNA and the accessibility of the target site may further control efficiency of silencing (Schubert et al., 2005). However, even if all the criteria are followed there are some targets that are refractory to RNAi-mediated silencing possibly due to the presence of stable secondary structures making the binding region inaccessible. All the factors suggested to take into consideration upon siRNA design still do not provide specific guidelines to make an efficient siRNA. Despite incomplete down-regulation of PML, there were a large number of cells in which PML nuclear speckles were no longer visible allowing us to establish any effects on APB composition. However, this was mainly clear using a mouse anti-PML antibody, while a rabbit anti-PML antibody revealed a background PML staining, which indicated that silencing was not complete (work in progress in the laboratory).

Despite these shortcomings, we decided to study the distribution of selected APB components in cells lacking, at least partially, PML expression. We found that in the absence of PML MRE11 association with APBs was reduced. This protein is part of a DNA damage response complex along with NBS1 and RAD50 (MRN complex). Previous reports have highlighted the importance of this complex, or specific members, for the correct assembly of APBs. NBS1 has been implicated in the recruitment of MRE11/Rad50 and BRCA1 to APBs (Wu et al., 2003). This work shows that in the absence of the correct recruitment of the abovementioned proteins to APBs there is not BrdU incorporation at APBs and long-term expression of NBS1 truncation mutants, which cause the delocalization of endogenous NBS1, leads to cell death suggesting that the correct assembly of these proteins into APBs plays a role in growth and proliferation of ALT cells. A recent report by Wei-Qin Jiang *et al.* (Jiang et al., 2005) proposed that overexpression of SP100, a known component of PML nuclear bodies, leads to the sequestration of the MRN complex which in turn leads to the inhibition of ALT. This was determined by a progressive telomere shortening of 121bp per

population doubling, a rate similar to that seen in telomerase-negative cells. Rapid telomere length changes were no longer seen and APBs were also no longer present within the nuclei of these cells. This effect was not seen in cells in which a C-terminal truncated mutant of Sp100 no longer able to bind the MRN complex was present. Proposing an essential role for this protein complex for the maintenance of ALT (Jiang et al., 2005). A more recent study by Jiang *et al.* demonstrated that in the absence of PML APB formation was reduced by up to 90% in cells lacking PML speckles. The authors suggest that PML is essential for the formation of APBs (Jiang et al., 2007). Our data suggest that PML is also important for the localization of MRE11 to APBs. Further studies on the effects of long-term PML down-regulation dissociation need to be carried out to determine any significant effects on the ALT mechanism.

TRF1 was also found to partially dissociate from APBs in the presence of reduced levels of PML. This protein is important for telomere maintenance. It is believed that TRF1 regulates telomere length through manipulation of telomerase activity. The longer the telomere, the greater the amount of TRF1 bound and telomerase activity is blocked. Conversely a short telomere has less TRF1 and has a greater chance of being elongated (Smogorzewska and de Lange, 2004). The role for TRF1 in telomere length appears important in cells that have active telomerase. ALT cells are believed to elongate telomeres through recombination and so the importance of TRF1 may be diminished in such an environment. A study carried out by Wu *et al.* also showed that upon alteration of APB status TRF1 was delocalized (Wu et al., 2003). However, they suggest that TRF1 is not critical for the localization of NBS1 or other associated proteins to APBs. These reports imply that TRF1 is not an important protein for the formation of APBs and telomere elongation in the absence of telomerase. Conversely, a more recent report demonstrated that TRF1 was an important component of APBs. Using siRNA against TRF1 and double labelling for PML/TRF2 and PNA/PML the authors suggest that there is a significant suppression of APBs (Jiang et al., 2007). A more detailed investigation into the role of TRF1 in APB formation is necessary in order to clarify its role.

TRF2 is an important protein in telomere maintenance and protection. It is known to be involved in the formation of the t-loop, and the absence of this protein leads to genetic instability and eventually senescence or cell death. Overexpression of this protein leads

to enhanced telomere attrition in primary human fibroblasts (Karlseder et al., 2002). This suggests that TRF2 can act as a negative regulator of telomere length. Upon PML down-regulation, we did not see any alteration in TRF2 localization to large or small speckles. Our data contradicts that reported by Jiang *et al.* In this report it is suggested that in the absence of PML TRF2 is no longer seen in nuclear speckles (Jiang et al., 2007). The authors use TRF2 as a marker for APBs in the absence of PML, where they report an almost complete reduction of APBs. However, the reason for disparate results could be that in order to enhance APBs cells were methionine restricted, whereas we report the effect of PML down-regulation in untreated cells. Alternatively we may not see a delocalization of TRF2 because it is not tightly associated with PML or simply that there was only a marginal displacement of TRF2 that was not detectable by immunofluorescence.

It has been shown that TRF1 forms a separate complex to TRF2 and that the two proteins do not directly interact but are linked through TIN2. Therefore the absence of an effect on TRF1 localization upon TRF2 down-regulation is not surprising. A small fraction of MRE11, on the other hand, has been reported to interact with TRF2 (Zhu et al., 2000). Therefore it would be logical to believe that there would be an effect on MRE11 in the absence of TRF2. This is not the case. PML is also unaffected by the lack of TRF2. We are in a position to exclude off-target effects of the RNAi oligo, because we confirmed the partial displacement of MRE11 and TRF1, and the lack of effect on TRF2 using two separate RNAi oligos targeting two different exons. Nevertheless, this effect could be due to transient down-regulation of PML and not be maintained in the long term.

4.5 Summary

This study determined the effect of PML and TRF2 transient down-regulation on the formation of APBs. PML was found to have an effect on the localization of MRE11 and TRF1 but not on TRF2. Vice versa, down-regulation of TRF2 was found not to affect the localization of these proteins. The data suggests that PML is also an important structural component for APB formation. The above data suggest that there may be two principal components necessary for the correct formation of APBs. The use of siRNA has only allowed the investigation of short term effects in the absence of PML and TRF2. To establish if the delocalization seen upon transient down-regulation is due to the disruption of a cellular process, such as telomere elongation, it is necessary to achieve stable down-regulation of TRF2 and PML. This will allow us to study effects on cell survival and morphology along with any effects on telomere maintenance and the ALT mechanism. To this end, we decided to downregulate PML and TRF2 using expression vectors encoding the relevant RNAi oligonucleotides and produce stable lines. This will be the subject of the next chapter.

Chapter 5) Stable Down-regulation of APB Components in an ALT Background.

5.1 Introduction

Primary cells can replicate a finite number of times and this is determined via the continuous erosion of telomeres every population doubling. During cell division short RNAs are used to prime DNA synthesis. Removal of these primers results in the formation of 8-12 nucleotide gaps, which do not pose a problem for circular genomes because each gap can be closed by extending a preceding Okazaki fragment. On a linear genome, the last RNA to prime lagging-strand synthesis will leave a gap that can not be filled in the absence of telomere maintenance mechanisms. There is a loss of 50-150bp/end/cell division in mammalian cells (Smogorzewska and de Lange, 2004), which eventually leads to senescence and apoptosis due to the activation of various cellular checkpoints. The biological and genomic consequences of telomere shortening have been well documented (Allsopp et al., 1992; Harley et al., 1990). Telomere length stabilization is required for cellular immortality. The great majority of cancers escape the limitations imposed by normal telomere shortening via activation of telomere maintenance mechanisms.

Although telomerase appears to be responsible for telomere maintenance in most cases, approximately 5% of human cancers have no detectable telomerase activity (Shay and Bacchetti, 1997) and appear to maintain their telomeres through Alternative Lengthening of Telomeres (ALT). One of the hallmarks of ALT is the appearance of ALT-associated PML-Nuclear bodies (APBs) of which PML is a component. PML has been implicated in the control of key tumor suppressive pathways and loss of expression is frequent in human cancers of various histological origins (Gurrieri et al., 2004; Rego et al., 2001). Evidence suggests that PML is important for the maintenance of correct cellular functions and that its disruption leads to de-regulation of many cellular processes such as tumor suppression and programmed cell death, thus increasing tumorigenic potential of cells. It is not clear what role PML plays in ALT cells and, for instance, whether it has tumour suppressive functions also in this context. It is also conceivable that in ALT cells PML may adopt a different role. In this respect, the function of the APBs in telomere maintenance is unclear, as it is unclear what role PML plays in it. It is important to note that a temporal correlation has been found between the immortalization event and the appearance of APBs. APBs have been found

only in ALT positive cell lines and tumours and not in mortal or telomerase positive cells (Yeager et al., 1999). A more recent report by Blanco and colleagues found that in telomerase null mice in which TRF2 (a telomere capping protein and APB component) was overexpressed, tumours with characteristics of ALT appeared and there was an increase in APBs. Conversely, when ALT is repressed APBs have been found to disappear. Somatic cell hybrids between telomerase positive cells and ALT cells caused ALT to be repressed and APBs to disappear (Perrem et al., 2001). More recently the disruption of these nuclear structures through the overexpression of sp100 was found to inhibit ALT (Jiang et al., 2005). These data strongly link APBs and ALT. It is possible that the function of APBs is to repair telomeric DNA that is recognized as genomic damage by the cell. However, a defined role for APBs has yet to be determined and it is possible that PML is involved in co-ordinating the function of these nuclear structures.

TRF2, another known component of APBs, is a sequence specific DNA binding protein that binds the duplex array of TTAGGG repeats at human telomeres. It has been shown to protect telomeres from end-to-end fusions through the formation of the t-loop (de Lange, 2002). The overexpression of TRF2 has been shown to cause telomere attrition (Blanco et al., 2007; Karlseder et al., 2002). Evidence has recently emerged suggesting a role for TRF2 as an oncogene in the absence of telomerase. Blanco and co-workers have reported that increased expression of TRF2 in telomerase deficient mice accelerated carcinogenesis and augmented telomere recombination implying TRF2 favoured the activation of ALT (Blanco et al., 2007). The overexpression of TRF2 has been shown to delay the onset of senescence by protecting critically short telomeres from fusion and repressing chromosome end-to-end fusions in pre-senescent cultures through the non-homologous end joining (NHEJ) mechanism (Karlseder et al., 1999; Karlseder et al., 2002; van Steensel et al., 1998). Uncapped telomeres resemble double strand breaks and it is the presence of the telomere capping complex, sheltrin (de Lange, 2005) that circumvents the activation of a DNA damage response. Despite these advances in understanding TRF2 functions, its role in ALT cells is presently unknown.

The aim of this study was to determine any effects on telomere maintenance in ALT in the absence of two APB components, PML and TRF2. Using vectors with shRNAs against either PML or TRF2 we were able to obtain U2OS clones stably expressing the short hairpin and significantly downregulating PML and TRF2 protein levels. We found

that there was no significant difference in clonogenicity between PML clones and control but there was a reduction in clonogenicity in TRF2 clones. TRF2 depleted clones still maintained MRE11 and TRF1 nuclear speckles, as seen in transient downregulation. Telomere length was altered in the absence of TRF2 but no significant difference was seen in PML depleted clones. TRF2 depleted clones were also found to be altered phenotypically with many multi-nucleated cells present and cells generally being larger than those of control clones.

5.2 Materials and Methods.

Detailed methodology of shRNA transfection, colony forming assays, single cell cloning, FACS, Western Southern blotting and immunofluorescence techniques can be found in Chapter 2.

5.3 Results

5.3.1 Stable Transfection of shRNA against PML and TRF2 in U2OS Cells

Elimination of PML is known not to affect cell viability, and $PML^{-/-}$ mice develop like normal littermates (Wang et al., 1998a). TRF2 depletion has been shown to cause cell death and senescence in tumor cell lines and primary cells, respectively (Karlseder et al., 1999; Karlseder et al., 2004b; Karlseder et al., 2002). The p53-proficient U2OS cell line was chosen to determine the effects of PML and TRF2 down-regulation on cell viability, proliferation and telomere length. U2OS are a well-characterized tumour cell line and derive from osteosarcoma, a tumor type believed to more readily activate ALT rather than telomerase. U2OS cells were transfected with shRNAs against PML (PML), TRF2 (T2) and an empty vector control (pRS). After a week of selection cells were fixed and stained with crystal violet to visualize colonies and determine an effect on cell viability (Figure 5.1a). The number of colonies was counted for cells transfected with the PML, TRF2 or control empty vector pRS. We found that cells transfected with the PML shRNA formed a similar number of colonies to control cells (Figure5.1a). Whereas, TRF2 shRNA transfected cells displayed a marked decrease in the number of

colonies formed (Figure 5.1a). It is important to note that cells lacking TRF2 were still able to form viable colonies, which could be further expanded.

To enable a closer examination of the effect of PML and TRF2 down-regulation on telomere length, single cell clones were picked and expanded for screening. Western blot analysis of cell lysates from each clone allowed us to determine which ones displayed the best down-regulation (Fig 5.1b). U2OS cells were transfected with two oligos against PML the first directed against the nuclear localization signal on exon VI (P-all), thus ensuring that all nuclear isoforms were targeted. The second was designed against exon II (EX2), which all PML isoforms contain and thus should target both nuclear and cytoplasmic isoforms. More than fifty clones were picked for each oligonucleotide, and only one clone from each transfection was found to have some extent of PML down-regulation (P-all39 and EX2-14), when compared to pRS transfected control cells (Fig 5.1b left panel). Both clones displayed almost complete down-regulation of the PML isoforms below 110kDa in size. However, the 110kDa band signal remained strong. This higher molecular weight band corresponds to the longer PML isoforms that are believed to co-migrate, PML I and PML II. We were unable to determine any effects on APBs by immunofluorescence. Although PML levels were significantly decreased by WB, the majority of cells still displayed punctuate nuclear staining of PML. APBs have been described as being larger than PML-NBs (Jiang et al., 2007; Yeager et al., 1999). In both P-all and exoII 14 clones large bodies were no longer seen however cells displayed smaller PML nuclear speckles that still partially colocalized with both MRE11 and TRF1 (not shown). This made it hard to assess the effect of stable PML down-regulation on APB components and no clear conclusion could be drawn.

Contrary to data reported to date we were able to obtain viable clones that no longer had detectable levels of TRF2 protein (Fig 5.1b right panel). Numerous clones displayed varying amounts of TRF2 down-regulation, with some displaying no protein (G10, D2), some with intermediate levels (C3, D10, E11) and some displaying no alterations in TRF2 protein levels (F8, C5) that were used as controls. Clones F8 and G10 were selected to carry out further investigations, with F8 acting as a control and G10 as a TRF2–deficient clone. Further analysis on cell death was carried out on the F8 and G10 clones. Cells were expanded and prepared for propidium iodide staining and cell death

analysis using FACS. The cell cycle profiles showed that there was a modest increase in cell death in G10, the TRF2 null clone (Figure 5.1c). The cell cycle profile implies that the elimination of TRF2 in U2OS cells does not affect cell proliferation or cell death when compared to the control clones.

5.3.2 Elimination of TRF2 does Not Affect MRE11/TRF1 Localization but Does Alter Cell Morphology.

We have shown in chapter 2 that transient down-regulation of TRF2 does not have any apparent effect on the localization of MRE11, TRF1 or PML (Figure 4.2). Having found that TRF2 negative clones were viable we wanted to determine if the effect of stable TRF2 down-regulation was the same as that seen in transient down-regulation experiments. F8 and G10 clones were examined by immunofluorescence to determine the localization of the abovementioned proteins. G10 cells no longer showed TRF2 in a nuclear speckled pattern; however PML still remained in large and small bodies within the nucleus (Figure 5.2a). F8 cells maintained TRF2 in nuclear speckles that colocalized with PML. The same is true of MRE11 and TRF1. When G10 cells were analysed to determine the presence of MRE11/TRF1 colocalization we found that even in the absence of TRF2, MRE11 and TRF1 still colocalized as in F8 cells (Figure 5.2a). These results exclude that what was seen in transient was due to an artefact of transfection.

Figure 5.1

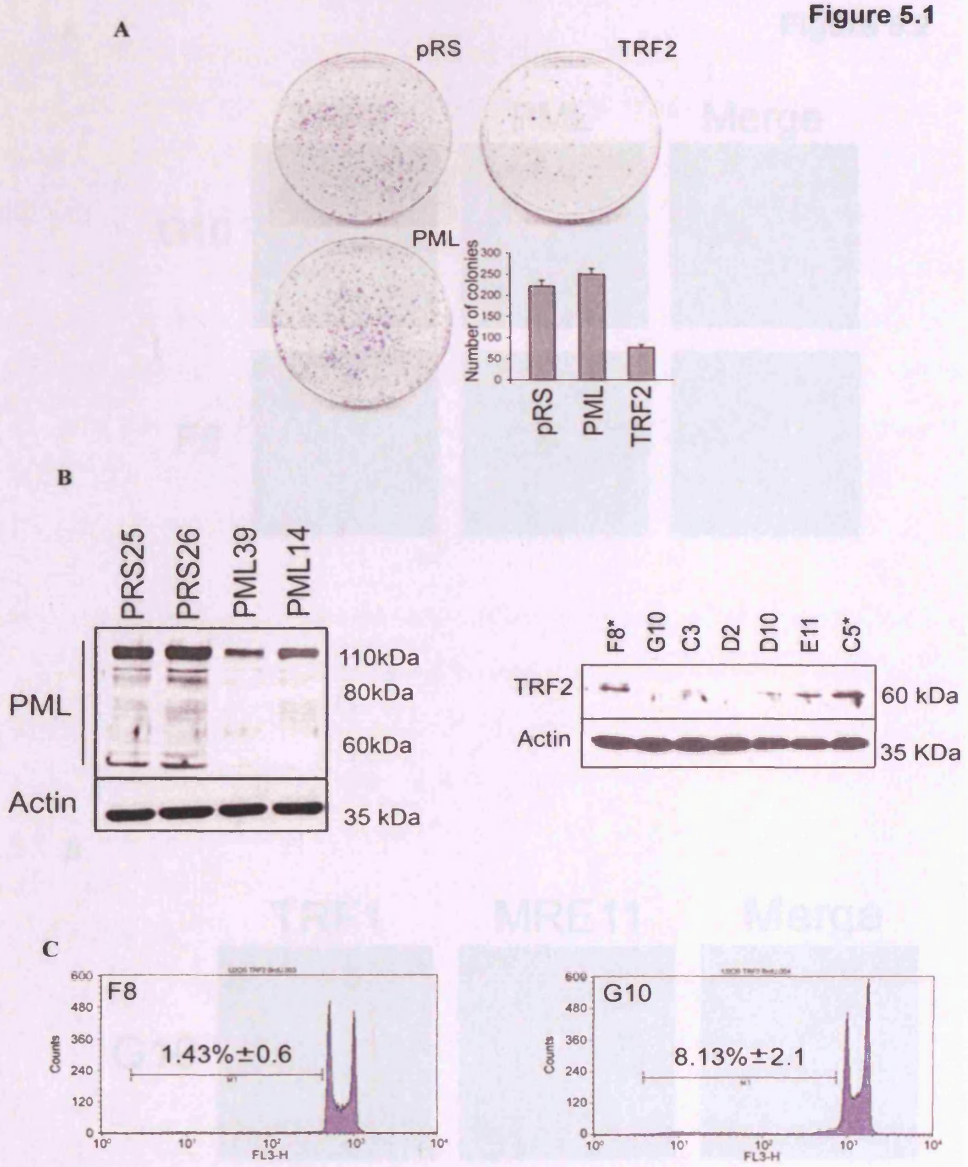

Figure 5.1 Stable depletion of PML and TRF2 by shRNA in U2OS cells. Cells were transfected with empty vector (PRS), PML oligos against exon II (II) and exon VI (P-all) or an oligo against TRF2 (T2). **(A)** U2OS cells were transfected with PRS, P-all or T2 and put in puromycin selection. Cells were methanol-fixed and stained with crystal violet to show the clonogenic potential of transfected cells. Number of colonies was quantified. Error bars represent ±1 standard deviation. **(B)** Clones were picked from cells transfected with PRS, P-all, II or T2 and lysates were collected. Western blot analysis showed that clone 39 of P-all transfected cells (P-all 39) and clone 14 of II transfected cells (PML 14) had depleted PML protein levels and. Western blot analysis of the lysates from TRF2 depleted clones showed some with no depletion (C5 and F8), partial depletion (C3, D10 and E11) and complete TRF2 depletion (G10). **(C)** Assessment of cell death induction in control F8 clone and TRF2 depleted G10 clone by FACS analysis no significant cell death in TRF2 depleted clone.

Figure 5.2

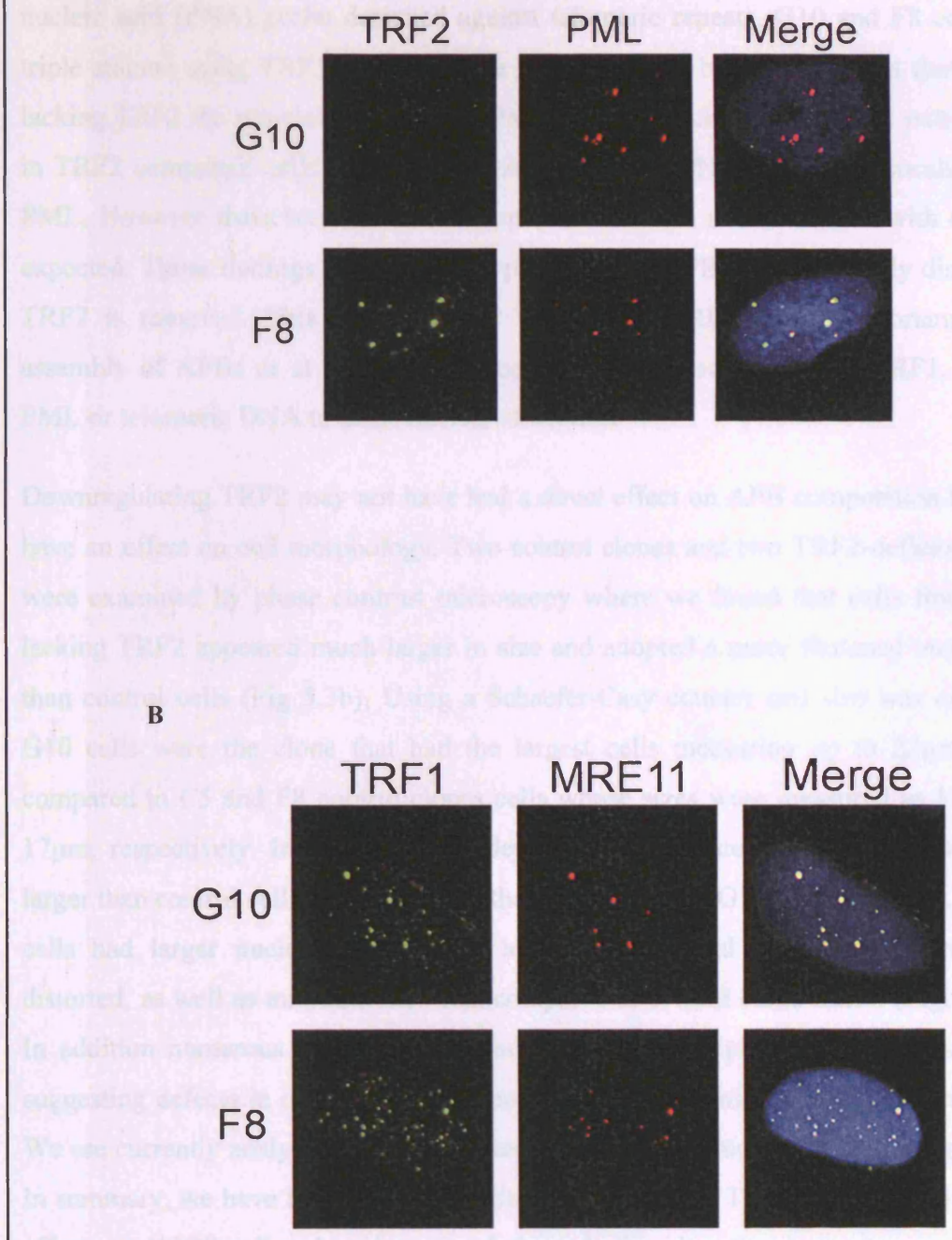

Figure 5.2 Stable TRF2 depletion does not affect MRE11, TRF1 or PML localization. Cells were PFA-fixed and stained by immunofluorescence using an anti-PML antibody, anti-TRF2 antibody, anti-TRF1 antibody and anti-MRE11 antibody. The merged confocal images of control TRF2 clone (F8) and TRF2 depleted clone (G10) determining the localization of TRF2 (green) and PML (red) **(A)** and TRF1 (green) and MRE11 (red) (**B**).

APBs are known to contain telomeric DNA. To ascertain that the nuclear speckles we were seeing in the absence of TRF2 did contain telomeric DNA we used a protein nucleic acid (PNA) probe designed against telomeric repeats. G10 and F8 cells were triple stained using TRF1, PML and the PNA probe. It became apparent that in cells lacking TRF2 the remaining TRF1 and PML nuclear speckles colocalized with PNA as in TRF2 competent cells (Figure 5.3a). All TRF1 and PNA speckles colocalized with PML, However there were some PML speckles that did not colocalize with either, as expected. These findings confirm our hypothesis that APBs are not clearly disrupted if TRF2 is removed. This reinforces our theory that TRF2 is not important for the assembly of APBs or at least is not necessary for the localization of TRF1, MRE11, PML or telomeric DNA to these nuclear structures.

Downregulating TRF2 may not have had a direct effect on APB composition but it did have an effect on cell morphology. Two control clones and two TRF2-deficient clones were examined by phase contrast microscopy where we found that cells from clones lacking TRF2 appeared much larger in size and adopted a more flattened morphology than control cells (Fig 5.3b). Using a Schaefer-Casy counter cell size was examined. G10 cells were the clone that had the largest cells measuring up to 22μm in size compared to C5 and F8 control clones cells whose sizes were measured as 16μm and 17μm, respectively. In another TRF2 depleted clone the cells were also found to be larger than control cells however not to the same degree as G10 cells (Figure 5.3c). G10 cells had larger nuclei that were no longer symmetrical but often elongated and distorted, as well as micronuclei, when compared to control clone nuclei (Figure 5.3d). In addition numerous G10 cells were seen to have multiple nuclei within each cell suggesting defects in cell division that could lead to genomic instability (Figure 5.3d). We are currently analyzing TRF2-depleted cells for the induction of endoreduplication. In summary, we have found that stable down-regulation of TRF2 had some unexpected effects on U2OS cell and nuclear morphology. Is this alteration in nuclear morphology due to an effect on telomere structure and/or maintenance?

Figure 5.3

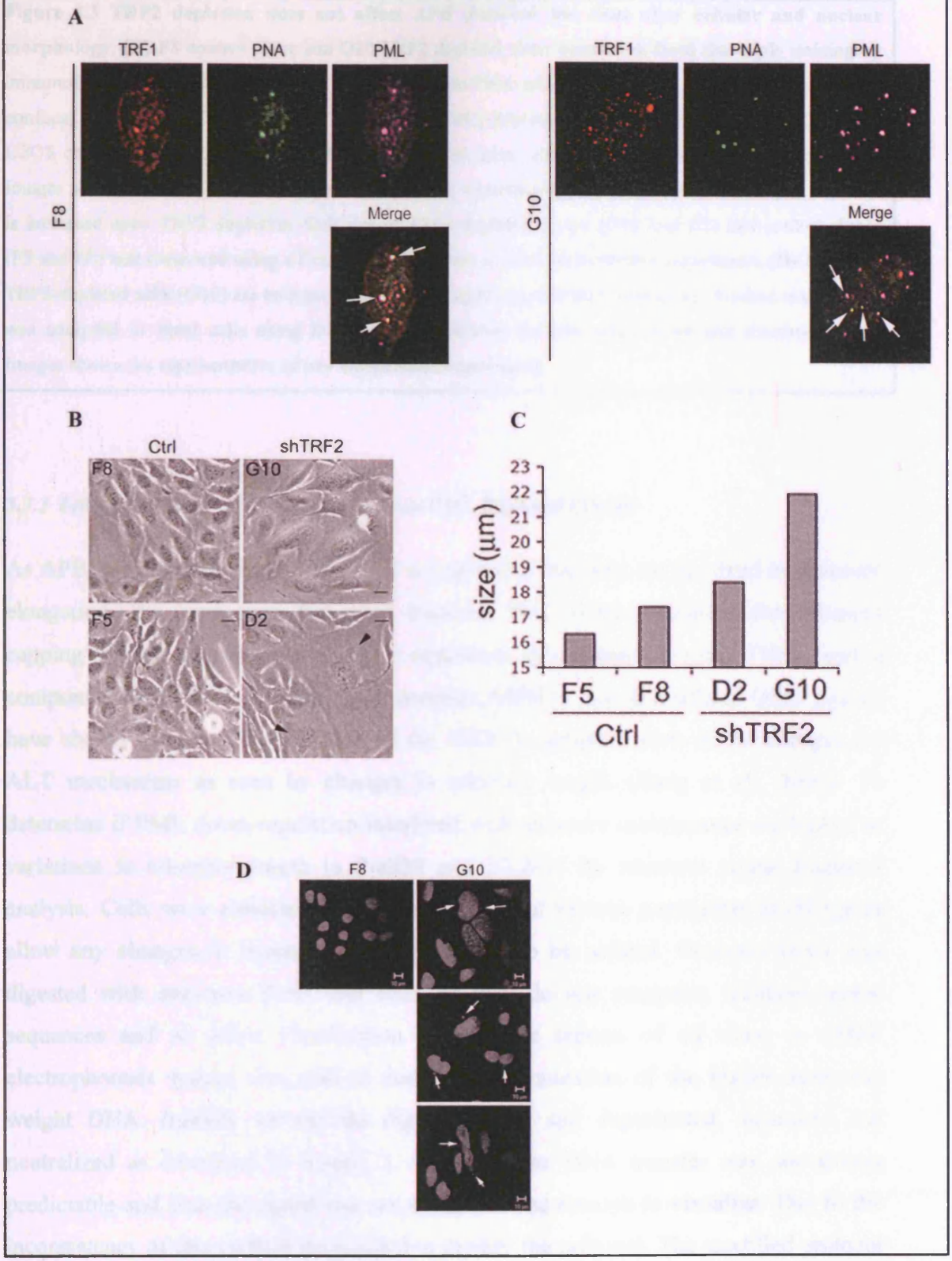
A
TRF1
PNA
PML
Merge
F8
G10
B
Ctrl
shTRF2
F8
G10
F5
D2
C
size (μm)
23
22
21
20
19
18
17
16
15
F5
F8
D2
G10
Ctrl
shTRF2
D
F8
G10

Figure 5.3 TRF2 depletion does not affect APB presence but does alter cellular and nuclear morphology. (A) F8 control clone and G10 TRF2 depleted clone were PFA-fixed and triple staining by immunofluorescence with TRF1 (red), PML (pink) and PNA probe (green) was performed. The merged confocal images show TRF1 and PML colocalize in TRF2-depleted cells and contain telomeric DNA. **(B)** U2OS cells lacking TRF2 (G10 and D2) are enlarged. Live cells were analyzed by light microscopy. Images shown are representative of three independent experiments. Bars represent 10 μM. **(C)** Cell size is increased upon TRF2 depletion. Cell size of TRF2 depleted clones (G10 and D2) and control clones (F5 and F8) was measured using a Coulter counter. Data of one representative experiment. **(D)** Nuclei of TRF2-depleted cells (G10) are enlarged, irregularly shaped and contain micronuclei. Nuclear morphology was analyzed in fixed cells using DAPI staining. Arrows indicate micronuclei and aberrant shapes. Images shown are representative of two independent experiments.

5.3.3 Telomere Repeat Fragment Analysis in PML Depleted Clones

As APBs appear with the onset of ALT it is possible that they are involved in telomere elongation. We have seen that upon transient PML down-regulation the telomere capping protein involved in negative regulation of telomere length, TRF1, and a component of the DNA damage repair complex, MRE11, are delocalized. Other reports have shown that the delocalization of the MRE11 complex from APBs disrupts the ALT mechanism as seen by changes in telomere length (Jiang et al., 2005). To determine if PML down-regulation interfered with telomere maintenance we looked at variations in telomere length in P-all39 and EX2-14 by telomere repeat fragment analysis. Cells were collected and DNA extracted at various population doublings to allow any changes in telomere length over time to be noticed. Genomic DNA was digested with enzymes HinfI and RsaI as they do not recognise telomere repeat sequences and so allow visualization of telomere repeats of all sizes. A CHEF electrophoresis system was used to ensure good separation of the higher molecular weight DNA. Initially we ran the digested DNA and depurinated, denatured and neutralized as described in chapter 2. However, the DNA transfer was not always predictable and thus the signal was not always strong enough to visualize. Due to the inconsistency of this method we decided to modify the protocol. The modified protocol substituted the depurination step with the gel being exposed to UV light, while

positively charged nylon membrane was used to transfer the DNA. These changes allowed clearer and more reliable data to be produced. Using the modified protocol we ran DNA samples from various population doublings of control and PML-downregulated samples (Fig 5.4). There is no clear difference in telomere length observed over time in the clones that lack PML when compared to control samples. Telomere lengths appear to remain stable. Both PML depleted clones display telomere lengths between 48kb and 6.5kb, much like control cells. The data from this study suggest that upon depletion of PML levels there is no significant difference in telomere maintenance over time. However it is important to note that PML was not completely downregulated in these clones.

Figure 5.4

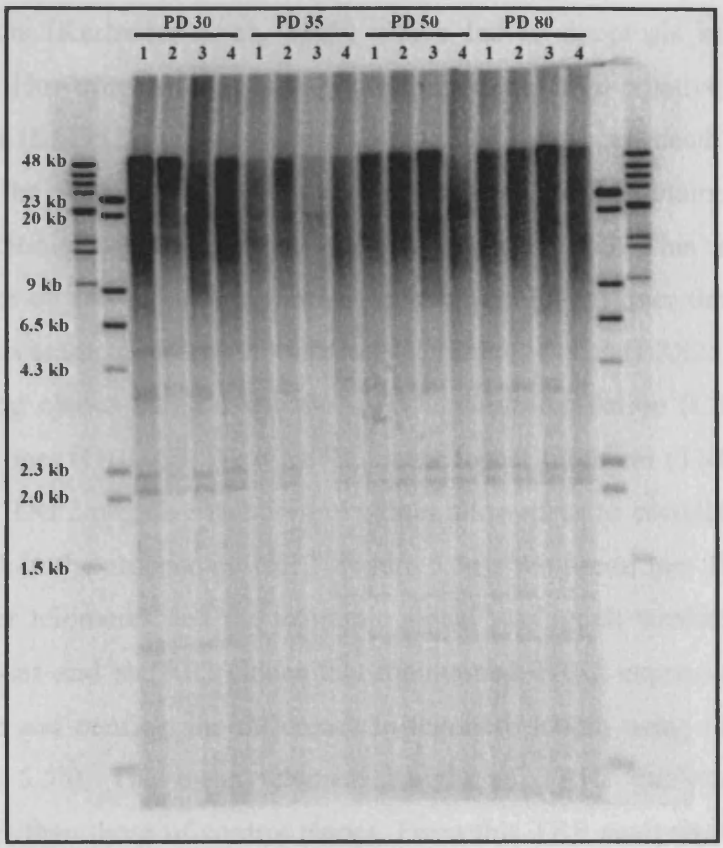

Figure 5.4 Telomere length changes in response to PML down-regulation. Southern blot of Hinf1/Rsa1 digested DNA from PML depleted clones with either P-ALL (lane 3) of EX2 (lane 4) and two control clones, pRS 25 (lane1) and pRS 26 (lane2). Each clone was passaged for 80 population doublings (PD) and samples were analysed at the indicated PDs. The blot was probed with a TTAGGG repeat probe to detect telomeric restriction fragments.

5.3.4 Telomere Repeat Fragment Analysis in TRF2 Depleted Clones.

To date there have been no reports of the effect of TRF2 down-regulation on telomere length in ALT. Overexpression studies have shown that there was an increased rate of telomere attrition in primary cells with little affect on the onset of senescence

(Karlseder et al., 2002). Other reports demonstrated that inhibition of TRF2 led to G-strand overhang loss and induced chromosome end fusions (van Steensel et al., 1998). There have been reports in which TRF2 has been inhibited through the use of dominant negative constructs (Karlseder et al., 1999) which led to apoptosis in a subset of mammalian cells. However this was done primarily in telomerase positive cells and the one ALT cell line (SAOS2) that was used showed no effect on cell death and this was said to be due to the absence of p53. By contrast, we were able to obtain stable TRF2-negative U2OS clones that were viable in the presence of p53. This allowed us to examine the effect of TRF2 down-regulation on telomere length over time in an ALT cell line. DNA was extracted from empty vector expressing clones (PRS25 and PRS26), shTRF2-expressing clones that did not show TRF2 down-regulation (C5, F8) and on TRF2-depleted clones (G10, C3, D2, C8). Telomere repeat fragment (TRF) analysis of DNA taken from TRF2 negative and control clones allowed us to establish differences in telomere length in the absence of TRF2 (Figure 5.5a). We found that TRF2 depleted clones had shorter telomeres and the telomeric signal was much weaker than that of empty vector clones and shTRF2 clones that maintained TRF2 expression. We were able to quantitate and confirm the difference in telomere length using the Telometric software (Figure 5.5b). The mean telomere lengths of TRF2 depleted clones are noticeably smaller than those of control clones. From this TRF analysis it appears that the down-regulation of TRF2 has a negative effect on telomere length in ALT cells. To date no reports have shown what the effect of TRF2 down-regulation on telomere length in ALT cells is. The above data are the first to suggest an effect on telomere length in the absence of TRF2 in ALT cells. We are currently analyzing telomere length also by different means (FlowFISH) in TRF2-depleted clones.

Figure 5.5

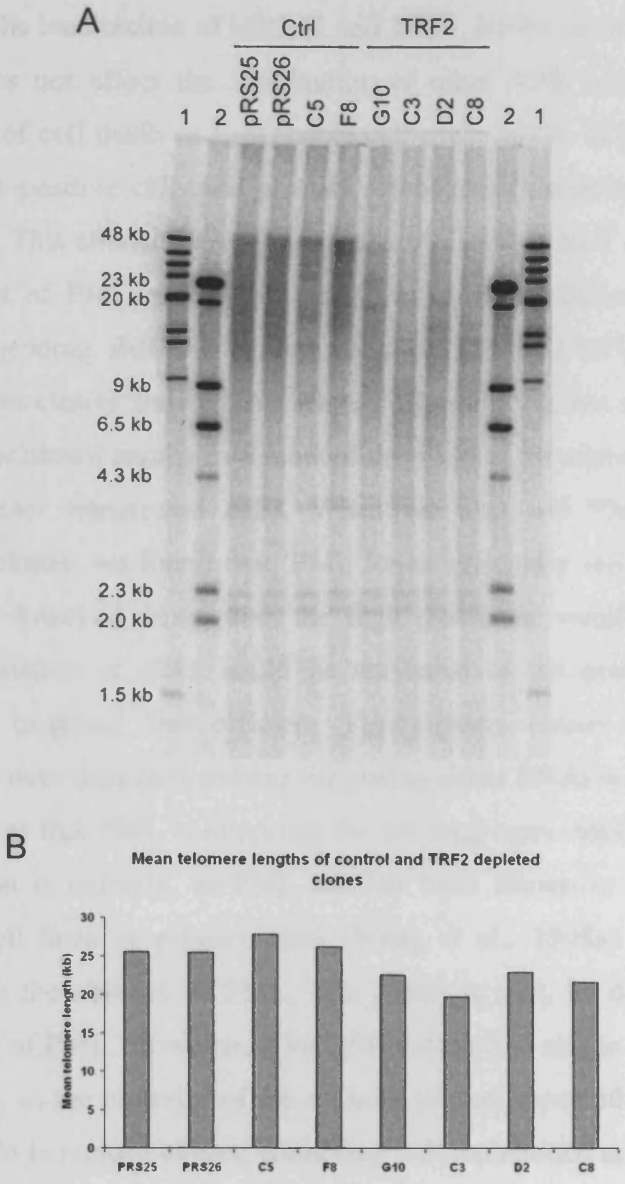

Figure 5.5 Telomere shortening in TRF2 depleted clones. Terminal restriction fragment length was analyzed by Southern blotting of genomic DNA from control empty vector transfected cells (pRS25 and pRS26) shRNA TRF2 transfected cells with no TRF2 depletion (C5 and F8) and TRF2 depleted cells (C3, C8, D2 and G10). **(B)** Telomere length analysis using the Telometrics programme, comparing control clones to TRF2 depleted clones. Mean telomere lengths of control clones (PRS25, PRS26, C5 and F8) differes from that of TRF2 depleted clones (G10, C3, D2 and C8).

5.4 Discussion

We previously determined the effect of transient PML and TRF2 silencing in U2OS cells. The results suggested that PML was an important component of APBs due to the effect on the localization of MRE11 and TRF1. However, we were surprised to find that TRF2 does not affect the localization of other APB components nor does it cause induction of cell death or irreversible cell cycle arrest, as previously demonstrated for telomerase-positive cells and primary fibroblasts (Karlseder et al., 1999; Karlseder et al., 2002). This alluded to a different role of TRF2 in ALT cells. In order to investigate the impact of PML and TRF2 long-term down-regulation, we stably overexpressed vectors encoding shRNAs against PML or TRF2 in U2OS cells. Colony formation experiments clearly showed that while PML silencing has no effect on colony number, TRF2 knockdown results in a marked decrease in the number of colonies compared to empty vector transfected cells. When we analyzed PML down-regulation in the resulting clones, we found that, PML lower molecular weight splice forms were more efficiently knocked down than the high molecular weight variants. The incomplete down-regulation of PML could be attributed to the presence of multiple isoforms rendering targeting less efficient. Furthermore, clones tend to lose PML down-regulation over time (not shown) suggesting either RNAi was not efficiently maintained over time or that PML is important for the long-term viability of ALT cells. The latter explanation is unlikely, as PML has not been shown to be required for survival of tumour cell lines or primary cells (Wang et al., 1998a) Colony formation was not affected in the absence of PML. This could, in part, be due to the incomplete down-regulation of PML. However, it was difficult to find single clones that displayed down-regulation, as the majority of the colonies picked appeared to have PML protein levels comparable to control clones, while they still maintained antibiotic resistance. The cells must therefore be capable of rejecting or silencing the construct over time. This phenomenon could happen in the majority of the selected cells. To test the role of PML in ALT, *Pml*$^{-/-}$ cells or animals could be used. However, this proved to be difficult as there are no reported reliable and faithful mouse models for ALT. For this reason we were dissuaded from using *Pml*$^{-/-}$ animals. A recent report has shown that TRF2 overexpression in the mouse skin appears to induce ALT in late-generation mice

lacking TERT (Blanco et al., 2007; Munoz et al., 2005). This mouse model could be crossed with *Pml*$^{-/-}$ mice in order to test the impact of Pml inactivation on ALT *in vivo*.

Several clones derived from U2OS cells transfected with TRF2 shRNA display a high degree of down-regulation, thus allowing us to analyze TRF2 function. This result is unexpected *per se*, as other reports have shown that TRF2 inactivation is incompatible with survival or proliferation in telomerase-positive cells, due to activation of DNA damage pathways (Karlseder et al., 1999; Karlseder et al., 2002) We found that TRF2 stable silencing did not affect PML colocalization with TRF1 and telomeric DNA, and the cell cycle analysis showed only few TRF2-depleted cells display apoptotic features (8-9%). These data contradict previous reports in which TRF2 functional inactivation led to rapid cell death in telomerase-positive cells (Karlseder et al., 1999). This study also included ALT SAOS2 cells that were proposed to be resistant to the cytotoxic effects of TRF2 inactivation due to p53 deficiency (Karlseder et al., 1999). Here we provide evidence to imply that p53 status cannot explain the observed lack of sensitivity as our study is carried out in U2OS cells, which possess an intact p53 pathway. TRF2 inactivation has been proposed to result in telomere uncapping, which in turn causes induction of genomic instability due to telomere fusions and consequent aberrant mitoses (Karlseder et al., 1999; van Steensel et al., 1998). Overall, our findings suggest that in ALT cells the telomere end structure could be different and/or that signalling originating at the telomere could be altered. We are currently investigating the induction of genomic instability in TRF2-depleted cells in order to determine if the effects of TRF2 depletion in ALT cells are similar to those seen in telomerase-positive and primary cells.

Upon examination of the effect of TRF2 down-regulation on telomere length we found that TRF2-depleted cells had shorter telomeres than controls. The telomeric signal seen by TRF was also less intense than that of control clones further suggesting a decrease of telomeric repeats in the absence of TRF2. Our data suggest that TRF2 plays a role in inhibition of telomere erosion. Reports have shown that TRF2 is important for the inhibition of non-homologous-end-joining (NHEJ) at chromosome ends (Smogorzewska and de Lange, 2002; van Steensel et al., 1998; Zhu et al., 2003) and is also able to limit homologous recombination (HR) (Wang et al., 2004). Wang *et al.* suggested that HR could contribute to telomere attrition as they observed telomeric

DNA circles in undisturbed cells. They also noted that there was a larger number of telomeric DNA circles in ALT cells and suggested that this was due to ALT cells having increase HR, which in the absence of telomerase could aid telomere maintenance. Our data suggest that TRF2 may be involved in limiting HR in ALT cells, hindering telomere erosion and promoting telomere lengthening. A recent report by Blanco *et al.* demonstrated that in the absence of telomerase overexpression of TRF2 resulted in telomere attrition in mouse keratinocytes (Blanco et al., 2007). It cannot be excluded that overexpression of TRF2 could affect the telomere end structure, thus affecting ALT. Interestingly, late-generation telomerase null / TRF2 animals were found to develop tumours with characteristic features of ALT, suggesting that in the presence of critically short telomeres TRF2 could stimulate the activation of ALT to maintain telomeric integrity. The minisatellite MS32 has been shown to be highly unstable in ALT cells (Jeyapalan et al., 2005). In future, it would be interesting to see if TRF2 inhibition affected the degree of instability.

Another characteristic of TRF2-deficient clones is that nuclear morphology is aberrant and nuclei are greatly enlarged. Several micronuclei are also present, a phenomenon which could due to aneuploidy or supernumerary centrosomes (Lazzerini Denchi et al., 2006). The overall cell diameter is also enlarged. Interestingly, a very recent report showed that TRF2 conditional inactivation in the regenerating mouse liver does not lead to cell death or senescence, but rather causes an increase of cell size very likely due to endoreduplication (Lazzerini Denchi et al., 2006).

5.5 Summary

In summary, we were able to obtain clones that display stable down-regulation of TRF2, while complete PML down-regulation was not achieved. Consequently, we were unable to detect any apparent changes in telomere length in PML depleted cells. In contrast, TRF2-depleted cells displayed altered cellular and nuclear morphology and form less colonies in a colony-forming assay. However, this was not due to induction of cell death, thus suggesting that in ALT cell lines, unlike in telomerase-positive cell lines, disruption of shelterin does not results in apoptosis. Importantly, we were able to detect changes in telomere length in TRF2-depleted clones. We found that in the

absence of TRF2, ALT cells had shorter telomeres and the intensity of the telomeric signal was also decreased. Taken together our data suggest a role for TRF2 in telomere elongation in the absence of telomerase.

Chapter 6) A Role of the ATM DNA Damage Response in ALT Cells

6.1 Introduction

DNA damage activates a multitude of signalling cascades that allow cells to either repair the damage or, if the break is too severe, cause the cell to undergo apoptosis. Alterations in a number of DNA damage response proteins can cause telomere dysfunction and lead to chromosomal instability. This suggests extensive functional interactions between telomere maintenance and DNA damage response mechanisms. Double-strand breaks (DSBs) are particularly effective in triggering the DNA damage response. In healthy cells, functional telomeres are recognised as DSBs in G2 phase of the cell cycle. Consequently the DNA-damage response is partially activated (Verdun et al., 2005). The protein encoded by the ATM gene belongs to the Phosphatidylinositol 3 and 4 (PI3/PI4)-kinase family. This protein is an important cell cycle checkpoint kinase that functions as a regulator of a wide variety of downstream proteins, including tumor suppressor proteins p53 and BRCA1, checkpoint kinase CHK2, checkpoint proteins RAD17 and RAD9, and DNA repair protein NBS1. It is believed to be a master controller of cell cycle checkpoint signalling pathways that are required for cell response to DNA damage and for genome stability. Mutations in this gene are associated with ataxia telangiectasia, an autosomal recessive disorder characterized by neurodegeneration, cell cycle checkpoint defects, radiosensitivity and cancer predisposition (Scott et al., 2002). Savitsky *et al.* (Savitsky et al., 1995) showed that the 350.6kDa protein displayed significant sequence similarities to several yeast, *Drosophila*, and mammalian phosphatidylinositol 3-prime (PI-3) kinases that are involved in mitogenic signal transduction, meiotic recombination, detection of DNA damage, and cell cycle control. Mutations in these genes cause a variety of phenotypes with features similar to those observed in human ataxia-telangiectasia cells.

Bi *et al.* and others (Bi et al., 2004; Oikemus et al., 2004; Queiroz-Machado et al., 2001; Scott et al., 2002; Silva et al., 2004; Song et al., 2004) have shown that mutations in the telomere fusion gene (*tefu*), which encodes the *Drosophila melanogaster* ATM homolog, lead to telomere fusions resulting in genome instability. Furthermore, the Mre11 and Rad50 proteins, involved in DNA damage response and repair along-side ATM, have been shown to serve in *Drosophila* telomere protection. These results are interesting because normal *Drosophila* telomeres are not elongated by telomerase. The

end of a *Drosophila* chromosome is enriched with retrotransposable elements. These elements specifically transpose to chromosome ends, compensating for the loss of chromosome sequences that occur with each replication cycle (Abad et al., 2004; Mason and Biessmann, 1995). The telomere maintaining function of ATM, Mre11, and Rad50 appears to be evolutionarily conserved and could be independent of a telomerase implying an important function in telomere maintenance in ALT.

Upon DNA damage ATM is activated and in turn phosphorylates a number of targets including p53. Phosphorylation occurs on Ser 15 of p53 and this allows the activation and transcription of downstream targets such as p21. This DNA damage cascade has been shown to occur in cells undergoing senescence due to critically short telomeres (d'Adda di Fagagna et al., 2003; Herbig et al., 2004). Replicative senescence can be abrogated by suppressing both the p53 and the $p16^{Ink4a}$/Retinoblastoma (RB) pathways either with SV40 large T or the combination of human papilloma virus (HPV) proteins HPV16 E6 and E7 respectively, extending the lifespan of a given cell population (Shay et al., 1991; Shay and Wright, 1989).

Recent evidence has implicated TRF2 as an important participant in the regulation of the senescence signal. TRF2 is essential for the protection of chromosome ends (de Lange, 2005; van Steensel et al., 1998) and its removal can result in end-to-end fusions and induction of cell cycle arrest or apoptosis. For instance, Karlseder *et al.* demonstrated that the inhibition of TRF2 can lead to the activation of the ATM/p53 pathway and eventually cause apoptosis (Karlseder et al., 1999). In contrast the over-expression of TRF2 prolonged the replicative lifespan of primary fibroblasts through the protection of critically short telomeres (Karlseder et al., 2002). Celli and de Lange demonstrated that the activation of the ATM pathway at chromosome ends does not require overhang degradation or other obvious DNA processing, suggesting that it is simply the uncapping of the telomeres that is necessary (Celli and de Lange, 2005).

This chapter will attempt to study the activation status of ATM in ALT cells at both steady state and following TRF2 down-regulation. We found that ATM is constitutively active in ALT cells and partially co-localizes with PML, TRF2 and telomeric DNA. In

TRF2-depleted cells we demonstrate an increase in ATM nuclear foci and activation of p53 and its downstream target p21. However, p53 is no longer seen in discrete nuclear foci in the absence of TRF2.

6.2 Materials and Methods

Detailed methodology of caffeine treatment, immunofluorescence and Western blotting techniques can be found in Chapter 2. Quantification was carried out on approximately 100 cells per experiment. Volovity 4.1 (Improvision Ltd. 2007) was used to generate the counts. Objects were found by intensity (lower limit 1000, upper limit 4095) for both red and green channels. In order to identify regions of colocalization the intersect function was used allowing the green channel to intersect the red. Intensities may vary depending on the quality of the image.

6.3 Results

6.3.1 ATM is constitutively phosphorylated at Serine 1981 in ALT cells

Recent reports have shown that inactivation of TRF2 in telomerase-positive tumour cells or primary fibroblasts causes telomere uncapping, allowing them to be recognized as DNA damage sites. This results in ATM activation and induction of p53-dependent cell death or cellular senescence (d'Adda di Fagagna et al., 2003; Di Micco et al., 2006; Karlseder et al., 1999; Mallette et al., 2007). The effect of TRF2 down-regulation in ALT cells has yet to be determined. Consequently we analyzed ATM activation by using an antibody that recognises phosphorylated serine 1981, which is an accepted activation marker.

6.3.1.1 P-ATM in ALT cells

Interestingly we found that phosphorylated ATM (P-ATM) was present in nuclear speckles in ALT cells (Figure 6.1a). In order to determine the specificity of the P-ATM, U2OS cells were treated with caffeine, which is an inhibitor of ATM and ATR. In cells cultured in 10mM caffeine the P-ATM signal steadily decreased over time until it was

almost completely abolished after 45 minutes (Figure 6.1b). Having confirmed the specificity of the antibody we wanted to know if P-ATM colocalized with PML and more specifically if it was present in APBs. Triple staining of U2OS and SAOS-2 cells with PNA, ATM and either TRF2 or PML was used to determine the localization of P-ATM. The number of P-ATM speckles per nucleus was counted as well as the number of ATM speckles that colocalized with PNA and TRF2 or PNA and PML in order to determine the proportion of P-ATM speckles associated with APBs (Figure 6.2 and 6.3). We found that in U2OS cells the average number of ATM speckles per nucleus was 10 and approximately half of these were found to colocalize with PNA and PML (Figure 6.2b) there was no significant difference between the number of ATM speckles seen to colocalize only with PML and those that colocalize with both PML and PNA suggesting that half of the ATM found in speckles in the nucleus of U2OS cells is in APBs. We also looked at the percentage of ATM speckles that colocalized with TRF2 and ATM in U2OS and SAOS (Figure 6.3a) cells. Again, we see that approximately half of the ATM speckles colocalize with both TRF2 and PNA in both the examined cell lines (Figure 6.3b). These data suggest that P-ATM can localize to APBs as well as to non-telomeric DNA damage foci in ALT cells.

Figure 6.1

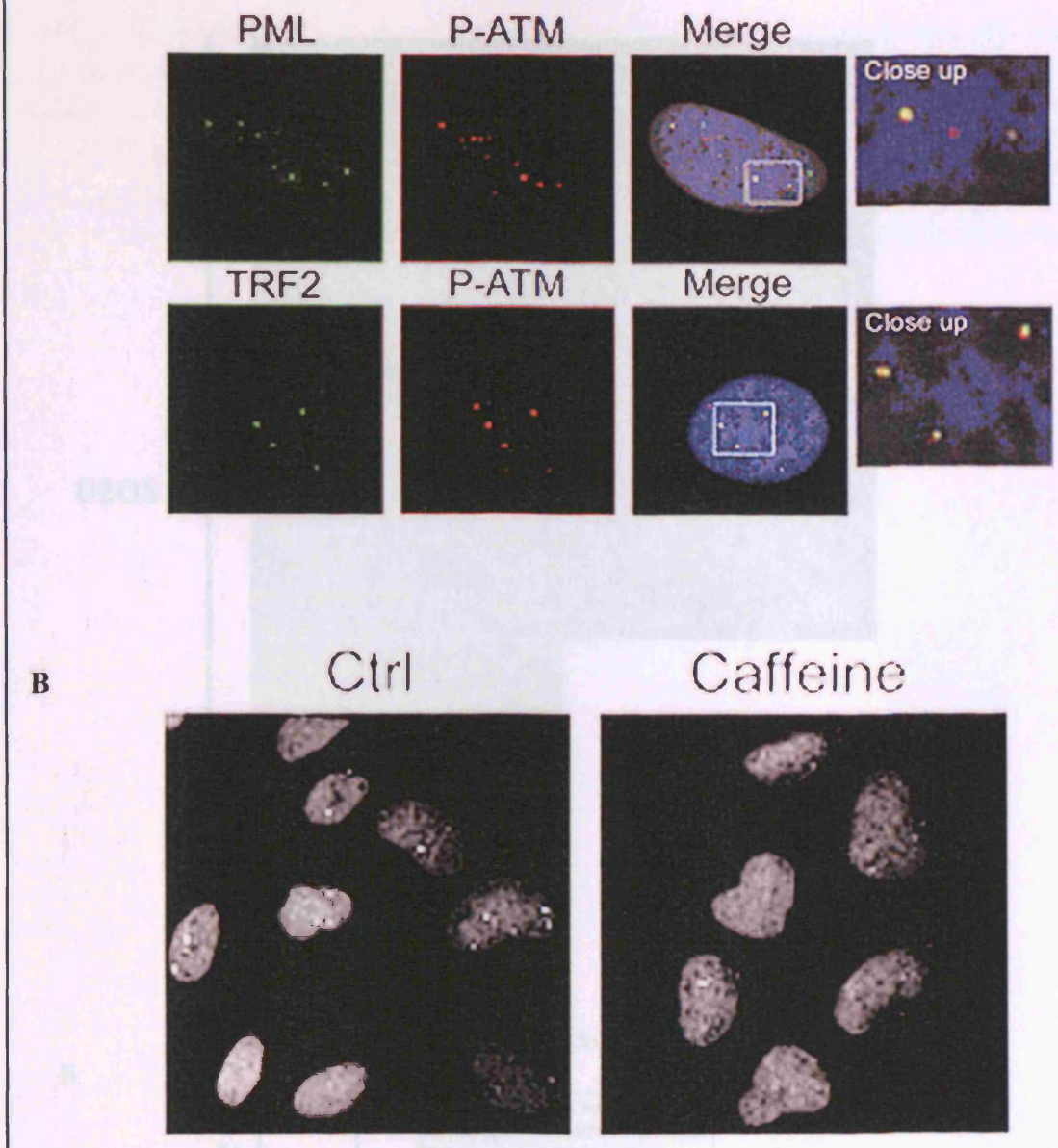

Figure 6.1 ATM is active and found in APBs in ALT cells. (A) U2OS cells were formalin-fixed and stained by immunofluorescence using an anti-PML antibody (green), an anti-TRF2 antibody (green) and an anti-S1981 ATM (P-ATM) antibody (red). The merged confocal images show P-ATM localization in nuclear speckles that colocalize with PML and TRF2. The nuclei are counterstained with DAPI (blue). (B) U2OS cells were treated with 10mM caffeine for 45 minutes, formalin-fixed and stained by immunofluorescence with an anti-S1981 ATM antibody. The confocal images demonstrate decreased P-ATM at APBs upon caffeine treatment.

Figure 6.2

A

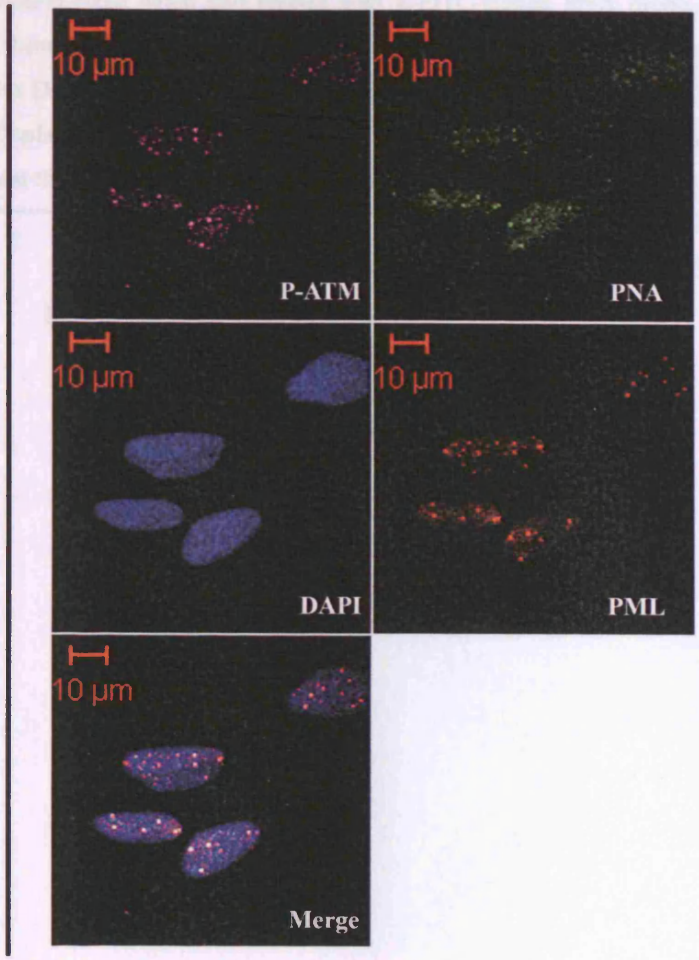

U2OS

B

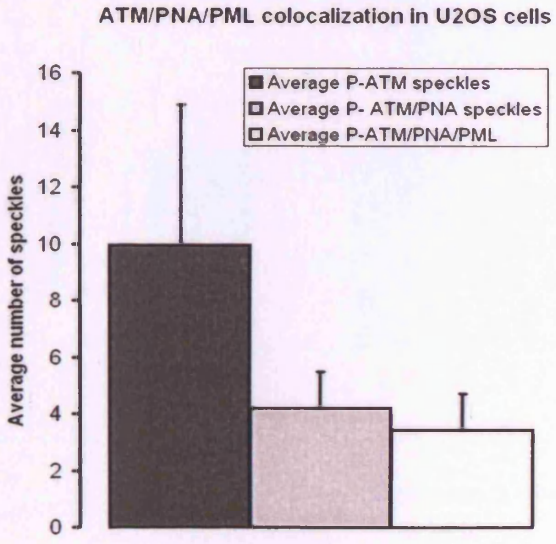

Figure 6.2 P-ATM colocalizes with PNA and PML in APBs. (A) U2OS cells were formalin-fixed and stained by immunofluorescence with an anti-PML antibody (red) and an anti-S1981 ATM antibody (P-ATM) (pink), formalin-fixed again and probed with a FITC-tagged PNA probe (green). The merged confocal image show P-ATM colocalizes with PML and PNA in nuclear speckles. Nuclei are counterstained with DAPI (blue). Size bars are in red. **(B)** The number of P-ATM speckles per nucleus and the number displaying colocalization with PNA or PML and PNA per nucleus were counted. Data are means of at least three experiments. Error bars are means ±1 standard deviation.

Figure 6.3

A

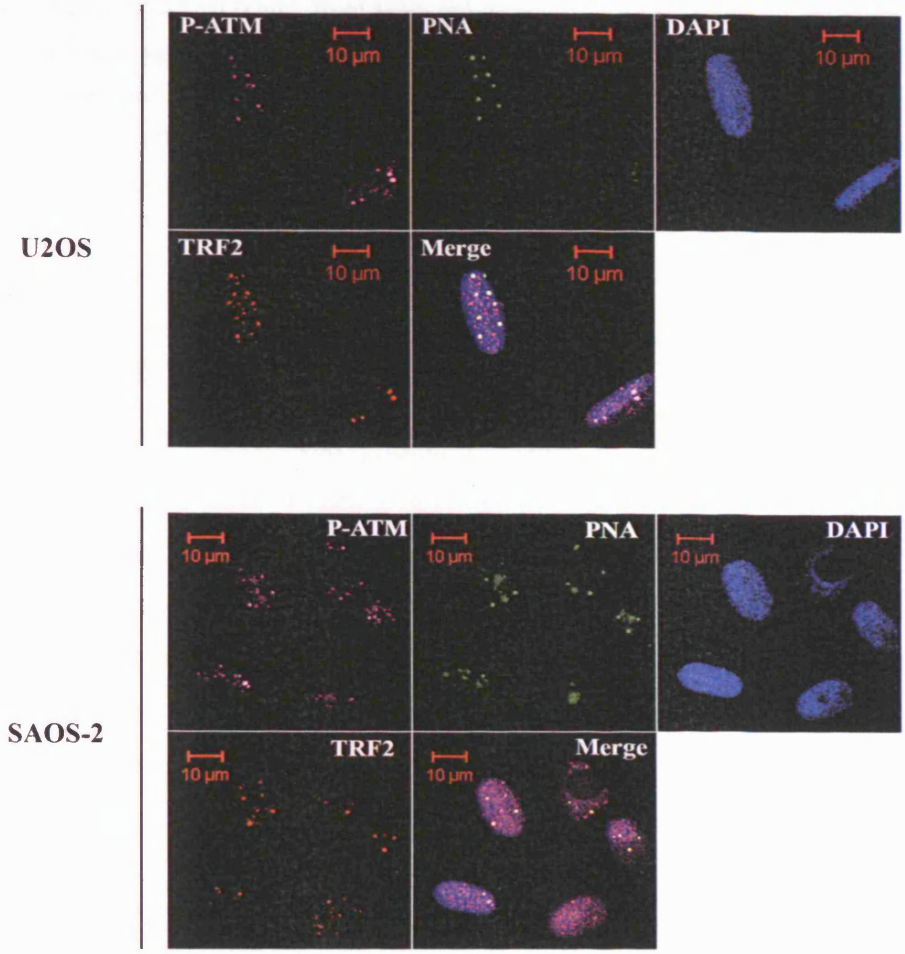
U2OS
P-ATM
PNA
DAPI
TRF2
Merge
SAOS-2
P-ATM
PNA
DAPI
TRF2
Merge
10 µm

B

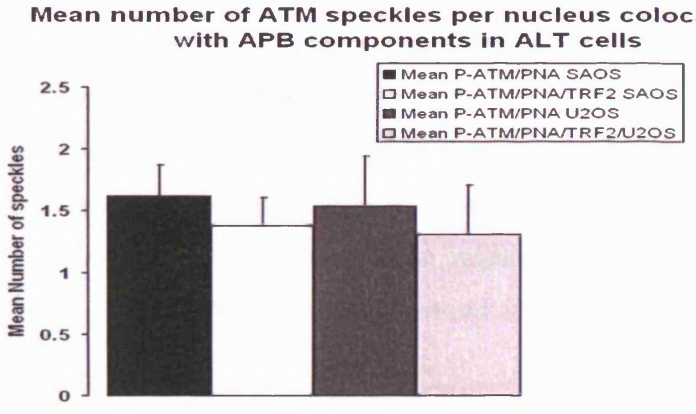
Mean number of ATM speckles per nucleus colocalizing with APB components in ALT cells
Mean P-ATM/PNA SAOS
Mean P-ATM/PNA/TRF2 SAOS
Mean P-ATM/PNA U2OS
Mean P-ATM/PNA/TRF2/U2OS
Mean Number of speckles
2.5
2
1.5
1
0.5
0

Figure 6.3 P-ATM is in APBs with PNA and TRF2 in SAOS and U2OS cells. (A) SAOS and U2OS cells were PFA-fixed and stained by immunofluorescence with an anti-TRF2 antibody (red), and ant-S1981 ATM antibody (P-ATM) (pink), fixed again and probed with a FITC-tagged PNA probe (PNA). The merged confocal images show P-ATM colocalizing with PNA and TRF2 in SAOS and U2OS cells. Nuclei are counterstained with DAPI (blue). Size bars are in red. **(B)** The number PNA and P-ATM colocalizing speckles or TRF2, PNA and P-ATM colocalizing speckles per nucleus were counted. Data are means of at least three experiments. Error bars are standard error of the mean.

6.3.1.2 P-ATM in TRF2 depleted cells.

Having established that ATM was present at APBs in an active conformation, as determined by the recognition of nuclear speckles by the phospho-specific antibody, we wanted to determine whether there was a difference in P-ATM localization in the absence of TRF2. ATM activation has been shown to occur in response to telomere damage. When telomeres become uncapped due to TRF2 inhibition, induction of apoptosis through the ATM/p53 pathway was reported (Karlseder et al., 1999). More recently, P-ATM was found to associate with telomeres upon inhibition of TRF2 (Takai et al., 2003). In this respect, we found a significant difference in the average number of P-ATM speckles seen in TRF2-depleted G10 versus control F8 cells (Figure 6.4a and c). TRF2 depleted cells had twice as many P-ATM nuclear speckles than control cells (Figure 6.4c). We went on to determine if there was also a difference in the proportion of P-ATM that colocalized with PML. We saw that there was a concomitant increase in the number of P-ATM/PML positive speckles in G10 TRF2-depleted cells compared to F8 control cells (Figure 6.4b and c). The above data suggest that, in the absence of TRF2, there is an increase in P-ATM and an increase in the amount of P-ATM/PML colocalization. However, it is likely that these additional ATM speckles are not localized to telomeres as the PNA staining observed in TRF2 depleted cells is very weak.

Figure 6.4

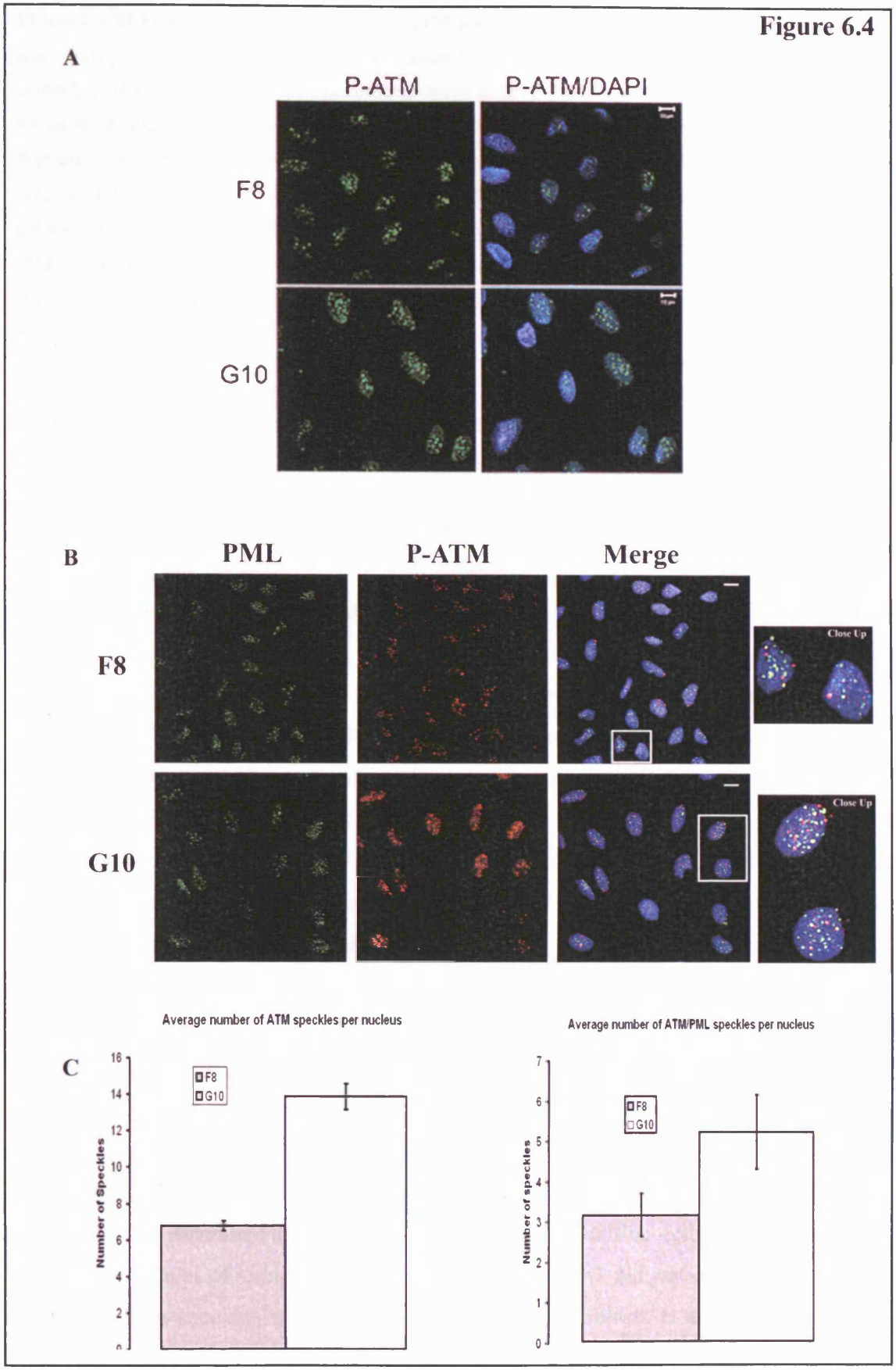
A
P-ATM
P-ATM/DAPI
F8
G10
B
PML
P-ATM
Merge
F8
G10
Close Up
Close Up
C
Average number of ATM speckles per nucleus
Number of Speckles
F8
G10
Average number of ATM/PML speckles per nucleus
Number of speckles
F8
G10

Figure 6.4 TRF2 depletion does not inhibit ATM phosphorylation. (A) TRF2 depleted clone (G10) and control clone (F8) were PFA-fixed and stained by immunofluorescence with anti-S1981 ATM antibody (P-ATM) (green).The merged confocal image shows P-ATM speckles present in both G10 and F8 nuclei. Nuclei are counterstained with DAPI (blue). Size bars are in the top right hand corner. **(B)** Formalin-fixed F8 and G10 cells were stained by immunofluorescence with an anti-PML antibody (green) and an anti-S1981 ATM antibody (P-ATM) (red). The merged confocal image shows colocalization of P-ATM with PML is not affected upon TRF2 depletion. Nuclei are counterstained with DAPI (blue). **(C)** The number of P-ATM speckles per nucleus (left panel) and the number of PML and P-ATM colocalizing speckles or per nucleus (right panel) were counted. Data are means of at least three experiments. Error bars are means ±1 standard deviation.

6.3.1.3 ATM targets and APBs

Activation of ATM due to DNA damage results in the activation of cell cycle checkpoints culminating in cell cycle arrest or apoptosis. It is believed that ATM autophosphorylation on serine 1981 is an important upstream event in the activation of these pathways. However, ATM does not appear to be a direct sensor of DNA damage (Banin et al., 1998; Smith et al., 1999; Suzuki et al., 1999) and several reports have suggested that the MRN complex is an upstream activator of ATM (Carson et al., 2003; Gatei et al., 2003; Uziel et al., 2003). NBS1, a component of the MRN complex, is phosphorylated by ATM on serine 343 at DSBs (Gatei et al., 2003). Our findings demonstrate that P-ATM is present in ALT cells at steady state and that a proportion of it is associated with APBs. We wanted to establish if ATM targets were also phosphorylated in ALT cells. We employed an antibody directed against ATM/ATR targets that recognises endogenous proteins containing the serine/threonine followed by a glutamine motif. ATM/ATR target nuclear speckles were found to colocalize with all P-ATM speckles (Figure 6.5a). We then looked more specifically at the phosphorylation status and localization patterns of a known ATM target and APB component, NBS1. A phospho-specific antibody directed against NBS1 enabled us to identify phosphorylated NBS1 in ALT cells that partially colocalized with PML (Figure 6.5a). To determine whether the presence of P-ATM in nuclear speckles was specific to ALT cells, we examined its localization in telomerase positive cells line and primary fibroblasts. Nuclei of telomerase-positive HeLa and MCF7 did not display ATM/ATR targets-positive speckles (Figure 6.5b). Primary BJ fibroblasts at early passage were also negative for P-ATM (Figure 6.5c.). In summary, our data clearly show that active

ATM is found in ALT cells at steady state, accumulates in APBs, and downstream targets are phosphorylated and partially colocalize with APBs.

Figure 6.5

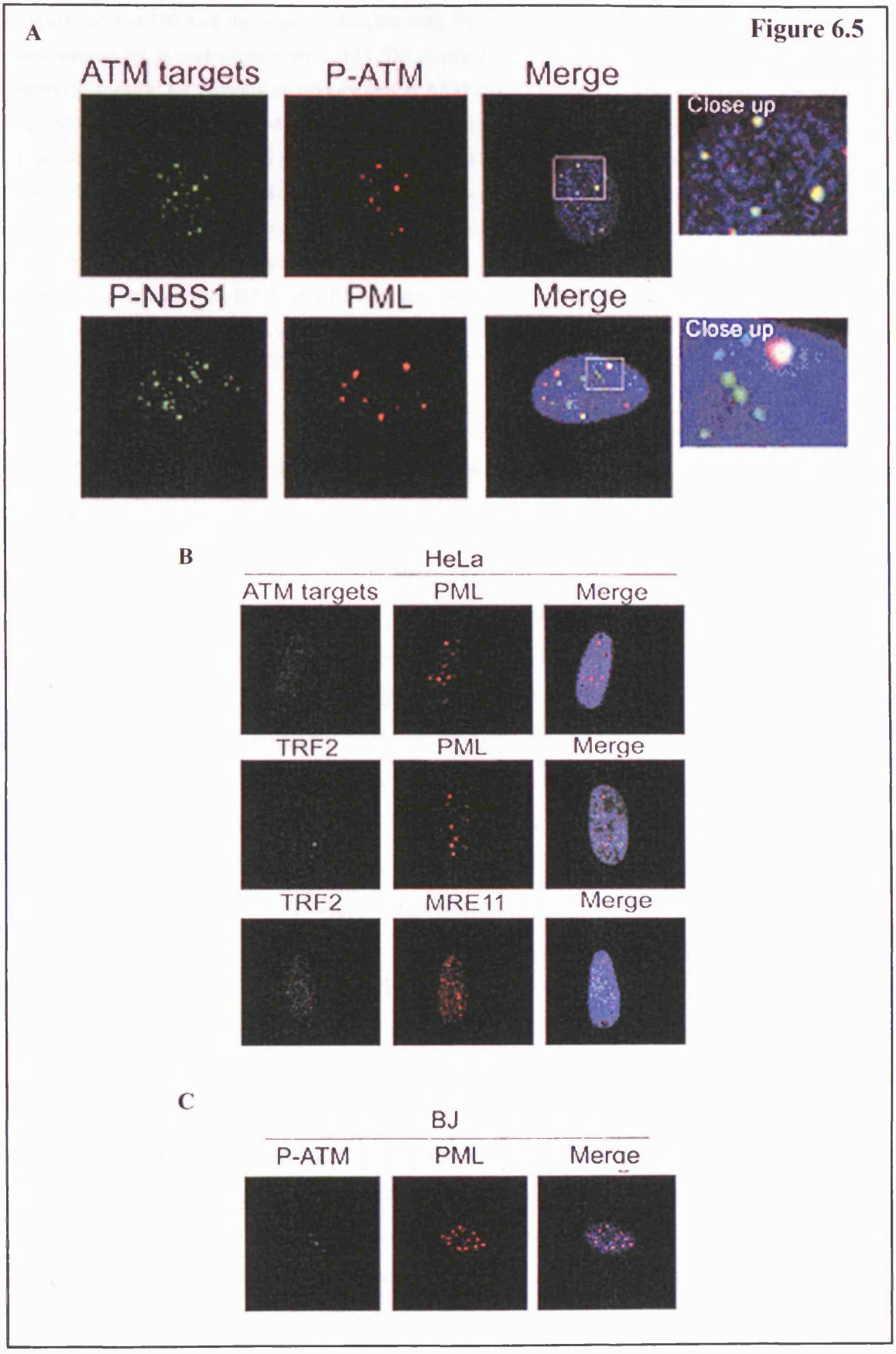
A
ATM targets
P-ATM
Merge
Close up
P-NBS1
PML
Merge
Close up
B
HeLa
ATM targets
PML
Merge
TRF2
PML
Merge
TRF2
MRE11
Merge
C
BJ
P-ATM
PML
Merge

Figure 6.5 P-ATM and its targets colocalize with PML only in ALT cells. All cells were PFA-fixed and stained by immunofluorescence. **(A)** The localization of ATM targets was analyzed using an antibody specific for proteins phosphorylated at ATM target sequences (green) in conjunction with an anti-S1981 ATM antibody (P-ATM) (top panel). The merged confocal image shows that ATM targets colocalize with P-ATM. Anti-phosphorylated NBS1 (P-NBS1) antibody was used to determine the colocalization between P-NBS1 and PML (bottom panels). Nuclei were stained using DAPI Figures shown are representative of two independent experiments. **(B)** HeLa cells lack APBs and are negative for ATM targets. Anti-ATM targets, anti-TRF2, anti-PML and anti-MRE11 antibodies were used. Nuclei were counterstained with DAPI. **(C)** BJ cells do not display P-ATM colocalization with PML. Anti-P-ATM and anti-PML antibodies were used, and nuclei were visualized using DAPI.

6.3.2 TRF2 controls p53 localization and activation in ALT cells

p53 is phosphorylated at Serine 15 upon ATM activation. As previously demonstrated, ATM is active in ALT cells at steady state. We therefore analyzed p53 phosphorylation status in ALT cells. A panel of ALT and telomerase-positive cell lines were examined by western blotting using a phospho-specific antibody (anti-P-Ser15), and we found that p53 was phosphorylated (P-p53) in three different ALT cell lines, VA13, GM847 and JFCF6 (Figure 6.6a). The isogenic telomerase positive cell line JFCF6-T, also displayed similar amounts of P-p53 (Figure 6.6a). JFCF6 and JFCF6-T are SV40 T antigen immortalized, thus suggesting that the presence of high P-p53 levels is due to the immortalization process or the presence of T antigen rather than to the ALT status. By contrast, p53 was not phosphorylated in the remaining telomerase-positive and ALT cell lines, such as U2OS and SUSM-1 (Figure 6.6a). We focused on U2OS cells as this was the only p53-proficient ALT cell line not immortalized using SV40. Interestingly, phosphorylation of p53 occurred in the absence of TRF2 in U2OS cells and its overall levels also increased (Figure 6.6b left panel). A concomitant increase of the p53 target gene and cell cycle inhibitor, p21, was also observed in the absence of TRF2 (Figure 6.6b left panel). In contrast, p53 proapoptotic targets, such Bax were not affected (Figure 6.6b right panel). Following confirmation of these differences by western blot, the localization of p53 in F8 U2OS cells was investigated. We found that more than 20% of cells displayed p53 in nuclear speckles, which were also positive for PML and TRF2 (Figure 6.7a). p53 colocalized with TRF1 and TRF2 also in untransfected U2OS

and SUSM-1 (Figure 6.7a and b), but not in telomerase-positive MCF-7 and HeLa (Figure 6.7c). SUSM-1 cells express only a mutated form of p53, however this did not influence its localization to APBs (Figure 6.7b) and (Mihara et al., 1996). To test whether p53-positive speckles contain telomeric DNA, we performed fluorescence in situ hybridization (FISH)/IF using a PNA probe specific for telomeric sequences and found that p53-containing foci colocalize with telomeric DNA during interphase (Figure 6.7a). The data presented here suggest that p53 accumulates at APBs, where it remains in an inactive and unphosphorylated state despite the presence of activated ATM. However, in the absence of TRF2 p53 is phosphorylated and activated, which coincides with its release from the APBs (Figure 6.6b).

Figure 6.6

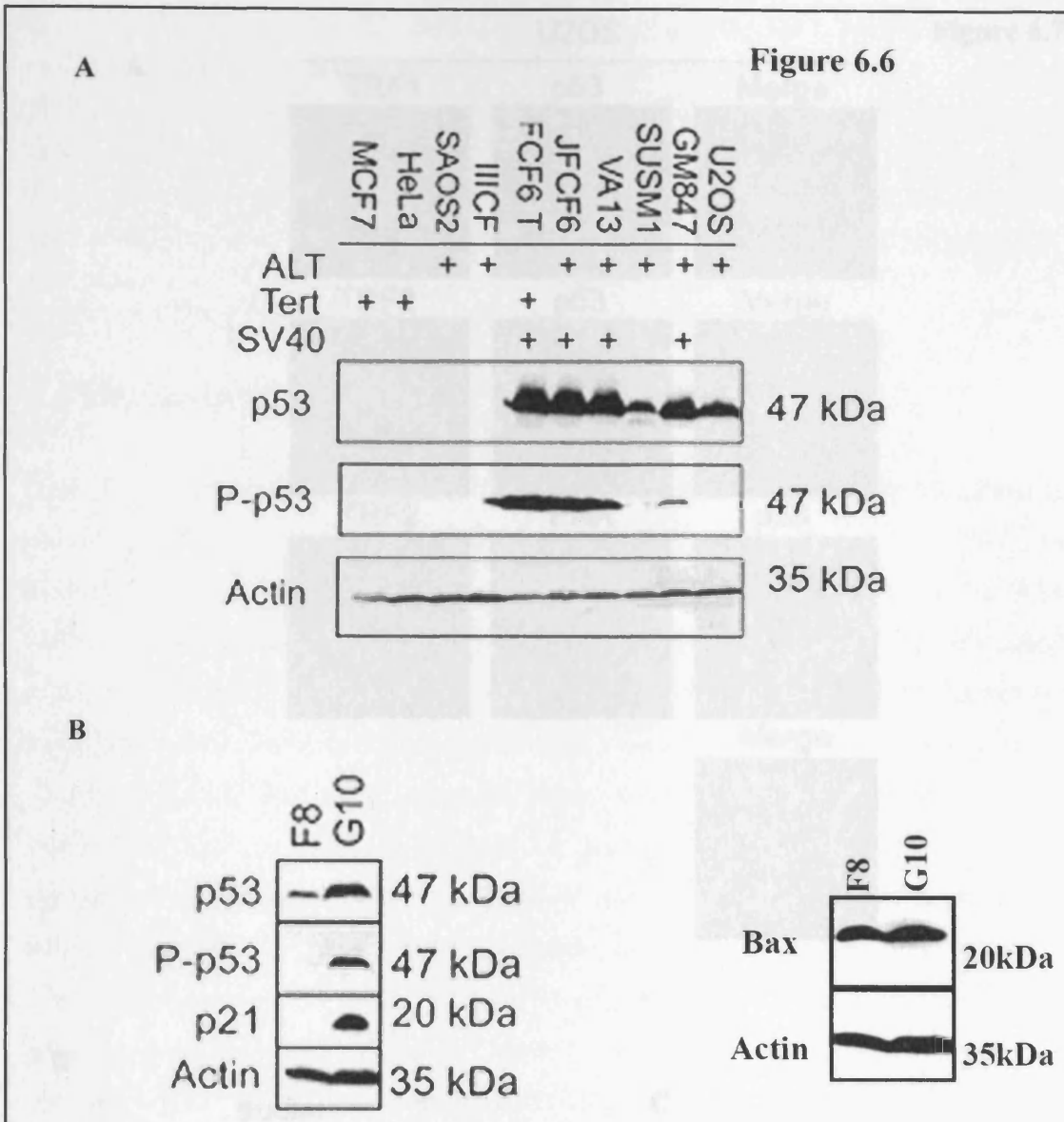

Figure 6.6 p53 is phosphorylated in TRF2 depleted cells. (A) ALT positive and telomerase positive cells were lysed and probed with anti-p53, anti-Actin and an antibody directed against p53 phosphorylated serine 15 (P-p53). Cells immortalized by SV40 are indicated. **(B)** TRF2 silencing results in an increase in p53 levels, its phosphorylation and the induction of p21. Control (F8) and TRF2-depleted (G10) clones were analyzed for p53, P-p53, p21 and Actin levels. Data shown are representative of two independent experiments.

Figure 6.7

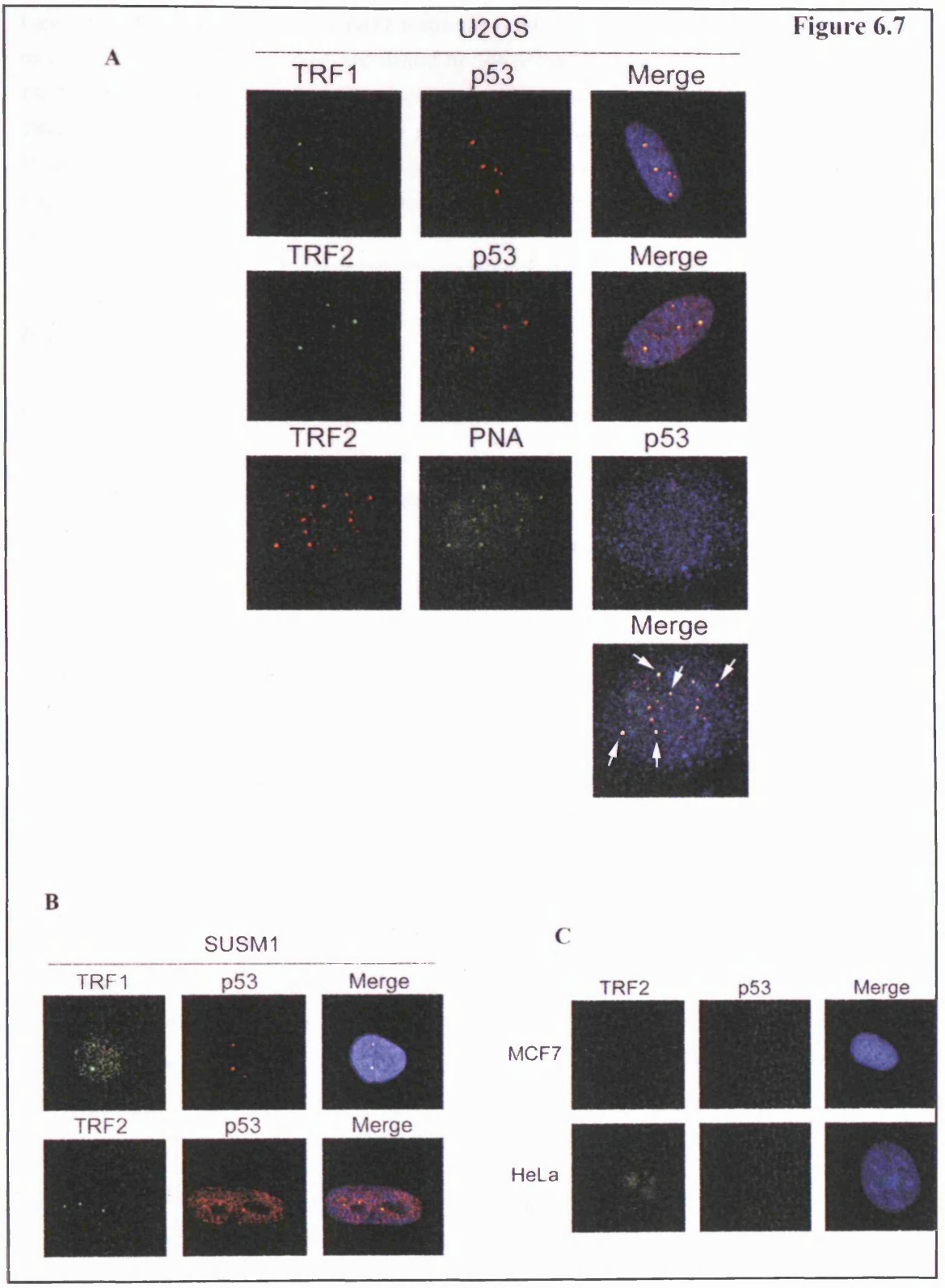
A
U2OS
TRF1
p53
Merge
TRF2
p53
Merge
TRF2
PNA
p53
Merge
B
SUSM1
TRF1
p53
Merge
TRF2
p53
Merge
C
TRF2
p53
Merge
MCF7
HeLa

Figure 6.7 p53 colocalization with TRF2 is specific to ALT cells. (A) p53 is found in APBs at steady state. U2OS cells were PFA-fixed and stained by immunofluorescence with anti-TRF1 (green), anti-TRF2 (green) and anti-p53 (red and blue) antibodies. The top two panels show p53 colocalizing with TRF1 and TRF2. The bottom panel shows p53 colocalizing also with PNA and TRF2 in APBs. **(B)** SUSM1 cells with mutated p53 also display p53 TRF1 or TRF2 colocalization. **(C)** Telomerase positive HeLa or MCF7 cells do not have p53 in nuclear speckles with TRF2. Nuclei are counterstained with DAPI (blue).

6.4 Discussion

Upon inactivation of TRF2 function telomeres become deprotected and uncapped and are recognized as damaged DNA ((Karlseder et al., 1999; Karlseder et al., 2002; van Steensel et al., 1998). Recent reports have shown that activation of the ATM/p53 pathway is responsible for cell death induction in tumour cell lines and senescence in primary fibroblasts following TRF2 inactivation (Karlseder et al., 1999; Karlseder et al., 2002),. In contrast, our results have shown that ATM is constitutively phosphorylated in ALT cells and forms nuclear foci, almost half of which colocalize with APB components. We indeed see an increase in the number of ATM nuclear speckles in the absence of TRF2 suggesting that telomeres are deprotected and that there is activation of the DNA damage response as previously reported (Karlseder et al., 1999; Karlseder et al., 2002; van Steensel et al., 1998). One of the hallmarks of ALT is genomic instability with increased rates of telomeric sister chromatid exchange (Londono-Vallejo et al., 2004) and minisatellite instability (Jeyapalan et al., 2005). Our data suggest that ATM is activated at steady state, but this does not result in either cell death or growth suppression. The precise reason for this is still unclear, as we found that downstream targets of ATM, such as NBS1 are phosphorylated suggesting that P-ATM is functionally active. It is possible that the localization of P-ATM to APBs is able to lessen the effect of ATM activation. Alternatively, the lack of activation of proapoptotic or growth suppressive downstream targets could protect ALT cells from ATM activation. TRF2 has been shown to directly interact with ATM, through the region containing the autophosphorylation site, and inhibit the ATM-dependent DNA damage response (Karlseder et al., 2004b). However, ALT cells appear to have constitutively active ATM. We see phosphorylation of downstream ATM targets that have been reported not to be phosphorylated upon overexpression of TRF2 dominant

negative mutants (Karlseder et al., 2004b). One explanation may be that, due to increased genomic instability, ATM is activated below the apoptosis threshold to allow DNA repair. The activation of G1/S, intra-S, and G2/M cell cycle check points by ATM is well documented. Primarily these blocks occur to allow cells to repair DNA damage. ALT cells may have developed a mechanism by which constitutive activation of ATM enables constant DNA damage repair in the absence of obvious cell cycle alterations. Another possibility is that activated ATM is involved in mechanisms regulating telomere maintenance. For instance, ATM and ATR have been found to play a role in telomere maintenance in yeast. In *S. cerevisiae* mutants lacking *atm* telomeres were shortened but stable. However, double mutants of *atm* and *atr* were found to have increased telomere fusions gross genome rearrangements and enter senescence (Craven et al., 2002; Mieczkowski et al., 2003; Ritchie et al., 1999). Similar findings were reported in *Drosophila.* ATM and ATR were found to control partially redundant pathways for telomere maintenance with the telomere fusions being more frequent in double mutants compared to single mutants (Bi et al., 2005). It is possible that in ALT cells the role of ATM in telomere maintenance is exacerbated to avoid excessive telomere dysfunction and cell death.. A role for ATM in telomere maintenance has been proposed in primary human fibroblasts, where it is important for correct telomere replication during S phase (Verdun et al., 2005; Verdun and Karlseder, 2006), Therefore, it cannot be excluded that active ATM is involved in ALT. Interestingly, BrdU incorporation at APBs is inhibited by caffeine treatment, thus suggesting that ATM (or ATR) is involved in replication of telomeric DNA (Nabetani et al., 2004). Our laboratory is currently investigating ATM function in ALT cells.

Activation of ATM results in p53 phosphorylation and induction of p53-mediated cell death or growth arrest, therefore we tested whether this was applicable to ALT cells. We analysed a panel of ALT and telomerase positive cell lines for p53 phosphorylation (P-p53) (Fig). There were some ALT and telomerase positive cell lines that appeared to have P-p53 at steady state. We believe that this is due to the immortalization process as it was only those that were immortalized with the SV40 large T antigen that displayed P-p53. Cells immortalized by carcinogen exposure such as SUSM-1 did not show P-p53 at steady state. Also osteosarcoma U2OS cells did not display P-p53. In contrast, it is only upon TRF2 silencing that p53 becomes phosphorylated and p21 induction is

observed in U2OS cells. Interestingly, we found p53 localized to APBs in a number of ALT cell lines. This also applies to SUSM-1 cells, which express a transcriptionally defective p53 mutant, thus suggesting that inactivating p53 mutations do not impair its targeting to APBs. We were unable to detect p53 and PML colocalization in telomerase-positive cells or primary fibroblasts. This suggests that at steady state p53 associates with PML in nuclear bodies only in cells where ALT is active. However, we did not look at a large enough selection of telomerase positive, primary or ALT cells to come to any concrete conclusions. Surprisingly, we found that phosphorylation and activations of p53 coincides with its release from APBs to the nucleoplasm following TRF2 silencing. In TRF2 depleted cells we also see an increase in p21 levels confirming that p53 is transcriptionally active in the absence of TRF2. A recent report by Razak and colleagues suggests that inhibition of p53 aids in the preferential activation of ALT (Razak et al., 2004). The authors suggest that p53 is associated with the telomeric complex in ALT cells and that is it able to inhibit DNA synthesis if its DNA binding activity is not altered. It is possible that the localization of p53 to APBs is a way to inhibit this function and allow recombination and telomere elongation to continue in ALT. TRF2 may be a key factor in the inhibition of p53-mediated ALT repression. TRF2 depletion-mediated release of p53 may be the first step in inhibiting ALT.

Our data imply a role for APBs in p53 activation regulation through TRF2. However, TRF2 down-regulation does not cause dissipation of other APB components (Chapter 4). We are unable to exclude the involvement of other APB components in p53 activation. Further studies looking at p53 activation and function in the absence of multiple APB components would allow firm conclusions to be drawn about the role of APBs in regulating p53 function. Overall, the evidence presented here suggests that, despite the presence of active ATM, TRF2 is able to inhibit p53 phosphorylation and activation at APBs. Based on the data presented here we propose a model for TRF2 function in ALT cells (Figure 6.8).

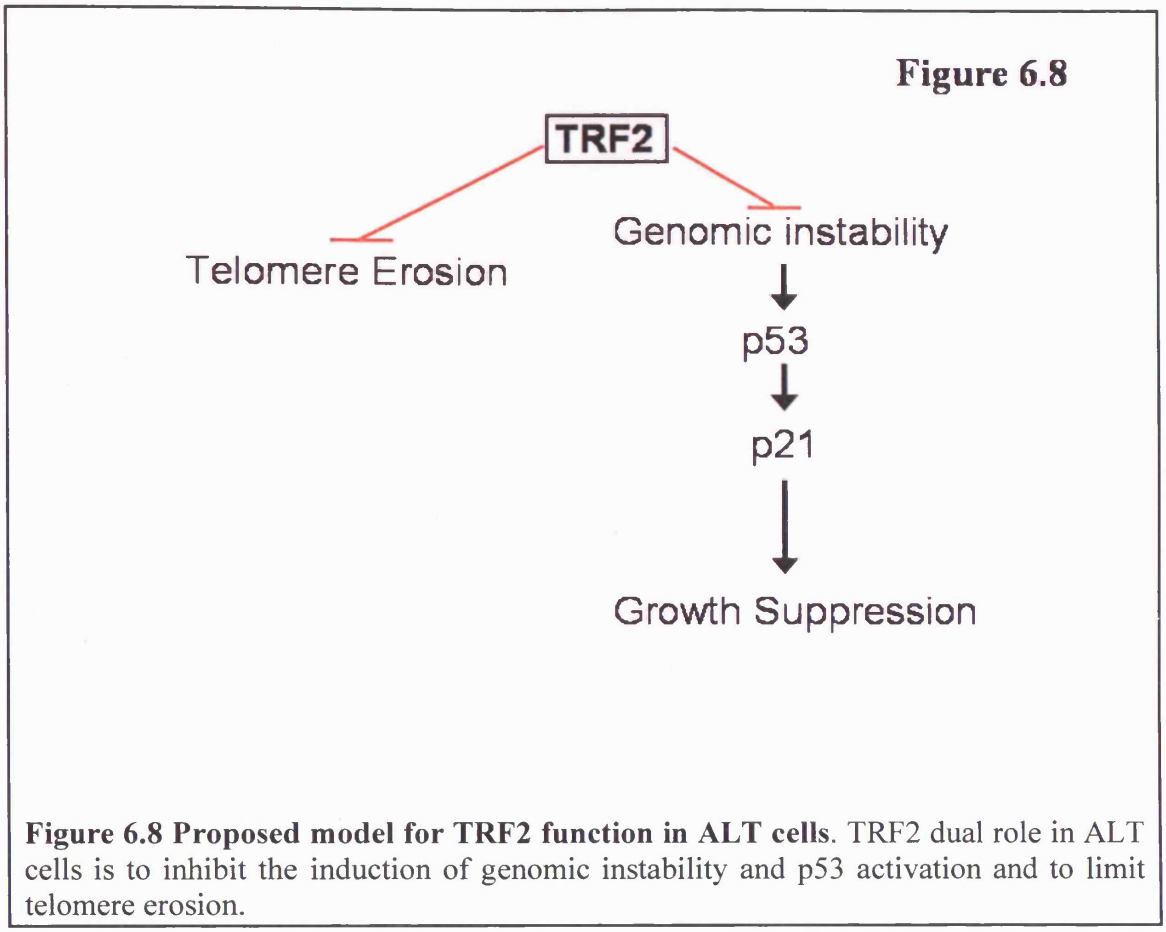

Figure 6.8 Proposed model for TRF2 function in ALT cells. TRF2 dual role in ALT cells is to inhibit the induction of genomic instability and p53 activation and to limit telomere erosion.

6.5 Summary

The data presented in this chapter have demonstrated that the DNA damage response protein, ATM, is constitutively active in ALT cells without inducing senescence or cell death. We suggest that the presence of active ATM at APBs is to aid in telomere repair and recombination. In the absence of TRF2 we show that p53 is delocalized from APBs and becomes transcriptionally active inducing p21 expression. We suggest that TRF2 is able to block p53 activation by ATM and thus prevent senescence and cell death. Overall the data implicate APBs in survival through their ability to regulate p53 activation.

Chapter 7) Discussion and Future work

7.1 Discussion

Work in this thesis has aimed to determine the role of PML and TRF2 in APB composition and telomere maintenance in ALT cells.

7.2 ALT-positive cells lines display a higher number of cells with APBs than previously reported.

Work in Chapter 3 aimed to determine the percentage of cells, of various cell lines, in which APBs were present. The colocalization of known components, MRE11, TRF1 and TRF2, with PML was used to identify APBs. Previous reports have suggested that only a small percentage of cells within a given population were positive for APBs (approximately 5%) (Yeager et al., 1999). The authors suggested that the low percentage of APB positive cells could be that APBs are only formed in a particular phase of the cell cycle or in cells that have exited the cell cycle. Another hypothesis put forward was that APBs represent reservoirs of telomeric DNA and associated proteins and are therefore present in cells actually undergoing telomere maintenance (Yeager et al., 1999). Alternatively, senescent cells are those positive for APBs. However this was found to be untrue by β-galactosidase assay. Suprisingly, using the above mentioned proteins as markers for APBs in a variety of ALT positive cells lines, we found a greater proportion of cells positive for APBs ranging from 10% in WI38VA13 cells to 30-40% in IIICF and JFCF6 cells. However, it was demonstrated that the percentage of APB positive cells increases with time in neo-immortalized IIICF cells (Yeager et al., 1999). It may be that the increased percentage of APB positive cells we see is due to the number of population doublings. Nevertheless, it is still not clear why we are able to see a greater number of APB positive cells in a given population compared to that reported in the literature. Recent studies by Jiang *et al.* (Jiang et al., 2005; Jiang et al., 2007) have used methionine restriction to increase the percentage of APB positive cells from 5% to approximately 60-70% in IIICF cells. We did not need to increase our percentage of APBs as our ALT cell lines already displayed a large proportion of cells positive for

APBs. There are no reports to say what the effect of methionine restriction is on ALT. It is possible that the resulting increase in APBs may be due to an alteration of ALT causing the cells to behave in an artificial manner. Interestingly, nuclear speckle size and number varied between cell strains. However, in the majority of cell lines examined it was the larger nuclear speckles that displayed colocalization of TRF1, TRF2 and MRE11 with PML. These findings are in agreement with those reported by Jiang *et al.* (Jiang et al., 2005). The authors state that APBs are larger than PML bodies seen in telomerase-positive cells and that the amount of telomere binding proteins found in APBs is greater than that seen at the telomere. Therefore, APBs are often seen as bright TRF1 or TRF2 foci whereas telomeres are often dimmer. This confirms that the bright nuclear structures that we found to contain MRE11, TRF1 and TRF2 along with PML are APBs.

Importantly, we did not see APBs in telomerase positive cells. In HeLa and MCF7 cells and the telomerase positive subclone of the JFCF6-T cells we did not detect any APBs. This is in concordance with reports that have found that the appearance of these nuclear structures tightly coincides with the presence of ALT within a cell line (Yeager et al., 1999). Our data confirms the specificity of these bodies as hallmarks of ALT.

The PML nuclear body is a structure that is known to be disrupted in the absence of PML. APBs resemble PML nuclear bodies in shape and are also composed of multiple proteins. A number of recent papers have attempted to determine the essential component(s) of APBs. A recent report has suggested that the MRN complex is important for APB formation and that its sequestration by overexpression of sp100 led to the disruption of these structures and the inhibition of ALT (Jiang et al., 2005). Furthermore, a study by Wu *et al.*. suggested that for the correct functional assembly of APBs Nijmen Breakage Syndrome 1 (NBS1) was necessary and that TRF1 was not an essential component of APBs (Wu et al., 2003; Wu et al., 2000). However a more recent paper by Jiang *et al.* demonstrated that TRF1 was essential for APB formation. siRNA depletion of TRF1 and other APB components such as TRF2, TIN2 and Rap1 was shown to decrease the percentage of APBs 10-fold (Jiang et al., 2007). Interestingly the authors also found that PML was important for the formation of these nuclear structures, and that in its absence there was a 90% decrease in the percentage of APBs. This suggests that PML is required for the formation of APBs as for PML-NBs.

However, these observations were made in cells that were methionine restricted to cause an increase in APB number. It is possible that the "novel" APBs generated in this manner are not identical in composition and structure to those found in normally cycling cells and thus may behave differently in the absence of specific components. The role of PML and TRF2 in the establishment of APBs in untreated ALT cells is not known.

7.3 Transient down-regulation of PML results in the delocalization of MRE11 and TRF1 but does not affect TRF2.

The data presented in Chapter 4 examined the importance of two APB components, TRF2 and PML, in the composition of APBs. Transient down-regulation of PML and TRF2 by siRNA allowed us to determine any short term effects on APBs. Our data suggest that PML is an important component of APBs, as its down-regulation led to the delocalization of TRF1 and MRE11. MRE11, a protein that is part of a DNA damage repair complex (MRN) along with NBS1 and RAD50, has been implicated in the formation of these structures. The overexpression of Sp100 caused the sequestration of the MRN complex that in turn disrupted APBs and eventually to the inhibition of ALT (Jiang et al., 2005). However, a more recent paper from the same lab demonstrated that sp100 was not an important component of APBs but that PML was (Jiang et al., 2007). The down-regulation of PML by siRNA was shown to disrupt APBs supporting our findings. Interestingly we did not see an effect on the localization of TRF2 in the absence of PML. TRF2 remained in bright nuclear speckles. This contradicts previous reports in which PML down-regulation resulted in the delocalization of TRF2 and the disruption of APBs (Jiang et al., 2007). However, the cell line used was different and APBs were induced through methionine restriction. The authors suggest that methionine restriction favours the assembly of APBs in ALT cells based on the report that a reduction in methylation in telomeric and subtelomeric regions led to an increase in telomeric recombination (Gonzalo et al., 2006). However this was reported to occur in embryonic stem cells that lacked DNA methyltransferases, and as the precise mechanism of ALT is not yet characterised it is difficult to say whether these cells will behave in a similar manner. Our data suggest that in unaltered cycling ALT cells, in the

absence of PML TRF2 remains in large nuclear speckles. Transient down-regulation of TRF2 was found to have no effect on the localization of MRE11, TRF1 or PML. We found that TRF1 and MRE11 colocalized with each other and with PML in the absence of TRF2 suggesting that APBs were still present. These data confirmed our hypothesis that TRF2 is not essential for the formation of APBs.

7.4 Stable down-regulation of PML has no significant effect on telomere maintenance in ALT cells.

Although a specific function of PML has not been reported, it has been implicated in many cellular processes such as transformation suppression, growth control and apoptosis. PML protein expression is frequently lost in human cancers of various histologic origins, and its loss is associated with tumor grade and progression in some tumor histotypes, such as prostate cancer and breast cancer (Gurrieri et al., 2004). The role of PML in ALT has not been determined. There are many hypotheses that suggest that PML and APBs are involved in telomere maintenance in ALT and Chapter 5 aimed to determine whether this was true. Clones stably expressing a shRNA against the nuclear localization signal in exon VI and one against exon II were used to identify any alterations in telomere length. Less than 4% of the clones displayed some degree of PML down-regulation. PML-depleted clones were maintained in culture over time to assess differences in telomere length. TRF analysis demonstrated that there was no significant difference in telomere length over time in the absence of PML. However, we were unable to obtain complete down-regulation of PML and the higher molecular weight bands corresponding in size to the PMLI and PMLII isoforms, albeit reduced in levels, remained. These were present in all clones picked and we were unable to find clones that no longer expressed these isoforms. The presence of a number of PML isoforms in PML-depleted clones could compensate for the depletion of other isoforms thus making it hard to come to any concrete conclusion about the effect of PML down-regulation on telomere length. Furthermore, after a certain time in culture PML levels returned to control levels. PML down-regulation did not affect clonogenicity of cells as expected as previous reports have shown that PML is not essential for survival *in vivo* or *in vitro* (Wang et al., 1998a; Wang et al., 1998b). To more clearly understand the

role of PML in ALT, *Pml*$^{-/-}$ cells or animals could be used. For instance, a recent report has shown that TRF2 overexpression in the mouse skin appears to induce ALT tumours in late generation mice lacking TERT ((Munoz et al., 2005); (Blanco et al., 2007)). This mouse model could be crossed with *Pml*$^{-/-}$ mice in order to test the impact of PML inactivation on ALT *in vivo*.

7.5 Transient TRF2 down-regulation does not affect the localization of PML, MRE11 or TRF1

Transient TRF2 down-regulation did not appear to affect APBs. However, previous reports have shown that inhibition of TRF2 function in primary and telomerase positive cells leads to irreversible cell cycle arrest and apoptosis (Karlseder et al., 1999), (Karlseder et al., 2002). We did not see any significant differences in cell death upon transient down-regulation of TRF2. However, we did see a significant decrease in colony formation in cells stably transfected with a shRNA against TRF2 compared to control cells. Surprisingly, we were able to obtain clones that displayed almost complete down-regulation of TRF2 suggesting that the response to TRF2 inactivation may be different in ALT cells (Karlseder et al., 1999), (Karlseder et al., 2002). Again we found that TRF2 stable down-regulation did not affect the localization of PML, TRF1 or MRE11 at early population doublings. Cell cycle analysis showed that there was not a large amount of cell death in TRF2-depleted cells, again contradicting reports that have shown that the inhibition of TRF2 led to rapid cell death in telomerase positive cells (Karlseder et al., 1999). Furthermore, as U2OS cells have functional p53, it appears that TRF2 depletion does not cause p53 activation in ALT cells. A study by Karlseder and colleagues suggested that cells lacking functional p53 such as SAOS-2 cells were resistant to the cytotoxic effects of TRF2 depletion (Karlseder et al., 1999). Our data suggest that lack of cytoxic effects may be not due to impaired p53 function, but rather to intrinsic differences of ALT cells. However, to confirm our data further studies on other p53-proficient ALT cell lines need to be carried out.

7.6 Stable depletion of TRF2 results in telomere shortening in ALT cells.

In order to determine if TRF2 depletion affected telomere maintenance we examined telomere length in TRF2-depleted cells over time. A recent report in which TRF2 was overexpressed in mouse keratinocytes lacking telomerase activity, found that there was an increase in ALT characteristics in the resulting skin tumours, such as increased telomere sister-chromatid exchange, appearance of APBs and an increase in extra-chromosomal telomere signals (Blanco et al., 2007). The authors suggest that the overexpression of TRF2 in the case of critically short telomeres may aid the de-repression of ALT. A possibility is that TRF2 is inducing telomere recombination through its association with other telomere-associated proteins such as WRN (Laud et al., 2005)and Pot1 (Wu et al., 2006). This report supports our findings that TRF2-depleted clones have a shorter mean telomere length than controls. We suggest that TRF2 is important for telomere maintenance in cells lacking active telomerase. However, further studies in different cell lines and reproduction of these results using the dominant negative TRF2 ($TRF2^{\Delta B\Delta M}$) need to be carried out to confirm that these results are not due to clonal variation or off target effects of the shRNA. Additionally, re-introduction of full length TRF2 into a TRF2-depleted clone should be carried out in order to determine whether telomere shortening and genomic instability are reversible in the presence of wild type TRF2. In this respect, preliminary findings generated after the completion of my thesis work indicate that $TRF2^{\Delta B\Delta M}$ can recapitulate most of the findings obtained using shRNA, including the telomere phenotype.

7.7 Clones stably downregulating TRF2 undergo radical morphological changes.

Another remarkable effect of TRF2 down-regulation occurred on cellular morphology. Cells from clones lacking TRF2 appeared larger and displayed a more flattened morphology than control cells. This is accompanied by an increase in the G2 phase of cell cycle, thus suggesting that these cells are partially arrested (this observation was done after the completion of my thesis work). The nuclear morphology of these cells is

also greatly altered, with many cells displaying multiple micronuclei which could be due to aneuploidy or supernumerary centrosomes (Lazzerini Denchi et al., 2006). A recent report in which TRF2 was conditionally knocked out in mouse hepatocytes established that there was no increase in cell death or senescence and that TRF2 was not essential for liver regeneration after partial hepatectomy (Lazzerini Denchi et al., 2006). The authors found that in TRF2 KO livers regeneration occurred without cell division but through endoreduplication and cell growth, and that this was a mechanism through which cells could circumvent chromosome segregation problems associated with telomeric fusions. This could be the case in our system, however further characterisation is needed in order to confirm this, such as metaphase spreads and γ-tubulin staining to visualize centrosomes and determine endoreduplication.

7.8 Active ATM is present in in ALT cells at steady state, and localizes to APBs.

TRF2 inactivation results in deprotection and uncapping of telomeres, which are then recognised as sites of DNA damage (van Steensel et al., 1998), (Karlseder et al., 1999), (Karlseder et al., 2002). The DNA damage pathway shown to be involved in induction of cell death in tumour cell lines and primary fibroblasts in the abence of TRF2 function is the ATM/p53 pathway (Karlseder et al., 1999), (Karlseder et al., 2002). The results presented in Chapter 6 aimed to analyze the status of ATM in ALT cells at steady state and following TRF2 silencing. Surprisingly, we found that ATM is constitutively active in ALT cell lines at steady state unlike in telomerase positive cell lines or primary human fibroblasts. This could be the reason for the different response to TRF2 down-regulation and the lack of cell death in ALT cells compared to that reported for telomerase positive and primary cells (Karlseder et al., 1999). Alternatively, there could be a block further downstream in the pathway that inhibits cell death but allows other functions of ATM to occur. In *Drosophila* and yeast it has been shown that ATM is important in telomere homeostasis (see Chapter 6). *Drosophila* and certain strains of yeast do not have telomerase activity and maintain their telomeres either by retrotransposition or by recombination; mechanisms that resemble ALT. It is likely that the components involved in maintaining telomere length in these organisms maintain

similar functions in ALT. More recently there have been reports of retrotransposition occurring in mammalian cells (Morrish et al., 2002), more specifically at telomeres (Morrish et al., 2007). The authors demonstrate that long interspersed element 1 (LINE-1) elements (17% of human DNA) are efficicently retrotransposed in Chinese hamster ovary (CHO) cells lines defective in non-homologous end joining (Morrish et al., 2002). Interestingly they found that transient expression of dominant negative TRF2 in these cells enabled telomere associated retrotransposition events (Morrish et al., 2007). The authors speculate that dysfunctional telomeres can serve as substrates for retrotransposition and that retrotransposition is an ancestral mechanism of RNA-mediated DNA repair. Cells that have activated ALT are believed to be maintain telomeres through recombination. However, the specific mechanism has not been determined. It is possible that dysfunctional telomeres in an ALT setting are elongated through retrotransposition as is the case in CHO cells and in *Drosophila.* Our results suggest that ATM is activated at steady state, but this does not result in either cell death or growth suppression. However the precise mechanism is still unknown. Activation of ATM may be below the threshold that initiates cell death. This enables it to phosphorylate some downstream targets such as Nbs1. Nbs1 has been shown to stimulate the endonuclease activity of MRE11 and that this was stimulated by ATP (Paull and Gellert, 1999). Paull and Gellert also showed that Mre11, complexed with Rad50 and Nbs1 could partially unwind or dissociate short DNA duplexes, and that this activity was specific for substrates with 3' overhangs (Paull and Gellert, 1999). It is possible that in ALT cells the phosphorylation of Nbs1 is necessary for the DNA processing function of the MRN complex. In this situation the activation of downstream targets of ATM is necessary for telomere maintenance but not for cell death. Furthermore, Bernardi *et al.* demonstrated that upon treatment with doxorubicin PML itself might be a target of ATM/ATR (Bernardi et al., 2004). One could be tempted to speculate that in ALT, PML phosphorylation by ATM could regulate the targeting of PML itself and other proteins to the APB. It is presently unknown whether PML is phosphorylated by ATM at steady state or upon TRF2 silencing in ALT cells.

7.9 Stable depletion of TRF2 causes an increase in phosphor-ATM nuclear speckles but no significant increase in cell death.

ATM was also shown to directly interact with TRF2 (Karlseder et al., 2004b). This interaction was shown to inhibit ATM autophosphorylation as it was shown to occur in the region containing the S1981. As previously mentioned our data suggests that ATM is phosphorylated and localizes to APBs. This finding is interesting as TRF2 is also present in APBs. It is likely that there is another component of these structures that blocks the direct interaction of TRF2 with ATM thus allowing it to be phosphorylated and possibly carry out a role in telomere maintenance in ALT cells. In order to determine whether the presence of TRF2 in APBs affected the function of P-ATM we examined the effect of TRF2 down-regulation on P-ATM localization and activation of downstream targets such as p53. It has been previously reported that inhibition of Trf2 results in the association of P-ATM with telomeres (Takai et al., 2003). Furthermore, ATM activation has been shown to occur in response to telomere uncapping due to TRF2 inhibition, resulting in the induction of apoptosis through the ATM/p53 pathway (Karlseder et al., 1999). Our data corroborate these reports, as in cells stably downregulating TRF2 there is an increase in P-ATM nuclear speckles suggesting that there is an increase in genomic instability. However, even though there is an increase in P-ATM we did not see a considerable increase in cell death contradicting the report that in the absence of TRF2 the activation of ATM results in cell death through p53. In TRF2 depleted clones we do see an increase in levels of P-p53 and we also see an increase in the levels of p21 suggesting that p53 is transcriptionally active in these cells. Our data clearly suggest that in the absence of TRF2 ALT cells behave differently to telomerase positive cells, and are able to survive even in the presence of activated ATM/p53 pathway.

7.10 ALT cells may survive in the absence of TRF2 through the activation of endoreduplication.

As mentioned above, cells depleted in TRF2 adopt a distorted morphology with enlarged nuclei. There are multiple reports that suggest that the accumulation of p21 is not only able to cause cell cycle arrest but is also able to modulate DNA endoreduplication (Bates et al., 1998; Niculescu et al., 1998). It is also interesting to note that p21 was shown to be inefficient in inhibiting DNA replication *in vivo* (Bates et al., 1998). Moreover, cells released form the p21 induced G2 block underwent endoreduplication before going through S phase and entering mitosis. The authors suggested a role for p21 in coupling DNA synthesis with mitosis. Ivanov *et al.* demonstrated that p53 mutant cells underwent mitotic catastrophe in response to genotoxic stress which caused cells to suppress mitosis and delay apoptosis resulting in endopolyploid cells (Ivanov et al., 2003). The above reports imply that p21 is involved in regulating endoreduplication. It is worth noting however, that these experiments were carried out in cells lacking functional p53 and Retinoblastoma (Rb) and most osteosarcoma cell lines lack pRb, which potently inhibits endoreduplication (Avni et al., 2003). Our data suggest that in the absence of TRF2 there is activation of p53, which in turn causes the transcription of p21. Possibly, the prolonged expression of p21 in TRF2 depleted clones could eventually lead to endoreduplication instead of cell death, probably as a result of the lack of functional pRb. Ivanov and colleagues suggest that after severe genotoxic insult endopolyploid cells have a transient survival advantage (Ivanov et al., 2003). With this in mind it is likely that in order to avoid cell death in the absence of TRF2, ALT cells are able to initiate endoreduplication. However, further work needs to be done in order to confirm that the altered nuclear morphology and size seen in TRF2 depleted cells is due to endoreduplication.

7.11 Future and Ongoing work.

The data presented in this study have demonstrated that there is a higher percentage of APBs present in ALT positive cells. We have shown that in the absence of PML some APB components such as TRF1 and MRE11 are delocalized whereas others, such as

TRF2, are not affected. The stable down-regulation of PML does not have a significant effect on telomere maintenance in ALT cells. However, TRF2 was shown to be dispensable for the localization of PML, TRF1 and MRE11 to APBs and stable depletion of TRF2 did not result in massive cell death. TRF2 was found to be important in telomere maintenance as in its absence there was a noticeable decrease in telomere length. Moreover, TRF2 depleted cells adopted a peculiar morphology and p53 phosphorylation was found to be increased compared to control cells. Furthermore, ATM was found to be constitutively active in ALT cells and localize to APBs. In the absence of TRF2, p21 was induced, and this may result in alterations in nuclear morphology and size. In order to ascertain that the above results are specifically due to the interference of the function of TRF2 and not to clonal variation or off-target effects, further work is being carried out using different tools to achieve the same goal. A dominant negative form of TRF2 ($TRF2^{\Delta B \Delta M}$) previously reported to inhibit TRF2 function (Karlseder et al., 1999; van Steensel et al., 1998), is being used to make single cell clones. This will enable the effect on APB components and telomere lengths to be assessed and determine whether the results achieved using a shRNA against TRF2 were specific. This will also exclude that the effects seen with the shRNA against TRF2 were due to clonal variation. In addition stable down-regulation of TRF2 is being done in other ALT cell lines including SUSM1cells. Upon TRF2 depletion we find that cells become enlarged. We hypothesized that this was due to endoreduplication. Metaphase spreads are being examined to confirm this. Furthermore, in order to more closely examine the effect on p53 activation and attempt to determine the sequence in which the observed changes occur, an inducible system in which TRF2 down-regulation is controlled by the addition of tetracycline is being constructed. The use of these systems will allow us to confirm our findings about the role of TRF2 in ALT cells.

7.12 Concluding remarks

As previously discussed the vast majority of tumours have been found to be telomerase-positive. This has led researchers to look for inhibitors of telomerase as a tool to inhibit cell proliferation and possibly tumour size. However, the discovery of telomerase-negative tumours that are able to maintain telomeres through alternative mechanisms, has meant that novel therapies need to be devised in order to target the telomere

elongation in this subset of human cancers. The recent discovery of the APB as a unique marker of ALT cells suggests that this structure may regulate the ALT mechanism. Therefore, it is of paramount importance to gain a clearer understanding of the role of these novel nuclear structures and their components in ALT, as this could result in the development of novel therapies specifically aimed at inhibiting telomere maintenance in ALT tumours. In this respect, our work demonstrates that the APB component TRF2 inhibits telomere erosion and p53 activation in ALT cells. The tumour suppressor PML promotes p53 activation in cells lacking functional TRF2, thus suggesting that its tumours suppressive function is inhibited in ALT tumours. Consequently, therapies aimed at inhibiting TRF2 function in ALT cells could result in inhibition of ALT and re-activation of tumour suppressive pathways. Finally, the hypothesis suggesting a potential role for ATM in ALT is very fascinating and needs to be tested.

References

Abad, J. P., De Pablos, B., Osoegawa, K., De Jong, P. J., Martin-Gallardo, A., and Villasante, A. (2004). TAHRE, a novel telomeric retrotransposon from Drosophila melanogaster, reveals the origin of Drosophila telomeres. Mol Biol Evol *21*, 1620-1624.

Abraham, R. T. (2001). Cell cycle checkpoint signaling through the ATM and ATR kinases. Genes Dev *15*, 2177-2196.

Agrawal, N., Dasaradhi, P. V., Mohmmed, A., Malhotra, P., Bhatnagar, R. K., and Mukherjee, S. K. (2003). RNA interference: biology, mechanism, and applications. Microbiol Mol Biol Rev *67*, 657-685.

Ahn, J. H., Brignole, E. J., 3rd, and Hayward, G. S. (1998). Disruption of PML subnuclear domains by the acidic IE1 protein of human cytomegalovirus is mediated through interaction with PML and may modulate a RING finger-dependent cryptic transactivator function of PML. Mol Cell Biol *18*, 4899-4913.

Ahuja, D., Saenz-Robles, M. T., and Pipas, J. M. (2005). SV40 large T antigen targets multiple cellular pathways to elicit cellular transformation. Oncogene *24*, 7729-7745.

Alcalay, M., Tomassoni, L., Colombo, E., Stoldt, S., Grignani, F., Fagioli, M., Szekely, L., Helin, K., and Pelicci, P. G. (1998). The promyelocytic leukemia gene product (PML) forms stable complexes with the retinoblastoma protein. Mol Cell Biol *18*, 1084-1093.

Alcalay, M., Zangrilli, D., Fagioli, M., Pandolfi, P. P., Mencarelli, A., Lo Coco, F., Biondi, A., Grignani, F., and Pelicci, P. G. (1992). Expression pattern of the RAR alpha-PML fusion gene in acute promyelocytic leukemia. Proc Natl Acad Sci U S A *89*, 4840-4844.

Alexander, K., and Hinds, P. W. (2001). Requirement for p27(KIP1) in retinoblastoma protein-mediated senescence. Mol Cell Biol *21*, 3616-3631.

Allsopp, R. C., Vaziri, H., Patterson, C., Goldstein, S., Younglai, E. V., Futcher, A. B., Greider, C. W., and Harley, C. B. (1992). Telomere length predicts replicative capacity of human fibroblasts. Proc Natl Acad Sci U S A *89*, 10114-10118.

Anton, L. C., Schubert, U., Bacik, I., Princiotta, M. F., Wearsch, P. A., Gibbs, J., Day, P. M., Realini, C., Rechsteiner, M. C., Bennink, J. R., and Yewdell, J. W. (1999). Intracellular localization of proteasomal degradation of a viral antigen. J Cell Biol *146*, 113-124.

Artandi, S. E., and DePinho, R. A. (2000). A critical role for telomeres in suppressing and facilitating carcinogenesis. Curr Opin Genet Dev *10*, 39-46.

Avni, D., Yang, H., Martelli, F., Hofmann, F., ElShamy, W. M., Ganesan, S., Scully, R., and Livingston, D. M. (2003). Active localization of the retinoblastoma protein in chromatin and its response to S phase DNA damage. Mol Cell *12*, 735-746.

Bailey, S. M., Brenneman, M. A., and Goodwin, E. H. (2004). Frequent recombination in telomeric DNA may extend the proliferative life of telomerase-negative cells. Nucleic Acids Res *32*, 3743-3751.

Bakkenist, C. J., and Kastan, M. B. (2003). DNA damage activates ATM through intermolecular autophosphorylation and dimer dissociation. Nature *421*, 499-506.

Banin, S., Moyal, L., Shieh, S., Taya, Y., Anderson, C. W., Chessa, L., Smorodinsky, N. I., Prives, C., Reiss, Y., Shiloh, Y., and Ziv, Y. (1998). Enhanced phosphorylation of p53 by ATM in response to DNA damage. Science *281*, 1674-1677.

Barrett, J. C., Annab, L. A., and Futreal, P. A. (1993). Genetic and molecular basis for cellular senescence. Adv Exp Med Biol *330*, 27-43.
Bates, S., Ryan, K. M., Phillips, A. C., and Vousden, K. H. (1998). Cell cycle arrest and DNA endoreduplication following p21Waf1/Cip1 expression. Oncogene *17*, 1691-1703.
Baumann, P., and Cech, T. R. (2001). Pot1, the putative telomere end-binding protein in fission yeast and humans. Science *292*, 1171-1175.
Bechter, O. E., Zou, Y., Shay, J. W., and Wright, W. E. (2003). Homologous recombination in human telomerase-positive and ALT cells occurs with the same frequency. EMBO Rep *4*, 1138-1143.
Belair, C. D., Yeager, T. R., Lopez, P. M., and Reznikoff, C. A. (1997). Telomerase activity: a biomarker of cell proliferation, not malignant transformation. Proc Natl Acad Sci U S A *94*, 13677-13682.
Bernardi, R., and Pandolfi, P. P. (2003). Role of PML and the PML-nuclear body in the control of programmed cell death. Oncogene *22*, 9048-9057.
Bernardi, R., Scaglioni, P. P., Bergmann, S., Horn, H. F., Vousden, K. H., and Pandolfi, P. P. (2004). PML regulates p53 stability by sequestering Mdm2 to the nucleolus. Nat Cell Biol *6*, 665-672.
Bertrand, P., Rouillard, D., Boulet, A., Levalois, C., Soussi, T., and Lopez, B. S. (1997). Increase of spontaneous intrachromosomal homologous recombination in mammalian cells expressing a mutant p53 protein. Oncogene *14*, 1117-1122.
Bi, X., Srikanta, D., Fanti, L., Pimpinelli, S., Badugu, R., Kellum, R., and Rong, Y. S. (2005). Drosophila ATM and ATR checkpoint kinases control partially redundant pathways for telomere maintenance. Proc Natl Acad Sci U S A *102*, 15167-15172.
Bi, X., Wei, S. C., and Rong, Y. S. (2004). Telomere protection without a telomerase; the role of ATM and Mre11 in Drosophila telomere maintenance. Curr Biol *14*, 1348-1353.
Bianchi, A., Smith, S., Chong, L., Elias, P., and de Lange, T. (1997). TRF1 is a dimer and bends telomeric DNA. Embo J *16*, 1785-1794.
Bianchi, A., Stansel, R. M., Fairall, L., Griffith, J. D., Rhodes, D., and de Lange, T. (1999). TRF1 binds a bipartite telomeric site with extreme spatial flexibility. Embo J *18*, 5735-5744.
Bilaud, T., Brun, C., Ancelin, K., Koering, C. E., Laroche, T., and Gilson, E. (1997). Telomeric localization of TRF2, a novel human telobox protein. Nat Genet *17*, 236-239.
Bischof, O., Kim, S. H., Irving, J., Beresten, S., Ellis, N. A., and Campisi, J. (2001). Regulation and localization of the Bloom syndrome protein in response to DNA damage. J Cell Biol *153*, 367-380.
Bischof, O., Kirsh, O., Pearson, M., Itahana, K., Pelicci, P. G., and Dejean, A. (2002). Deconstructing PML-induced premature senescence. Embo J *21*, 3358-3369.
Bissonnette, N., and Hunting, D. J. (1998). p21-induced cycle arrest in G1 protects cells from apoptosis induced by UV-irradiation or RNA polymerase II blockage. Oncogene *16*, 3461-3469.
Blackburn, E. H. (1991). Structure and function of telomeres. Nature *350*, 569-573.
Blackburn, E. H. (1994). Telomeres: no end in sight. Cell *77*, 621-623.
Blanco, R., Munoz, P., Flores, J. M., Klatt, P., and Blasco, M. A. (2007). Telomerase abrogation dramatically accelerates TRF2-induced epithelial carcinogenesis. Genes Dev *21*, 206-220.
Blasco, M. A. (2005). Telomeres and human disease: ageing, cancer and beyond. Nat Rev Genet *6*, 611-622.

Blasco, M. A., Lee, H. W., Hande, M. P., Samper, E., Lansdorp, P. M., DePinho, R. A., and Greider, C. W. (1997). Telomere shortening and tumor formation by mouse cells lacking telomerase RNA. Cell *91*, 25-34.
Blasco, M. A., Rizen, M., Greider, C. W., and Hanahan, D. (1996). Differential regulation of telomerase activity and telomerase RNA during multi-stage tumorigenesis. Nat Genet *12*, 200-204.
Boddy, M. N., Duprez, E., Borden, K. L., and Freemont, P. S. (1997). Surface residue mutations of the PML RING finger domain alter the formation of nuclear matrix-associated PML bodies. J Cell Sci *110 (Pt 18)*, 2197-2205.
Boisvert, F. M., Hendzel, M. J., and Bazett-Jones, D. P. (2000). Promyelocytic leukemia (PML) nuclear bodies are protein structures that do not accumulate RNA. J Cell Biol *148*, 283-292.
Bond, J. A., Haughton, M. F., Rowson, J. M., Smith, P. J., Gire, V., Wynford-Thomas, D., and Wyllie, F. S. (1999). Control of replicative life span in human cells: barriers to clonal expansion intermediate between M1 senescence and M2 crisis. Mol Cell Biol *19*, 3103-3114.
Bond, J. A., Wyllie, F. S., and Wynford-Thomas, D. (1994). Escape from senescence in human diploid fibroblasts induced directly by mutant p53. Oncogene *9*, 1885-1889.
Borden, K. L. (2000). RING domains: master builders of molecular scaffolds? J Mol Biol *295*, 1103-1112.
Borden, K. L. (2002). Pondering the promyelocytic leukemia protein (PML) puzzle: possible functions for PML nuclear bodies. Mol Cell Biol *22*, 5259-5269.
Borden, K. L., Boddy, M. N., Lally, J., O'Reilly, N. J., Martin, S., Howe, K., Solomon, E., and Freemont, P. S. (1995). The solution structure of the RING finger domain from the acute promyelocytic leukaemia proto-oncoprotein PML. Embo J *14*, 1532-1541.
Borden, K. L., Campbell Dwyer, E. J., and Salvato, M. S. (1998). An arenavirus RING (zinc-binding) protein binds the oncoprotein promyelocyte leukemia protein (PML) and relocates PML nuclear bodies to the cytoplasm. J Virol *72*, 758-766.
Borden, K. L., CampbellDwyer, E. J., and Salvato, M. S. (1997). The promyelocytic leukemia protein PML has a pro-apoptotic activity mediated through its RING domain. FEBS Lett *418*, 30-34.
Borden, K. L., Lally, J. M., Martin, S. R., O'Reilly, N. J., Solomon, E., and Freemont, P. S. (1996). In vivo and in vitro characterization of the B1 and B2 zinc-binding domains from the acute promyelocytic leukemia protooncoprotein PML. Proc Natl Acad Sci U S A *93*, 1601-1606.
Bradshaw, P. S., Stavropoulos, D. J., and Meyn, M. S. (2005). Human telomeric protein TRF2 associates with genomic double-strand breaks as an early response to DNA damage. Nat Genet *37*, 193-197.
Brien, T. P., Kallakury, B. V., Lowry, C. V., Ambros, R. A., Muraca, P. J., Malfetano, J. H., and Ross, J. S. (1997). Telomerase activity in benign endometrium and endometrial carcinoma. Cancer Res *57*, 2760-2764.
Broccoli, D., Chong, L., Oelmann, S., Fernald, A. A., Marziliano, N., van Steensel, B., Kipling, D., Le Beau, M. M., and de Lange, T. (1997a). Comparison of the human and mouse genes encoding the telomeric protein, TRF1: chromosomal localization, expression and conserved protein domains. Hum Mol Genet *6*, 69-76.
Broccoli, D., Godley, L. A., Donehower, L. A., Varmus, H. E., and de Lange, T. (1996). Telomerase activation in mouse mammary tumors: lack of detectable telomere shortening and evidence for regulation of telomerase RNA with cell proliferation. Mol Cell Biol *16*, 3765-3772.

Broccoli, D., Smogorzewska, A., Chong, L., and de Lange, T. (1997b). Human telomeres contain two distinct Myb-related proteins, TRF1 and TRF2. Nat Genet *17*, 231-235.
Broccoli, D., Young, J. W., and de Lange, T. (1995). Telomerase activity in normal and malignant hematopoietic cells. Proc Natl Acad Sci U S A *92*, 9082-9086.
Brugarolas, J., Chandrasekaran, C., Gordon, J. I., Beach, D., Jacks, T., and Hannon, G. J. (1995). Radiation-induced cell cycle arrest compromised by p21 deficiency. Nature *377*, 552-557.
Bryan, T. M., Englezou, A., Dalla-Pozza, L., Dunham, M. A., and Reddel, R. R. (1997). Evidence for an alternative mechanism for maintaining telomere length in human tumors and tumor-derived cell lines. Nat Med *3*, 1271-1274.
Bryan, T. M., Englezou, A., Gupta, J., Bacchetti, S., and Reddel, R. R. (1995). Telomere elongation in immortal human cells without detectable telomerase activity. Embo J *14*, 4240-4248.
Buchhop, S., Gibson, M. K., Wang, X. W., Wagner, P., Sturzbecher, H. W., and Harris, C. C. (1997). Interaction of p53 with the human Rad51 protein. Nucleic Acids Res *25*, 3868-3874.
Burger, A. M., Bibby, M. C., and Double, J. A. (1997). Telomerase activity in normal and malignant mammalian tissues: feasibility of telomerase as a target for cancer chemotherapy. Br J Cancer *75*, 516-522.
Buscemi, G., Savio, C., Zannini, L., Micciche, F., Masnada, D., Nakanishi, M., Tauchi, H., Komatsu, K., Mizutani, S., Khanna, K., *et al.* (2001). Chk2 activation dependence on Nbs1 after DNA damage. Mol Cell Biol *21*, 5214-5222.
Campisi, J. (1997). The biology of replicative senescence. Eur J Cancer *33*, 703-709.
Campisi, J., Dimri, G. P., Nehlin, J. O., Testori, A., and Yoshimoto, K. (1996). Coming of age in culture. Exp Gerontol *31*, 7-12.
Canman, C. E., Lim, D. S., Cimprich, K. A., Taya, Y., Tamai, K., Sakaguchi, K., Appella, E., Kastan, M. B., and Siliciano, J. D. (1998). Activation of the ATM kinase by ionizing radiation and phosphorylation of p53. Science *281*, 1677-1679.
Canman, C. E., Wolff, A. C., Chen, C. Y., Fornace, A. J., Jr., and Kastan, M. B. (1994). The p53-dependent G1 cell cycle checkpoint pathway and ataxia-telangiectasia. Cancer Res *54*, 5054-5058.
Cao, L., Alani, E., and Kleckner, N. (1990). A pathway for generation and processing of double-strand breaks during meiotic recombination in S. cerevisiae. Cell *61*, 1089-1101.
Cao, Y., Li, H., Deb, S., and Liu, J. P. (2002). TERT regulates cell survival independent of telomerase enzymatic activity. Oncogene *21*, 3130-3138.
Carbone, R., Pearson, M., Minucci, S., and Pelicci, P. G. (2002). PML NBs associate with the hMre11 complex and p53 at sites of irradiation induced DNA damage. Oncogene *21*, 1633-1640.
Carney, J. P., Maser, R. S., Olivares, H., Davis, E. M., Le Beau, M., Yates, J. R., 3rd, Hays, L., Morgan, W. F., and Petrini, J. H. (1998). The hMre11/hRad50 protein complex and Nijmegen breakage syndrome: linkage of double-strand break repair to the cellular DNA damage response. Cell *93*, 477-486.
Carson, C. T., Schwartz, R. A., Stracker, T. H., Lilley, C. E., Lee, D. V., and Weitzman, M. D. (2003). The Mre11 complex is required for ATM activation and the G2/M checkpoint. Embo J *22*, 6610-6620.
Celli, G. B., and de Lange, T. (2005). DNA processing is not required for ATM-mediated telomere damage response after TRF2 deletion. Nat Cell Biol *7*, 712-718.

Cerone, M. A., Londono-Vallejo, J. A., and Bacchetti, S. (2001). Telomere maintenance by telomerase and by recombination can coexist in human cells. Hum Mol Genet *10*, 1945-1952.
Cerosaletti, K. M., and Concannon, P. (2003). Nibrin forkhead-associated domain and breast cancer C-terminal domain are both required for nuclear focus formation and phosphorylation. J Biol Chem *278*, 21944-21951.
Cesare, A. J., and Griffith, J. D. (2004). Telomeric DNA in ALT cells is characterized by free telomeric circles and heterogeneous t-loops. Mol Cell Biol *24*, 9948-9957.
Chai, Y., Koppenhafer, S. L., Shoesmith, S. J., Perez, M. K., and Paulson, H. L. (1999). Evidence for proteasome involvement in polyglutamine disease: localization to nuclear inclusions in SCA3/MJD and suppression of polyglutamine aggregation in vitro. Hum Mol Genet *8*, 673-682.
Chang, B. D., Broude, E. V., Dokmanovic, M., Zhu, H., Ruth, A., Xuan, Y., Kandel, E. S., Lausch, E., Christov, K., and Roninson, I. B. (1999). A senescence-like phenotype distinguishes tumor cells that undergo terminal proliferation arrest after exposure to anticancer agents. Cancer Res *59*, 3761-3767.
Charette, S. J., and Landry, J. (2000). The interaction of HSP27 with Daxx identifies a potential regulatory role of HSP27 in Fas-induced apoptosis. Ann N Y Acad Sci *926*, 126-131.
Chen, G. Q., Zhu, J., Shi, X. G., Ni, J. H., Zhong, H. J., Si, G. Y., Jin, X. L., Tang, W., Li, X. S., Xong, S. M., *et al.* (1996). In vitro studies on cellular and molecular mechanisms of arsenic trioxide (As2O3) in the treatment of acute promyelocytic leukemia: As2O3 induces NB4 cell apoptosis with downregulation of Bcl-2 expression and modulation of PML-RAR alpha/PML proteins. Blood *88*, 1052-1061.
Chen, L., Trujillo, K., Ramos, W., Sung, P., and Tomkinson, A. E. (2001). Promotion of Dnl4-catalyzed DNA end-joining by the Rad50/Mre11/Xrs2 and Hdf1/Hdf2 complexes. Mol Cell *8*, 1105-1115.
Chen, L. Y., and Chen, J. D. (2003). Daxx silencing sensitizes cells to multiple apoptotic pathways. Mol Cell Biol *23*, 7108-7121.
Chin, L., Tam, A., Pomerantz, J., Wong, M., Holash, J., Bardeesy, N., Shen, Q., O'Hagan, R., Pantginis, J., Zhou, H., *et al.* (1999). Essential role for oncogenic Ras in tumour maintenance. Nature *400*, 468-472.
Chong, L., van Steensel, B., Broccoli, D., Erdjument-Bromage, H., Hanish, J., Tempst, P., and de Lange, T. (1995). A human telomeric protein. Science *270*, 1663-1667.
Ciapponi, L., Cenci, G., Ducau, J., Flores, C., Johnson-Schlitz, D., Gorski, M. M., Engels, W. R., and Gatti, M. (2004). The Drosophila Mre11/Rad50 complex is required to prevent both telomeric fusion and chromosome breakage. Curr Biol *14*, 1360-1366.
Condemine, W., Takahashi, Y., Zhu, J., Puvion-Dutilleul, F., Guegan, S., Janin, A., and de The, H. (2006). Characterization of endogenous human promyelocytic leukemia isoforms. Cancer Res *66*, 6192-6198.
Costanzo, V., Paull, T., Gottesman, M., and Gautier, J. (2004). Mre11 assembles linear DNA fragments into DNA damage signaling complexes. PLoS Biol *2*, E110.
Counter, C. M., Avilion, A. A., LeFeuvre, C. E., Stewart, N. G., Greider, C. W., Harley, C. B., and Bacchetti, S. (1992). Telomere shortening associated with chromosome instability is arrested in immortal cells which express telomerase activity. Embo J *11*, 1921-1929.
Counter, C. M., Gupta, J., Harley, C. B., Leber, B., and Bacchetti, S. (1995). Telomerase activity in normal leukocytes and in hematologic malignancies. Blood *85*, 2315-2320.

Counter, C. M., Meyerson, M., Eaton, E. N., Ellisen, L. W., Caddle, S. D., Haber, D. A., and Weinberg, R. A. (1998). Telomerase activity is restored in human cells by ectopic expression of hTERT (hEST2), the catalytic subunit of telomerase. Oncogene *16*, 1217-1222.
Court, R., Chapman, L., Fairall, L., and Rhodes, D. (2005). How the human telomeric proteins TRF1 and TRF2 recognize telomeric DNA: a view from high-resolution crystal structures. EMBO Rep *6*, 39-45.
Craven, R. J., Greenwell, P. W., Dominska, M., and Petes, T. D. (2002). Regulation of genome stability by TEL1 and MEC1, yeast homologs of the mammalian ATM and ATR genes. Genetics *161*, 493-507.
d'Adda di Fagagna, F., Reaper, P. M., Clay-Farrace, L., Fiegler, H., Carr, P., Von Zglinicki, T., Saretzki, G., Carter, N. P., and Jackson, S. P. (2003). A DNA damage checkpoint response in telomere-initiated senescence. Nature *426*, 194-198.
D'Orazi, G., Cecchinelli, B., Bruno, T., Manni, I., Higashimoto, Y., Saito, S., Gostissa, M., Coen, S., Marchetti, A., Del Sal, G., *et al.* (2002). Homeodomain-interacting protein kinase-2 phosphorylates p53 at Ser 46 and mediates apoptosis. Nat Cell Biol *4*, 11-19.
Dahlen, M., Olsson, T., Kanter-Smoler, G., Ramne, A., and Sunnerhagen, P. (1998). Regulation of telomere length by checkpoint genes in Schizosaccharomyces pombe. Mol Biol Cell *9*, 611-621.
Daniel, C. W., Aidells, B. D., Medina, D., and Faulkin, L. J., Jr. (1975). Unlimited division potential of precancerous mouse mammary cells after spontaneous or carcinogen-induced transformation. Fed Proc *34*, 64-67.
Daniel, M. T., Koken, M., Romagne, O., Barbey, S., Bazarbachi, A., Stadler, M., Guillemin, M. C., Degos, L., Chomienne, C., and de The, H. (1993). PML protein expression in hematopoietic and acute promyelocytic leukemia cells. Blood *82*, 1858-1867.
de Lange, T. (2002). Protection of mammalian telomeres. Oncogene *21*, 532-540.
de Lange, T. (2005). Shelterin: the protein complex that shapes and safeguards human telomeres. Genes Dev *19*, 2100-2110.
de Lange, T., Shiue, L., Myers, R. M., Cox, D. R., Naylor, S. L., Killery, A. M., and Varmus, H. E. (1990). Structure and variability of human chromosome ends. Mol Cell Biol *10*, 518-527.
de The, H., Lavau, C., Marchio, A., Chomienne, C., Degos, L., and Dejean, A. (1991). The PML-RAR alpha fusion mRNA generated by the t(15;17) translocation in acute promyelocytic leukemia encodes a functionally altered RAR. Cell *66*, 675-684.
Degos, L., and Wang, Z. Y. (2001). All trans retinoic acid in acute promyelocytic leukemia. Oncogene *20*, 7140-7145.
Dellaire, G., Ching, R. W., Ahmed, K., Jalali, F., Tse, K. C., Bristow, R. G., and Bazett-Jones, D. P. (2006). Promyelocytic leukemia nuclear bodies behave as DNA damage sensors whose response to DNA double-strand breaks is regulated by NBS1 and the kinases ATM, Chk2, and ATR. J Cell Biol *175*, 55-66.
Desbois, C., Rousset, R., Bantignies, F., and Jalinot, P. (1996). Exclusion of Int-6 from PML nuclear bodies by binding to the HTLV-I Tax oncoprotein. Science *273*, 951-953.
Di Micco, R., Fumagalli, M., Cicalese, A., Piccinin, S., Gasparini, P., Luise, C., Schurra, C., Garre, M., Nuciforo, P. G., Bensimon, A., *et al.* (2006). Oncogene-induced senescence is a DNA damage response triggered by DNA hyper-replication. Nature *444*, 638-642.

Dimri, G. P., Lee, X., Basile, G., Acosta, M., Scott, G., Roskelley, C., Medrano, E. E., Linskens, M., Rubelj, I., Pereira-Smith, O., and et al. (1995). A biomarker that identifies senescent human cells in culture and in aging skin in vivo. Proc Natl Acad Sci U S A *92*, 9363-9367.
Dolganov, G. M., Maser, R. S., Novikov, A., Tosto, L., Chong, S., Bressan, D. A., and Petrini, J. H. (1996). Human Rad50 is physically associated with human Mre11: identification of a conserved multiprotein complex implicated in recombinational DNA repair. Mol Cell Biol *16*, 4832-4841.
Dong, Z., Zhong, Q., and Chen, P. L. (1999). The Nijmegen breakage syndrome protein is essential for Mre11 phosphorylation upon DNA damage. J Biol Chem *274*, 19513-19516.
Dupre, A., Boyer-Chatenet, L., and Gautier, J. (2006). Two-step activation of ATM by DNA and the Mre11-Rad50-Nbs1 complex. Nat Struct Mol Biol *13*, 451-457.
Duprez, E., Saurin, A. J., Desterro, J. M., Lallemand-Breitenbach, V., Howe, K., Boddy, M. N., Solomon, E., de The, H., Hay, R. T., and Freemont, P. S. (1999). SUMO-1 modification of the acute promyelocytic leukaemia protein PML: implications for nuclear localisation. J Cell Sci *112 (Pt 3)*, 381-393.
Dyck, J. A., Maul, G. G., Miller, W. H., Jr., Chen, J. D., Kakizuka, A., and Evans, R. M. (1994). A novel macromolecular structure is a target of the promyelocyte-retinoic acid receptor oncoprotein. Cell *76*, 333-343.
Ecsedy, J. A., Michaelson, J. S., and Leder, P. (2003). Homeodomain-interacting protein kinase 1 modulates Daxx localization, phosphorylation, and transcriptional activity. Mol Cell Biol *23*, 950-960.
Ellis, N. A., Groden, J., Ye, T. Z., Straughen, J., Lennon, D. J., Ciocci, S., Proytcheva, M., and German, J. (1995). The Bloom's syndrome gene product is homologous to RecQ helicases. Cell *83*, 655-666.
Elmore, L. W., Rehder, C. W., Di, X., McChesney, P. A., Jackson-Cook, C. K., Gewirtz, D. A., and Holt, S. E. (2002). Adriamycin-induced senescence in breast tumor cells involves functional p53 and telomere dysfunction. J Biol Chem *277*, 35509-35515.
Eskiw, C. H., Dellaire, G., Mymryk, J. S., and Bazett-Jones, D. P. (2003). Size, position and dynamic behavior of PML nuclear bodies following cell stress as a paradigm for supramolecular trafficking and assembly. J Cell Sci *116*, 4455-4466.
Everett, R. D., Lomonte, P., Sternsdorf, T., Driel, R. v., and Orr, A. (1999). Cell cycle regulation of PML modification and ND10 composition. Journal of Cell Science *112*, 4581-4588.
Fagioli, M., Alcalay, M., Pandolfi, P. P., Venturini, L., Mencarelli, A., Simeone, A., Acampora, D., Grignani, F., and Pelicci, P. G. (1992). Alternative splicing of PML transcripts predicts coexpression of several carboxy-terminally different protein isoforms. Oncogene *7*, 1083-1091.
Fagioli, M., Alcalay, M., Tomassoni, L., Ferrucci, P. F., Mencarelli, A., Riganelli, D., Grignani, F., Pozzan, T., Nicoletti, I., Grignani, F., and Pelicci, P. G. (1998). Cooperation between the RING + B1-B2 and coiled-coil domains of PML is necessary for its effects on cell survival. Oncogene *16*, 2905-2913.
Falck, J., Coates, J., and Jackson, S. P. (2005). Conserved modes of recruitment of ATM, ATR and DNA-PKcs to sites of DNA damage. Nature *434*, 605-611.
Fang, D., Wang, H. Y., Fang, N., Altman, Y., Elly, C., and Liu, Y. C. (2001). Cbl-b, a RING-type E3 ubiquitin ligase, targets phosphatidylinositol 3-kinase for ubiquitination in T cells. J Biol Chem *276*, 4872-4878.

Ferbeyre, G., de Stanchina, E., Querido, E., Baptiste, N., Prives, C., and Lowe, S. W. (2000). PML is induced by oncogenic ras and promotes premature senescence. Genes Dev *14*, 2015-2027.
Ferguson, D. O., Sekiguchi, J. M., Chang, S., Frank, K. M., Gao, Y., DePinho, R. A., and Alt, F. W. (2000). The nonhomologous end-joining pathway of DNA repair is required for genomic stability and the suppression of translocations. Proc Natl Acad Sci U S A *97*, 6630-6633.
Fogal, V., Gostissa, M., Sandy, P., Zacchi, P., Sternsdorf, T., Jensen, K., Pandolfi, P. P., Will, H., Schneider, C., and Del Sal, G. (2000). Regulation of p53 activity in nuclear bodies by a specific PML isoform. Embo J *19*, 6185-6195.
Fuchs, B. C., Perez, J. C., Suetterlin, J. E., Chaudhry, S. B., and Bode, B. P. (2004). Inducible antisense RNA targeting amino acid transporter ATB0/ASCT2 elicits apoptosis in human hepatoma cells. Am J Physiol Gastrointest Liver Physiol *286*, G467-478.
Gana, Y., Moa, Y., Johnstona, J. r., Lua, J., Wientjesa, M. G., and Aua, J. L.-S. (2002). Telomere maintenance in telomerase-positive human ovarian SKOV-3 cells cannot be retarded by complete inhibition of telomerase. FEBS Letters *527*, 10-14.
Garkavtsev, I., Hull, C., and Riabowol, K. (1998). Molecular aspects of the relationship between cancer and aging: tumor suppressor activity during cellular senescence. Exp Gerontol *33*, 81-94.
Gatei, M., Sloper, K., Sorensen, C., Syljuasen, R., Falck, J., Hobson, K., Savage, K., Lukas, J., Zhou, B. B., Bartek, J., and Khanna, K. K. (2003). Ataxia-telangiectasia-mutated (ATM) and NBS1-dependent phosphorylation of Chk1 on Ser-317 in response to ionizing radiation. J Biol Chem *278*, 14806-14811.
Ghosal, G., and Muniyappa, K. (2005). Saccharomyces cerevisiae Mre11 is a high-affinity G4 DNA-binding protein and a G-rich DNA-specific endonuclease: implications for replication of telomeric DNA. Nucleic Acids Res *33*, 4692-4703.
Gilson, E., Roberge, M., Giraldo, R., Rhodes, D., and Gasser, S. M. (1993). Distortion of the DNA double helix by RAP1 at silencers and multiple telomeric binding sites. J Mol Biol *231*, 293-310.
Girdwood, D., Bumpass, D., Vaughan, O. A., Thain, A., Anderson, L. A., Snowden, A. W., Garcia-Wilson, E., Perkins, N. D., and Hay, R. T. (2003). P300 transcriptional repression is mediated by SUMO modification. Mol Cell *11*, 1043-1054.
Goddard, A. D., Borrow, J., Freemont, P. S., and Solomon, E. (1991). Characterization of a zinc finger gene disrupted by the t(15;17) in acute promyelocytic leukemia. Science *254*, 1371-1374.
Goldstein, S. (1990). Replicative senescence: the human fibroblast comes of age. Science *249*, 1129-1133.
Gonzalez-Suarez, E., Samper, E., Ramirez, A., Flores, J. M., Martin-Caballero, J., Jorcano, J. L., and Blasco, M. A. (2001). Increased epidermal tumors and increased skin wound healing in transgenic mice overexpressing the catalytic subunit of telomerase, mTERT, in basal keratinocytes. Embo J *20*, 2619-2630.
Gonzalo, S., Jaco, I., Fraga, M. F., Chen, T., Li, E., Esteller, M., and Blasco, M. A. (2006). DNA methyltransferases control telomere length and telomere recombination in mammalian cells. Nat Cell Biol *8*, 416-424.
Goodwin, E. C., and DiMaio, D. (2000). Repression of human papillomavirus oncogenes in HeLa cervical carcinoma cells causes the orderly reactivation of dormant tumor suppressor pathways. Proc Natl Acad Sci U S A *97*, 12513-12518.

Gorski, M. M., Romeijn, R. J., Eeken, J. C., de Jong, A. W., van Veen, B. L., Szuhai, K., Mullenders, L. H., Ferro, W., and Pastink, A. (2004). Disruption of Drosophila Rad50 causes pupal lethality, the accumulation of DNA double-strand breaks and the induction of apoptosis in third instar larvae. DNA Repair (Amst) *3*, 603-615.
Gostissa, M., Hengstermann, A., Fogal, V., Sandy, P., Schwarz, S. E., Scheffner, M., and Del Sal, G. (1999). Activation of p53 by conjugation to the ubiquitin-like protein SUMO-1. Embo J *18*, 6462-6471.
Gottschling, D. E., and Zakian, V. A. (1986). Telomere proteins: specific recognition and protection of the natural termini of Oxytricha macronuclear DNA. Cell *47*, 195-205.
Greenberg, R. A., Chin, L., Femino, A., Lee, K. H., Gottlieb, G. J., Singer, R. H., Greider, C. W., and DePinho, R. A. (1999). Short dysfunctional telomeres impair tumorigenesis in the INK4a(delta2/3) cancer-prone mouse. Cell *97*, 515-525.
Greenwell, P. W., Kronmal, S. L., Porter, S. E., Gassenhuber, J., Obermaier, B., and Petes, T. D. (1995). TEL1, a gene involved in controlling telomere length in S. cerevisiae, is homologous to the human ataxia telangiectasia gene. Cell *82*, 823-829.
Griffith, J., Bianchi, A., and de Lange, T. (1998). TRF1 promotes parallel pairing of telomeric tracts in vitro. J Mol Biol *278*, 79-88.
Griffith, J. D., Comeau, L., Rosenfield, S., Stansel, R. M., Bianchi, A., Moss, H., and de Lange, T. (1999). Mammalian telomeres end in a large duplex loop. Cell *97*, 503-514.
Grimwade, D., Howe, K., Langabeer, S., Davies, L., Oliver, F., Walker, H., Swirsky, D., Wheatley, K., Goldstone, A., Burnett, A., and Solomon, E. (1996). Establishing the presence of the t(15;17) in suspected acute promyelocytic leukaemia: cytogenetic, molecular and PML immunofluorescence assessment of patients entered into the M.R.C. ATRA trial. M.R.C. Adult Leukaemia Working Party. Br J Haematol *94*, 557-573.
Grimwade, D., and Solomon, E. (1997). Characterisation of the PML/RAR alpha rearrangement associated with t(15;17) acute promyelocytic leukaemia. Curr Top Microbiol Immunol *220*, 81-112.
Grobelny, J. V., Godwin, A. K., and Broccoli, D. (2000). ALT-associated PML bodies are present in viable cells and are enriched in cells in the G(2)/M phase of the cell cycle. J Cell Sci *113 Pt 24*, 4577-4585.
Guiducci, C., Cerone, M. A., and Bacchetti, S. (2001). Expression of mutant telomerase in immortal telomerase-negative human cells results in cell cycle deregulation, nuclear and chromosomal abnormalities and rapid loss of viability. Oncogene *20*, 714-725.
Guo, A., Salomoni, P., Luo, J., Shih, A., Zhong, S., Gu, W., and Pandolfi, P. P. (2000a). The function of PML in p53-dependent apoptosis. Nat Cell Biol *2*, 730-736.
Guo, A., Salomoni, P., Luo, J., Shih, A., Zhong, S., Gu, W., and Paolo Pandolfi, P. (2000b). The function of PML in p53-dependent apoptosis. Nat Cell Biol *2*, 730-736.
Gurrieri, C., Capodieci, P., Bernardi, R., Scaglioni, P. P., Nafa, K., Rush, L. J., Verbel, D. A., Cordon-Cardo, C., and Pandolfi, P. P. (2004). Loss of the tumor suppressor PML in human cancers of multiple histologic origins. J Natl Cancer Inst *96*, 269-279.
Haber, J. E. (1998). The many interfaces of Mre11. Cell *95*, 583-586.
Hahn, W. C., Stewart, S. A., Brooks, M. W., York, S. G., Eaton, E., Kurachi, A., Beijersbergen, R. L., Knoll, J. H., Meyerson, M., and Weinberg, R. A. (1999). Inhibition of telomerase limits the growth of human cancer cells. Nat Med *5*, 1164-1170.

Hakin-Smith, V., Jellinek, D. A., Levy, D., Carroll, T., Teo, M., Timperley, W. R., McKay, M. J., Reddel, R. R., and Royds, J. A. (2003). Alternative lengthening of telomeres and survival in patients with glioblastoma multiforme. Lancet *361*, 836-838.
Hammond, S. M., Bernstein, E., Beach, D., and Hannon, G. J. (2000). An RNA-directed nuclease mediates post-transcriptional gene silencing in Drosophila cells. Nature *404*, 293-296.
Hanada, K., Ukita, T., Kohno, Y., Saito, K., Kato, J., and Ikeda, H. (1997). RecQ DNA helicase is a suppressor of illegitimate recombination in Escherichia coli. Proc Natl Acad Sci U S A *94*, 3860-3865.
Hanaoka, S., Nagadoi, A., and Nishimura, Y. (2005). Comparison between TRF2 and TRF1 of their telomeric DNA-bound structures and DNA-binding activities. Protein Sci *14*, 119-130.
Hannon, G. J. (2002). RNA interference. Nature *418*, 244-251.
Hara, E., Tsurui, H., Shinozaki, A., Nakada, S., and Oda, K. (1991). Cooperative effect of antisense-Rb and antisense-p53 oligomers on the extension of life span in human diploid fibroblasts, TIG-1. Biochem Biophys Res Commun *179*, 528-534.
Harle-Bachor, C., and Boukamp, P. (1996). Telomerase activity in the regenerative basal layer of the epidermis inhuman skin and in immortal and carcinoma-derived skin keratinocytes. Proc Natl Acad Sci U S A *93*, 6476-6481.
Harley, C. B. (1991). Telomere loss: mitotic clock or genetic time bomb? Mutat Res *256*, 271-282.
Harley, C. B., Futcher, A. B., and Greider, C. W. (1990). Telomeres shorten during ageing of human fibroblasts. Nature *345*, 458–460.
Harmon, F. G., and Kowalczykowski, S. C. (1998). RecQ helicase, in concert with RecA and SSB proteins, initiates and disrupts DNA recombination. Genes Dev *12*, 1134-1144.
Harrington, L., McPhail, T., Mar, V., Zhou, W., Oulton, R., Bass, M. B., Arruda, I., and Robinson, M. O. (1997). A mammalian telomerase-associated protein. Science *275*, 973-977.
Harris, C. C., and Hollstein, M. (1993). Clinical implications of the p53 tumor-suppressor gene. N Engl J Med *329*, 1318-1327.
Hayflick, L. (1965). The Limited in Vitro Lifetime of Human Diploid Cell Strains. Exp Cell Res *37*, 614-636.
Hayflick, L., and Moorhead, P. S. (1961). The serial cultivation of human diploid cell strains. Exp Cell Res *25*, 585-621.
Henderson, S., Allsopp, R., Spector, D., Wang, S. S., and Harley, C. (1996). In situ analysis of changes in telomere size during replicative aging and cell transformation. J Cell Biol *134*, 1-12.
Henson, J. D., Hannay, J. A., McCarthy, S. W., Royds, J. A., Yeager, T. R., Robinson, R. A., Wharton, S. B., Jellinek, D. A., Arbuckle, S. M., Yoo, J., *et al.* (2005). A robust assay for alternative lengthening of telomeres in tumors shows the significance of alternative lengthening of telomeres in sarcomas and astrocytomas. Clin Cancer Res *11*, 217-225.
Henson, J. D., Neumann, A. A., Yeager, T. R., and Reddel, R. R. (2002). Alternative lengthening of telomeres in mammalian cells. Oncogene *21*, 598-610.
Herbig, U., Jobling, W. A., Chen, B. P., Chen, D. J., and Sedivy, J. M. (2004). Telomere shortening triggers senescence of human cells through a pathway involving ATM, p53, and p21(CIP1), but not p16(INK4a). Mol Cell *14*, 501-513.

Hiyama, E., Gollahon, L., Kataoka, T., Kuroi, K., Yokoyama, T., Gazdar, A. F., Hiyama, K., Piatyszek, M. A., and Shay, J. W. (1996). Telomerase activity in human breast tumors. J Natl Cancer Inst *88*, 116-122.
Hiyama, K., Hirai, Y., Kyoizumi, S., Akiyama, M., Hiyama, E., Piatyszek, M. A., Shay, J. W., Ishioka, S., and Yamakido, M. (1995). Activation of telomerase in human lymphocytes and hematopoietic progenitor cells. J Immunol *155*, 3711-3715.
Hockemeyer, D., Daniels, J. P., Takai, H., and de Lange, T. (2006). Recent expansion of the telomeric complex in rodents: Two distinct POT1 proteins protect mouse telomeres. Cell *126*, 63-77.
Hockemeyer, D., Sfeir, A. J., Shay, J. W., Wright, W. E., and de Lange, T. (2005). POT1 protects telomeres from a transient DNA damage response and determines how human chromosomes end. Embo J *24*, 2667-2678.
Hofmann, T. G., Moller, A., Sirma, H., Zentgraf, H., Taya, Y., Droge, W., Will, H., and Schmitz, M. L. (2002). Regulation of p53 activity by its interaction with homeodomain-interacting protein kinase-2. Nat Cell Biol *4*, 1-10.
Hofmann, T. G., and Will, H. (2003). Body language: the function of PML nuclear bodies in apoptosis regulation. Cell Death Differ *10*, 1290-1299.
Hollenbach, A. D., Sublett, J. E., McPherson, C. J., and Grosveld, G. (1999). The Pax3-FKHR oncoprotein is unresponsive to the Pax3-associated repressor hDaxx. Embo J *18*, 3702-3711.
Honda, R., and Yasuda, H. (2000). Activity of MDM2, a ubiquitin ligase, toward p53 or itself is dependent on the RING finger domain of the ligase. Oncogene *19*, 1473-1476.
Hopfner, K. P., Karcher, A., Shin, D. S., Craig, L., Arthur, L. M., Carney, J. P., and Tainer, J. A. (2000). Structural biology of Rad50 ATPase: ATP-driven conformational control in DNA double-strand break repair and the ABC-ATPase superfamily. Cell *101*, 789-800.
Horvath, M. P., Schweiker, V. L., Bevilacqua, J. M., Ruggles, J. A., and Schultz, S. C. (1998). Crystal structure of the Oxytricha nova telomere end binding protein complexed with single strand DNA. Cell *95*, 963-974.
Houghtaling, B. R., Cuttonaro, L., Chang, W., and Smith, S. (2004). A dynamic molecular link between the telomere length regulator TRF1 and the chromosome end protector TRF2. Curr Biol *14*, 1621-1631.
Hsiao, R., Sharma, H. W., Ramakrishnan, S., Keith, E., and Narayanan, R. (1997). Telomerase activity in normal human endothelial cells. Anticancer Res *17*, 827-832.
Huang, C. L., Deng, M. L., Guo, R. J., Wu, M. T., Liu, F. Z., Liang, Y. M., and Qiao, Q. D. (1988). A study on the induction of differentiation of human leukemic cells by harringtonine combined with cytarabine. Leukemia *2*, 518-522.
Huschtscha, L. I., and Reddel, R. R. (1999). p16(INK4a) and the control of cellular proliferative life span. Carcinogenesis *20*, 921-926.
Ishov, A. M., Sotnikov, A. G., Negorev, D., Vladimirova, O. V., Neff, N., Kamitani, T., Yeh, E. T., Strauss, J. F., 3rd, and Maul, G. G. (1999). PML is critical for ND10 formation and recruits the PML-interacting protein daxx to this nuclear structure when modified by SUMO-1. J Cell Biol *147*, 221-234.
Ishov, A. M., Vladimirova, O. V., and Maul, G. G. (2004). Heterochromatin and ND10 are cell-cycle regulated and phosphorylation-dependent alternate nuclear sites of the transcription repressor Daxx and SWI/SNF protein ATRX. J Cell Sci *117*, 3807-3820.
Ivanov, A., Cragg, M. S., Erenpreisa, J., Emzinsh, D., Lukman, H., and Illidge, T. M. (2003). Endopolyploid cells produced after severe genotoxic damage have the potential to repair DNA double strand breaks. J Cell Sci *116*, 4095-4106.

Ivanov, E. L., Sugawara, N., White, C. I., Fabre, F., and Haber, J. E. (1994). Mutations in XRS2 and RAD50 delay but do not prevent mating-type switching in Saccharomyces cerevisiae. Mol Cell Biol *14*, 3414-3425.
Jang, M. S., Ryu, S. W., and Kim, E. (2002). Modification of Daxx by small ubiquitin-related modifier-1. Biochem Biophys Res Commun *295*, 495-500.
Jensen, K., Shiels, C., and Freemont, P. S. (2001). PML protein Isoforms and the RBCC/TRIM motif. Oncogene, 7223-7233.
Jeyapalan, J. N., Varley, H., Foxon, J. L., Pollock, R. E., Jeffreys, A. J., Henson, J. D., Reddel, R. R., and Royle, N. J. (2005). Activation of the ALT pathway for telomere maintenance can affect other sequences in the human genome. Hum Mol Genet *14*, 1785-1794.
Jiang, W. Q., Zhong, Z. H., Henson, J. D., Neumann, A. A., Chang, A. C., and Reddel, R. R. (2005). Suppression of alternative lengthening of telomeres by Sp100-mediated sequestration of the MRE11/RAD50/NBS1 complex. Mol Cell Biol *25*, 2708-2721.
Jiang, W. Q., Zhong, Z. H., Henson, J. D., and Reddel, R. R. (2007). Identification of candidate alternative lengthening of telomeres genes by methionine restriction and RNA interference. Oncogene.
Joazeiro, C. A., and Weissman, A. M. (2000). RING finger proteins: mediators of ubiquitin ligase activity. Cell *102*, 549-552.
Johnson, F. B., Marciniak, R. A., McVey, M., Stewart, S. A., Hahn, W. C., and Guarente, L. (2001). The Saccharomyces cerevisiae WRN homolog Sgs1p participates in telomere maintenance in cells lacking telomerase. Embo J *20*, 905-913.
Kakizuka, A., Miller, W. H., Jr., Umesono, K., Warrell, R. P., Jr., Frankel, S. R., Murty, V. V., Dmitrovsky, E., and Evans, R. M. (1991). Chromosomal translocation t(15;17) in human acute promyelocytic leukemia fuses RAR alpha with a novel putative transcription factor, PML. Cell *66*, 663-674.
Kamei, H. (1997). Cystine starvation induces reversible large-body formation from nuclear bodies in T24 cells. Exp Cell Res *237*, 207-216.
Kamitani, T., Kito, K., Nguyen, H. P., Wada, H., Fukuda-Kamitani, T., and Yeh, E. T. (1998). Identification of three major sentrinization sites in PML. J Biol Chem *273*, 26675-26682.
Kang, J., Ferguson, D., Song, H., Bassing, C., Eckersdorff, M., Alt, F. W., and Xu, Y. (2005). Functional interaction of H2AX, NBS1, and p53 in ATM-dependent DNA damage responses and tumor suppression. Mol Cell Biol *25*, 661-670.
Karlseder, J., Broccoli, D., Dai, Y., Hardy, S., and de Lange, T. (1999). p53- and ATM-dependent apoptosis induced by telomeres lacking TRF2. Science *283*, 1321-1325.
Karlseder, J., Hoke, K., Mirzoeva, O. K., Bakkenist, C., Kastan, M. B., Petrini, J. H., and de Lange, T. (2004a). The telomeric protein TRF2 binds the ATM kinase and can inhibit the ATM-dependent DNA damage response. PLoS Biol *2*, E240.
Karlseder, J., Hoke, K., Mirzoeva, O. K., Bakkenist, C., Kastan, M. B., Petrini, J. H., and Lange Td, T. (2004b). The Telomeric Protein TRF2 Binds the ATM Kinase and Can Inhibit the ATM-Dependent DNA Damage Response. PLoS Biol *2*, E240.
Karlseder, J., Smogorzewska, A., and de Lange, T. (2002). Senescence induced by altered telomere state, not telomere loss. Science *295*, 2446-2449.
Kastner, P., Perez, A., Lutz, Y., Rochette-Egly, C., Gaub, M. P., Durand, B., Lanotte, M., Berger, R., and Chambon, P. (1992). Structure, localization and transcriptional properties of two classes of retinoic acid receptor alpha fusion proteins in acute promyelocytic leukemia (APL): structural similarities with a new family of oncoproteins. Embo J *11*, 629-642.

Katakura, Y., Nakata, E., Miura, T., and Shirahata, S. (1999). Transforming growth factor beta triggers two independent-senescence programs in cancer cells. Biochem Biophys Res Commun *255*, 110-115.
Katayama, H., Sasai, K., Kawai, H., Yuan, Z. M., Bondaruk, J., Suzuki, F., Fujii, S., Arlinghaus, R. B., Czerniak, B. A., and Sen, S. (2004). Phosphorylation by aurora kinase A induces Mdm2-mediated destabilization and inhibition of p53. Nat Genet *36*, 55-62.
Kelleher, C., Kurth, I., and Lingner, J. (2005). Human protection of telomeres 1 (POT1) is a negative regulator of telomerase activity in vitro. Mol Cell Biol *25*, 808-818.
Kentsis, A., and Borden, K. L. (2000). Construction of macromolecular assemblages in eukaryotic processes and their role in human disease: linking RINGs together. Curr Protein Pept Sci *1*, 49-73.
Khan, M. M., Nomura, T., Kim, H., Kaul, S. C., Wadhwa, R., Shinagawa, T., Ichikawa-Iwata, E., Zhong, S., Pandolfi, P. P., and Ishii, S. (2001a). Role of PML and PML-RARalpha in Mad-mediated transcriptional repression. Mol Cell *7*, 1233-1243.
Khan, M. M., Nomura, T., Kim, H., Kaul, S. C., Wadhwa, R., Zhong, S., Pandolfi, P. P., and Ishii, S. (2001b). PML-RARalpha alleviates the transcriptional repression mediated by tumor suppressor Rb. J Biol Chem *276*, 43491-43494.
Khelifi, A. F., D'Alcontres, M. S., and Salomoni, P. (2005). Daxx is required for stress-induced cell death and JNK activation. Cell Death Differ *12*, 724-733.
Kim, M. M., Rivera, M. A., Botchkina, I. L., Shalaby, R., Thor, A. D., and Blackburn, E. H. (2001). A low threshold level of expression of mutant-template telomerase RNA inhibits human tumor cell proliferation. Proc Natl Acad Sci U S A *98*, 7982-7987.
Kim, N. W., Piatyszek, M. A., Prowse, K. R., Harley, C. B., West, M. D., Ho, P. L., Coviello, G. M., Wright, W. E., Weinrich, S. L., and Shay, J. W. (1994). Specific association of human telomerase activity with immortal cells and cancer. Science *266*, 2011-2015.
Kim, S. H., Han, S., You, Y. H., Chen, D. J., and Campisi, J. (2003). The human telomere-associated protein TIN2 stimulates interactions between telomeric DNA tracts in vitro. EMBO Rep *4*, 685-691.
Kim, S. H., Kaminker, P., and Campisi, J. (1999). TIN2, a new regulator of telomere length in human cells. Nat Genet *23*, 405-412.
Klugbauer, S., and Rabes, H. M. (1999). The transcription coactivator HTIF1 and a related protein are fused to the RET receptor tyrosine kinase in childhood papillary thyroid carcinomas. Oncogene *18*, 4388-4393.
Koken, M. H., Puvion-Dutilleul, F., Guillemin, M. C., Viron, A., Linares-Cruz, G., Stuurman, N., de Jong, L., Szostecki, C., Calvo, F., Chomienne, C., and et al. (1994). The t(15;17) translocation alters a nuclear body in a retinoic acid-reversible fashion. Embo J *13*, 1073-1083.
Kurki, S., Latonen, L., and Laiho, M. (2003). Cellular stress and DNA damage invoke temporally distinct Mdm2, p53 and PML complexes and damage-specific nuclear relocalization. J Cell Sci *116*, 3917-3925.
Kurreck, J. (2006). siRNA Efficiency: Structure or Sequence-That Is the Question. J Biomed Biotechnol *2006*, 83757.
Kurz, E. U., and Lees-Miller, S. P. (2004). DNA damage-induced activation of ATM and ATM-dependent signaling pathways. DNA Repair (Amst) *3*, 889-900.
Kyo, S., Takakura, M., Kohama, T., and Inoue, M. (1997). Telomerase activity in human endometrium. Cancer Res *57*, 610-614.

Lackinger, D., and Kaina, B. (2000). Primary mouse fibroblasts deficient for c-Fos, p53 or for both proteins are hypersensitive to UV light and alkylating agent-induced chromosomal breakage and apoptosis. Mutat Res *457*, 113-123.
Lafarga, M., Berciano, M. T., Pena, E., Mayo, I., Castano, J. G., Bohmann, D., Rodrigues, J. P., Tavanez, J. P., and Carmo-Fonseca, M. (2002). Clastosome: a subtype of nuclear body enriched in 19S and 20S proteasomes, ubiquitin, and protein substrates of proteasome. Mol Biol Cell *13*, 2771-2782.
Lallemand-Breitenbach, V., Zhu, J., Puvion, F., Koken, M., Honore, N., Doubeikovsky, A., Duprez, E., Pandolfi, P. P., Puvion, E., Freemont, P., and de The, H. (2001). Role of promyelocytic leukemia (PML) sumolation in nuclear body formation, 11S proteasome recruitment, and As2O3-induced PML or PML/retinoic acid receptor alpha degradation. J Exp Med *193*, 1361-1371.
Lane, D. P., and Crawford, L. V. (1979). T antigen is bound to a host protein in SV40-transformed cells. Nature *278*, 261-263.
Langley, E., Pearson, M., Faretta, M., Bauer, U. M., Frye, R. A., Minucci, S., Pelicci, P. G., and Kouzarides, T. (2002). Human SIR2 deacetylates p53 and antagonizes PML/p53-induced cellular senescence. Embo J *21*, 2383-2396.
Laud, P. R., Multani, A. S., Bailey, S. M., Wu, L., Ma, J., Kingsley, C., Lebel, M., Pathak, S., DePinho, R. A., and Chang, S. (2005). Elevated telomere-telomere recombination in WRN-deficient, telomere dysfunctional cells promotes escape from senescence and engagement of the ALT pathway. Genes Dev *19*, 2560-2570.
Lavin, M. F., and Shiloh, Y. (1997). The genetic defect in ataxia-telangiectasia. Annu Rev Immunol *15*, 177-202.
Lazzerini Denchi, E., Celli, G., and de Lange, T. (2006). Hepatocytes with extensive telomere deprotection and fusion remain viable and regenerate liver mass through endoreduplication. Genes Dev *20*, 2648-2653.
Le Douarin, B., Zechel, C., Garnier, J. M., Lutz, Y., Tora, L., Pierrat, P., Heery, D., Gronemeyer, H., Chambon, P., and Losson, R. (1995). The N-terminal part of TIF1, a putative mediator of the ligand-dependent activation function (AF-2) of nuclear receptors, is fused to B-raf in the oncogenic protein T18. Embo J *14*, 2020-2033.
Le, X. F., Vallian, S., Mu, Z. M., Hung, M. C., and Chang, K. S. (1998). Recombinant PML adenovirus suppresses growth and tumorigenicity of human breast cancer cells by inducing G1 cell cycle arrest and apoptosis. Oncogene *16*, 1839-1849.
Le, X. F., Yang, P., and Chang, K. S. (1996). Analysis of the growth and transformation suppressor domains of promyelocytic leukemia gene, PML. J Biol Chem *271*, 130-135.
Lee, H. W., Blasco, M. A., Gottlieb, G. J., Horner, J. W., 2nd, Greider, C. W., and DePinho, R. A. (1998). Essential role of mouse telomerase in highly proliferative organs. Nature *392*, 569-574.
Lee, J. H., and Paull, T. T. (2004). Direct activation of the ATM protein kinase by the Mre11/Rad50/Nbs1 complex. Science *304*, 93-96.
Lee, J. H., and Paull, T. T. (2005). ATM activation by DNA double-strand breaks through the Mre11-Rad50-Nbs1 complex. Science *308*, 551-554.
Levis, R. W. (1989). Viable deletions of a telomere from a Drosophila chromosome. Cell *58*, 791-801.
Levy, M. Z., Allsopp, R. C., Futcher, A. B., Greider, C. W., and Harley, C. B. (1992). Telomere end-replication problem and cell aging. J Mol Biol *225*, 951-960.
Li, B., Oestreich, S., and de Lange, T. (2000a). Identification of human Rap1: implications for telomere evolution. Cell *101*, 471-483.

Li, H., Leo, C., Zhu, J., Wu, X., O'Neil, J., Park, E. J., and Chen, J. D. (2000b). Sequestration and inhibition of Daxx-mediated transcriptional repression by PML. Mol Cell Biol *20*, 1784-1796.
Lin, H. K., Bergmann, S., and Pandolfi, P. P. (2004). Cytoplasmic PML function in TGF-beta signalling. Nature *431*, 205-211.
Liu, D., Safari, A., O'Connor, M. S., Chan, D. W., Laegeler, A., Qin, J., and Songyang, Z. (2004). PTOP interacts with POT1 and regulates its localization to telomeres. Nat Cell Biol *6*, 673-680.
Loayza, D., and De Lange, T. (2003). POT1 as a terminal transducer of TRF1 telomere length control. Nature *423*, 1013-1018.
Loayza, D., Parsons, H., Donigian, J., Hoke, K., and de Lange, T. (2004). DNA binding features of human POT1: a nonamer 5'-TAGGGTTAG-3' minimal binding site, sequence specificity, and internal binding to multimeric sites. J Biol Chem *279*, 13241-13248.
Lombard, D. B., and Guarente, L. (2000). Nijmegen breakage syndrome disease protein and MRE11 at PML nuclear bodies and meiotic telomeres. Cancer Res *60*, 2331-2334.
Londono-Vallejo, J. A., Der-Sarkissian, H., Cazes, L., Bacchetti, S., and Reddel, R. R. (2004). Alternative lengthening of telomeres is characterized by high rates of telomeric exchange. Cancer Res *64*, 2324-2327.
Louria-Hayon, I., Grossman, T., Sionov, R. V., Alsheich, O., Pandolfi, P. P., and Haupt, Y. (2003). The promyelocytic leukemia protein protects p53 from Mdm2-mediated inhibition and degradation. J Biol Chem *278*, 33134-33141.
Luciani, J. J., Depetris, D., Usson, Y., Metzler-Guillemain, C., Mignon-Ravix, C., Mitchell, M. J., Megarbane, A., Sarda, P., Sirma, H., Moncla, A., *et al.* (2006). PML nuclear bodies are highly organised DNA-protein structures with a function in heterochromatin remodelling at the G2 phase. J Cell Sci *119*, 2518-2531.
Luderus, M. E., van Steensel, B., Chong, L., Sibon, O. C., Cremers, F. F., and de Lange, T. (1996). Structure, subnuclear distribution, and nuclear matrix association of the mammalian telomeric complex. J Cell Biol *135*, 867-881.
Lundblad, V., and Blackburn, E. H. (1993). An alternative pathway for yeast telomere maintenance rescues est1- senescence. Cell *73*, 347-360.
Lundblad, V., and Szostak, J. W. (1989). A mutant with a defect in telomere elongation leads to senescence in yeast. Cell *57*, 633-643.
Luo, J., Nikolaev, A. Y., Imai, S., Chen, D., Su, F., Shiloh, A., Guarente, L., and Gu, W. (2001). Negative control of p53 by Sir2alpha promotes cell survival under stress. Cell *107*, 137-148.
Luo, K. Q., and Chang, D. C. (2004). The gene-silencing efficiency of siRNA is strongly dependent on the local structure of mRNA at the targeted region. Biochem Biophys Res Commun *318*, 303-310.
Lupas, A. (1996). Coiled coils: new structures and new functions. Trends Biochem Sci *21*, 375-382.
Makarov, V. L., Hirose, Y., and Langmore, J. P. (1997). Long G tails at both ends of human chromosomes suggest a C strand degradation mechanism for telomere shortening. Cell *88*, 657-666.
Mallette, F. A., Gaumont-Leclerc, M. F., and Ferbeyre, G. (2007). The DNA damage signaling pathway is a critical mediator of oncogene-induced senescence. Genes Dev *21*, 43-48.

Maser, R. S., Monsen, K. J., Nelms, B. E., and Petrini, J. H. (1997). hMre11 and hRad50 nuclear foci are induced during the normal cellular response to DNA double-strand breaks. Mol Cell Biol *17*, 6087-6096.
Mason, J. M., and Biessmann, H. (1995). The unusual telomeres of Drosophila. Trends Genet *11*, 58-62.
Matsutani, N., Yokozaki, H., Tahara, E., Tahara, H., Kuniyasu, H., Haruma, K., Chayama, K., Yasui, W., and Tahara, E. (2001). Expression of telomeric repeat binding factor 1 and 2 and TRF1-interacting nuclear protein 2 in human gastric carcinomas. Int J Oncol *19*, 507-512.
Maul, G. G. (1998). Nuclear domain 10, the site of DNA virus transcription and replication. Bioessays *20*, 660-667.
Maul, G. G., Jensen, D. E., Ishov, A. M., Herlyn, M., and Rauscher, F. J., 3rd (1998). Nuclear redistribution of BRCA1 during viral infection. Cell Growth Differ *9*, 743-755.
Maul, G. G., Negorev, D., Bell, P., and Ishov, A. M. (2000). Review: properties and assembly mechanisms of ND10, PML bodies, or PODs. J Struct Biol *129*, 278-287.
Maul, G. G., Yu, E., Ishov, A. M., and Epstein, A. L. (1995). Nuclear domain 10 (ND10) associated proteins are also present in nuclear bodies and redistribute to hundreds of nuclear sites after stress. J Cell Biochem *59*, 498-513.
McEachern, M. J., and Blackburn, E. H. (1996). Cap-prevented recombination between terminal telomeric repeat arrays (telomere CPR) maintains telomeres in Kluyveromyces lactis lacking telomerase. Genes Dev *10*, 1822-1834.
McElligott, R., and Wellinger, R. J. (1997). The terminal DNA structure of mammalian chromosomes. Embo J *16*, 3705-3714.
Mehle, C., Piatyszek, M. A., Ljungberg, B., Shay, J. W., and Roos, G. (1996). Telomerase activity in human renal cell carcinoma. Oncogene *13*, 161-166.
Melnick, A., and Licht, J. D. (1999). Deconstructing a disease: RARalpha, its fusion partners, and their roles in the pathogenesis of acute promyelocytic leukemia. Blood *93*, 3167-3215.
Meroni, G., and Diez-Roux, G. (2005). TRIM/RBCC, a novel class of 'single protein RING finger' E3 ubiquitin ligases. Bioessays *27*, 1147-1157.
Metcalfe, J. A., Parkhill, J., Campbell, L., Stacey, M., Biggs, P., Byrd, P. J., and Taylor, A. M. (1996). Accelerated telomere shortening in ataxia telangiectasia. Nat Genet *13*, 350-353.
Michaelson, J. S., Bader, D., Kuo, F., Kozak, C., and Leder, P. (1999). Loss of Daxx, a promiscuously interacting protein, results in extensive apoptosis in early mouse development. Genes Dev *13*, 1918-1923.
Michaelson, J. S., and Leder, P. (2003). RNAi reveals anti-apoptotic and transcriptionally repressive activities of DAXX. J Cell Sci *116*, 345-352.
Mieczkowski, P. A., Mieczkowska, J. O., Dominska, M., and Petes, T. D. (2003). Genetic regulation of telomere-telomere fusions in the yeast Saccharomyces cerevisae. Proc Natl Acad Sci U S A *100*, 10854-10859.
Mihara, K., Iijima, M., Kondo, T., and Namba, M. (1996). Selective expression of mutated p53 in human cells immortalized with either 4-nitroquinoline 1-oxide or 60Co gamma rays. Cell Struct Funct *21*, 111-116.
Minucci, S., Maccarana, M., Cioce, M., De Luca, P., Gelmetti, V., Segalla, S., Di Croce, L., Giavara, S., Matteucci, C., Gobbi, A., *et al.* (2000). Oligomerization of RAR and AML1 transcription factors as a novel mechanism of oncogenic activation. Mol Cell *5*, 811-820.

Mirzoeva, O. K., and Petrini, J. H. (2001a). DNA damage-dependent nuclear dynamics of the Mre11 complex. Mol Cell Biol *21*, 281-288.
Mirzoeva, O. K., and Petrini, J. H. J. (2001b). DNA Damage-Dependent Nuclear Dynamics of the
Mre11 Complex. Molecular and Cellular Biology *21*, 281-288.
Morrish, T. A., Garcia-Perez, J. L., Stamato, T. D., Taccioli, G. E., Sekiguchi, J., and Moran, J. V. (2007). Endonuclease-independent LINE-1 retrotransposition at mammalian telomeres. Nature *446*, 208-212.
Morrish, T. A., Gilbert, N., Myers, J. S., Vincent, B. J., Stamato, T. D., Taccioli, G. E., Batzer, M. A., and Moran, J. V. (2002). DNA repair mediated by endonuclease-independent LINE-1 retrotransposition. Nat Genet *31*, 159-165.
Mu, Z. M., Chin, K. V., Liu, J. H., Lozano, G., and Chang, K. S. (1994). PML, a growth suppressor disrupted in acute promyelocytic leukemia. Mol Cell Biol *14*, 6858-6867.
Munarriz, E., Barcaroli, D., Stephanou, A., Townsend, P. A., Maisse, C., Terrinoni, A., Neale, M. H., Martin, S. J., Latchman, D. S., Knight, R. A., *et al.* (2004). PIAS-1 is a checkpoint regulator which affects exit from G1 and G2 by sumoylation of p73. Mol Cell Biol *24*, 10593-10610.
Munoz, P., Blanco, R., and Blasco, M. A. (2006). Role of the TRF2 telomeric protein in cancer and ageing. Cell Cycle *5*, 718-721.
Munoz, P., Blanco, R., Flores, J. M., and Blasco, M. A. (2005). XPF nuclease-dependent telomere loss and increased DNA damage in mice overexpressing TRF2 result in premature aging and cancer. Nat Genet *37*, 1063-1071.
Muntoni, A., and Reddel, R. R. (2005). The first molecular details of ALT in human tumor cells. Hum Mol Genet *14 Spec No. 2*, R191-196.
Muratani, M., Gerlich, D., Janicki, S. M., Gebhard, M., Eils, R., and Spector, D. L. (2002). Metabolic-energy-dependent movement of PML bodies within the mammalian cell nucleus. Nature Cell Biology *4*, 106-110.
Murnane, J. P., Sabatier, L., Marder, B. A., and Morgan, W. F. (1994). Telomere dynamics in an immortal human cell line. Embo J *13*, 4953-4962.
Myers, J. S., and Cortez, D. (2006). Rapid activation of ATR by ionizing radiation requires ATM and Mre11. J Biol Chem *281*, 9346-9350.
Nabetani, A., Yokoyama, O., and Ishikawa, F. (2004). Localization of hRad9, hHus1, hRad1, and hRad17 and caffeine-sensitive DNA replication at the alternative lengthening of telomeres-associated promyelocytic leukemia body. J Biol Chem *279*, 25849-25857.
Nairz, K., and Klein, F. (1997). mre11S--a yeast mutation that blocks double-strand-break processing and permits nonhomologous synapsis in meiosis. Genes Dev *11*, 2272-2290.
Naito, T., Matsuura, A., and Ishikawa, F. (1998). Circular chromosome formation in a fission yeast mutant defective in two ATM homologues. Nat Genet *20*, 203-206.
Naka, K., Ikeda, K., and Motoyama, N. (2002). Recruitment of NBS1 into PML oncogenic domains via interaction with SP100 protein. Biochem Biophys Res Commun *299*, 863-871.
Natarajan, S., and McEachern, M. J. (2002). Recombinational telomere elongation promoted by DNA circles. Mol Cell Biol *22*, 4512-4521.
Nefkens, I., Negorev, D. G., Ishov, A. M., Michaelson, J. S., Yeh, E. T., Tanguay, R. M., Muller, W. E., and Maul, G. G. (2003). Heat shock and Cd2+ exposure regulate PML and Daxx release from ND10 by independent mechanisms that modify the induction of heat-shock proteins 70 and 25 differently. J Cell Sci *116*, 513-524.

Neves, H., Ramos, C., da Silva, M. G., Parreira, A., and Parreira, L. (1999). The nuclear topography of ABL, BCR, PML, and RARalpha genes: evidence for gene proximity in specific phases of the cell cycle and stages of hematopoietic differentiation. Blood *93*, 1197-1207.
Niculescu, A. B., 3rd, Chen, X., Smeets, M., Hengst, L., Prives, C., and Reed, S. I. (1998). Effects of p21(Cip1/Waf1) at both the G1/S and the G2/M cell cycle transitions: pRb is a critical determinant in blocking DNA replication and in preventing endoreduplication. Mol Cell Biol *18*, 629-643.
Niida, H., Matsumoto, T., Satoh, H., Shiwa, M., Tokutake, Y., Furuichi, Y., and Shinkai, Y. (1998). Severe growth defect in mouse cells lacking the telomerase RNA component. Nat Genet *19*, 203-206.
O'Brien, W., Stenman, G., and Sager, R. (1986). Suppression of tumor growth by senescence in virally transformed human fibroblasts. Proc Natl Acad Sci U S A *83*, 8659-8663.
Oh, B. K., Kim, Y. J., Park, C., and Park, Y. N. (2005). Up-regulation of telomere-binding proteins, TRF1, TRF2, and TIN2 is related to telomere shortening during human multistep hepatocarcinogenesis. Am J Pathol *166*, 73-80.
Oikemus, S. R., McGinnis, N., Queiroz-Machado, J., Tukachinsky, H., Takada, S., Sunkel, C. E., and Brodsky, M. H. (2004). Drosophila atm/telomere fusion is required for telomeric localization of HP1 and telomere position effect. Genes Dev *18*, 1850-1861.
Olovnikov, A. M. (1971). [Principle of marginotomy in template synthesis of polynucleotides]. Dokl Akad Nauk SSSR *201*, 1496-1499.
Opresko, P. L., Mason, P. A., Podell, E. R., Lei, M., Hickson, I. D., Cech, T. R., and Bohr, V. A. (2005). POT1 stimulates RecQ helicases WRN and BLM to unwind telomeric DNA substrates. J Biol Chem *280*, 32069-32080.
Opresko, P. L., von Kobbe, C., Laine, J. P., Harrigan, J., Hickson, I. D., and Bohr, V. A. (2002). Telomere-binding protein TRF2 binds to and stimulates the Werner and Bloom syndrome helicases. J Biol Chem *277*, 41110-41119.
Palmero, I., McConnell, B., Parry, D., Brookes, S., Hara, E., Bates, S., Jat, P., and Peters, G. (1997). Accumulation of p16INK4a in mouse fibroblasts as a function of replicative senescence and not of retinoblastoma gene status. Oncogene *15*, 495-503.
Paull, T. T., and Gellert, M. (1999). Nbs1 potentiates ATP-driven DNA unwinding and endonuclease cleavage by the Mre11/Rad50 complex. Genes Dev *13*, 1276-1288.
Pearson, M., Carbone, R., Sebastiani, C., Cioce, M., Fagioli, M., Saito, S., Higashimoto, Y., Appella, E., Minucci, S., Pandolfi, P. P., and Pelicci, P. G. (2000). PML regulates p53 acetylation and premature senescence induced by oncogenic Ras. Nature *406*, 207-210.
Peng, H., Begg, G. E., Schultz, D. C., Friedman, J. R., Jensen, D. E., Speicher, D. W., and Rauscher, F. J., 3rd (2000). Reconstitution of the KRAB-KAP-1 repressor complex: a model system for defining the molecular anatomy of RING-B box-coiled-coil domain-mediated protein-protein interactions. J Mol Biol *295*, 1139-1162.
Perlman, R., Schiemann, W. P., Brooks, M. W., Lodish, H. F., and Weinberg, R. A. (2001). TGF-beta-induced apoptosis is mediated by the adapter protein Daxx that facilitates JNK activation. Nat Cell Biol *3*, 708-714.
Perrem, K., Colgin, L. M., Neumann, A. A., Yeager, T. R., and Reddel, R. R. (2001). Coexistence of alternative lengthening of telomeres and telomerase in hTERT-transfected GM847 cells. Mol Cell Biol *21*, 3862-3875.

Petrini, J. H., and Stracker, T. H. (2003). The cellular response to DNA double-strand breaks: defining the sensors and mediators. Trends Cell Biol *13*, 458-462.
Petrini, J. H., Walsh, M. E., DiMare, C., Chen, X. N., Korenberg, J. R., and Weaver, D. T. (1995). Isolation and characterization of the human MRE11 homologue. Genomics *29*, 80-86.
Queiroz-Machado, J., Perdigao, J., Simoes-Carvalho, P., Herrmann, S., and Sunkel, C. E. (2001). tef: a mutation that causes telomere fusion and severe genome rearrangements in Drosophila melanogaster. Chromosoma *110*, 10-23.
Quignon, F., De Bels, F., Koken, M., Feunteun, J., Ameisen, J. C., and de The, H. (1998). PML induces a novel caspase-independent death process. Nat Genet *20*, 259-265.
Ramirez, R. D., Wright, W. E., Shay, J. W., and Taylor, R. S. (1997). Telomerase activity concentrates in the mitotically active segments of human hair follicles. J Invest Dermatol *108*, 113-117.
Rathmell, J. C., and Thompson, C. B. (1999). The central effectors of cell death in the immune system. Annu Rev Immunol *17*, 781-828.
Razak, Z. R., Varkonyi, R. J., Kulp-McEliece, M., Caslini, C., Testa, J. R., Murphy, M. E., and Broccoli, D. (2004). p53 differentially inhibits cell growth depending on the mechanism of telomere maintenance. Mol Cell Biol *24*, 5967-5977.
Reddel, R. R. (2003). Alternative lengthening of telomeres, telomerase, and cancer. Cancer Letters *194*, 155-162.
Regad, T., Saib, A., Lallemand-Breitenbach, V., Pandolfi, P. P., de The, H., and Chelbi-Alix, M. K. (2001). PML mediates the interferon-induced antiviral state against a complex retrovirus via its association with the viral transactivator. Embo J *20*, 3495-3505.
Rego, E. M., Wang, Z. G., Peruzzi, D., He, L. Z., Cordon-Cardo, C., and Pandolfi, P. P. (2001). Role of promyelocytic leukemia (PML) protein in tumor suppression. J Exp Med *193*, 521-529.
Reymond, A., Meroni, G., Fantozzi, A., Merla, G., Cairo, S., Luzi, L., Riganelli, D., Zanaria, E., Messali, S., Cainarca, S., *et al.* (2001). The tripartite motif family identifies cell compartments. Embo J *20*, 2140-2151.
Reynolds, A., Leake, D., Boese, Q., Scaringe, S., Marshall, W. S., and Khvorova, A. (2004). Rational siRNA design for RNA interference. Nat Biotechnol *22*, 326-330.
Reznikoff, C. A., Yeager, T. R., Belair, C. D., Savelieva, E., Puthenveettil, J. A., and Stadler, W. M. (1996). Elevated p16 at senescence and loss of p16 at immortalization in human papillomavirus 16 E6, but not E7, transformed human uroepithelial cells. Cancer Res *56*, 2886-2890.
Rheinwald, J. G., Hahn, W. C., Ramsey, M. R., Wu, J. Y., Guo, Z., Tsao, H., De Luca, M., Catricala, C., and O'Toole, K. M. (2002). A two-stage, p16(INK4A)- and p53-dependent keratinocyte senescence mechanism that limits replicative potential independent of telomere status. Mol Cell Biol *22*, 5157-5172.
Ritchie, K. B., Mallory, J. C., and Petes, T. D. (1999). Interactions of TLC1 (which encodes the RNA subunit of telomerase), TEL1, and MEC1 in regulating telomere length in the yeast Saccharomyces cerevisiae. Mol Cell Biol *19*, 6065-6075.
Ritchie, K. B., and Petes, T. D. (2000). The Mre11p/Rad50p/Xrs2p complex and the Tel1p function in a single pathway for telomere maintenance in yeast. Genetics *155*, 475-479.

Robles, S. J., and Adami, G. R. (1998). Agents that cause DNA double strand breaks lead to p16INK4a enrichment and the premature senescence of normal fibroblasts. Oncogene *16*, 1113-1123.
Rodriguez, M. S., Desterro, J. M., Lain, S., Midgley, C. A., Lane, D. P., and Hay, R. T. (1999). SUMO-1 modification activates the transcriptional response of p53. Embo J *18*, 6455-6461.
Rogan, E. M., Bryan, T. M., Hukku, B., Maclean, K., Chang, A. C., Moy, E. L., Englezou, A., Warneford, S. G., Dalla-Pozza, L., and Reddel, R. R. (1995). Alterations in p53 and p16INK4 expression and telomere length during spontaneous immortalization of Li-Fraumeni syndrome fibroblasts. Mol Cell Biol *15*, 4745-4753.
Roth, C. W., Kobeski, F., Walter, M. F., and Biessmann, H. (1997). Chromosome end elongation by recombination in the mosquito Anopheles gambiae. Mol Cell Biol *17*, 5176-5183.
Sager, R. (1991). Senescence as a mode of tumor suppression. Environ Health Perspect *93*, 59-62.
Saito, T., Schneider, A., Martel, N., Mizumoto, H., Bulgay-Moerschel, M., Kudo, R., and Nakazawa, H. (1997). Proliferation-associated regulation of telomerase activity in human endometrium and its potential implication in early cancer diagnosis. Biochem Biophys Res Commun *231*, 610-614.
Salomoni, P., Bernardi, R., Bergmann, S., Changou, A., Tuttle, S., and Pandolfi, P. P. (2005). The promyelocytic leukemia protein PML regulates c-Jun function in response to DNA damage. Blood *105*, 3686-3690.
Salomoni, P., and Pandolfi, P. P. (2002). The role of PML in tumor suppression. Cell *108*, 165-170.
Saurin, A. J., Borden, K. L., Boddy, M. N., and Freemont, P. S. (1996). Does this have a familiar RING? Trends Biochem Sci *21*, 208-214.
Savitsky, K., Sfez, S., Tagle, D. A., Ziv, Y., Sartiel, A., Collins, F. S., Shiloh, Y., and Rotman, G. (1995). The complete sequence of the coding region of the ATM gene reveals similarity to cell cycle regulators in different species. Hum Mol Genet *4*, 2025-2032.
Scaglioni, P. P., Yung, T. M., Cai, L. F., Erdjument-Bromage, H., Kaufman, A. J., Singh, B., Teruya-Feldstein, J., Tempst, P., and Pandolfi, P. P. (2006). A CK2-dependent mechanism for degradation of the PML tumor suppressor. Cell *126*, 269-283.
Scheel, C., Schaefer, K. L., Jauch, A., Keller, M., Wai, D., Brinkschmidt, C., van Valen, F., Boecker, W., Dockhorn-Dworniczak, B., and Poremba, C. (2001). Alternative lengthening of telomeres is associated with chromosomal instability in osteosarcomas. Oncogene *20*, 3835-3844.
Scheffner, M., Werness, B. A., Huibregtse, J. M., Levine, A. J., and Howley, P. M. (1990). The E6 oncoprotein encoded by human papillomavirus types 16 and 18 promotes the degradation of p53. Cell *63*, 1129-1136.
Schubert, S., Grunweller, A., Erdmann, V. A., and Kurreck, J. (2005). Local RNA target structure influences siRNA efficacy: systematic analysis of intentionally designed binding regions. J Mol Biol *348*, 883-893.
Scott, S. P., Bendix, R., Chen, P., Clark, R., Dork, T., and Lavin, M. F. (2002). Missense mutations but not allelic variants alter the function of ATM by dominant interference in patients with breast cancer. Proc Natl Acad Sci U S A *99*, 925-930.
Seeler, J. S., and Dejean, A. (1999). The PML nuclear bodies: actors or extras? Curr Opin Genet Dev *9*, 362-367.

Seo, S. R., Ferrand, N., Faresse, N., Prunier, C., Abecassis, L., Pessah, M., Bourgeade, M. F., and Atfi, A. (2006). Nuclear retention of the tumor suppressor cPML by the homeodomain protein TGIF restricts TGF-beta signaling. Mol Cell *23*, 547-559.
Serrano, M., Hannon, G. J., and Beach, D. (1993). A new regulatory motif in cell-cycle control causing specific inhibition of cyclin D/CDK4. Nature *366*, 704-707.
Serrano, M., Lin, A. W., McCurrach, M. E., Beach, D., and Lowe, S. W. (1997). Oncogenic ras provokes premature cell senescence associated with accumulation of p53 and p16INK4a. Cell *88*, 593-602.
Sfeir, A. J., Chai, W., Shay, J. W., and Wright, W. E. (2005). Telomere-end processing the terminal nucleotides of human chromosomes. Mol Cell *18*, 131-138.
Shay, J. W., and Bacchetti, S. (1997). A survey of telomerase activity in human cancer. Eur J Cancer *33*, 787-791.
Shay, J. W., and Gazdar, A. F. (1997). Telomerase in the early detection of cancer. J Clin Pathol *50*, 106-109.
Shay, J. W., Pereira-Smith, O. M., and Wright, W. E. (1991). A role for both RB and p53 in the regulation of human cellular senescence. Exp Cell Res *196*, 33-39.
Shay, J. W., and Wright, W. E. (1989). Quantitation of the frequency of immortalization of normal human diploid fibroblasts by SV40 large T-antigen. Exp Cell Res *184*, 109-118.
Shen, T. H., Lin, H. K., Scaglioni, P. P., Yung, T. M., and Pandolfi, P. P. (2006). The mechanisms of PML-nuclear body formation. Mol Cell *24*, 331-339.
Sherr, C. J. (1996). Cancer cell cycles. Science *274*, 1672-1677.
Sherr, C. J., and DePinho, R. A. (2000). Cellular senescence: mitotic clock or culture shock? Cell *102*, 407-410.
Shiloh, Y. (1997). Ataxia-telangiectasia and the Nijmegen breakage syndrome: related disorders but genes apart. Annu Rev Genet *31*, 635-662.
Shiloh, Y., and Kastan, M. B. (2001). ATM: genome stability, neuronal development, and cancer cross paths. Adv Cancer Res *83*, 209-254.
Shore, D. (1994). RAP1: a protean regulator in yeast. Trends Genet *10*, 408-412.
Silva, E., Tiong, S., Pedersen, M., Homola, E., Royou, A., Fasulo, B., Siriaco, G., and Campbell, S. D. (2004). ATM is required for telomere maintenance and chromosome stability during Drosophila development. Curr Biol *14*, 1341-1347.
Skinner, P. J., Koshy, B. T., Cummings, C. J., Klement, I. A., Helin, K., Servadio, A., Zoghbi, H. Y., and Orr, H. T. (1997). Ataxin-1 with an expanded glutamine tract alters nuclear matrix-associated structures. Nature *389*, 971-974.
Smith, G. C., Cary, R. B., Lakin, N. D., Hann, B. C., Teo, S. H., Chen, D. J., and Jackson, S. P. (1999). Purification and DNA binding properties of the ataxia-telangiectasia gene product ATM. Proc Natl Acad Sci U S A *96*, 11134-11139.
Smith, M. L., and Fornace, A. J., Jr. (1997). p53-mediated protective responses to UV irradiation. Proc Natl Acad Sci U S A *94*, 12255-12257.
Smith, S., and de Lange, T. (1997). TRF1, a mammalian telomeric protein. Trends Genet *13*, 21-26.
Smogorzewska, A., and de Lange, T. (2002). Different telomere damage signaling pathways in human and mouse cells. Embo J *21*, 4338-4348.
Smogorzewska, A., and de Lange, T. (2004). Regulation of telomerase by telomeric proteins. Annu Rev Biochem *73*, 177-208.
Smogorzewska, A., Karlseder, J., Holtgreve-Grez, H., Jauch, A., and de Lange, T. (2002). DNA ligase IV-dependent NHEJ of deprotected mammalian telomeres in G1 and G2. Curr Biol *12*, 1635-1644.

Smogorzewska, A., van Steensel, B., Bianchi, A., Oelmann, S., Schaefer, M. R., Schnapp, G., and de Lange, T. (2000). Control of human telomere length by TRF1 and TRF2. Mol Cell Biol *20*, 1659-1668.
Song, J. J., and Lee, Y. J. (2003a). Effect of glucose concentration on activation of the ASK1-SEK1-JNK1 signal transduction pathway. J Cell Biochem *89*, 653-662.
Song, J. J., and Lee, Y. J. (2003b). Role of the ASK1-SEK1-JNK1-HIPK1 signal in Daxx trafficking and ASK1 oligomerization. J Biol Chem *278*, 47245-47252.
Song, J. J., and Lee, Y. J. (2004). Tryptophan 621 and serine 667 residues of Daxx regulate its nuclear export during glucose deprivation. J Biol Chem *279*, 30573-30578.
Song, K., Jung, D., Jung, Y., Lee, S. G., and Lee, I. (2000). Interaction of human Ku70 with TRF2. FEBS Lett *481*, 81-85.
Song, Y. H., Mirey, G., Betson, M., Haber, D. A., and Settleman, J. (2004). The Drosophila ATM ortholog, dATM, mediates the response to ionizing radiation and to spontaneous DNA damage during development. Curr Biol *14*, 1354-1359.
Stansel, R. M., de Lange, T., and Griffith, J. D. (2001). T-loop assembly in vitro involves binding of TRF2 near the 3' telomeric overhang. Embo J *20*, 5532-5540.
Stein, G. H., Beeson, M., and Gordon, L. (1990). Failure to phosphorylate the retinoblastoma gene product in senescent human fibroblasts. Science *249*, 666-669.
Stein, G. H., and Dulic, V. (1995). Origins of G1 arrest in senescent human fibroblasts. Bioessays *17*, 537-543.
Sternsdorf, T., Grotzinger, T., Jensen, K., and Will, H. (1997). Nuclear dots: actors on many stages. Immunobiology *198*, 307-331.
Stewart, G. S., Maser, R. S., Stankovic, T., Bressan, D. A., Kaplan, M. I., Jaspers, N. G., Raams, A., Byrd, P. J., Petrini, J. H., and Taylor, A. M. (1999). The DNA double-strand break repair gene hMRE11 is mutated in individuals with an ataxia-telangiectasia-like disorder. Cell *99*, 577-587.
Stiff, T., Reis, C., Alderton, G. K., Woodbine, L., O'Driscoll, M., and Jeggo, P. A. (2005). Nbs1 is required for ATR-dependent phosphorylation events. Embo J *24*, 199-208.
Suzuki, K., Kodama, S., and Watanabe, M. (1999). Recruitment of ATM protein to double strand DNA irradiated with ionizing radiation. J Biol Chem *274*, 25571-25575.
Takai, H., Smogorzewska, A., and de Lange, T. (2003). DNA damage foci at dysfunctional telomeres. Curr Biol *13*, 1549-1556.
Tanaka, H., Mendonca, M. S., Bradshaw, P. S., Hoelz, D. J., Malkas, L. H., Meyn, M. S., and Gilley, D. (2005). DNA damage-induced phosphorylation of the human telomere-associated protein TRF2. Proc Natl Acad Sci U S A *102*, 15539-15544.
Tang, J., Qu, L. K., Zhang, J., Wang, W., Michaelson, J. S., Degenhardt, Y. Y., El-Deiry, W. S., and Yang, X. (2006). Critical role for Daxx in regulating Mdm2. Nat Cell Biol *8*, 855-862.
Taylor, R. S., Ramirez, R. D., Ogoshi, M., Chaffins, M., Piatyszek, M. A., and Shay, J. W. (1996). Detection of telomerase activity in malignant and nonmalignant skin conditions. J Invest Dermatol *106*, 759-765.
Teng, S. C., Chang, J., McCowan, B., and Zakian, V. A. (2000). Telomerase-independent lengthening of yeast telomeres occurs by an abrupt Rad50p-dependent, Rif-inhibited recombinational process. Mol Cell *6*, 947-952.
Teng, S. C., and Zakian, V. A. (1999). Telomere-telomere recombination is an efficient bypass pathway for telomere maintenance in Saccharomyces cerevisiae. Mol Cell Biol *19*, 8083-8093.

Topcu, Z., Mack, D. L., Hromas, R. A., and Borden, K. L. (1999). The promyelocytic leukemia protein PML interacts with the proline-rich homeodomain protein PRH: a RING may link hematopoiesis and growth control. Oncogene *18*, 7091-7100.
Torii, S., Egan, D. A., Evans, R. A., and Reed, J. C. (1999). Human Daxx regulates Fas-induced apoptosis from nuclear PML oncogenic domains (PODs). Embo J *18*, 6037-6049.
Tournier, C., Hess, P., Yang, D. D., Xu, J., Turner, T. K., Nimnual, A., Bar-Sagi, D., Jones, S. N., Flavell, R. A., and Davis, R. J. (2000). Requirement of JNK for stress-induced activation of the cytochrome c-mediated death pathway. Science *288*, 870-874.
Trotman, L. C., Alimonti, A., Scaglioni, P. P., Koutcher, J. A., Cordon-Cardo, C., and Pandolfi, P. P. (2006). Identification of a tumour suppressor network opposing nuclear Akt function. Nature *441*, 523-527.
Trotman, L. C., Niki, M., Dotan, Z. A., Koutcher, J. A., Di Cristofano, A., Xiao, A., Khoo, A. S., Roy-Burman, P., Greenberg, N. M., Van Dyke, T., *et al.* (2003). Pten dose dictates cancer progression in the prostate. PLoS Biol *1*, E59.
Tsubouchi, H., and Ogawa, H. (2000). Exo1 roles for repair of DNA double-strand breaks and meiotic crossing over in Saccharomyces cerevisiae. Mol Biol Cell *11*, 2221-2233.
Tsukamoto, T., Hashiguchi, N., Janicki, S. M., Tumbar, T., Belmont, A. S., and Spector, D. L. (2000). Visualization of gene activity in living cells. Nat Cell Biol *2*, 871-878.
Ulaner, G. A., Hoffman, A. R., Otero, J., Huang, H. Y., Zhao, Z., Mazumdar, M., Gorlick, R., Meyers, P., Healey, J. H., and Ladanyi, M. (2004). Divergent patterns of telomere maintenance mechanisms among human sarcomas: sharply contrasting prevalence of the alternative lengthening of telomeres mechanism in Ewing's sarcomas and osteosarcomas. Genes Chromosomes Cancer *41*, 155-162.
Uziel, T., Lerenthal, Y., Moyal, L., Andegeko, Y., Mittelman, L., and Shiloh, Y. (2003). Requirement of the MRN complex for ATM activation by DNA damage. Embo J *22*, 5612-5621.
van Steensel, B., and de Lange, T. (1997). Control of telomere length by the human telomeric protein TRF1. Nature *385*, 740-743.
van Steensel, B., Smogorzewska, A., and de Lange, T. (1998). TRF2 protects human telomeres from end-to-end fusions. Cell *92*, 401-413.
Vaziri, H., and Benchimol, S. (1996). From telomere loss to p53 induction and activation of a DNA-damage pathway at senescence: the telomere loss/DNA damage model of cell aging. Exp Gerontol *31*, 295-301.
Vaziri, H., and Benchimol, S. (1998). Reconstitution of telomerase activity in normal human cells leads to elongation of telomeres and extended replicative life span. Curr Biol *8*, 279-282.
Vaziri, H., Dessain, S. K., Ng Eaton, E., Imai, S. I., Frye, R. A., Pandita, T. K., Guarente, L., and Weinberg, R. A. (2001). hSIR2(SIRT1) functions as an NAD-dependent p53 deacetylase. Cell *107*, 149-159.
Verdun, R. E., Crabbe, L., Haggblom, C., and Karlseder, J. (2005). Functional human telomeres are recognized as DNA damage in G2 of the cell cycle. Mol Cell *20*, 551-561.
Verdun, R. E., and Karlseder, J. (2006). The DNA damage machinery and homologous recombination pathway act consecutively to protect human telomeres. Cell *127*, 709-720.

Waldman, T., Lengauer, C., Kinzler, K. W., and Vogelstein, B. (1996). Uncoupling of S phase and mitosis induced by anticancer agents in cells lacking p21. Nature *381*, 713-716.
Wang, R. C., Smogorzewska, A., and de Lange, T. (2004). Homologous recombination generates T-loop-sized deletions at human telomeres. Cell *119*, 355-368.
Wang, Z. G., Delva, L., Gaboli, M., Rivi, R., Giorgio, M., Cordon-Cardo, C., Grosveld, F., and Pandolfi, P. P. (1998a). Role of PML in cell growth and the retinoic acid pathway. Science *279*, 1547-1551.
Wang, Z. G., Ruggero, D., Ronchetti, S., Zhong, S., Gaboli, M., Rivi, R., and Pandolfi, P. P. (1998b). PML is essential for multiple apoptotic pathways. Nat Genet *20*, 266-272.
Watson, J. D. (1972). Origin of concatemeric T7 DNA. Nat New Biol *239*, 197-201.
Wei, X., Yu, Z. K., Ramalingam, A., Grossman, S. R., Yu, J. H., Bloch, D. B., and Maki, C. G. (2003). Physical and functional interactions between PML and MDM2. J Biol Chem *278*, 29288-29297.
Weis, K., Rambaud, S., Lavau, C., Jansen, J., Carvalho, T., Carmo-Fonseca, M., Lamond, A., and Dejean, A. (1994). Retinoic acid regulates aberrant nuclear localization of PML-RAR alpha in acute promyelocytic leukemia cells. Cell *76*, 345-356.
Wells, S. I., Aronow, B. J., Wise, T. M., Williams, S. S., Couget, J. A., and Howley, P. M. (2003). Transcriptome signature of irreversible senescence in human papillomavirus-positive cervical cancer cells. Proc Natl Acad Sci U S A *100*, 7093-7098.
Williamson, J. R., Raghuraman, M. K., and Cech, T. R. (1989). Monovalent cation-induced structure of telomeric DNA: the G-quartet model. Cell *59*, 871-880.
Wright, W. E., Tesmer, V. M., Huffman, K. E., Levene, S. D., and Shay, J. W. (1997). Normal human chromosomes have long G-rich telomeric overhangs at one end. Genes Dev *11*, 2801-2809.
Wu, G., Jiang, X., Lee, W. H., and Chen, P. L. (2003). Assembly of functional ALT-associated promyelocytic leukemia bodies requires Nijmegen Breakage Syndrome 1. Cancer Res *63*, 2589-2595.
Wu, G., Lee, W. H., and Chen, P. L. (2000). NBS1 and TRF1 colocalize at promyelocytic leukemia bodies during late S/G2 phases in immortalized telomerase-negative cells. Implication of NBS1 in alternative lengthening of telomeres. J Biol Chem *275*, 30618-30622.
Wu, L., Multani, A. S., He, H., Cosme-Blanco, W., Deng, Y., Deng, J. M., Bachilo, O., Pathak, S., Tahara, H., Bailey, S. M., *et al.* (2006). Pot1 deficiency initiates DNA damage checkpoint activation and aberrant homologous recombination at telomeres. Cell *126*, 49-62.
Xiao, Y., and Weaver, D. T. (1997). Conditional gene targeted deletion by Cre recombinase demonstrates the requirement for the double-strand break repair Mre11 protein in murine embryonic stem cells. Nucleic Acids Res *25*, 2985-2991.
Xu, H. J., Zhou, Y., Ji, W., Perng, G. S., Kruzelock, R., Kong, C. T., Bast, R. C., Mills, G. B., Li, J., and Hu, S. X. (1997). Reexpression of the retinoblastoma protein in tumor cells induces senescence and telomerase inhibition. Oncogene *15*, 2589-2596.
Xu, Z. X., Timanova-Atanasova, A., Zhao, R. X., and Chang, K. S. (2003). PML colocalizes with and stabilizes the DNA damage response protein TopBP1. Mol Cell Biol *23*, 4247-4256.

Xu, Z. X., Zou, W. X., Lin, P., and Chang, K. S. (2005). A role for PML3 in centrosome duplication and genome stability. Mol Cell *17*, 721-732.
Yang, S., Kuo, C., Bisi, J. E., and Kim, M. K. (2002). PML-dependent apoptosis after DNA damage is regulated by the checkpoint kinase hCds1/Chk2. Nat Cell Biol *4*, 865-870.
Yang, X., Khosravi-Far, R., Chang, H. Y., and Baltimore, D. (1997). Daxx, a novel Fas-binding protein that activates JNK and apoptosis. Cell *89*, 1067-1076.
Yankiwski, V., Marciniak, R. A., Guarente, L., and Neff, N. F. (2000). Nuclear structure in normal and Bloom syndrome cells. Proc Natl Acad Sci U S A *97*, 5214-5219.
Yasuda, S., Inoue, K., Hirabayashi, M., Higashiyama, H., Yamamoto, Y., Fuyuhiro, H., Komure, O., Tanaka, F., Sobue, G., Tsuchiya, K., *et al.* (1999). Triggering of neuronal cell death by accumulation of activated SEK1 on nuclear polyglutamine aggregations in PML bodies. Genes Cells *4*, 743-756.
Yasumoto, S., Kunimura, C., Kikuchi, K., Tahara, H., Ohji, H., Yamamoto, H., Ide, T., and Utakoji, T. (1996). Telomerase activity in normal human epithelial cells. Oncogene *13*, 433-439.
Ye, J. Z., Hockemeyer, D., Krutchinsky, A. N., Loayza, D., Hooper, S. M., Chait, B. T., and de Lange, T. (2004). POT1-interacting protein PIP1: a telomere length regulator that recruits POT1 to the TIN2/TRF1 complex. Genes Dev *18*, 1649-1654.
Yeager, T. R., Neumann, A. A., Englezou, A., Huschtscha, L. I., Noble, J. R., and Reddel, R. R. (1999). Telomerase-negative Immortalized Human Cells Contain a Novel Type of Promyelocytic Leukemia (PML) Body. Cancer Rearch *59*, 4175-4179.
Zhang, X., Mar, V., Zhou, W., Harrington, L., and Robinson, M. O. (1999). Telomere shortening and apoptosis in telomerase-inhibited human tumor cells. Genes Dev *13*, 2388-2399.
Zhong, S., Hu, P., Ye, T.-Z., Stan, R., Ellis, N. A., and Pandol, P. P. (1999). A role for PML and the nuclear body in genomic stability. Oncogene *18*, 7941-7947.
Zhong, S., Muller, S., Ronchetti, S., Freemont, P. S., Dejean, A., and Pandolfi, P. P. (2000a). Role of SUMO-1-modified PML in nuclear body formation. Blood *95*, 2748-2752.
Zhong, S., Salomoni, P., Ronchetti, S., Guo, A., Ruggero, D., and Pandolfi, P. P. (2000b). Promyelocytic leukemia protein (PML) and Daxx participate in a novel nuclear pathway for apoptosis. J Exp Med *191*, 631-640.
Zhong, Z., Shiue, L., Kaplan, S., and de Lange, T. (1992). A mammalian factor that binds telomeric TTAGGG repeats in vitro. Mol Cell Biol *12*, 4834-4843.
Zhu, J., Koken, M. H., Quignon, F., Chelbi-Alix, M. K., Degos, L., Wang, Z. Y., Chen, Z., and de The, H. (1997). Arsenic-induced PML targeting onto nuclear bodies: implications for the treatment of acute promyelocytic leukemia. Proc Natl Acad Sci U S A *94*, 3978-3983.
Zhu, J., Wang, H., Bishop, J. M., and Blackburn, E. H. (1999). Telomerase extends the lifespan of virus-transformed human cells without net telomere lengthening. Proc Natl Acad Sci U S A *96*, 3723-3728.
Zhu, J., Woods, D., McMahon, M., and Bishop, J. M. (1998). Senescence of human fibroblasts induced by oncogenic Raf. Genes Dev *12*, 2997-3007.
Zhu, X. D., Kuster, B., Mann, M., Petrini, J. H., and de Lange, T. (2000). Cell-cycle-regulated association of RAD50/MRE11/NBS1 with TRF2 and human telomeres. Nat Genet *25*, 347-352.

Zhu, X. D., Niedernhofer, L., Kuster, B., Mann, M., Hoeijmakers, J. H., and de Lange, T. (2003). ERCC1/XPF removes the 3' overhang from uncapped telomeres and represses formation of telomeric DNA-containing double minute chromosomes. Mol Cell *12*, 1489-1498.

Publications arising from this work

Khelifi AF, D'Alcontres MS, Salomoni P (2005). Daxx is required for stress-induced cell death and JNK activation. Cell Death Differ **(7):724-33**

Stagno D'Alcontres M., Mendez-Bermudez A., Royle N.J. and Salomoni P. **The telomere-binding protein TRF2 protects ALT cells from PML-dependent p53 activation and telomere erosion.** Submitted to the Journal of Cell Biology July 2007.